



Inflammation and end-organ damage with obesity and gender

By Ian Bloor, BSc (Hons)

Thesis submitted to the University of Nottingham
for the degree of Doctor of Philosophy

September 2011

Abstract

Latest epidemiological data suggests that 1.5 billion adults worldwide are obese or overweight. Excess weight and adipocyte hypertrophy have long been associated with contributing to low-grade systemic inflammation through elevated adipokine secretion. These increased endocrine signals further augment the metabolic dysfunction related to the presence of obesity. A chronic exposure to obesity mediated inflammation is also suggested to be responsible for progression of renal pathology and eventual end-stage organ failure. In human clinical statistics, these factors indicate a gender disparity, as males demonstrate much faster progression rates of obesity-linked renal disease than females. Therefore, the aim of this thesis was to investigate the role of gender in obesity mediated inflammation in the development of renal disease using a large animal model i.e. sheep.

Post-natal female and male sheep were exposed to a lean or obesogenic environment by restricting physical activity from ≈ 3 months to ≈ 17 months of age. Analysis of body composition and adipose tissue physiology, morphology and deposition identified the development of moderate obesity following chronic exposure to a low physical environment, although no differences were observed with gender. With obesity, both genders demonstrated metabolic irregularities; males showed hyperinsulinaemia and females displayed hypercortisolism. Gene expression analysis identified an up-regulation of inflammatory related genes in perirenal adipose tissue (PAT) and kidney in obese males, a finding not seen in females, although obese females exhibited an up-regulation in glucocorticoid receptor abundance in PAT. Furthermore, the males demonstrated adaptations in renal structure and function with obesity, modifications not observed in females.

The main conclusion of my thesis is that after the development of obesity, males appear much more sensitive to the metabolic, inflammatory and renal adaptations associated with an obese condition. Females displayed a down-regulation of inflammatory genes with obesity which I propose acts as a protective mechanism against the progression of renal disease, perhaps mediated by an immunosuppressive glucocorticoid action in adipose tissue. It is also possible that sex hormones play a role in obesity inflammatory renal disease development, postulated to occur through HPA activation and epigenetic alterations.

Acknowledgements

Firstly, I would like to thank my funding organisations, the British Journal of Anaesthesia and the Royal College of Anaesthetists whose financial support allowed me to complete my studies and PhD in Nottingham. I am also most grateful for the generous travel grants awarded to me by the University of Nottingham and Physiological Society which enabled me to present my work at both national and international scientific conferences.

My sincerest thanks go to my project supervisors Professors Michael Symonds and Ravi Mahajan for providing excellent support, direction and advice throughout my study period. Many thanks go to all the staff and students within the Academic Division of Child Health and Obstetrics and Gynaecology Department at the Queen's Medical Centre, Nottingham who have made my time at the University of Nottingham both enjoyable and productive. In particular I would like to thank Dr Helen Budge for all her help and advice with regards to translating my research within a professional and clinical setting.

Special thanks to Dr Sylvain Sebert who performed all the animal experimentation work including the sheep handling and husbandry, data generation and collection for the animal activity and morphometric measurements, and finally all tissue and plasma sample collection for subsequent laboratory analysis. Also thanks to Catherine Pincott-Allen, Mark Pope and Victoria Wilson for their excellent technical support and expertise which allowed me to conduct my experimental analysis with confidence and proficiency.

Finally, I would like to thank my family and friends for all their support during the three years of my studies, in particular Nicola for her continuous encouragement, financial support and for help with proof-reading my thesis.

Table of contents

Abstract.....	iii
Acknowledgements	iv
Table of contents	v
Declaration	xi
Abbreviations	xii
List of figures	xv
List of tables	xxiii
Chapter 1 - Introduction	1
1.1 Obesity and overweight.....	1
1.1.1 Gender dimorphism in obesity	3
1.1.2 Maternal nutrition in the development of obesity	4
1.2 Adipose tissue.....	7
1.2.1 Adipocyte alterations with obesity	8
1.2.2 Adipose tissue as an endocrine organ	9
1.2.3 Obesity and insulin resistance	12
1.3 Inflammation and the immune response.....	14
1.3.1 Obesity induced inflammation	14
1.3.2 Gender and adipose tissue depot differences in inflammation	18
1.4 The kidney structure and function.....	19
1.4.1 Glomerular filtration rate	23
1.4.2 The kidney as a target organ in an obese condition	24
1.4.3 Pathophysiology of hypertension, metabolic abnormalities and obesity tissue in renal disease	25
1.4.4 The renin-angiotensin-aldosterone system.....	28
1.4.5 Sex differences in obesity mediated renal nephropathy	30
1.4.6 Perirenal adipose tissue	31
1.4.7 Hyperlipidaemia and the progression of renal lipotoxicity	31
1.5 The role of glucocorticoids in obesity and inflammation	33
1.6 Gene expression.....	36
1.7 Genes, cytokines and proteins involved in obesity mediated inflammation and renal nephropathy	38
1.7.1 Glucocorticoids.....	38
1.7.1.1 11 β hydroxysteroid dehydrogenase type 1	38
1.7.1.2 11 β hydroxysteroid dehydrogenase type 2	38
1.7.1.3 Glucocorticoid Receptor	39

1.7.2 Appetite regulators	40
1.7.2.1 Adiponectin and adiponectin receptors.....	40
1.7.2.2 Leptin and leptin receptor	41
1.7.3 Markers of pro-inflammation	42
1.7.3.1 Interferon- γ	42
1.7.3.2 Interleukin-6	42
1.7.3.3 Interleukin-18	43
1.7.3.4 Monocyte chemoattractant protein-1 and C-C motif receptor 2	43
1.7.3.5 Tumour necrosis factor- α	44
1.7.4 Markers of anti-inflammation	45
1.7.4.1 Interleukin-10	45
1.7.4.2 Inducible nitric oxide synthase and nitric oxide	46
1.7.4.3 Peroxisome proliferating activated receptor- γ	47
1.7.5 Lipid sensing receptors	47
1.7.5.1 Cluster of differentiation-14	47
1.7.5.2 Toll-like receptor 4.....	48
1.7.6 Cell adhesion molecules.....	49
1.7.6.1 Intercellular adhesion molecule 1	49
1.7.6.2 Vascular cell adhesion molecule-1	50
1.7.7 Cellular proliferation and apoptosis	50
1.7.7.1 Caspase-3.....	50
1.7.7.2 Proliferating cell nuclear antigen	51
1.7.8 Renal molecules	51
1.7.8.1 Erythropoietin receptor	51
1.7.8.2 Renin	52
1.7.9 Gene, cytokine and protein summary	53
1.8 The sheep as an experimental model for obesity	55
1.9 Main hypothesis and aims.....	57
Chapter 2 - Materials and methods	58
2.1 Procedural & legislative declaration.....	58
2.2 Study design.....	59
2.2.1 Animals, diets and environments	59
2.2.2 Physiological measurements.....	62
2.2.3 Dual x-ray absorptiometry	62
2.2.4 Plasma sampling.....	62
2.2.5 Post mortem analysis	63
2.3 Tissue analysis.....	64

2.4 Ribonucleic acid extraction.....	65
2.4.1 RNA extraction procedure	65
2.4.2 Polymerase chain reaction	66
2.4.3 Reverse transcription PCR.....	68
2.4.4 Quantitative PCR	69
2.4.4.1 Reference genes in Q-PCR.....	72
2.4.5 Development of oligonucleotide primers for Q-PCR.....	74
2.4.6 RT-PCR procedure.....	77
2.4.7 Hot start PCR procedure	78
2.4.8 Agarose gel electrophoresis & DNA extraction	78
2.4.8.1 Agarose gel electrophoresis & DNA extraction procedure.....	79
2.4.9 Q-PCR procedure	80
2.5 Histology	82
2.5.1 Histological tissue processing	82
2.5.2 Haematoxylin and eosin staining.....	83
2.5.2.1 H&E staining procedure	83
2.5.2.2 Glomerular H&E analysis.....	84
2.5.2.3 Perirenal adipocyte H&E analysis.....	84
2.5.3 Masson’s trichrome staining	84
2.5.3.1 Masson’s trichrome staining procedure	85
2.5.4 Immunohistochemistry	85
2.5.4.1 IHC procedure	86
2.6 Plasma metabolite analysis	88
2.6.1 Glucose analysis	88
2.6.2 Non-esterified fatty acids analysis.....	88
2.6.3 Triglyceride analysis.....	89
2.6.4 Plasma metabolite analysis procedure	89
2.6.5 Plasma creatinine analysis	90
2.6.5.1 Plasma creatinine analysis procedure	90
2.6.6 Plasma cytokine analysis	90
2.6.6.1 Plasma cytokine analysis procedure.....	91
2.7 Triglyceride analysis	93
2.7.1 Triglyceride analysis procedure.....	93
2.8 Thiobarbituric acid reactive substances analysis	95
2.8.1 TBARS procedure.....	96
2.8.2 Bicinchoninic acid total protein determination.....	97
2.8.2.1 BCA assay procedure.....	97

2.9 Western blotting.....	98
2.9.1 Western blot protein extraction procedure	98
2.9.2 Western blot polyacrylamide gel electrophoresis procedure	99
2.9.3 Western blot semi-dry blotting procedure	100
2.9.4 Western blot protein detection procedure.....	100
2.10 Statistical analysis	102
Chapter 3 – The effect of gender and obesity on systemic metabolism and adipose tissue physiology	104
3.1 Introduction and aims	104
3.1.1 Hypothesis.....	104
3.2 Materials and methods	105
3.3 The ovine model of obesity and maternal nutrition.....	106
3.4 Results.....	107
3.4.1 The effects of an obesogenic environment and gender and their contribution to body weight and adipose tissue deposition.....	107
3.4.1.1 The effect of an obesogenic environment and gender on perirenal adipose tissue and adipocyte development.....	112
3.4.2 The effect of increased adiposity on plasma hormones and metabolites	116
3.4.2.1 The effect of increased adiposity on triglyceride accumulation in muscle.....	128
3.5 Discussion	130
3.5.1 An obesogenic environment and obesity development	130
3.5.2 Changes in adipose tissue deposition, location and physiology.....	132
3.5.3 Metabolic adaptations with obesity and gender	134
3.5.4 Lipid deposition, peroxidation and lipotoxicity with gender and obesity	137
3.5.5 Conclusion and summary.....	138
Chapter 4 – The effects of gender and obesity on the perirenal adipose tissue inflammatory genotype	140
4.1 Introduction and aims	140
4.1.1 Hypothesis.....	140
4.2 Materials and methods	140
4.3 Results.....	141
4.3.1 The effect of moderate obesity and gender on the metabolic genotype in perirenal adipose tissue.....	141
4.3.2 The effect of moderate obesity and gender on the glucocorticoid genotype in perirenal adipose tissue.....	142

4.3.3 The effect of moderate obesity and gender on the inflammatory genotype in perirenal adipose tissue.....	144
4.4 Discussion	147
4.4.1 Metabolic gene expression of PAT in response to moderate obesity	147
4.4.2 Glucocorticoid and inflammatory gene expression of PAT in response to moderate obesity	149
4.4.3 Conclusion and summary.....	151
Chapter 5 – The effects of gender and obesity on renal physiology, function and inflammation.....	153
5.1 Introduction and aims	153
5.1.1 Hypothesis.....	153
5.2 Materials and methods	154
5.3 Results.....	154
5.3.1 The effect of moderate obesity and gender on renal morphology, physiology and function.	154
5.3.1.1 Glomerular physiology	155
5.3.1.2 Haemodynamic parameters.....	158
5.3.1.3 Glomerular cellular proliferation and apoptosis	158
5.3.1.4 Renal triglyceride accumulation and oxidative stress	161
5.3.1.5 Renal collagen deposition.....	162
5.3.1.6 Plasma creatinine and renal function	164
5.3.2 The effect of moderate obesity and gender on the renal inflammatory genotype.	167
5.3.2.1 Glucocorticoid renal gene expression	167
5.3.2.2 Pro-inflammatory renal cytokine expression	168
5.3.2.3 Anti-inflammatory renal gene expression	171
5.3.2.4 Lipid sensing receptor renal gene expression	171
5.3.2.5 Cell adhesion molecule renal gene expression.....	173
5.3.2.6 Renal molecule gene expression	173
5.3.3 The effect of moderate obesity and gender on inflammatory protein expression	174
5.3.3.1 Renal TLR4 protein expression.....	174
5.3.3.2 Systemic IL-6 and TNF- α protein concentrations	176
5.4 Discussion	177
5.4.1 Alterations in renal and glomerular physiology and function with moderate obesity	177
5.4.2 Changes in renal inflammatory gene transcription.....	181
5.4.3 Development of renal lipid deposition	184

5.4.4 Conclusions and summary	185
Chapter 6 – Conclusion	187
6.1 General aims	187
6.1.1 Development of moderate obesity.....	187
6.1.2 Gender disparity in obesity mediated inflammation	188
6.1.3 Summary	188
6.2 Study limitations	191
6.2.1 Sheep model of obesity	191
6.2.2 Maternal nutritional intervention.....	191
6.2.3 Histological analysis	192
6.2.4 Gene expression	192
6.2.5 Protein expression	192
6.3 Future work and perspectives	193
6.3.1 Physiology and inflammatory profile of other adipose depots.....	193
6.3.2 Epigenetic factors	193
6.3.3 Sex hormone analysis	193
6.3.4 Original project proposal.....	194
6.4 Final remarks.....	194
References.....	195
Appendices	218
Appendix A – Abstracts, original presentation and conferences attended	218
Appendix B – Details of suppliers	223

Declaration

The work in this thesis was performed within the Academic Child Health Division, School of Clinical Sciences, University of Nottingham between October 2008 and September 2011.

This thesis illustrates my own work, completed under the supervision of Professor Michael Symonds and Professor Ravi Mahajan. This report is an accurate representation of the work performed and no other study reproducing this work, to my knowledge, has been carried out within the University of Nottingham.

Ian Bloor

September 2011

Abbreviations

11 β HSD – 11 beta hydroxysteroid dehydrogenase
A – Fed to appetite
AAP – 4-aminoantipyrine
ACE – Angiotension converting enzyme
ACTB – Beta-actin
ACTH – Adrenocorticotropic hormone
ADP – Adenosine diphosphate
ANOVA – Analysis of variance
APS – Ammonium persulphate
ATP – Adenosine triphosphate
ATR – Angiotensin receptor
AUC – Area under the curve
BCA – Bicinchoninic Acid
BHT – Butylated hydrotoluene
BMI – Body mass index
BSA – Bovine serum albumin
CCD – Charge coupled device
CCR2 – Chemokine (C-C motif) receptor 2
CD14 – Cluster of differentiation 14
cdNA – Complimentary deoxyribonucleic acid
Cl⁻ – Chloride ion
CNS – Central nervous system
COSHH – Control of substances hazardous to health
CRF – Corticotropin releasing factor
CRP – C reactive protein
CVD – Cardiovascular disease
DAB – 3,3 diaminobenzidine
DMSO – Dimethyl sulfoxide
DNA – Deoxyribonucleic acid
dNTP – Deoxyribonucleotide
DTT - Dithiothreitol
DXA – Dual x-ray absorptiometry
EARNEST – Early nutrition programming project
EDTA – Ethylenediaminetetraacetic acid
eGFR – Estimated glomerular filtration rate
ELISA – Enzyme linked immunosorbent assay
eNOS – Endothelial nitric oxide synthase
EPO - Erythropoietin
EPOR – Erythropoietin receptor
ER – Endoplasmic reticulum
ESRD – End stage renal disease
FADD – Fas associated with death domain
FSGS – Focal segmental glomerulosclerosis
GFR – Glomerular filtration rate
GLUT4 – Glucose transporter type 4
GR – Glucocorticoid receptor

GTT – Glucose tolerance test
H₂O – Water
H₂O₂ – Hydrogen peroxide
H&E – Haematoxylin and eosin
HCl – Hydrochloric acid
HCO₃⁻ – Bicarbonate ion
HIER – Heat induced epitope retrieval
HPA – Hypothalamic pituitary adrenal axis
HSE – Health survey of England
ICAM1 – Intercellular adhesion molecule 1
IFN γ – Interferon gamma
IHC – Immunohistochemistry
IL – Interleukin
iNOS – Inducible nitric oxide synthase
IRS1 – Insulin receptor substrate 1
L – Lean environment
LBP – Lipid binding protein
LD – Longissimus dorsi
LF – Lean females
LM – Lean males
LPS – Lipopolysaccharide
MCP1 – Monocyte chemoattractant protein 1
MDA – Malondialdehyde
MHC – Major histocompatibility complex
MIF – Macrophage migration factor
mRNA – Messenger ribonucleic acid
MyD88 – Myeloid differentiation factor 88
N – Nutrient restriction
Na⁺ – Sodium ion
NADPH – Nicotinamide adenine dinucleotide phosphate
NCBI – National centre for biotechnology information
NEFA – Non esterified fatty acid
NF κ B – Nuclear factor kappa-light-chain-enhancer of activated B cells
NICE – National institute of clinical excellence
NO – Nitric oxide
NS – Not significant
O – Obesogenic environment
O₂ – Oxygen
O₂⁻ – Superoxide anion
OF – Obese females
OM – Obese males
ONOO⁻ – Oxidising peroxynitrite anion
PAT – Perirenal adipose tissue
PBS – Phosphate buffered saline
PCNA – Proliferating cell nuclear antigen
PCR – Polymerase chain reaction
PET – Positive emitting topography
PMA – Polymolybdic acid

POMC – Proopiomelanocortin
PPAR γ – Peroxisome proliferator activated receptor gamma
PVDF – Polyvinylidene fluoride
QPCR – Quantitative polymerase chain reaction
r18s – Ribosomal 18s
RAAS – Renin angiotensin aldosterone system
RIP – Receptor interacting protein
RNA – Ribonucleic acid
ROS – Reactive oxidative species
RPL19 – L19 ribosomal protein
RPO – Large ribosomal protein
RTPCR – Reverse transcription polymerase chain reaction
S – Significant
SDS – Sodium dodecyl sulphate
SODD – Silencer of death domain
TAE – Tris-acetate-EDTA
TBA – Thiobarbituric acid
TBARS – Thiobarbituric acid reactive substances
TEMED – N,N,N,N,Tetramethylethylenediamine
TOOS – N-ethyl-N(2hydroxy-3-sulphopropyl)m-toluidine
TLR4 – Toll like receptor 4
TNF α – Tumour necrosis factor alpha
TNFR $_1$ – Tumour necrosis factor receptor 1
TRADD – TNF receptor associated death domain
Tris – *Tris*(hydroxymethyl)aminomethane
tRNA – Transfer ribonucleic acid
TTBS – Tris buffered saline with Tween[®]
TZD – Thiazolidinedione
VCAM1 – Vascular cell adhesion molecule 1
VEGF – Vascular endothelial growth factor
WHO – World health organisation
YWHAZ – Tyrosine 3-monooxygenase/tryptophan 5-monooxygenase activation protein

List of figures

Figure 1.1: <i>Body mass index calculation</i>	1
Figure 1.2: <i>Summary of Hales and Barker 'Thrifty Phenotype' hypothesis⁸</i>	5
Figure 1.3: <i>Microscopic sections of brown adipose tissue (A) and white adipose tissue (B)</i>	7
Figure 1.4: <i>Insulin mediated glucose uptake via binding of insulin to insulin receptor which initiates signal transduction and glucose transport in to cells through GLUT4 action⁵²</i>	13
Figure 1.5: <i>Summary diagram of the mechanisms involved in obesity induced inflammation</i>	17
Figure 1.6: <i>A – Cross section of kidney, depicting cortical and medullary regions of the organ. Striated regions show pyramidal papillae. B – A nephron; the basic functional filtration unit, which performs majority of organ functions. Renal tubule portion of nephron located within medullary region. C – A detailed image of a nephron. The Bowman's capsule is a double walled capsule containing the glomerular capillary tuft (glomerulus), these two structures constitute the renal corpuscle. The majority are located in the cortical region, with juxtamedullary corpuscles being the exception^{74,75,76,77,78}</i>	20
Figure 1.7: <i>A cross section of a renal corpuscle. The vascular poles of the glomerulus are located at the openings of the proximal convoluted tubule and the efferent and afferent arterioles. The capillary tuft consists of endothelial cells, covering podocytes and filtration slits. The juxtaglomerular apparatus comprises of the mesangial matrix and macula densa^{77,79}</i>	21
Figure 1.8: <i>Cockcroft-Gault creatinine clearance estimation formula used to calculate GFR in human adults⁸⁸</i>	23
Figure 1.9: <i>Interactive relationship towards chronic kidney disease by visceral obesity, hypertension and metabolic abnormalities⁹²</i>	25
Figure 1.10: <i>Microscopic histological kidney sections showing glomerular apparatus. Image A shows a healthy glomerulus with an open and complete capillary tuft and open Bowman's space. Image B shows a thickening and scarring of the capillary tuft and a closed Bowman's space, an indication of glomerulosclerosis⁹⁷</i>	26
Figure 1.11: <i>Summary of mechanisms involved in obesity mediated kidney function impairment, showing hypertension and metabolic abnormality pathways¹⁰⁴</i>	28
Figure 1.12: <i>Summary diagram of the renin-angiotension-aldosterone system; a decrease in blood pressure is sensed by the juxtaglomerular apparatus resulting in an up-regulation of renin. Renin acts on circulating angiotensinogen to form inactive angiotensin I, converted to active angiotensin II by angiotensin converting enzyme (ACE). Angiotensin II acts to both increase arterial blood pressure and activates aldosterone synthesis in the adrenal cortex. Aldosterone increases salt retention in the renal tubules resulting in additional arterial blood pressure increase¹⁰⁹</i>	29

Figure 1.13: Summary of the hypothalamus-pituitary-adrenal (HPA) axis. A stress signal activates the hypothalamus which synthesizes corticotropin releasing factor (CRF), in turn stimulating the formation of proopiomelanocortin (POMC) and adrenocorticotrophic hormone (ACTH). ACTH results in glucocorticoid (cortisol) production in the adrenal cortex which inhibits immune cell and downstream cytokine synthesis. In obesity, the stress signal is elevated leading to additional immune suppression and potential cortisol dysfunction. Adapted from Slominski et al¹⁴⁵. 35

Figure 1.14: Summary of protein synthesis via gene transcription and translation. RNA polymerase converts nuclear DNA strand to precursor mRNA which is then converted to mature mRNA by spliceosome proteins. After transport of mRNA to cytoplasm, translation via ribosomal tRNA anti-codons occurs forming an amino acid chain and eventual protein^{55,150}. 37

Figure 1.15: Enzymatic reactions catalysed by 11 β hydroxysteroid dehydrogenase types 1 and 2 (11 β HSD1 and 2). 11 β HSD1 converts inactive cortisone to active cortisol by reduction of ketone to hydroxyl group via NADPH, conversely 11 β HSD2 catalyses the opposite reaction via NAD⁺. The human and rodent forms of the glucocorticoid molecules are represented by 1-2a and 1-2b respectively¹⁵². 39

Figure 1.16: TNF trimer binding to TNF-R1 resulting in recruitment of signaling proteins into the receptor complex, which can then lead to either apoptotic or proliferative pathways¹⁸³. 45

Figure 1.17: Summary of cellular membrane bound toll-like receptor 4 (TLR4) and cluster of differentiation-14 (CD14) lipopolysaccharide (LPS) activation cluster pathway. Lipid binding protein (LBP) presents LPS or lipid component of free fatty acid to receptor stimulating nuclear transcription factor NF- κ B. Activation of TLR4 pathway results in up-regulation of pro-inflammatory cytokines and stimulation of immune response²⁰⁵. 49

Figure 1.18: Regulation of erythropoiesis by negative feedback loop mechanism. Erythropoietin (EPO) is produced by the kidney resulting in increased circulating EPO in response to detection of abnormal oxygen tension²¹⁶. 52

Figure 1.19: Summary of mechanism pathways involved in obesity activated inflammation and subsequent renal nephropathy¹¹³⁻²⁰⁴. 54

Figure 2.1: Initial experimental animal groups: N = nutrient restricted (60% of normal energy requirements), A = fed to appetite (150% of normal energy requirements), L = lean environment, O = obesogenic environment, and breakdown of groups into gender. Four animals between the NL and NO groups expired during the experimental procedure. 61

Figure 2.2: Final experimental animal groups: LF = lean females, OF = obese females, LM = lean males and OM = obese males. Four female animals expired during the experimental procedure. 61

Figure 2.3: Basic theory of polymerase chain reaction. Template DNA is amplified exponentially in an enzymatic reaction of temperature controlled cycles by complimentary oligonucleotide primers. 67

Figure 2.4: Diagram of reverse transcription polymerase chain reaction. A random primer binds to single stranded mRNA and sequence is elongated by a transcriptase enzyme to create cDNA. Template of double stranded cDNA is then amplified by classic PCR. 69

Figure 2.5: Typical 'sigmoidal' curves in Q-PCR. Fluorescent signal crosses threshold and increases exponentially until plateau from expenditure of reagents or cycle number. Red lines represent external standards, green are unknown samples and blue represent negative controls. 70

Figure 2.6: Standard curve from Q-PCR. Cycle number at cycle threshold is plotted against logarithm of known dilution series to produce linearised graph of exponential PCR reaction. Correlation coefficient (R^2) and reaction efficiency (E) are then calculated. 71

Figure 2.7: Typical melt curve from Q-PCR. The single peak indicates specificity of product amplified. 72

Figure 2.8: Comparison of three genes r18s, YWHAZ and ACTB. Crossing threshold of each gene was determined against 32 samples to validate use as mRNA reference gene. 73

Figure 2.9: Graphical output from geNorm software in analysis of four reference genes. A lower M value represents a higher stability. A combination of RPL19 and RPO were determined to have the highest stability of the reference genes analysed, and were used to calculate PAT sample gene expression. 74

Figure 2.10: Antibody action in direct and indirect immunostaining method. Direct IHC uses a specific primary antibody conjugate to bind to target antigen, producing a signal for measurement, e.g. colour development. Indirect IHC uses a secondary antibody conjugate to bind to the primary antibody to form an antigen-primary-secondary antibody complex to produce the signal, an increased specificity method for antigen detection²⁶³. 86

Figure 2.11: Principle enzymatic reaction involved in glucose analysis reaction^{266,267}. 88

Figure 2.12: Principle enzymatic reaction involved in NEFA analysis reaction^{268,269}. ... 88

Figure 2.13: Principle enzymatic chemical reaction involved in triglyceride analysis reaction²⁷⁰. 89

Figure 2.14: Enzymatic reaction involved in plasma creatinine analysis²⁷¹ 90

Figure 2.15: Stages of sandwich ELISA. A: Microplate is coated with capture antibody, and non-specific binding sites blocked with blocking agent. B: Sample containing target antigen introduced to well. C: Primary antibody applied to bind to target antigen. D: Secondary antibody with enzyme conjugate applied to primary antibody complex. Protein complex emits fluorescent signal after addition of chemical reagent. 91

Figure 2.16: Malondialdehyde-thiobarbituric acid adduct formation²⁷⁴ 95

Figure 3.1: Review of experimental animal model used throughout my thesis: LF = lean female, OF = obese female, LM = lean male and OM = obese male sheep. Four female animals expired during the experimental procedure.105

Figure 3.2: Area under curve (AUC) of mean activity per 24 hour period of lean female (LF; n=6), obese female (OF; n=8), lean male (LM; n=10) and obese male (OM; n=9) sheep. Values are mean \pm SEM. Statistical difference is denoted by *** = $p < 0.001$ (ANOVA).108

Figure 3.3: Ratio of energy intake to physical activity of lean female (LF; n=6), obese female (OF; n=8), lean male (LM; n=10) and obese male (OM; n=9) sheep. Values are mean \pm SEM. Statistical difference is denoted by *** = $p < 0.001$ (ANOVA).109

Figure 3.4: Representative microscopic slides of haematoxylin and eosin stained perirenal adipose tissue (PAT) of lean female (A), obese female (B), lean male (C) and obese male (D) sheep. Adipocyte membranes (pink stained boundaries marked by arrow E) in obese groups are enlarged and more polygonal in shape, thus contain more lipid area (white non-stained region; arrow F). Blue stained nuclei in obese samples appear pushed to periphery of adipocyte membrane (arrow G). Slides are displayed at 20x magnification.112

Figure 3.5: Adipocyte perimeter (μm) of perirenal adipocytes of lean female (LF; n=7), obese female (OF; n=8), lean male (LM; n=10) and obese male (OM; n=9) sheep. Values are mean \pm SEM. Statistical difference is denoted by *** = $p < 0.001$ (ANOVA).113

Figure 3.6: Adipocyte area (μm^2) of perirenal adipocytes of lean female (LF; n=7), obese female (OF; n=8), lean male (LM; n=10) and obese male (OM; n=9) sheep. Values are mean \pm SEM. Statistical difference is denoted by *** = $p < 0.001$ (ANOVA).113

Figure 3.7: Relationship between PAT mass (g) and perirenal adipocyte area (μm^2) of total sheep (n=34). Correlation analysis showed a statistical significance where $p < 0.0001$ and $r^2 = 0.85$ (Pearson's correlation coefficient).114

Figure 3.8: Frequency distribution (%) of perirenal adipocyte area for lean female (LF; n=311) and lean male (LM; n=465) sheep. Variance of distribution between groups by F-test showed significance, where $p = 0.0002$115

Figure 3.9: Frequency distribution (%) of perirenal adipocyte area for obese female (OF; n=242) and obese male (OM; n=301) sheep. Variance of distribution between groups showed no statistical significance.115

Figure 3.10: GTT plasma insulin baseline (ng/ml) of lean female (LF; n=7), obese female (OF; n=6), lean male (LM; n=10) and obese male (OM; n=7) sheep. Values are mean \pm SEM. Statistical difference is denoted by ** = $p < 0.005$ (Kruskal-Wallis).116

Figure 3.11: GTT plasma insulin time course measurements of lean female (LF; n=7) and obese female (OF; n=6) sheep. Values are mean \pm SEM. Statistical difference is denoted by ** = $p < 0.005$ between LF and OF at time point 20m; *** = $p < 0.001$ between LF and OF at time point 10m (Two-way ANOVA with repeated measures). 117

Figure 3.12: GTT plasma insulin time course measurements of lean male (LM; n=10) and obese male (OM; n=7) sheep. Values are mean \pm SEM.118

Figure 3.13: GTT plasma insulin AUC (ng/ml) of lean female (LF; n=7), obese female (OF; n=6), lean male (LM; n=10) and obese male (OM; n=7) sheep. Values are mean \pm SEM. Statistical difference is denoted by * = $p < 0.05$ (Kruskal-Wallis).118

Figure 3.14: Relationship between total fat mass (g) and plasma insulin AUC (ng/ml) of female (n=12) sheep. Correlation analysis showed no statistical significance where $p = 0.16$ and $r^2 = 0.21$ (Pearson's correlation coefficient).119

Figure 3.15: Relationship between total fat mass (g) and plasma insulin AUC (ng/ml) of male (n=17) sheep. Correlation analysis showed statistical significance where $p = 0.003$ and $r^2 = 0.46$ (Pearson's correlation coefficient).119

Figure 3.16: Baseline plasma leptin (ng/ml) of lean female (LF; n=7), obese female (OF; n=9), lean male (LM; n=11) and obese male (OM; n=9) sheep. Values are mean \pm SEM.120

Figure 3.17: Plasma leptin time course measurements after feeding for lean female (LF; n=7) and obese female (OF; n=9) sheep. Values are mean ± SEM. Statistical differences are denoted by * = p<0.05 between LF-OF at time point 8h; *** = p<0.001 between LF-OF at time point 24h (Two-way ANOVA with repeated measures).121

Figure 3.18: Plasma leptin time course measurements after feeding for lean male (LM; n=11) and obese male (OM; n=9) sheep. Values are mean ± SEM. Statistical differences are denoted by ** = p<0.01 between LM-OM at time point 4h, *** = p<0.001 between LM-OM at time point 8h and 24h (Two-way ANOVA with repeated measures).121

Figure 3.19: Plasma leptin AUC (ng/ml) of lean female (LF; n=7), obese female (OF; n=9), lean male (LM; n=11) and obese male (OM; n=9) sheep. Values are mean ± SEM. Statistical differences are denoted by ** = p<0.005; *** = p<0.001 (ANOVA).122

Figure 3.20: Relationship between total fat mass (g) and plasma leptin AUC (ng/ml) of total sheep (n=36). Correlation analysis showed a statistical significance where p<0.0001 and r² = 0.64 (Pearson's correlation coefficient).122

Figure 3.21: Relationship between GTT plasma insulin AUC (ng/ml) and plasma leptin AUC (ng/ml) of total sheep (n=30). Correlation analysis showed no significant difference where p=0.02 and r² = 0.18 (Pearson's correlation coefficient).123

Figure 3.22: Baseline plasma cortisol (nmol/l) of lean female (LF; n=7), obese female (OF; n=9), lean male (LM; n=11) and obese male (OM; n=9) sheep. Values are mean ± SEM. Statistical difference is denoted by ** = p<0.005 (ANOVA).123

Figure 3.23: Plasma cortisol time course measurements after feeding for lean female (LF; n=7) and obese female (OF; n=9) sheep. Values are mean ± SEM. Statistical differences are denoted by * = p<0.05 between LF-OF at time point 0h, 8h and 24h; ** = p<0.01 between LF-OF at time point 0h and 4h (Two-way ANOVA with repeated measures).124

Figure 3.24: Plasma cortisol time course measurements after feeding for lean male (LF; n=11) and obese male (OF; n=9) sheep. Values are mean ± SEM.125

Figure 3.25: Plasma cortisol AUC (nmol/l) of lean female (LF; n=7), obese female (OF; n=9), lean male (LM; n=11) and obese male (OM; n=9) sheep. Values are mean ± SEM. Statistical difference is denoted by ** = p<0.005 (ANOVA).125

Figure 3.26: Relationship between omental + PAT mass (g) and plasma cortisol AUC (nmol/l) of female sheep (n=16). Correlation analysis showed a statistical significance where p=0.0003 and r² = 0.63 (Pearson's correlation coefficient).126

Figure 3.27: Relationship between omental + PAT mass (g) and plasma cortisol AUC (nmol/l) of male sheep (n=20). Correlation analysis showed no statistical significance where p=0.25 and r² = 0.07 (Pearson's correlation coefficient).126

Figure 3.28: Triglyceride deposition in mg per g longissimus dorsi (LD) muscle of lean female (LF; n=7), obese female (OF; n=9), lean male (LM; n=11) and obese male (OM; n=9) sheep. Values are mean ± SEM. Statistical difference is denoted by * = p<0.05 (Kruskal-Wallis).128

Figure 3.29: Relationship between GTT plasma insulin AUC (ng/ml) and muscle triglycerides (mg/g) of total sheep (n=30). Correlation analysis showed no statistical significance where p=0.20 and r² = 0.06 (Pearson's correlation coefficient).129

Figure 3.30: Summary of findings in effect of gender and obesity on systemic metabolism and adipose tissue physiology. HPA – Hypothalamic pituitary adrenal axis.139

Figure 4.1: Glucocorticoid receptor (GR) GeNorm mRNA expression values of lean female (LF; n=7), obese female (OF; n=9), lean male (LM; n=11) and obese male (OM; n=8) sheep in PAT. Values are mean \pm SEM. Statistical difference is denoted by * = $p < 0.05$ (ANOVA).142

Figure 4.2: 11 β -hydroxysteroid dehydrogenase type 1 (11 β HSD1) GeNorm mRNA expression values of lean female (LF; n=7), obese female (OF; n=9), lean male (LM; n=11) and obese male (OM; n=8) sheep in PAT. Values are mean \pm SEM. Statistical difference is denoted by * = $p < 0.05$ (Kruskal-Wallis).143

Figure 4.3: 11 β -hydroxysteroid dehydrogenase type 2 (11 β HSD2) GeNorm mRNA expression values of lean female (LF; n=7), obese female (OF; n=9), lean male (LM; n=11) and obese male (OM; n=8) sheep in PAT. Values are mean \pm SEM. Statistical difference is denoted by * = $p < 0.05$ (Kruskal-Wallis).144

Figure 4.4: Interleukin-6 (IL-6) GeNorm mRNA expression values of lean female (LF; n=7), obese female (OF; n=9), lean male (LM; n=11) and obese male (OM; n=8) sheep in PAT. Values are mean \pm SEM. Statistical difference is denoted by * = $p < 0.05$ (Kruskal-Wallis).145

Figure 4.5: Monocyte chemoattractant protein-1 (MCP-1) GeNorm mRNA expression values of lean female (LF; n=7), obese female (OF; n=9), lean male (LM; n=11) and obese male (OM; n=8) sheep in PAT. Values are mean \pm SEM. Statistical difference is denoted by * = $p < 0.05$ (Kruskal-Wallis).145

Figure 4.6: Toll-like receptor 4 (TLR4) GeNorm mRNA expression values of lean female (LF; n=7), obese female (OF; n=9), lean male (LM; n=11) and obese male (OM; n=8) sheep in PAT. Values are mean \pm SEM. Statistical difference is denoted by * = $p < 0.05$ (ANOVA).146

Figure 4.7: Summary of findings in effect of gender and obesity on perirenal adipose tissue (PAT) inflammatory genotype. 11 β HSD1/2 – 11beta hydroxysteroid dehydrogenase type-1/2; GR- α – Glucocorticoid receptor- α ; HPA – Hypothalamic pituitary adrenal axis.152

Figure 5.1: Representative haematoxylin & eosin (H&E) 5 μ m stained microscopic sections at 20x magnification; A – lean female, B – obese female, C – lean male and D – obese male sheep. The pink coloured stain represents connective tissue, red blood cells and non-nucleated cellular material shown by arrow E. Blue/black staining represents cellular nuclei (arrow F). The circular structures are the glomeruli (arrow G). In area and cell count analysis \approx 40 glomeruli were analysed for each animal.156

Figure 5.2: Glomerular area mean average (μ m²) of lean female (LF; n=7), obese female (OF; n=9), lean male (LM; n=9) and obese male (OM; n=9) sheep. Values are mean \pm SEM. Statistical difference is denoted by ** = $p < 0.005$ (ANOVA).156

Figure 5.3: Glomerular nucleated cell number mean average of lean female (LF; n=7), obese female (OF; n=9), lean male (LM; n=9) and obese male (OM; n=9) sheep. Values are mean \pm SEM. Statistical difference is denoted by * = $p < 0.05$; ** = $p < 0.005$ (Kruskal-Wallis).157

Figure 5.4: Relationship between glomerular area (μ m²) and glomerular nucleated cell number of total sheep (n=34). Correlation analysis showed a statistical significance where $p < 0.0001$ and $r^2 = 0.82$ (Pearson's correlation coefficient).157

Figure 5.5: Representative capase-3 (1:50 primary antibody dilution) immunohistochemistry 5µm stained microscopic sections at 10x magnification; A – lean female, B – obese female, C – lean male and D – obese male sheep. The brown coloured stain represents positively stained nuclei shown by arrow E. Blue staining represents negatively stained nuclei (arrow F).159

Figure 5.6: Representative proliferating cell nuclear antigen (PCNA, 1:4000 primary antibody dilution) immunohistochemistry 5µm stained microscopic sections at 10x magnification; A – lean female, B – obese female, C – lean male and D – obese male sheep. The brown coloured stain represents positively stained nuclei shown by arrow E. Blue staining represents negatively stained nuclei (arrow F).160

Figure 5.7: Triglyceride deposition in mg per g kidney of lean female (LF; n=7), obese female (OF; n=9), lean male (LM; n=10) and obese male (OM; n=9) sheep. Values are mean ± SEM. Statistical difference is denoted by ** = p<0.005 (ANOVA).161

Figure 5.8: Renal thiobarbituric acid reactive substance (TBARS) measurements of lean female (LF; n=7), obese female (OF; n=9), lean male (LM; n=10) and obese male (OM; n=9) sheep. Values are mean ± SEM.162

Figure 5.9: Representative Masson trichrome staining for collagen 5µm stained microscopic sections at 5x magnification; A – lean female, B – obese female, C – lean male and D – obese male sheep. The red coloured stain represents keratin and connective tissue (arrow G), green colour represents staining of collagen peptides (arrow H) and blue/black staining represents cellular nuclei (arrow J). Images E and F represent over-stained samples, possibly due to increased dehydration during tissue processing.163

Figure 5.10: Plasma creatinine (nmol/µl) of lean female (LF; n=7), obese female (OF; n=9), lean male (LM; n=11) and obese male (OM; n=9) sheep. Values are mean ± SEM. Statistical difference is denoted by ** = p<0.005 (ANOVA).164

Figure 5.11: Plasma creatinine corrected for lean mass (nmol/µl/kg) of lean female (LF; n=7), obese female (OF; n=9), lean male (LM; n=11) and obese male (OM; n=9) sheep. Values are mean ± SEM. Statistical difference is denoted by * = p<0.05 (ANOVA).165

Figure 5.12: Relationship between lean mass (kg) and plasma creatinine corrected for lean mass (nmol/µl/kg) of female sheep (n=15). Correlation analysis showed no statistical significance where p=0.82 and r² = 0.004 (Pearson’s correlation coefficient).166

Figure 5.13: Relationship between lean mass (kg) and plasma creatinine corrected for lean mass (nmol/µl/kg) of male sheep (n=15). Correlation analysis showed a statistical significance where p=0.0004 and r² = 0.51 (Pearson’s correlation coefficient).166

Figure 5.14: 11β-hydroxysteroid dehydrogenase type 2 (11βHSD2) 2^{-(ΔCt)} mRNA expression values of lean female (LF; n=7), obese female (OF; n=9), lean male (LM; n=10) and obese male (OM; n=9) sheep in renal tissue. Values are mean ± SEM. Statistical difference is denoted by * = p<0.05; ** = p<0.005 (Kruskal-Wallis).167

Figure 5.15: Glucocorticoid receptor (GR) 2^{-(ΔCt)} mRNA expression values of lean female (LF; n=7), obese female (OF; n=9), lean male (LM; n=10) and obese male (OM; n=9) sheep in renal tissue. Values are mean ± SEM. Statistical difference is denoted by *** = p<0.001 (ANOVA).168

Figure 5.16: Interferon- γ ($IFN-\gamma$) $2^{-\Delta Ct}$ mRNA expression values of lean female (LF; n=7), obese female (OF; n=9), lean male (LM; n=10) and obese male (OM; n=9) sheep in renal tissue. Values are mean \pm SEM. Statistical difference is denoted by ** = $p < 0.005$ (ANOVA).169

Figure 5.17: Tumour necrosis factor- α (TNF- α) $2^{-\Delta Ct}$ mRNA expression values of lean female (LF; n=7), obese female (OF; n=9), lean male (LM; n=10) and obese male (OM; n=9) sheep in renal tissue. Values are mean \pm SEM. Statistical difference is denoted by * = $p < 0.05$ (Kruskal-Wallis).170

Figure 5.18: Cluster of differentiation 14 (CD14) $2^{-\Delta Ct}$ mRNA expression values of lean female (LF; n=7), obese female (OF; n=9), lean male (LM; n=10) and obese male (OM; n=9) sheep in renal tissue. Values are mean \pm SEM. Statistical difference is denoted by ** = $p < 0.005$ (ANOVA).172

Figure 5.19: Toll-like receptor 4 (TLR4) $2^{-\Delta Ct}$ mRNA expression values of lean female (LF; n=7), obese female (OF; n=9), lean male (LM; n=10) and obese male (OM; n=9) sheep in renal tissue. Values are mean \pm SEM. Statistical difference is denoted by ** = $p < 0.005$; *** = $p < 0.001$ (ANOVA).172

Figure 5.20: Representative Western blot image for toll-like receptor 4 (TLR4) a 100kDa protein; 1:500 TLR4 mouse primary antibody dilution; 1:2000 rabbit anti-mouse secondary antibody dilution on 20 μ g random protein samples. Arrow A identifies the faint protein band at approximately 100kDa, referenced against protein standard lane identified by arrow B. The main protein band (\approx 50kDa) identified by arrow C is unknown.174

Figure 5.21: Representative Western blot image for toll-like receptor 4 (TLR4) negative control; 1:1000 non-immune mouse serum dilution; 1:2000 rabbit anti-mouse secondary antibody dilution on 20 μ g random protein samples. Faint 100kDa band is still present in negative control identified by arrow A. Protein standard lane identified by arrow B.175

Figure 5.22: Representative toll-like receptor 4 (TLR4) immunohistochemistry 5 μ m stained microscopic sections at 10x magnification; A - 1:100 primary antibody dilution, B - negative control. The brown coloured stain represents positively stained area which appeared to be due to non-specific binding shown by arrow D. Blue staining represents negatively stained nuclei (arrow E).175

Figure 5.23: Summary diagram of male response to obesity and its effect on renal morphology and inflammatory gene expression. None of these renal adaptations were displayed by females in response to obesity. ESRD - End stage renal disease.186

Figure 6.1: Obesity induced inflammatory gene expression and metabolic pathways in PAT and renal tissue exhibited by females in my study.189

Figure 6.2: Obesity induced inflammatory gene expression and metabolic pathways in PAT and renal tissue exhibited by males in my study.190

List of tables

Table 1.1: <i>The international classification of adult underweight, overweight and obesity according to BMI³.</i>	2
Table 1.2: <i>Adipokines secreted by white adipose tissue and their function and effect^{26,48}.</i>	11
Table 1.3: <i>Summary of effects in obesity on inflammatory outcomes in relation to gender and adipose depots.</i>	18
Table 2.1: <i>General parameter guidelines for optimal polymerase chain reaction primer design²³⁸.</i>	68
Table 2.2: <i>Reference gene primer sequences for mRNA quantification.</i>	75
Table 2.3: <i>Inflammatory gene primer sequences for mRNA quantification.</i>	76
Table 2.4: <i>Additional gene primer sequences for mRNA quantification.</i>	77
Table 2.5: <i>Hot start PCR program conditions. Second phase of program repeats for 35 cycles.</i>	78
Table 2.6: <i>QPCR program conditions. * denotes range of optimal temperatures for genes analysed.</i>	81
Table 3.1: <i>Energy intake (MJ/kg/24 hours) throughout post-natal environment intervention of lean female (LF), obese female (OF), lean male (LM) and obese male (OM) sheep. Values are means ± SEM. NS = no significant differences, S = significance where only one of two comparable groups display significance; statistical difference is denoted by ^{ab}, ** = p<0.005 (ANOVA).</i>	107
Table 3.2: <i>Body weight parameter measurements of lean female (LF), obese female (OF), lean male (LM) and obese male (OM) sheep. Values are mean ± SEM. NS = no significant difference, S = significance where only one of two comparable groups display significance; statistical differences are denoted by * = p<0.05; ^{ab}, ** = p<0.005; *** = p<0.001, (ANOVA). Body weight corrected for fat mass, Lean mass and Lean mass:total fat mass ratio analyses treated with Kruskal-Wallis statistical test.</i>	110
Table 3.3: <i>Adipose tissue depot measurements of lean female (LF), obese female (OF), lean male (LM) and obese male (OM) sheep. Values are mean ± SEM. NS = no significant difference, S = significance where only one of two comparable groups display significance; statistical differences are denoted by ^{ab}, * = p<0.05; ** = p<0.005; *** = p<0.001 (ANOVA). Omental (kg) and relative subcutaneous analyses treated with Kruskal-Wallis statistical test.</i>	111
Table 3.4: <i>Plasma metabolite measurements for glucose, non-esterified fatty acids (NEFAs) and triglycerides (mmol/l) of lean female (LF), obese female (OF), lean male (LM) and obese male (OM) sheep. NS = no significant difference (ANOVA). Plasma glucose analysis treated with Kruskal-Wallis statistical test.</i>	127
Table 4.1: <i>Leptin and leptin receptor GeNorm mRNA gene expression values of lean female (LF), obese female (OF), lean male (LM) and obese male (OM) sheep in PAT. Values are mean ± SEM. NS = no significant difference (Kruskal-Wallis).</i>	141

Table 4.2: *Adiponectin and adiponectin receptor GeNorm mRNA gene expression values of lean female (LF), obese female (OF), lean male (LM) and obese male (OM) sheep in PAT. Values are mean ± SEM. NS = no significant difference, S = significance where only one of two comparable groups display significance; statistical difference is denoted by ^{ab} = p<0.005 (Kruskal-Wallis).*.....142

Table 5.1: *Kidney weight (g) and relative kidney weight (g/kg body weight) of lean female (LF), obese female (OF), lean male (LM) and obese male (OM) sheep. Values are mean ± SEM. NS = no significant difference, S = significance where only one of two comparable groups display significance; statistical differences are denoted by ^{ab}, * = p<0.05; ** = p<0.005 (ANOVA). Relative kidney weight analysis treated with Kruskal-Wallis statistical test.*154

Table 5.2: *Heart rate (bpm), systolic, diastolic and mean blood pressure (mmHg) measurements for lean female (LF), obese female (OF), lean male (LM) and obese male (OM) sheep. Values are mean ± SEM. NS = no significant difference (ANOVA).*158

Table 5.3: *Total and glomerular staining % of caspase-3 and proliferating cell nuclear antigen (PCNA) of lean female (LF), obese female (OF), lean male (LM) and obese male (OM) sheep. Values are mean ± SEM. NS = no significant difference, S = significance where only one of two comparable groups display significance; statistical difference is denoted by * = p<0.05 (ANOVA).*.....161

Table 5.4: *Collagen index (arbitrary units) for lean female (LF), obese female (OF), lean male (LM) and obese male (OM) sheep. Values are mean ± SEM. NS = no significant difference (Kruskal-Wallis).*163

Table 5.5: *Interleukin-6 (IL-6) and interleukin-18 (IL-18) 2^{-(ΔCt)} mRNA gene expression values of lean female (LF), obese female (OF), lean male (LM) and obese male (OM) sheep in renal tissue. Values are mean ± SEM. NS = no significant difference, S = significance where only one of two comparable groups display significance; statistical difference is denoted by ^{ab} = p<0.05 (ANOVA). IL-18 analysis treated with Kruskal-Wallis statistical test.*168

Table 5.6: *Chemokine C-C motif receptor 2 (CCR2) and monocyte chemoattractant protein-1 (MCP-1) 2^{-(ΔCt)} mRNA gene expression values of lean female (LF), obese female (OF), lean male (LM) and obese male (OM) sheep in renal tissue. Values are mean ± SEM. NS = no significant difference, S = significance where only one of two comparable groups display significance; statistical differences are denoted by ** = p<0.005; *** = p<0.001 (ANOVA). MCP-1 analysis treated with Kruskal-Wallis statistical test.*.....169

Table 5.7: *Interleukin-10 (IL-10), inducible nitric oxide synthase (iNOS) and peroxisome proliferator activated receptor-γ (PPAR-γ) 2^{-(ΔCt)} mRNA gene expression values of lean female (LF), obese female (OF), lean male (LM) and obese male (OM) sheep in renal tissue. Values are mean ± SEM. NS = no significant difference, S = significance where only one of two comparable groups display significance; statistical difference is denoted by ^{ab} = p<0.05. iNOS analysis treated with ANOVA statistical test.*171

Table 5.8: *Intracellular cell adhesion molecule-1 (ICAM-1) and vascular cell adhesion molecule (VCAM-1) 2^{-(ΔCt)} mRNA gene expression values of lean female (LF), obese female (OF), lean male (LM) and obese male (OM) sheep in renal tissue. Values are mean ± SEM. NS = no significant difference, S = significance where only one of two comparable groups display significance; statistical differences are denoted by ^{ab}, ** = p<0.005 (ANOVA).*.....173

Table 5.9: *EPOR* (erythropoietin receptor) and renin $2^{-(\Delta Ct)}$ mRNA expression values of lean female (LF; n=7), obese female (OF; n=9), lean male (LM; n=10) and obese male (OM; n=9) sheep in renal tissue. Values are mean \pm SEM. Statistical differences are denoted by ** = $p < 0.005$; ^{ab} = $p < 0.001$ (ANOVA). Renin analysis treated with Kruskal-Wallis statistical test.173

Chapter 1 - Introduction

My thesis reports a study of juvenile onset obesity in sheep and the influence of gender on inflammatory responses in the kidney and surrounding perirenal adipose tissue. This chapter will discuss and summarise the contemporary epidemiological and experimental animal research on obesity in relation to gender, the kidney and inflammation, previously published.

1.1 Obesity and overweight

Obesity can be defined as the excessive or abnormal accumulation of fat in adipose tissue, resulting in increased morbidity and mortality. The World Health Organization (WHO) achieves classification of obesity by calculating the Body Mass Index (BMI) of an individual shown in Figure 1.1. BMI is a simple index calculated by dividing an individual's weight (kg) by the square of their height (m²) and, although an approximate method of determining body fat mass, is a widely accepted measurement. As BMI does not distinguish between fat and muscular mass, the National Institute for Clinical Excellence (NICE) recommend the use of BMI in conjunction with waist circumference to estimate adiposity, with measurements of 102cm and 88cm in men and women respectively being classed as raised waist circumferences¹.

$$\text{BMI} = \text{Weight (kg)} / \text{Height (m}^2\text{)}$$

Figure 1.1: *Body mass index calculation*

Table 1.1 (p2) shows the international classification of adult underweight, overweight and obesity according to BMI. For example, an adult who weighed 90kg and measured 1.81 metres, their BMI would equal $90\text{kg}/1.81\text{ m}^2 = 27.47$, which would indicate a pre obese individual according to BMI calculation. Due to the difficulty in estimating fat mass in children aged 5-14, no applied standard definition of obesity currently exists, however the WHO are developing an international growth reference for school-aged children².

Classification	BMI (kg/m ²)	
	Principal cut-off points	Additional cut-off points
Severe Thinness	<16.00	<16.00
Moderate Thinness	16.00 - 16.99	16.00 - 16.99
Mild Thinness	17.00 - 18.49	17.00 - 18.49
Underweight	<18.50	<18.50
Normal Range	18.50 - 24.99	18.50 - 22.99
		23.00 - 24.99
Overweight	≥25.00	≥25.00
Pre-obese	25.00 - 29.99	25.00 - 27.49
		27.50 - 29.99
Obese	≥30.00	≥
Obese class I	30.00 - 34.99	30.00 - 32.49
		32.49 - 34.99
Obese class II	35.00 - 39.99	35.00 - 37.49
		37.49 - 39.99
Obese class III	≥40.00	≥40.00

Table 1.1: *The international classification of adult underweight, overweight and obesity according to BMI³.*

Obesity and overweight have reached epidemic global proportions, affecting both industrialised and developing countries. Latest statistics from the WHO suggest that in 2008 approximately 1.5 billion adults over the age of 20 were overweight, of which 200 million men and 300 million women were classed as obese. These levels are predicted to rise to 2.3 billion, 300 and 400 million respectively by 2015. It is also estimated globally that as many as 43 million children under 5 were overweight in 2010. In 2008, the annual Health Survey for England (HSE) reported that approximately a quarter of all adults in England (24-25%) were obese and 66% of men and 58% of women were overweight⁴. In 2007 31% of boys and 29% girls aged 2-15 were estimated to be obese or overweight, however recent figures suggest that childhood obesity rates may have stabilised⁴. Due to this increasing global prevalence, obesity and its associated comorbidities are now one of the leading preventable causes of mortality worldwide, and it is estimated that obesity and its related conditions cost the UK National Health Service around £4.2 billion a year⁵. Weight gain and obesity are attributed to an increase in the ratio of calorie consumption to calorie expenditure. Research into this imbalance has identified a combination of behavioral, environmental and genetic factors⁶; however the current and predicted incidence of obesity in the UK implies that behavioral and socio-economic factors, i.e. modern sedentary lifestyles and dietary issues, especially in poorer social classes are involved to a greater extent than genetic factors⁴.

It has also been hypothesised that some metabolic adult diseases, for example changes in susceptibility to developing obesity may have early life or foetal origins^{7,8}.

Obesity has been linked to exaggerated morbidity and mortality, and increased risk factors associated with obesity include development of insulin resistance, type 2 diabetes, hypertension, coronary heart disease, stroke, cancer, gallbladder disease, osteoarthritis, asthma and sleep apnea⁹. The World Health Organization classify the presence of central obesity, defined by BMI and waist to hip ratio, as one of the risk criteria for metabolic syndrome alongside diabetes mellitus type II, hyperglycaemia, hypertension, dyslipidaemia, microalbuminuria and chronic low-grade inflammation¹⁰.

1.1.1 Gender dimorphism in obesity

Risk factors associated with obesity depend not only on the amount of accumulated fat tissue, but also on its anatomical distribution. In central obesity which is more prevalent in males, fat tissue tends to be accumulated in the upper body, i.e. increased intra-abdominal and ectopic visceral fat deposits¹¹. Yet in pre-menopausal females, increased subcutaneous fat is accumulated in peripheral and lower body areas, i.e. gluteal and femoral regions¹¹. This gender dimorphism in fat distribution has been highlighted in past research and it is well established that females tend to have a higher percentage of total body adiposity to males. However despite this, BMI matched males are shown to have nearly twice the amount of visceral adipose tissue compared to females¹¹. Research has also identified that fat redistribution occurs in females from aging, particularly during and beyond menopause, where lower body region adiposity changes to central adiposity¹². This lower amount of visceral adiposity in pre-menopausal females is believed to be linked to the lower prevalence of obesity related metabolic conditions or metabolic syndrome, such as hypertension, diabetes, hyperlipidaemia and cardiovascular disease (CVD) than seen in BMI matched males¹³.

This lower prevalence of obesity related morbidities seen in females does however converge with the male population after menopause¹⁴, suggesting an involvement of female sex hormones in adiposity development and possible protection from obesity linked conditions, which will be discussed in subsequent chapters.

Despite this gender dimorphism in fat storage where pre-menopausal females may present a healthier obese metabolic profile than males, obese individuals still have an increased risk of morbidity than the general population¹⁵.

1.1.2 Maternal nutrition in the development of obesity

In 1991, Hales and Barker published the 'Thrifty Phenotype' hypothesis, which proposed that in a poor nutritional foetal environment, metabolic adaptations occur such as an enhanced capacity to store fat through alterations in insulin sensitivity and an adaptive response to optimize the growth of key organs at a detriment to growth of less important organs, including the development of fat⁸. The hypothesis suggested that these adaptations are strategies for survival in similarly poor nutritional post-natal environments, but when exposed to over-nutrition, maternally nutritionally restricted offspring become more at risk to develop metabolic disorders like obesity and diabetes mellitus type II^{7,8}. There is now a considerable amount of scientific evidence to support the hypothesis that inappropriate prenatal or early postnatal nutrition may predispose individuals to developing obesity and linked metabolic conditions in later life^{8,16,17,18}. A diagrammatical representation of the 'Thrifty Phenotype' hypothesis is shown in Figure 1.2, p5.

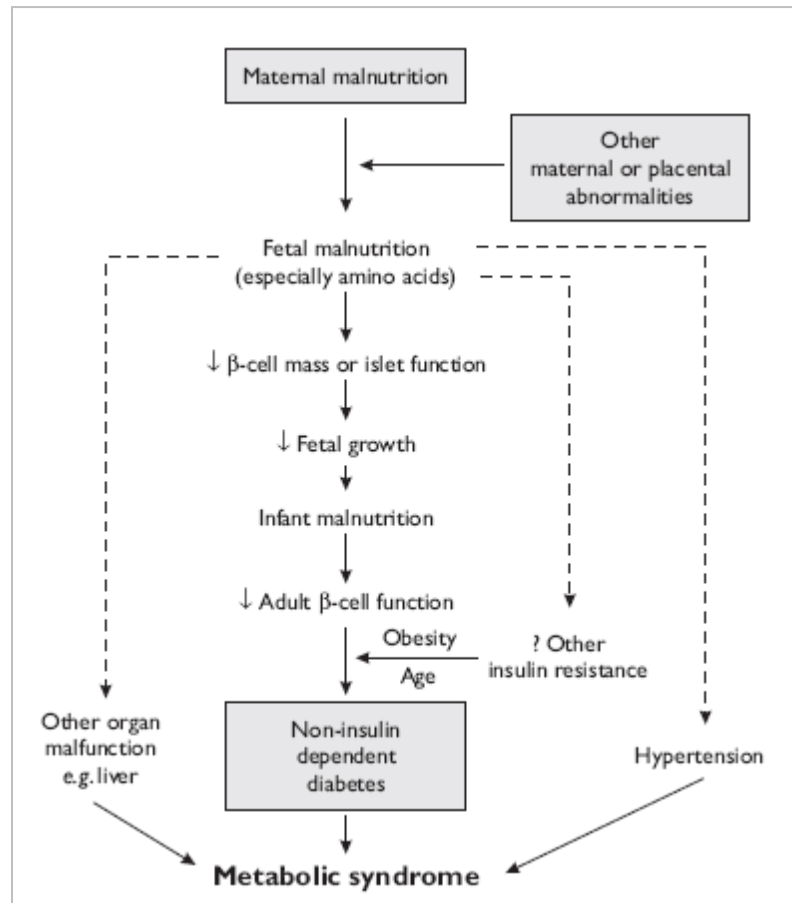


Figure 1.2: Summary of Hales and Barker 'Thrifty Phenotype' hypothesis⁸.

Early work on the 1944-45 'Dutch Famine Birth Cohort' study first highlighted that 19 year old males exposed *in utero* to the Dutch famine showed higher rates of obesity than those conceived before or after the famine period¹⁶. This rate of obesity was higher in offspring exposed to intrauterine undernutrition in early gestation compared to the mid to late gestation and non-exposed males¹⁶. A follow up study of the cohort identified that maternal malnutrition during early gestation was associated with higher rates of obesity in females but not males at 50 years of age¹⁷. Additional studies all based on subjects exposed to the Dutch famine study indicate that exposure to restricted maternal nutrition at any stage of gestation can lead to increased risk of disease later in adult life^{18,19,20}. As the Dutch famine study was a unique opportunity for such research in humans, animal models are now utilised to study suboptimal nutrition at specific stages of gestation in order to elucidate the mechanisms responsible for prenatal nutritional programming. Maternal undernutrition during early to mid gestation in sheep resulted in increased development in adiposity in the offspring at birth²¹.

Studies in rodent models show that exposure to maternal overnutrition and maternal obesity during pregnancy and through lactation is associated with the development of obesity in the offspring^{22, 23}.

An additional rodent study suggested that maternal overnutrition independent of maternal obesity and postnatal diet produced an obese phenotype of male and female offspring²⁴. In both the animal and human models of gestational dietary manipulations, both under and over-nutrition appear to promote the development of obesity in the offspring. Furthermore, foetal programming studies in adult sheep through pre-natal under-nutrition identified an imbalance in glucose-insulin homeostasis in nutritionally restricted animals²⁵. These studies indicate that a suboptimal maternal diet during critical periods of foetal development, impacts on immediate postnatal and later adult health through alterations in adipose tissue development and changes to the metabolic milieu.

1.2 Adipose tissue

Adipose tissue is fibrous connective tissue with a highly organised vasculature mainly composed of fat cells (adipocytes), but also containing a variety of other cells such as endothelial cells, fibroblasts and macrophages²⁶. It serves as both an insulating layer and energy store and is found in a range of subcutaneous and intra-abdominal organ depots around the body. There are two types of adipose tissue; white adipose tissue, and brown adipose tissue. The two different types of adipose tissue differ substantially in structure and function. Brown adipocytes are polygonal in shape, highly vascularised, contain high numbers of mitochondria and contain a number of small lipid inclusions (multilocular). In contrast, white adipocytes contain a single, large central lipid inclusion (unilocular) which flattens the nucleus and pushes it towards the periphery, and have very few mitochondria²⁷, as shown in Figure 1.3.

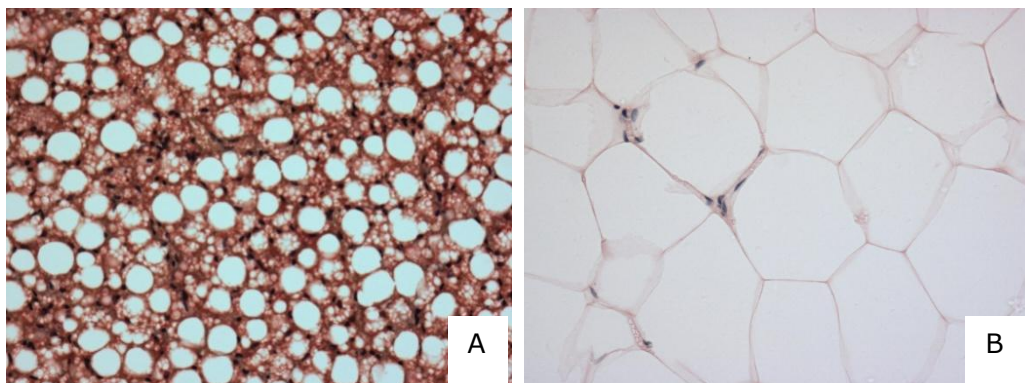


Figure 1.3: *Microscopic sections of brown adipose tissue (A) and white adipose tissue (B).*

Brown adipose tissue produces heat via non-shivering thermogenesis which maintains body temperature in neonates and small mammals²⁸. It was initially suggested that brown adipose tissue present in the body, predominantly located in the internal adipose depots, regresses with age immediately after birth where it is completely converted into white adipose tissue by adulthood²⁹. Recent research has shown that adult humans retain a small amount of brown adipose tissue in the superclavicular region, which was determined by glucose uptake using positron emitting topography (PET) scans³⁰. It is now also recognised that rather than both adipocyte types being derived from the same preadipocyte lineage that BAT maybe derived from skeletal muscle precursors³¹. Although relatively small amounts of brown adipose tissue exist in adults, white adipose tissue's function and action is responsible for the majority of its associated metabolic properties³⁴.

The primary functions of white adipose tissue are passive insulation and energy storage which is implemented through the accumulation and mobilisation of non-esterified fatty acids (NEFAs). It has also been identified as being an important endocrine organ, actively communicating by sending and receiving different types of signals, and as a result playing a central role in lipid and energy metabolism³².

1.2.1 Adipocyte alterations with obesity

Free fatty acids are accumulated in white adipocytes and esterified into triglycerides for storage. Once utilisation of triglycerides for energy is required, they undergo lipolysis and are hydrolysed to glycerol and NEFAs that are transported by the bloodstream to other tissues, mainly muscle and liver³³. However with obesity, white adipose tissue increases storage of intracellular triglyceride stores, causing enlargement of the cell, termed hypertrophy³⁴. Initially it was thought that adipocyte cell number was established during childhood, but it is now understood that the progression of obesity in adults who were not obese during childhood, show hyperplastic adipose tissue development³⁴, which is also demonstrated in some animal models³⁵. This adipocyte differentiation is believed to be induced by prolonged adipocyte hypertrophy during the development of obesity.

Morphological and functional variation occurs between subcutaneous and visceral adipocytes. Subcutaneous adipose tissue is comprised of well organised, tightly packed spherical lobules, whereas intra-abdominal adipose depots appear highly vascularised with disorganised, irregular shaped lobules³⁶. Females have larger subcutaneous adipocytes when compared to omental adipocytes, possibly leading to a lower storage capacity in visceral depots for triglycerides, leading to more rapid lipid saturation, increased lipolysis and possible omental adipocyte cell dysfunction³⁷. In contrast, opposite results were found in another study, which again demonstrated that subcutaneous adipocytes were larger than omental fat cells in females, but subcutaneous adipocytes displayed increased lipolysis compared to omental fat. Although less active, the omental adipocytes displayed higher sensitivity to lipolytic stimuli through antagonism of the β -adrenergic receptor, suggesting omental fatty-acid flux was caused by increased generation of free fatty acids rather than greater lipolysis³⁸.

Evidence suggests that adipocyte hyperplasia rather than hypertrophy occurs in females during fat mass expansion. This observation was reported in gluteal but not visceral adipose tissue depots, although adipocyte hypertrophy was observable in gluteal fat depots when compared to a lean counterpart³⁹. Subcutaneous but not omental fat depots in obese females, also showed a positive correlation in size with total fat mass³⁹.

These results indicate that during subcutaneous adipose tissue expansion in females, adipose tissue mass is developing through adipogenesis, lipolysis and adipocyte hypertrophy. Theoretically allowing for subcutaneous depots in females to store larger amounts lipids, and thus limiting fat accumulation in visceral compartments.

1.2.2 Adipose tissue as an endocrine organ

Adipose tissue secretes a range of proteins, both hormones and cytokines (termed adipokines) that play important functional local and systemic roles in metabolism, immune responses, reproduction and the cardiovascular system⁴⁰. In obesity, hypertrophic adipocytes increase production and secretion of adipokines in circulation, and that adipokine expression correlates to adipocyte size⁴¹. In total, over 50 molecular entities have been identified as being secreted from adipocytes. The entirety of these secretions along with other lipid moieties released by the adipocytes constitutes the secretome⁴². Table 1.2 (p11) shows a summarised table of adipokines secreted by white adipose tissue and their respective functions.

It is thought some of these adipokine secretions signal to induce macrophage recruitment and infiltration in adipose tissue, as macrophage numbers are significantly higher in expanding adipose tissue depots⁴³. The accumulative effect of increased inflammatory adipokine secretion with additional macrophage recruitment and activation is one of the mechanisms proposed to contribute to the chronic low-grade inflammation, associated with obesity.

Early research on excess adipose tissue accumulation discovered that circulating plasma NEFAs are elevated in obese individuals⁴⁴. Excess plasma NEFA concentrations inhibit insulin action on skeletal muscle glucose uptake and suppress hepatic glucose production leading to increased circulating insulin (hyperinsulinaemia) and insulin resistance⁴⁵.

Raised circulating insulin plays a pleiotropic role to promote further adipose storage and inhibiting lipolysis which promotes preadipocyte differentiation and increasing fatty acid synthesis. This results in additional adipose tissue expanse and reinforces insulin resistance, leading to development of subsequently linked conditions, such as diabetes mellitus type II, hypertension and CVD. In humans, macrophage moderated adipose tissue inflammation with obesity is a further contributory factor towards the development of insulin resistance⁴⁶. However other studies have shown that plasma NEFA concentrations are not significantly increased in obese subjects without diabetes mellitus type II. Under these conditions NEFA circulation is controlled through increased NEFA turnover and metabolism, yet these controls are impaired in the presence of insulin resistance and altered by excess dietary fatty acids and during energy consumption⁴⁷.

To date the exact developmental mechanisms of both pro-inflammation and insulin resistance through adipose tissue and NEFA signaling in obesity are not entirely understood, yet appear to be involved in a complex feedback system.

Adipokine	Function/Effect
Adipocyte lipid binding protein	Regulates systemic glucose and lipid metabolism
Adipocyte trypsin	Immune stress response
Adiponectin	Regulates glucose level and metabolism of lipids in energy production
Angiotensin	Blood vessel constriction, release of vasopressin & aldosterone which increase blood pressure
Apelin	Regulation of body fluid homeostasis
C-reactive protein	Inflammatory response, insulin resistance
Cholesteryl ester transfer protein	Mediates the transfer of cholesteryl esters and triglycerides between lipoprotein particles
Hormone sensitive lipase	Hydrolysis of triglycerides for NEFA mobilisation
Insulin-like growth factor	Insulin effects & cell growth/development
Interleukin 1β (IL-1β)	Inflammatory response
Interleukin 6 (IL-6)	Immune stress response, insulin resistance
Interleukin 8 (IL-8)	Immune stress response
Interleukin 10 (IL-10)	Anti-inflammatory effect
Interleukin 18 (IL-18)	Inflammatory response
Leptin	Regulates energy uptake/expenditure (appetite and metabolism)
Lipoprotein lipase	Mediates lipid uptake
Macrophage migration inhibitory factor β (MIF-β)	Immune stress response
Metallothionein	Immune stress response
Monobutyrin	Vasodilatation of the microvessel
Monocyte chemotactic protein 1 (MCP-1)	Immune stress response
Perilipin	Regulates lipid metabolism
Peroxisome proliferator-activated protein-γ (PPAR-γ)	Lipid metabolism, vascular homeostasis, inflammation
Plasminogen activator inhibitor-1 (PAI-1)	Vascular homeostasis
Resistin	Inflammatory response, insulin resistance
Retinol binding protein	Lipid metabolism
Steroid hormones	Lipid metabolism, insulin resistance
Transforming growth factor-β	Cell adhesion and migration, growth and differentiation
Tumour necrosis factor-α (TNF-α)	Immune stress response, insulin resistance
Uncoupling proteins	Energy balance and thermoregulation
Visfatin	Insulin resistance
Zinc-alpha2-glycoprotein	Lipid metabolism

Table 1.2: Adipokines secreted by white adipose tissue and their function and effect^{26,48}.

1.2.3 Obesity and insulin resistance

Insulin is a signalling hormone involved in the regulation of carbohydrate and lipid metabolism. Immediately after food consumption, a rapid increase of blood glucose occurs which stimulates pancreatic β -cells to synthesize insulin. Circulating insulin then facilitates the suppression of hepatic gluconeogenesis and modulates the entry and uptake of glucose through the major glucose transporter (GLUT4) action in liver, muscle and adipose tissue for conversion and storage to glycogen and later utilisation⁴⁹, as summarised in Figure 1.4, p13. In the presence of obesity, the normal insulin sensing mechanism suffers dysregulation, this impairment of insulin-responsiveness appears in all insulin sensitive tissues thought to arise from a down-regulation of GLUT4⁴⁹. Decreased stimulation of insulin mediated glucose transport and subsequent impaired glucose storage and metabolism leads to an insulin resistant state at a cellular level, resulting in hyperglycaemia and the development of diabetes mellitus type II. Obesity has also been demonstrated to contribute to insulin resistance through reduced insulin binding to its receptor, modulated by an impaired phosphorylation of the receptor and decreased tyrosine kinase activity in muscle and adipose tissue⁴⁹. The obesity mediated mechanisms of insulin resistance are complex and not fully elucidated, however it is hypothesised that the endocrine function of adipose tissue and the elevated secretions in NEFAs, glycerol, cytokines and other signalling molecules from adipocytes observed in obesity, all contribute to the development of obesity related insulin resistance⁵⁰.

Whilst insulin resistance positively correlates to visceral fat mass and BMI, epidemiological studies have highlighted that weight loss and reduction in central adipose depot size improves insulin sensitivity⁵¹.

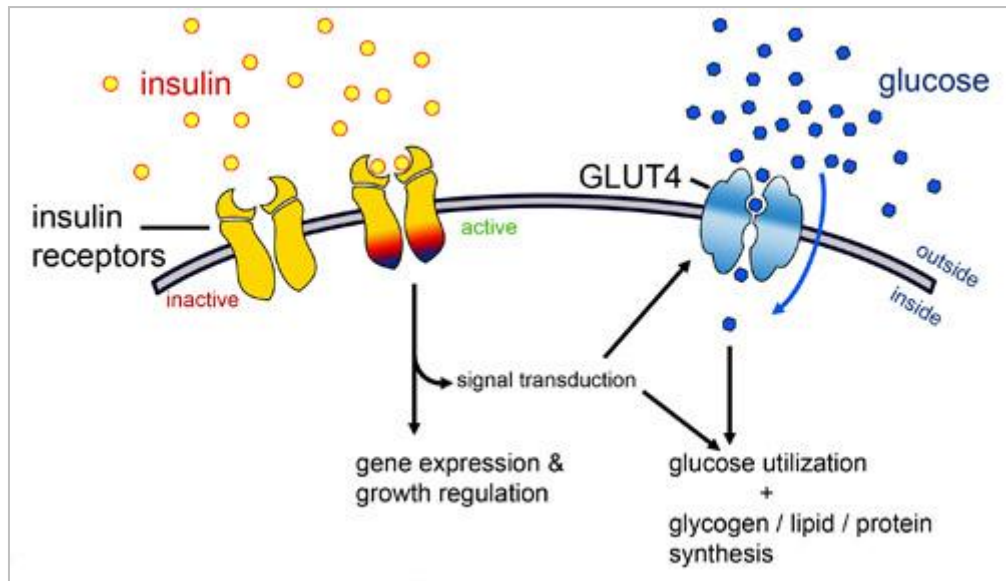


Figure 1.4: *Insulin mediated glucose uptake via binding of insulin to insulin receptor which initiates signal transduction and glucose transport in to cells through GLUT4 action⁵².*

1.3 Inflammation and the immune response

The human immune response consists of a number of complex molecular pathways and is composed of both the innate (non-specific) and adaptive (immunological memory) immune systems⁵³. These protect the host organism from infection and also differentiate between host cells and pathogens, although if this system fails, auto-immune disease can occur⁵⁴. When an antigen penetrates an external barrier and enters the body, immune responses, both cell mediated and humoral, are activated. The antigen may be attacked and ingested by phagocytic cells such as monocytes, macrophages, neutrophils or dendritic cells⁵³. Certain immune cells can also act as antigen presenting cells (APC) to initiate and further develop the immune response. Surface major histocompatibility complex (MHC) proteins bind with invading organism fragments which communicate with helper T-cells which in turn stimulates B-cells and cytotoxic T-cells; activation of the adaptive immune system⁵⁵.

In addition to this system, the presence of infection, injury or stress triggers cells to secrete chemical signals such as cytokines, chemokines and proteins that induce inflammation to protect surrounding tissues. This attracts immune cells that are involved in complex biochemical complement cascades activated by antibodies to destroy target cells⁵⁶. The host response to immune system agonists includes regulation of the cytokine response, cell-adhesion molecule expression, production of oxidative stress factors and cell death⁵⁷. Inflammatory responses can over or under react due to an uncoupling of the pro and anti-inflammatory mediator balance which can lead to further tissue damage⁵⁸.

1.3.1 Obesity induced inflammation

It is now established conditions such as obesity and hyperinsulinaemia stimulate the immune system, specifically activating a chronic low-grade pro-inflammatory state. Excess adipose tissue mass has been shown to positively correlate with expression of the pro-inflammatory gene, tumour necrosis factor- α (TNF- α)⁵⁹. It is a gene not only involved in immune cell signaling and further cytokine recruitment, but may contribute to insulin resistance by decreasing the uptake of glucose in response to insulin by inhibiting tyrosine phosphorylation of insulin receptor substrate-1 (IRS-1)^{59,60}. This is further evidence of the interlinked and complex nature of obesity, adipose tissue and insulin resistance.

Other markers of pro-inflammation, such as concentrations of plasma cytokines and the acute phase C-reactive protein (CRP), are positively correlated with adipose tissue mass⁴², emphasising the association between inflammation and obesity. CRP is also considered to be an independent biomarker in the development of CVD⁴², highlighting the relationship between obesity induced inflammation and additional morbidities.

As described in Table 1.2 (p11), adipose tissue is responsible for the synthesis and secretion of numerous molecular signals, but of particular interest in an obese pro-inflammatory status are the immune-modulating adipokines. In an obese condition it has been demonstrated that immunological adipokines from the interleukin family, both pro and anti-inflammatory molecules interleukin-6 (IL-6) and interleukin-10 (IL-10), show up-regulated expression and increased circulating plasma concentrations^{61,62,63}. The monocyte/macrophage recruitment molecule, monocyte chemoattractant protein-1 (MCP-1) and its receptor chemokine C-C motif receptor 2 (CCR2) also show up-regulation in the presence of obesity⁶⁴. These inflammatory molecules are also believed to contribute to the development of insulin resistance^{62,64}.

Numerous mechanisms may be driving adipose tissue induced inflammation, including increased adipokine synthesis, circulating NEFAs and triglycerides resulting from adipocyte hyperplasia and hypertrophy. Adipocyte hypertrophy has also been linked to increased apoptosis and crown-like structure development⁶⁵, which may be responsible for cumulative macrophage signalling and recruitment. In addition, immune cell infiltration of adipose tissue occurs via elevated adipokine cross-talk, contributing to further adipokine synthesis and macrophage accumulation. It is hypothesised that the non-fat cell fraction of adipose tissue is responsible for the majority of relative adipokine expression⁶⁶. One of the mechanisms thought to contribute to increased non-fat cell development in obesity, is via microcirculatory dysfunction and hypoxia caused by adipocyte enlargement⁶⁷. Hypoxic adipose tissue stimulates vascular synthesis and remodelling via up-regulation of the vascular endothelial growth factor (VEGF) gene, allowing for endothelial growth leading to additional immune cell infiltration and signalling, creating a continuous chronic inflammation feedback loop⁶⁷.

Finally, recent research has demonstrated that the metabolic hormones leptin and adiponectin, which are known to be direct signallers on the hypothalamus in the regulation of appetite and primarily synthesised in adipose tissue, also modulate an immune response in obesity linked inflammation, via both direct and indirect mechanisms^{68,69}. Figure 1.5, p17 summarises the complex nature of obesity induced inflammatory pathways.

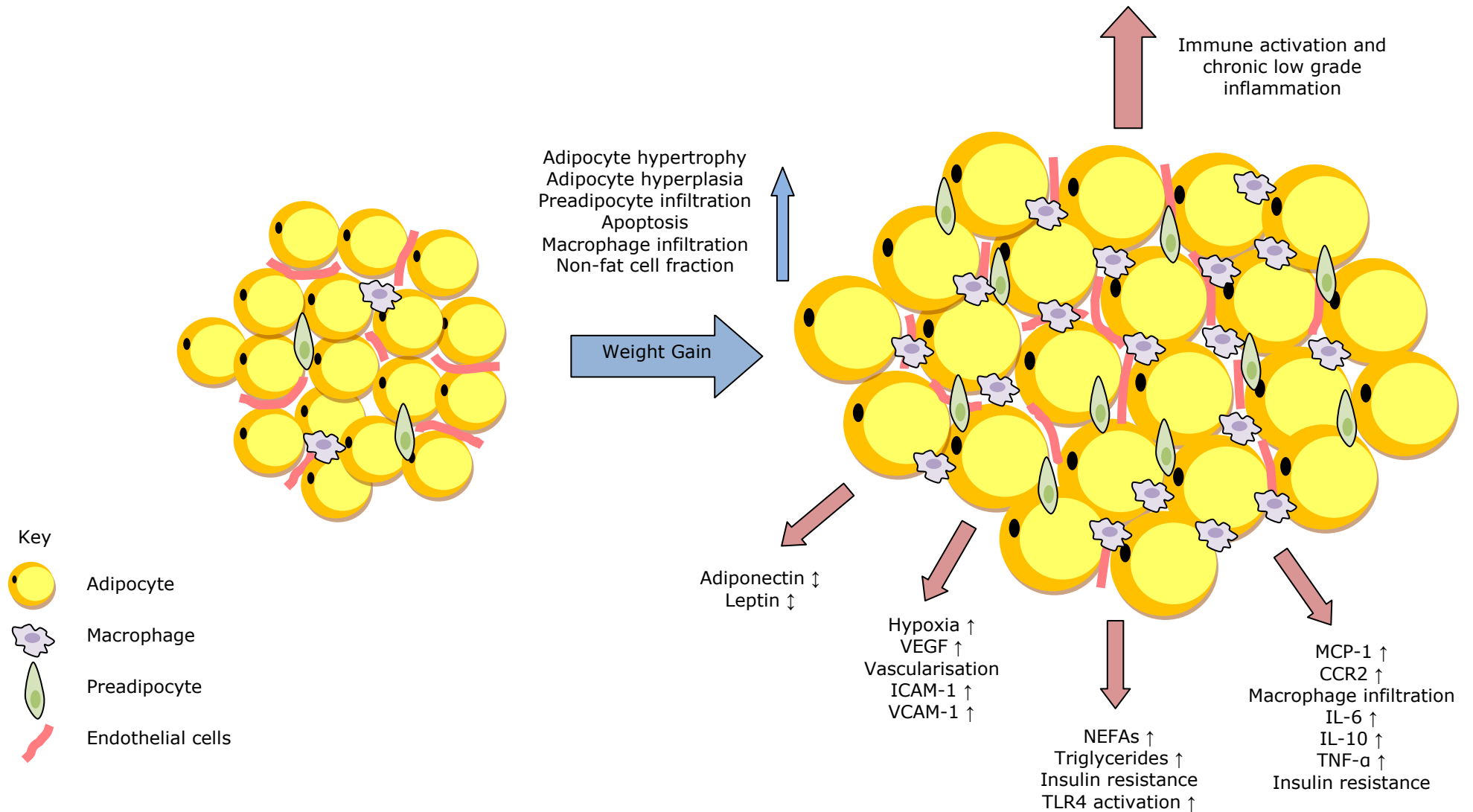


Figure 1.5: Summary diagram of the mechanisms involved in obesity induced inflammation.

1.3.2 Gender and adipose tissue depot differences in inflammation

Different adipose tissue depots display heterogeneity between genders and their metabolic profiles. A study in comparing gender and gluteal and intra-abdominal visceral adipose depots to their respective inflammatory protein markers has shown that visceral adiposity is significantly associated with elevated IL-6 and CRP plasma concentrations. The study also demonstrated a trend showing increasing subcutaneous thigh adiposity in females resulting in lower concentrations of the same inflammatory proteins⁷⁰. These results suggest that visceral adipose tissue is a predictor of inflammatory protein concentration and that obese females may show a reduced obesity linked inflammatory profile. Adipose tissue from extremely obese females has also been identified as synthesising higher levels of inflammatory adipokines compared to leaner females, regardless of locale⁶⁶. Additional studies have shown conflicting results in comparison of subcutaneous and omental adipose depots. In visceral adipose tissue, MCP-1 and TNF- α expression is down-regulated or equal to gene expression in subcutaneous fat⁶⁶. Yet IL-6, CCR2 and macrophage migration factor (MIF) gene expression is up-regulated in visceral compared to subcutaneous adipose tissue depots^{71,72}, however none of these studies examined age or gender differences. Adipose tissue inflammatory profiles may show heterogeneity between gender and depot location, although the literature presents varied conclusions, summarised in Table 1.3. It is possible that any heterogeneity displayed is due to differences in the adipose depot components, i.e. relative fraction of non-fat cells and adipocyte number and size, although obesity certainly impacts and promotes an inflammatory profile in adipose tissue.

Source	Species	Gender	Adipose depot	Outcome
Alvehus et al (2010)	Human	Both	Visceral to subcutaneous	CCR2 expression \uparrow MIF expression \uparrow
Beasley et al (2009)	Human	Males to females	Visceral	Plasma IL-6 \uparrow Plasma CRP \uparrow
Beasley et al (2009)	Human	Males to Females	Subcutaneous	Plasma IL-6 \downarrow Plasma CRP \downarrow Plasma TNF- α \downarrow
Cinti et al (2005)	Mice	Males only	Total	Adipocyte death \uparrow Macrophage infiltration \uparrow
Cinti et al (2005)	Humans	Both	Visceral to subcutaneous	MCP-1 expression \downarrow TNF- α expression \downarrow
Fain et al (2004)	Humans	Females only	Visceral to subcutaneous	Adipokine secretion \uparrow

Table 1.3: Summary of effects in obesity on inflammatory outcomes in relation to gender and adipose depots.

The elevated chronic inflammatory status observed in obesity alongside the associated obesity comorbidities, is hypothesised to be a mechanism behind a more widespread systemic injury, targeting organ systems such as the heart, liver and kidneys⁷³. My project investigates the nature of potential obesity mediated inflammation and its effects on the kidneys.

1.4 The kidney structure and function

In humans and most mammalian species, the kidneys are two highly complex reniform shaped organs located in the retroperitoneal space conjoined to an adrenal gland and located anteriorly atop each organ. They consist of a number of extremely specialised cells, organised in a three dimensional pattern, that perform a variety of important biological functions, including filtering blood to remove waste metabolites, fluid homeostasis, hormone production and regulation of blood pH and pressure^{74,75,76,77}. Kidney parenchyma consists mainly of two sections, an outer cortical (cortex) portion and an inner medullary (medulla) portion, see Figure 1.6, p20. The kidney consists of multilobular, pyramidal elevations called renal papillae which project from the cortical medullary junction into the renal sinus, a cavity surrounded by the kidney parenchyma and occupied by the renal pelvis, renal calyces, nerve fibres and adipose tissue. The renal sinus leads to the renal hilum allowing access of the kidney to the renal veins, arteries and ureter^{74,75,76,77}. Contained within the pyramidal papillae are the functional units of the kidney, called nephrons, see Figure 1.6, p20. There are approximately between 800,000 and 1.2 million nephrons in each human kidney⁷⁴. Nephrons consist of the renal corpuscle and renal tubules. The renal corpuscle is comprised of the Bowman's capsule, a double walled, spherical case structure which encapsulates a glomerular capillary tuft (the glomerulus as shown in Figure 1.7, p21).

Renal corpuscles are located at the basal pole of the nephron, which are almost all exclusively located within the cortical region of the kidney, with juxtamedullary renal corpuscles being the exception. The renal tubule consists of the convoluted and straight proximal tubule and peritubular capillary network, the loop of Henle, the convoluted and straight distal tubule and finally the collecting duct. The renal tubule is located at the apex pole of the nephron and is located within the medullary region of the kidney^{74,75,76,77}. The glomerulus is a three dimensional ball of capillaries, these capillaries consist of endothelial cells and a basement membrane, whose exterior is coated by renal podocytes and form filtration slits with adjacent podocytes.

Each glomerulus contains two vascular poles; located at one of the vascular poles is a specialised matrix of connective tissue comprised of mesangial cells which fill the void between adjacent capillaries. Located at the same vascular pole, are particular epithelial cells connected to the distal tubule termed the macula densa. The mesangial matrix and macula densa are called the juxtaglomerular apparatus⁷⁷.

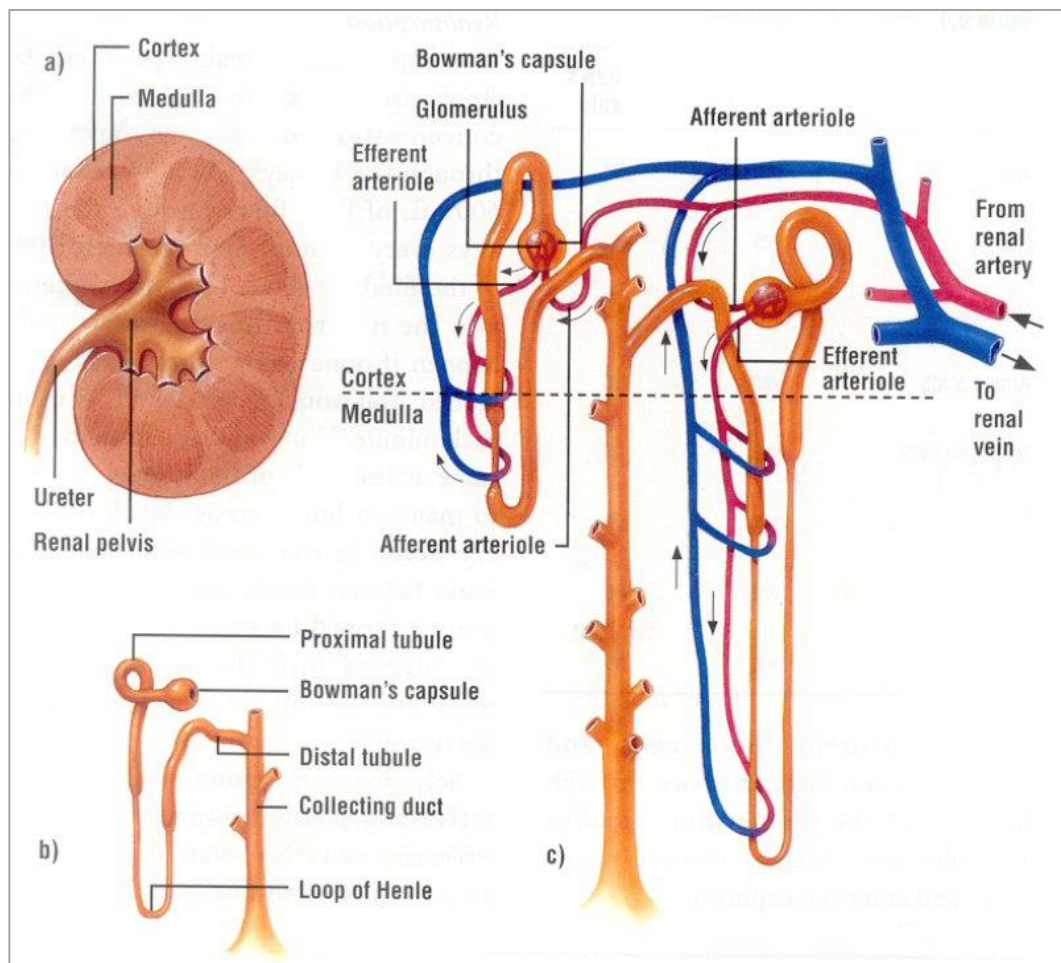


Figure 1.6: A – Cross section of kidney, depicting cortical and medullary regions of the organ. Striated regions show pyramidal papillae. B – A nephron; the basic functional filtration unit, which performs majority of organ functions. Renal tubule portion of nephron located within medullary region. C – A detailed image of a nephron. The Bowman's capsule is a double walled capsule containing the glomerular capillary tuft (glomerulus), these two structures constitute the renal corpuscle. The majority are located in the cortical region, with juxtamedullary corpuscles being the exception^{74,75,76,77,78}.

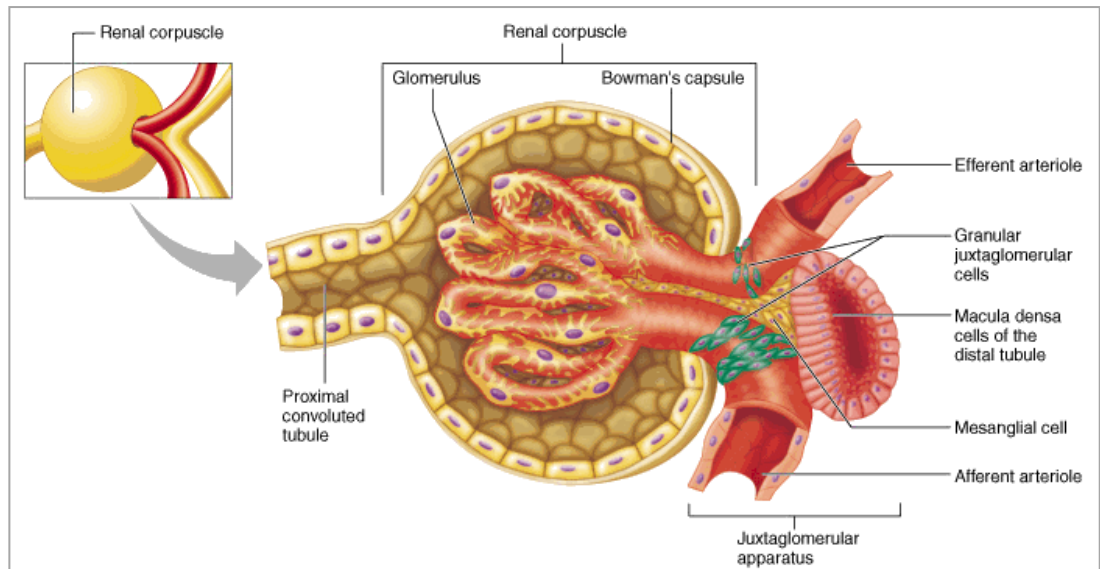


Figure 1.7: A cross section of a renal corpuscle. The vascular poles of the glomerulus are located at the openings of the proximal convoluted tubule and the efferent and afferent arterioles. The capillary tuft consists of endothelial cells, covering podocytes and filtration slits. The juxtaglomerular apparatus comprises of the mesangial matrix and macula densa^{77,79}.

The kidneys are supplied with blood from the renal arteries which branch into smaller interlobular arteries that run along the medullary-cortex border, the afferent arterioles which supply the glomeruli, branch off these interlobular arteries^{74,80,81}. After entering the glomerulus at a higher pressure than the remaining kidney microvasculature, blood is filtered through the glomerular capillaries. The volume of fluid filtered through the kidney during a set unit of time is a clinical measure of kidney function called the glomerular filtration rate (GFR). Filtration occurs via hydrostatic and oncotic 'Starling forces' through the podocyte fashioned filtration slits, forming urinary filtrate which is then excreted into the Bowman's capsule and transported to the proximal tubule⁸⁰. Filtered blood from the glomerulus enters the efferent arteriole and passes to the interlobular veins. After the urinary filtrate has passed into the proximal tubule, ions, molecules and waste metabolites are reabsorbed and secreted between the peritubular capillary network and the proximal tubule via passive and active transport processes^{74,80,81}. Specialised reabsorption transport proteins and ion pumps which transport glucose, amino acids, bicarbonate ions (HCO_3^-) and sodium chloride ions (Na^+ and Cl^-) facilitate the transfer of these molecules back to circulation. Increased solute concentration in the blood subsequently impacts on its osmotic pressure allowing for water to also be reabsorbed from the urinary filtrate. These reabsorption and secretion mechanisms occur at various degrees throughout the loop of Henle depending on solute concentrations until urinary filtrate reaches the distal tubule and collecting duct⁷⁷.

Whilst still undergoing reabsorption and secretion, the distal tubule reacts to the concentration of arginine vasopressin (anti-diuretic hormone), to either decrease urine volume and water excretion or increase urine dilution and urine volume^{74,80,81}. Finally urea and waste metabolites are passed through the collecting duct and ureter to be stored in the bladder ready for excretion.

The kidney is also responsible for the production of various hormones, for example the macula densa senses abnormalities in plasma sodium chloride concentrations at the afferent arteriole, and in response produces renin^{74,82}, a protein involved in the renin-angiotensin-aldosterone system (RAAS). In response to hypoxia, fibroblasts in the renal cortex promote transcription of erythropoietin (EPO), a hormone that regulates erythrocyte production⁸³. These hormones will be discussed in greater detail in subsequent sections.

1.4.1 Glomerular filtration rate

As GFR is accepted to be the best overall measure of kidney function, in determination of GFRs, clinical practice regularly measures either endogenous or exogenous biomarker clearance from serum by urine excretion. It is important that the biomarker used is not reabsorbed by the kidney and freely filtered by the glomerulus, examples of exogenous and endogenous biomarkers are inulin (a plant polysaccharide) and creatinine (a metabolite of muscle synthesised creatine phosphate) respectively^{84,85}. Generally, to avoid the administration of an exogenous biomarker, creatinine is used in the measure of GFR. To measure GFR, both serum and timed urinary samples are collected to determine a creatinine clearance rate, however creatinine generation is dependent on muscle mass and is also secreted by the proximal tubule, so GFR readings can be over or underestimated using this urinary clearance method^{84,86}. Additionally timed urinary collections can also prove problematic to achieve accurate results. Therefore standard clinical practice is to use an estimated GFR calculation based on serum creatinine measurement. There are a variety of estimation formulae available, but routinely, the Cockcroft and Gault (in adults, see Figure 1.8) or Schwartz (in children)⁸⁷ equations are the standard mathematical estimated GFR formulae. These equations take parameters such as age, weight, height and sex into consideration to calculate an accurate estimation of GFR^{84,86}. In animal studies GFRs are determined by the serum and urinary excretion methods using either endogenous or exogenous biomarker clearance rather than formulating eGFR equations for multiple animal species⁸⁵. By using GFR and eGFR measurements it is possible to monitor the progression of chronic kidney disease. Measurements implying a reduction in GFR, hypofiltration or extreme hyperfiltration are often signs of nephropathy and kidney damage⁸⁴.

$$\text{Estimated creatinine clearance (eCr)} = \frac{(140 - \text{age}) \times \text{mass [kg]} \times 0.85 \text{ [if female]}}{72 \times \text{serum creatinine [mg/dl]}}$$

Figure 1.8: Cockcroft-Gault creatinine clearance estimation formula used to calculate GFR in human adults⁸⁸.

1.4.2 The kidney as a target organ in an obese condition

The kidneys are sensitive to subtle changes in blood flow volume and oxygen delivery, where chronic exposure to such alterations often leads to impairment and damage of the nephrons. As previously discussed, obesity has consistently been associated with the development of hypertension, diabetes mellitus type II and metabolic syndrome, conditions that directly impact on kidney function. It is therefore logical to suggest that the presence of obesity plays a key role in the development and progression of chronic kidney disease. The relationship between an increasing BMI and impairment of renal haemodynamics is also evident in subjects without obesity⁸⁹. However, it has been reported that obesity as an independent risk factor without the presence of its comorbidities hypertension, diabetes mellitus type II and dyslipidaemia, does not significantly increase the risk of cardiovascular morbidity and mortality in either gender⁹⁰. Conversely, once obesity is combined with hypertension, the risk of cardiovascular morbidity and mortality is dramatically increased, in both genders, albeit with females showing a decreased risk compared to males⁹⁰. Nevertheless, obese subjects are at an increased risk of hypertension, but it appears the reverse is also true and that hypertensive subjects are predisposed to gain more weight⁹¹. The evidence from these studies suggests that obesity, hypertension and metabolic abnormalities interact and this amplifies their individual contribution towards CVD, summarised in Figure 1.9, p25, which is further amplified by additional genetic and socio-environmental factors associated with obesity development.

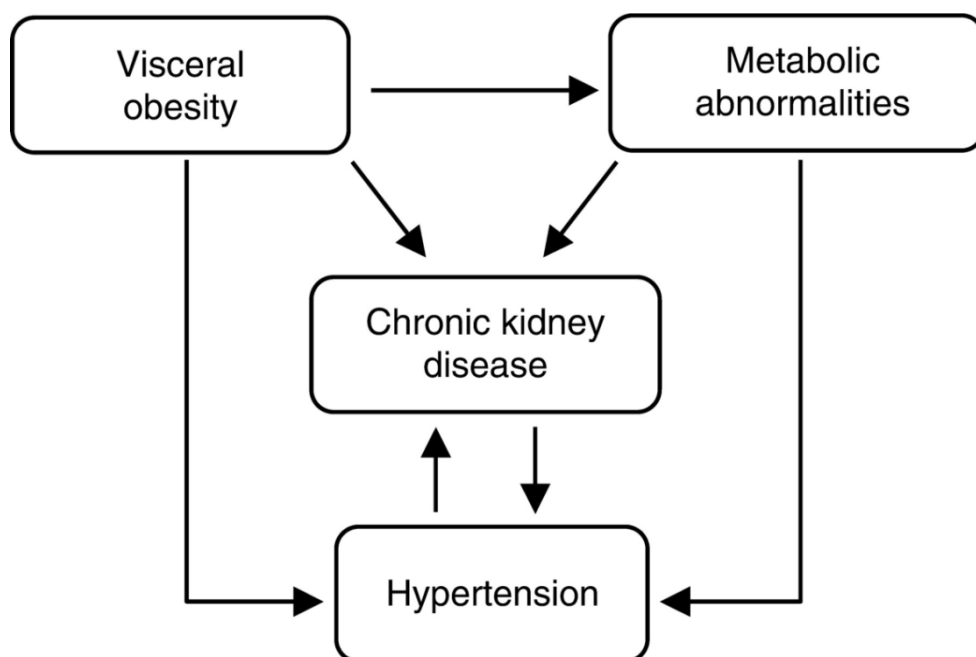


Figure 1.9: Interactive relationship towards chronic kidney disease by visceral obesity, hypertension and metabolic abnormalities⁹².

1.4.3 Pathophysiology of hypertension, metabolic abnormalities and obesity tissue in renal disease

Although the mechanistic knowledge of hypertensive renal damage is fairly limited, it is believed that during sustained hypertension, renal microvascular endothelial tissue responds by an up-regulation of vasoactive molecules, such as endothelin, inter-cellular adhesion molecule-1 (ICAM-1) and vascular cell adhesion molecule-1 (VCAM-1)⁹³. These molecules play a role in recruitment and activation of immune cells which may be involved in the constriction of renal vessels and sclerosis of muscle and endothelial tissue of the renal microvasculature seen in hypertension⁸¹. The afferent arterioles which supply the nephrons and excretory system with blood, also undergo hyalinisation (the deposition of glycoproteins and lipids from plasma), which occurs to a greater extent with elevated plasma lipids as seen in obesity. This in turn exposes the glomerular capillary apparatus to glomerular hypertension, leading to conditions such as focal segmental glomerulosclerosis (FSGS) shown in Figure 1.10 (p26) and glomerular injury responsible for continued hypertension⁸¹. Glomerulosclerosis is the scarring of the glomeruli, whereby sustained vascular mechanical injury induces the production and deposition of types I, II, III, IV, V and VI collagen in the glomerular basement membrane. Immunohistological staining has demonstrated that collagen synthesis and deposition in glomerulosclerosis is due solely to podocyte and glomerular cells⁹⁴.

The process of glomerulosclerosis development leads to a reduction in nephron number, hyperfiltration of remaining glomeruli and an overall reduction in filtration efficiency, usually diagnosed by the presence of proteinuria and haematuria. It has been established that in obese, proteinuric patients with elevated GFRs, a consistent finding in the renal pathology of these patients has been glomerular hypertrophy, or glomerulomegaly⁹⁵. The hallmarks of glomerulopathy in obese humans have often been both the presence of FSGS and glomerulomegaly, which are clinical signs of kidney disease, alongside other clinical observations such as proteinuria, fluctuations in GFR and renal vasodilatation⁹⁶.

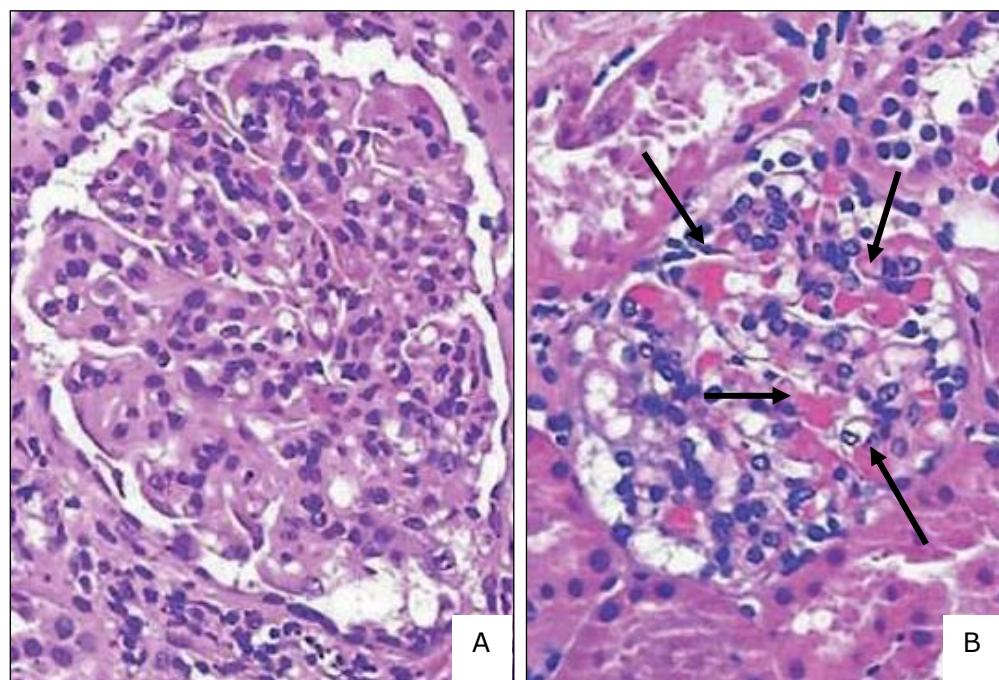


Figure 1.10: *Microscopic histological kidney sections showing glomerular apparatus. Image A shows a healthy glomerulus with an open and complete capillary tuft and open Bowman's space. Image B shows a thickening and scarring of the capillary tuft and a closed Bowman's space, an indication of glomerulosclerosis⁹⁷.*

The majority of histological based studies researching glomerulopathy in obesity have been conducted using animal kidney biopsy experiments. These studies have highlighted glomerular alterations such as an enlarged Bowman's space, capillary membrane thickening, glomerular hypertrophy accompanied by an increased cellular and mesangial matrix proliferation and elevated expression of growth and immune molecules⁹⁶.

One of the mechanisms thought to contribute towards visceral obesity and increased NEFA derived hypertension and glomerulopathy is through activation of the RAAS by stimulating the sympathetic nervous system, triggered by hyperleptinaemia and hyperinsulinaemia. Stimulation of renin production leads to an up-regulation of angiotension I and II, a pathway involved in vasoconstriction and hypertension⁹⁸. Additionally the presence of central obesity is positively correlated to the prevalence of diabetes mellitus type II⁹⁹. Increased circulating insulin from adipose tissue hypertrophy, hyperlipidaemia and subsequent elevated inflammatory profile induces insulin resistance¹⁰⁰ preventing circulating glucose being converted to storable glycogen, leading to hyperglycaemia and eventual diabetes mellitus type II. Chronic presence of diabetes mellitus type II leads to initial diabetic nephropathy, characterised by a thickening of the glomerulus, glomerular hypertrophy and mesangial expansion¹⁰¹, affecting GFR and elevating proteinuria. Continued exposure causes further injury to the kidney glomeruli, concluding in FSGS, glomerular nephritis, glomerular necrosis and eventual end stage renal disease (ESRD)¹⁰².

The WHO reports that 10-20% of diabetes mellitus type II patients suffer mortality from diabetes related kidney disease¹⁰³. Figure 1.11, p28 elaborates on the interactive pathways between visceral obesity, hypertension and metabolic abnormalities contributing to chronic kidney disease.

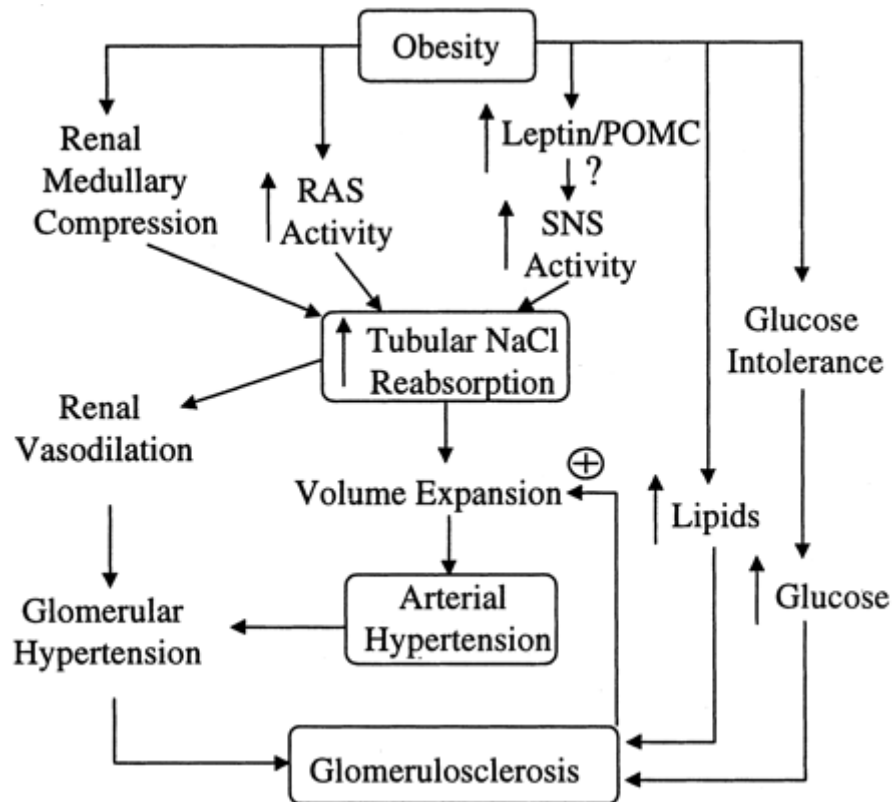


Figure 1.11: Summary of mechanisms involved in obesity mediated kidney function impairment, showing hypertension and metabolic abnormality pathways¹⁰⁴.

1.4.4 The renin-angiotensin-aldosterone system

The RAAS is a critical regulator of arterial blood pressure through the control of extracellular fluid volume, sodium homeostasis and vascular resistance¹⁰⁵. Production of renin by the granular cells of the juxtaglomerular apparatus is stimulated via three primary mechanisms; a decrease in sodium chloride concentrations detected by the macula densa, a decrease in arterial blood pressure detected by baroreceptor mechanism located within the afferent arteriole and sympathetic nervous system activation via β_1 adrenoreceptors¹⁰⁶. Upon stimulation of the RAAS, circulating plasma renin is increased. Active renin (also known as angiotensinogenase) cleaves the substrate angiotensinogen which is produced by the liver, to form the inactive peptide angiotensin I. Angiotensin converting enzyme (ACE) converts angiotensin I to angiotensin II by catalytic cleavage. Angiotensin II action is mediated by two receptors, angiotensin receptor-1 (AT₁) and angiotensin receptor-2 (AT₂). Formation of the AT₁-angiotensin II complex mediates afferent and efferent arteriole vasoconstriction and elevation of sodium ion and fluid reabsorption¹⁰⁵. Furthermore, angiotensin II is a regulatory factor in the synthesis of aldosterone, stimulating production in the adrenal cortex via AT₁ binding.

Aldosterone is a mineralocorticoid which binds to glucocorticoid receptor (GR) located in the proximal and distal tubules of nephrons. This process regulates sodium ion reabsorption and potassium ion secretion via an elevation in ion pump and protein transport¹⁰⁷. Overall the activation of the RAAS (summarised in Figure 1.12) results in systemic vasoconstriction and an elevation of systemic arterial blood pressure coupled with reduced blood flow, a system which is routinely targeted by pharmacological inhibition to treat hypertension and associated cardiovascular conditions¹⁰⁵. An over-stimulated RAAS is associated with the development of obesity, hypertension and metabolic syndrome, a mechanism possibly derived by angiotensin II mediated adipocyte growth and differentiation¹⁰⁸.

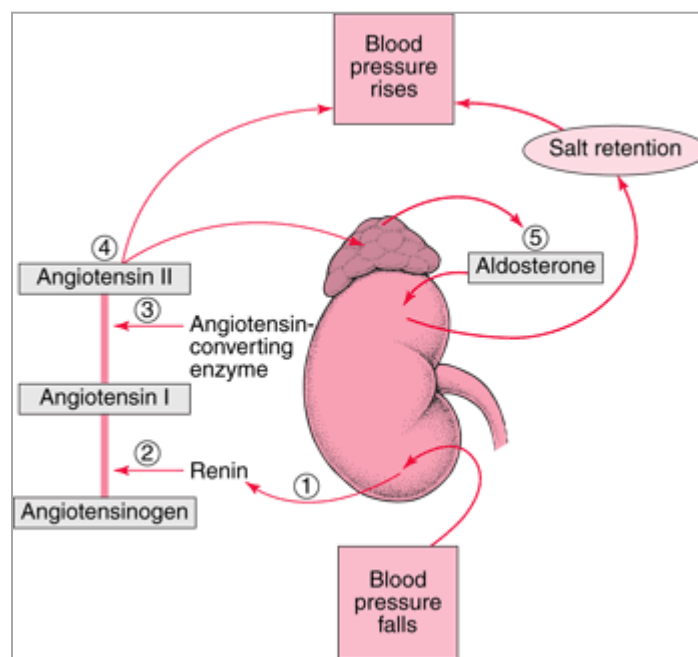


Figure 1.12: Summary diagram of the renin-angiotensin-aldosterone system; a decrease in blood pressure is sensed by the juxtaglomerular apparatus resulting in an up-regulation of renin. Renin acts on circulating angiotensinogen to form inactive angiotensin I, converted to active angiotensin II by angiotensin converting enzyme (ACE). Angiotensin II acts to both increase arterial blood pressure and activates aldosterone synthesis in the adrenal cortex. Aldosterone increases salt retention in the renal tubules resulting in additional arterial blood pressure increase¹⁰⁹.

1.4.5 Sex differences in obesity mediated renal nephropathy

As previously discussed, females appear to be at a reduced risk from renal nephropathy compared to males. Males also appear to suffer from faster progression of a number of nephropathies¹¹⁰. It is suggested that this gender disparity in both humans and animals may be attributable to differences in diet, glomerular haemodynamics, glomerular size and the direct actions of sex hormones¹¹⁰. A study on both testosterone and oestradiol action on mesangial cell proliferation and collagen synthesis demonstrated that whilst testosterone had no effect, oestradiol suppressed mesangial cell proliferation and collagen synthesis, a potential mechanism behind slower glomerulosclerosis progression seen in female subjects¹¹¹. In regards to the sexual dimorphism in cardiovascular parameters, males display higher arterial blood pressures and higher plasma renin activity than pre-menopausal females or post-menopausal females treated with oestrogen replacement therapy¹¹². It is therefore hypothesised that these differences are regulated by sex hormone stimulation and suppression of the RAAS. Several experimental animal studies have reported that oestrogen both up-regulates plasma angiotensinogen, and down regulates renin, ACE and AT₁¹¹³, in effect suppressing the RAAS. Experimental studies using rats have demonstrated that male rats display higher renal angiotensinogen levels than females, which are significantly increased during puberty and decreased after castration, and renal angiotensinogen mRNA expression is up-regulated in females exposed to exogenous testosterone^{114,115}. This evidence suggests that sex hormones play an important role in the regulation of blood pressure from action through the RAAS, one of the potential mechanisms which may account for the gender disparity seen in the progression of renal nephropathy and CVD.

1.4.6 Perirenal adipose tissue

Surrounding the fibrous kidney capsule is a variable layer of perinephric or perirenal adipose tissue (PAT) used for heat generation in neonates, and for protective cushioning and supporting the organ's retroperitoneal position after the neonatal period¹¹⁶. In animals fed a high-fat diet, obesity development and the enlargement of adipose tissue depots is not solely limited to classic visceral, subcutaneous and gluteal regions but also to a further extension in visceral ectopic adipose depots¹¹⁷. Raised ectopic adipose tissue with obesity effects depots around the cardiovascular apparatus, including the kidneys, heart and associated vasculature¹¹⁷. In an obese condition perirenal adipose tissue enlargement and subsequent adipose infiltration of the renal sinus may result in direct physical compression of the renal medullary architecture and microvasculature, leading to a restriction of tubule blood flow¹¹⁸. Consequently compression of renal nephron apparatus could result in impaired fluid and sodium reabsorption, leading to activation of the RAAS and contributing to obesity mediated hypertensive renal nephropathy. Perirenal adipose tissue thickness has been described as an independent predictor of chronic kidney disease and increased renal resistance¹¹⁸. Ectopic renal adipogenesis and enlarged ectopic adipose storage has been demonstrated to increase lipid deposition in renal cortical tissue of rats¹¹⁹. Excess accumulation of intra-renal lipids are also linked to renal lipotoxicity and lipid mediated insulin resistance and associated inflammation^{117,120}.

1.4.7 Hyperlipidaemia and the progression of renal lipotoxicity

In obesity, the excess lipid accumulation in adipose tissue contributes to adipocyte hypertrophy and systemic dyslipidaemia. As previously discussed, visceral and ectopic adipocytes appear to have a lower storage capacity for triglycerides compared to subcutaneous adipocytes³⁷. With obesity, hypertrophy of these specific depot adipocytes is increasingly linked to a hyperlipidaemic status¹²¹. However obesity is not only associated with increased adipocyte lipogenesis and hyperlipidaemia linked adipocyte hypertrophy, but may contribute towards lipid accumulation and deposition in non-adipose tissue and non-adipocytes. Saturation of lipids in non-adipose tissue, a process termed lipotoxicity, impairs and damages tissue via metabolic cellular dysfunction and tissue injury pathways¹²². Adverse consequences of excess lipid deposition have been observed in a number of different organs and tissues, including skeletal muscle, pancreas, liver, heart and kidney¹²³.

In skeletal muscle, intracellular accumulated NEFAs activate a serine/threonine kinase cascade resulting in reduced phosphorylation of insulin receptor substrate-1, a critical pathway of insulin resistance genesis¹²⁴. Such interference in insulin receptor signalling, results in further accumulation of intracellular NEFA metabolites, fatty acid coenzyme A and diacylglycerol¹²⁵.

In the progression of lipotoxicity induced renal injury, filtered NEFAs carried on albumin through the proximal tubule, trigger the inflammatory state observed in proteinuria. Accumulating albumin carried NEFAs stimulate macrophage infiltration of proximal tubule epithelial cells, demonstrated in patients with proteinuria derived nephrotic syndrome by initial monocyte and macrophage foam cell precursor infiltration¹²⁶. Inflammatory cascade activation via macrophage infiltration and cytokine recruitment is believed to significantly increase tubular cell stress, injury and apoptosis, leading to general tubulointerstitial injury and renal nephropathy¹²³. In acute renal failure models, excess unmetabolised NEFAs can induce mitochondrial dysfunction and activation of nuclear factor kappa light chain enhancer activated B cell (NF-κB). These pathways are both mechanisms of excess lipid induced cell death¹²⁷. Excess NEFAs have also been linked to an increase in cellular oxidative stress and further cellular apoptosis, observed by an up-regulation in nitric oxide production¹²³.

1.5 The role of glucocorticoids in obesity and inflammation

A member of the steroidal hormones family, glucocorticoids are primarily synthesised and secreted by the adrenal cortex, although recent data suggests that they are also synthesised within local organ and tissue systems too¹²⁸. They regulate a number of metabolic physiological processes and maintain immune related homeostasis through interactions with GR, present in almost all tissue¹²⁹. These hormones are responsible for the maintenance and increase of blood glucose concentrations via hepatic gluconeogenesis by stimulation of lipolysis for glycerol formation from adipocyte stored triglycerides and through inhibition of glucose uptake by adipose and muscle tissue. Glucocorticoids also have a potent anti-inflammatory and immunosuppressive action, and are used pharmacologically in treatment of inflammatory and auto-immune disorders¹³⁰.

Regulation of glucocorticoid synthesis is controlled by activation of the hypothalamic–pituitary–adrenal (HPA) axis, a neuroendocrine negative feedback loop, and the RAAS. In response to systemic stress or decreased circulating levels of glucocorticoids, adrenocorticotrophic hormone (ACTH) is produced by the pituitary gland via hypothalamic synthesis and signalling of corticotrophin releasing hormone (CRH) and steroidogenic peptide proopiomelanocortin (POMC). ACTH stimulates production of glucocorticoids in the adrenal gland. Additionally, glucocorticoid synthesis in certain tissues is regulated by the 11 β hydroxysteroid dehydrogenase family of enzymes¹³¹. In central obesity both human and rodent models have reported that activity of the HPA and RAAS axes are increased^{98,132}, evidence that visceral obesity is a form of systemic stress. A link between HPA activity and modification in body fat distribution via increased intra-abdominal fat development has also been reported^{133,134}.

Energy balance is controlled via hormonal stimulation from signalling molecules including leptin, adiponectin, insulin and cortisol or corticosterone (the predominant glucocorticoids in humans and rodents respectively) on the HPA axis. Energy hormone concentrations undergo fluxes during pre and postprandial periods of appetite regulation¹³⁵, but with obesity this hormonal signalling milieu is dysregulated. For example, patients with Cushing's syndrome, which is the prolonged exposure of the body to increased levels of plasma cortisol (hypercortisolism), central obesity is a prominent feature¹³⁶.

In fact with obesity, cortisol secretions are increased although circulating concentrations of cortisol in obese subjects are normal or low suggesting that cortisol clearance rate is elevated¹³⁷, confirmed by raised urinary cortisol excretion¹³⁴.

Obese human and rodent studies have demonstrated that intracellular tissue hypercortisolism exists due to increased activity of 11 β -hydroxysteroid dehydrogenase type 1 (11 β HSD1), an enzyme which converts inactive cortisone to active cortisol, reported to be up-regulated in omental but not subcutaneous adipose tissue depots^{134,136,138}. Though in human males, central obesity has been described to inhibit hepatic 11 β HSD1 activity compared to pre-menopausal women¹³⁴.

Changes in 11 β HSD1 expression contribute towards development of insulin resistance, hypertension and associated metabolic syndrome¹³⁹. With respect to cortisol action within the kidney, 11 β HSD2, an enzyme that converts active cortisol to inactive cortisone is expressed in the tubular nephron architecture to prevent inappropriate stimulation of GR and anti-inflammatory action by cortisol¹³⁸. The response of kidney 11 β HSD2 expression to abdominal obesity is so far unknown, although mutations of the 11 β HSD2 gene are linked to development of primary hypertension¹⁴⁰. The 11 β -hydroxysteroid family of enzymes can be regulated by a number of molecular factors, some influenced by the presence of central obesity such as insulin, TNF- α and sex hormones¹³⁸.

One of the suggested anti-inflammatory mechanisms of cortisol is inhibition of monocyte-macrophage differentiation and function, demonstrated to be suppressed in the presence of cortisol. After removal of cortisol, normal monocyte-macrophage differentiation and proliferation rates are restored¹⁴¹. Furthermore proteins involved in innate immunity up-regulated by the presence of lipopolysaccharide (LPS), are down regulated in the presence of cortisol¹⁴². It also inhibits synthesis of numerous cytokines, immune transcription mediators (i.e. NF- κ B) and cell surface molecules involved in the immune response^{143,144}. Although the mechanisms involved in the relationship between obesity, gender, glucocorticoids and inflammation are not completely understood, imbalance of HPA activity from obesity and cortisol dysfunction are potential mediators of adverse clinical outcomes. Figure 1.13, p35 summarises the pathways of glucocorticoid action in obesity and inflammation.

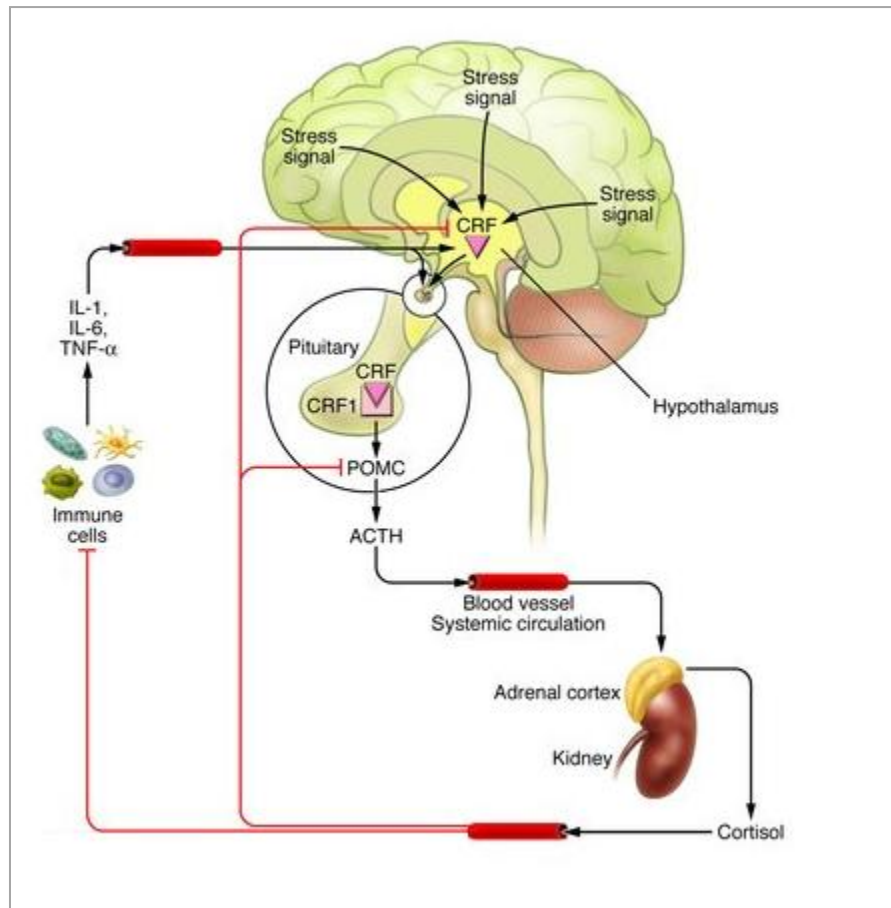


Figure 1.13: Summary of the hypothalamus-pituitary-adrenal (HPA) axis. A stress signal activates the hypothalamus which synthesizes corticotropin releasing factor (CRF), in turn stimulating the formation of proopiomelanocortin (POMC) and adrenocorticotrophic hormone (ACTH). ACTH results in glucocorticoid (cortisol) production in the adrenal cortex which inhibits immune cell and downstream cytokine synthesis. In obesity, the stress signal is elevated leading to additional immune suppression and potential cortisol dysfunction. Adapted from Slominski et al¹⁴⁵.

1.6 Gene expression

Gene expression is an important analytical tool to determine the amounts of a functional gene product derived from nuclear DNA. In eukaryotes, initially the DNA gene sequence is duplicated by RNA polymerase to form a primary precursor-messenger RNA (mRNA) transcript; a single complimentary molecular strand of genetic information⁵⁵. Precursor-mRNA is then spliced by spliceosome proteins to remove the introns from the sequence leaving only an exon comprised mature mRNA sequence. This functional mRNA sequence is then translated to an amino acid sequence via ribosomal transfer RNA (tRNA) anti-codon interaction, synthesising one amino acid per three nucleotide mRNA bases (codon)⁵⁵. Translated mRNA products are the initial amino acid sequences of the coded protein, which undergo post-translational modification into their secondary and tertiary structures for their functional purposes⁵⁵. The gene expression, transcription and translation mechanism is summarised in Figure 1.14, p37. Gene expression analysis evaluates the levels of mature mRNA within individual cells or a specific amount of whole tissue.

Gene expression is a key factor with regards to regulation of cellular activity, and since any alteration in gene expression would reflect changes in cellular mechanisms such as proliferation, survival or differentiation¹⁴⁶, the ability to quantify transcription levels of specific genes is essential to any research into gene function. Gene expression profiling is widely used in biological research, especially within animal model studies in response to applied experimental manipulations or interventions. These studies have identified multiple gene function and regulation fluctuations observed in numerous tissues mediated by both obesity and renal nephropathy^{147,148}. Gene expression data must be supplemented with protein expression analysis to corroborate the successful transcription of mature mRNA to expressed protein, which generally show a positive correlation¹⁴⁹.

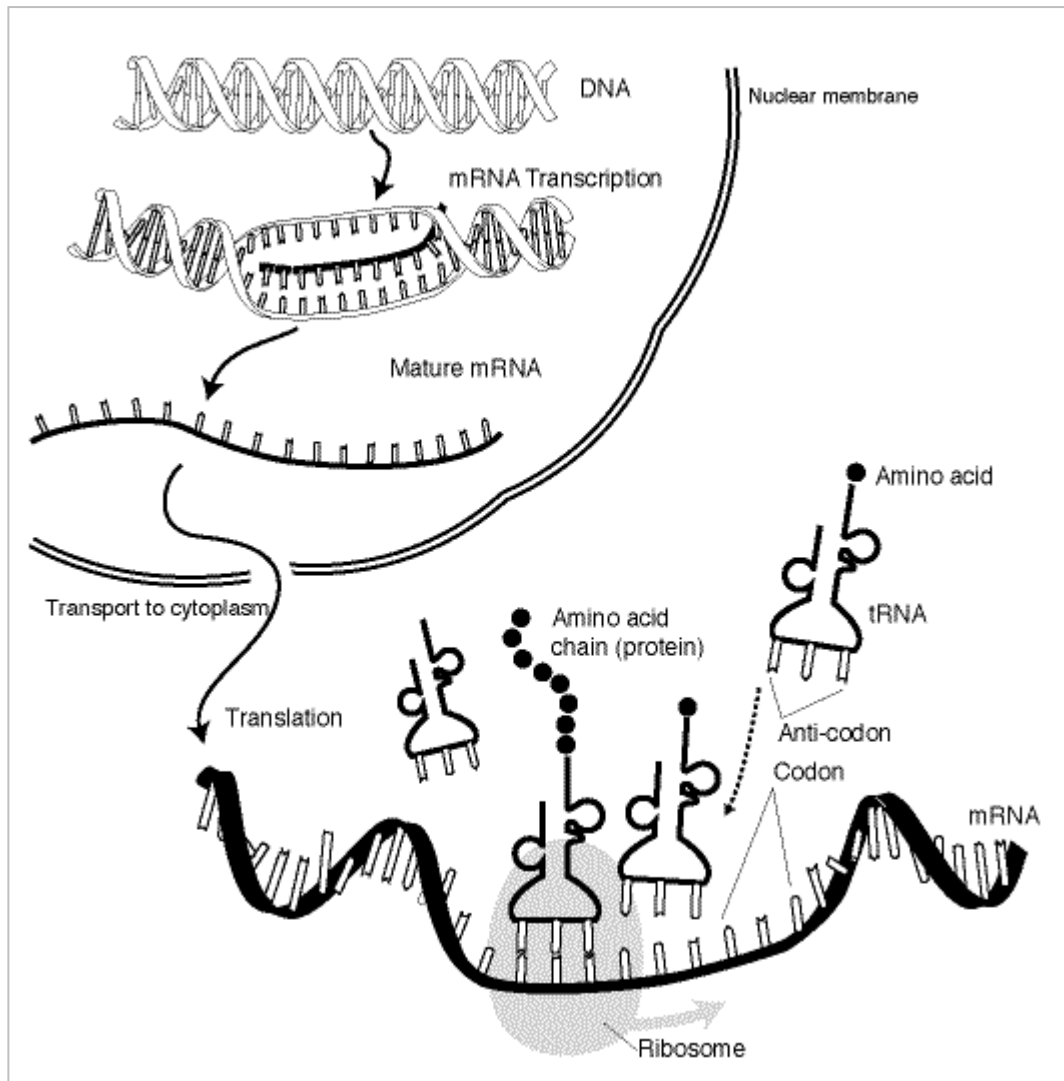


Figure 1.14: Summary of protein synthesis via gene transcription and translation. RNA polymerase converts nuclear DNA strand to precursor mRNA which is then converted to mature mRNA by spliceosome proteins. After transport of mRNA to cytoplasm, translation via ribosomal tRNA anti-codons occurs forming an amino acid chain and eventual protein^{55,150}.

1.7 Genes, cytokines and proteins involved in obesity mediated inflammation and renal nephropathy

Numerous cytokines and proteins are involved in the cellular mechanisms and pathways of the immune response and inflammation. Although not a comprehensive list, this section will discuss the functional roles of certain renal hormones, proteins and cytokines involved in inflammation and their response in the presence of obesity and how they contribute towards the development or prevention of renal nephropathy.

1.7.1 Glucocorticoids

1.7.1.1 11 β hydroxysteroid dehydrogenase type 1

The type 1 isoform of the hydroxysteroid dehydrogenase enzyme located in the endoplasmic reticulum (ER), is a bidirectional enzyme which principally acts as an oxoreductase enzyme to convert inactive cortisone to the active glucocorticoid cortisol (corticosterone in rodents), leading to amplified local glucocorticoid action¹⁵¹. 11 β HSD1 appears primarily in the liver and adipose tissue, and acts by reducing inactive cortisone to cortisol by concomitant reduction of nicotinamide adenine dinucleotide phosphate (NADPH)¹⁵². The enzyme has been shown to be expressed by human adipocytes and preadipocytes, and expression levels are positively correlated with BMI. Its expression is significantly up-regulated in omental adipose tissue in obesity compared to peripheral adipose depots and lean control subjects¹⁵³. Using rodent models, over expression of 11 β HSD1 in visceral adipose tissue is linked to the development of hyperglycaemia, dyslipidaemia, insulin resistance and hypertension, conditions associated with the metabolic syndrome. In 11 β HSD1 knockout mice however, visceral adipose accumulation is reduced¹⁵⁴. Expression of 11 β HSD1 has been observed in rodent renal architecture, including the distal tubules, aldosterone target cells and collecting duct, but no substantial levels of 11 β HSD1 have been observed in human or sheep kidneys¹³⁹.

1.7.1.2 11 β hydroxysteroid dehydrogenase type 2

The type 2 isozyme of the hydroxysteroid dehydrogenase enzyme, 11 β HSD2, has a converse action to that of 11 β HSD1, and converts active cortisol to inactive cortisone. 11 β HSD2 catalyses the conversion of cortisol by oxidative dehydrogenation to cortisone, a reaction facilitated by the co-factor NAD⁺¹⁵². The reaction mechanisms of the heterogeneous 11 β hydroxysteroid dehydrogenase family are shown in Figure 1.15, p39.

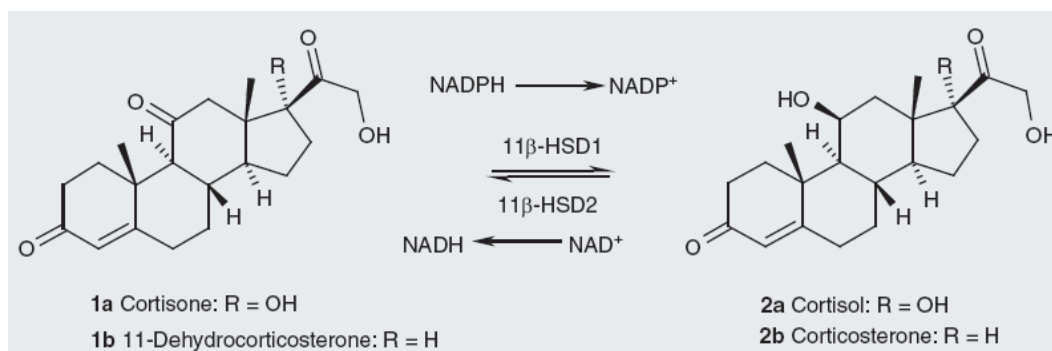


Figure 1.15: Enzymatic reactions catalysed by 11 β hydroxysteroid dehydrogenase types 1 and 2 (11 β HSD1 and 2). 11 β HSD1 converts inactive cortisone to active cortisol by reduction of ketone to hydroxyl group via NADPH, conversely 11 β HSD2 catalyses the opposite reaction via NAD⁺. The human and rodent forms of the glucocorticoid molecules are represented by 1-2a and 1-2b respectively¹⁵².

11 β HSD2 is present in mineralocorticoid receptor target tissues, including kidney, and prevents inappropriate glucocorticoid-mineralocorticoid receptor activation through conversion of cortisol to cortisone¹⁵⁵. Defects or mutations in 11 β HSD2 expression, thought to arise from elevated sodium reabsorption, have been observed to result in cortisol-dependent apparent mineralocorticoid excess which clinically manifests itself as severe hypertension, suppressed plasma renin activity, hypokalaemia, reduced aldosterone levels, abnormal kidney histology and interstitial fibrosis¹⁵⁶. Histological analysis of 11 β HSD2 knockout rodent models, have demonstrated distal nephron hypertrophy and hyperplasia¹⁵⁷. Obesity action on 11 β HSD2 expression in the human kidney is unknown to date, although one recent human study suggests that 11 β HSD2 activity is elevated in obesity resulting in an intensified supply of cortisone from the kidney for extra-renal 11 β HSD1 conversion which may fuel development of visceral adiposity and insulin resistance¹⁵⁸.

1.7.1.3 Glucocorticoid Receptor

As discussed, the GR is a nuclear receptor located in the cellular cytoplasm of almost all tissue, intended for the glucocorticoid family of steroid hormones¹²⁹. Glucocorticoid binding to GR primarily initiates transcription of numerous genes and factors involved in metabolic homeostasis; additionally glucocorticoid binding contributes to an anti-inflammatory status through immunosuppressive action on monocyte and macrophage differentiation^{130,141}. In humans, two GR isoforms have been identified, GR- α and GR- β , which originate from the same gene splicing. GR- α has been described as the active form of GR, demonstrated to be the default expressed GR in human cells and GR- β the inactive form¹⁵⁹, which does not bind glucocorticoid ligands or initiate gene transcription.

Mutations and polymorphisms in the GR sequence have been linked to GR- β expression, resulting in decreased glucocorticoid responsiveness and glucocorticoid resistance¹⁶⁰.

In response to obesity, GR- α mRNA expression was down-regulated in subcutaneous adipose tissue depots of obese patients compared to lean subjects, although this alteration was not observed in visceral adipose tissue. The authors of the study suggested that the glucocorticoid insensitivity displayed by obese patients may have been due to dysregulation in expression of GR- α :GR- β ratio, although visceral adipose depots were still responsive to local glucocorticoid synthesis¹⁶¹.

1.7.2 Appetite regulators

1.7.2.1 Adiponectin and adiponectin receptors

Adiponectin is a 244kDa adipose tissue specific protein hormone derived from adipocytes and is one of the most abundant gene transcripts in adipose tissue. Plasma adiponectin exists as a full-length polypeptide or globular form, which can bind and stimulate two cell surface receptors, adiponectin receptor 1 and adiponectin receptor 2. Activation of an adiponectin receptor mediates pathways involved in cellular energy homeostasis, glucose uptake and fatty acid activation¹⁶². In contrast to other adipokines in humans and mice, adiponectin mRNA expression and plasma levels are decreased with obesity and presence of the metabolic syndrome, a trend that is reversed in subjects with weight loss¹⁶³. Obesity is also believed to contribute to a reduction in adiponectin sensitivity through decreased adiponectin receptor expression¹⁶². Mice studies have demonstrated that down-regulation of adiponectin expression and decreased plasma adiponectin, correlates with insulin resistance. Exogenous doses of adiponectin were observed to decrease insulin resistance by reducing triglyceride content in liver and muscle of obese mice¹⁶⁴. In a study investigating the relationship between adiponectin and cardiovascular and renal disease, a 1 μ g/ml increase of plasma adiponectin was associated with a decreased risk of CVD. Likewise, patients with chronic kidney disease and ischemic heart disease, had lower plasma levels of adiponectin compared to patients without, suggesting that hypoadiponectinaemia is a predictor of CVD¹⁶⁵, indicating that adiponectin may additionally possess anti-inflammatory properties. This is supported by an observation that plasma adiponectin suppresses macrophage differentiation¹⁶⁶.

1.7.2.2 Leptin and leptin receptor

Leptin is a 16kDa adipose tissue derived protein hormone which signals through binding to the leptin receptor and plays a role in regulation of appetite and energy homeostasis through food intake signaling and satiety control. The primary target of leptin receptor binding is located in the hypothalamus, although recent studies have identified additional peripheral targets for leptin action¹⁶⁷. Activation of leptin receptor inhibits appetite by suppressing synthesis of feeding stimulant molecules, such as neuropeptide Y¹⁶⁷. The initial discovery of an 'obese' gene in the 1950s, later identified as leptin, demonstrated that a mutation or defect in transcription of the gene led to a phenotype of excessive appetite and development of severe obesity in mice¹⁶⁸. Exogenous introduction of leptin in these animals reversed both appetite and adipose tissue mass¹⁶⁸. It is now well established that adipose tissue mass levels and BMI positively correlate to circulating plasma leptin levels, which is observed in both genders albeit with obese females exhibiting higher plasma leptin levels than their male counterparts¹⁶⁹. The proposed mechanism driving the observed sexual leptin dimorphism is via the stimulating and suppressive effect of oestrogen and testosterone respectively¹⁷⁰.

It is thought that the chronic exposure of higher leptin levels observed in obese subjects leads to leptin desensitisation and development of leptin resistance; thus a dysregulation of leptin action in appetite regulation and energy homeostasis occurs. Hyperleptinaemia has additionally been associated with development of insulin resistance, suggesting a role in the metabolic syndrome¹⁶⁹. More recent research has identified leptin as a member of the cytokine family that possesses additional secondary immune and inflammatory properties, suggesting a mediator between nutritional status and the immune response. Periods of malnutrition or starvation and subsequent decreased circulating leptin signal are associated with abnormalities and suppression of the immune system¹⁷¹. In experimental animal models, using LPS as an inflammatory stimulus is associated with an up-regulation of leptin mRNA and circulating plasma leptin. This increase in leptin is believed to directly regulate the synthesis of the inflammatory cytokines and activate monocyte/macrophage through stimulation of IFN- γ ¹⁷². Leptin has also been identified as an anti-apoptotic and proliferative molecule which is reported to mediate the glomerular endothelial proliferation exhibited in glomerulosclerosis, a process amplified with an up-regulation of the RAAS¹⁷².

1.7.3 Markers of pro-inflammation

1.7.3.1 Interferon- γ

IFN- γ originally termed macrophage activating factor, activates macrophages which stimulate immune cell recruitment and produce inflammatory cytokines in an effective innate immune response¹⁷³. It is produced by various immune cells, such as natural killer cells, lymphocytes, APCs, and B and T cells via an innate immune system crosstalk, where macrophage pathogen recognition mediates cytokine production, additional immune cell recruitment and further IFN- γ synthesis and macrophage activation¹⁷³. Glucocorticoid action and anti-inflammatory cytokines have been described as negative regulators of IFN- γ production¹⁷³. In cases of glomerulonephritis, macrophage accumulation correlates with renal dysfunction, additional activation of these renal infiltrated macrophages by IFN- γ increased proteinuria and glomerular proliferation of macrophages¹⁷⁴.

Exposure of macrophages to IFN- γ results in up-regulation and increased production of inducible nitric oxide synthase (iNOS) and adhesion molecules, suggesting that IFN- γ activation of macrophages augments and modulates renal injury¹⁷⁴. In support of this finding, IFN- γ suppression by glucocorticoids reduced proliferation and recruitment of macrophages to inflamed glomeruli¹⁷⁴.

1.7.3.2 Interleukin-6

An important multifunctional cytokine, IL-6 has both pro and anti-inflammatory properties and is involved in the acute phase and immune response. It is produced by a number of tissues and cells including adipose tissue, monocytes, fibroblasts, macrophages, endothelial tissue B-cells and T-cells in the presence of injury, trauma or stress¹⁷⁵. This cytokine transmits its biological signal through two protein receptors on the cell, a specific binding molecule, interleukin 6 receptor and membrane bound glycoprotein 130. IL-6 forms complexes with these protein receptors, which in turn activates the receptor complex initiating a signal transduction cascade, such as the Janus kinases and signal transducers and activators of transcription pathway¹⁷⁵. This cascade simply transforms a signal into a response such as regulation of cell proliferation, differentiation and cell apoptosis.

It is expressed and produced by numerous tissues including adipose tissue, and as previously discussed, obese subjects displayed elevated plasma IL-6 concentrations which correlated with levels of insulin resistance⁶¹. Patients diagnosed with ESRD have poorer outcomes in the presence of elevated IL-6 plasma concentrations¹⁷⁶.

1.7.3.3 Interleukin-18

Interleukin 18 (IL-18) is structurally homologous to IL-1, but is expressed by both immune and non-immune cells and its receptor belongs to the IL1R and TLR superfamily¹⁷⁷. IL-18 mediates T helper cell immune responses in conjunction with interleukin 12 (IL-12) when presented with a microbial agent such as LPS, which induces IFN- γ by stimulating T and natural killer cells. IL-18 also stimulates expression of other cytokines involved in immunity and inflammation¹⁷⁷. Over production of IL-18 can lead to severe pro-inflammatory disorders varying from auto-immune diseases to inflammatory organ tissue damage. In contrast, mice studies have shown that IL-18 deficient subjects develop obesity and insulin resistance compared to wild type, which may indicate a similar role for IL-18 in energy intake and insulin sensitivity homeostasis as seen with IL-6 and TNF- α ¹⁷⁸. Urinary IL-18 in children was increased in patients with acute kidney injury (AKI) prior to urinary creatinine elevation, demonstrating the potential of IL-18 as an independent biomarker for kidney damage and inflammatory morbidity¹⁷⁹.

1.7.3.4 Monocyte chemoattractant protein-1 and C-C motif receptor 2

MCP-1 is a member of the chemokine family, and is produced by a number of immune cells. It binds to membrane bound CCR2 proteins which are highly expressed on monocyte and activated T cell surfaces. This receptor bound MCP1-CCR2 complex primarily is involved in attracting monocytes, T-lymphocytes and natural killer cells to the site of injury or stress. MCP-1 has been shown to up-regulate the synthesis of IL-6 in epithelial cells and *in vitro* models have shown TNF- α concentration being amplified by an increase of MCP-1 expression. Obesity and increased adipose depot size has been linked with elevated mRNA expression of MCP-1 leading to higher MCP-1 plasma concentrations⁶⁴. Obese mice engineered to over express the MCP-1 gene exhibited increased macrophage infiltration in adipose tissue, increased hepatic triglyceride deposition and insulin resistance, while MCP-1 knockout mice demonstrated reduced insulin resistance⁶⁴.

MCP-1/CCR2 complex formation has also been suggested to be a major promoter of inflammation, macrophage infiltration, fibrosis and tissue damage exhibited in diabetic nephropathy¹⁸⁰.

1.7.3.5 Tumour necrosis factor- α

A multifunctional cytokine, TNF- α is involved in the immune response, inflammation, growth promotion and growth inhibition of an organism. Similar to all cytokines, TNF- α is widely secreted by a number of tissues and cells including macrophages and monocytes. It binds and communicates with two receptors, type I (TNF-R1) and type II (TNF-R2) which belong to the TNF gene superfamily¹⁸¹. The molecule exists as both a membrane bound protein and a soluble form trimer, but is initially produced as a type II membrane protein. The membrane bound form is then converted by proteolytic cleavage to the soluble form by TNF- α converting enzyme. When a TNF- α trimer binds to TNF-R1, silencer of death domain (SODD) proteins are dissociated from the TNF-R1 receptor complex and TNF-receptor associated death domain (TRADD) proteins are recruited into the receptor complex¹⁸¹. TNF-R1-TRADD complex proteins can recruit TNF receptor-associated factor 2 proteins, FAS-associated protein with death domain (FADD) proteins and receptor interacting protein (RIP) kinase enzymes. This protein recruitment produces TNF-R1 signaling complexes involved in the activation of a number of signaling pathways including mitogen-activated protein kinase (MAPK), nuclear factor (NF)- κ B and caspase dependent apoptotic pathways¹⁸², see Figure 1.16, p45. These pathways play important roles in inflammatory responses, cell growth, differentiation, proliferation and pro and anti-apoptotic functions.

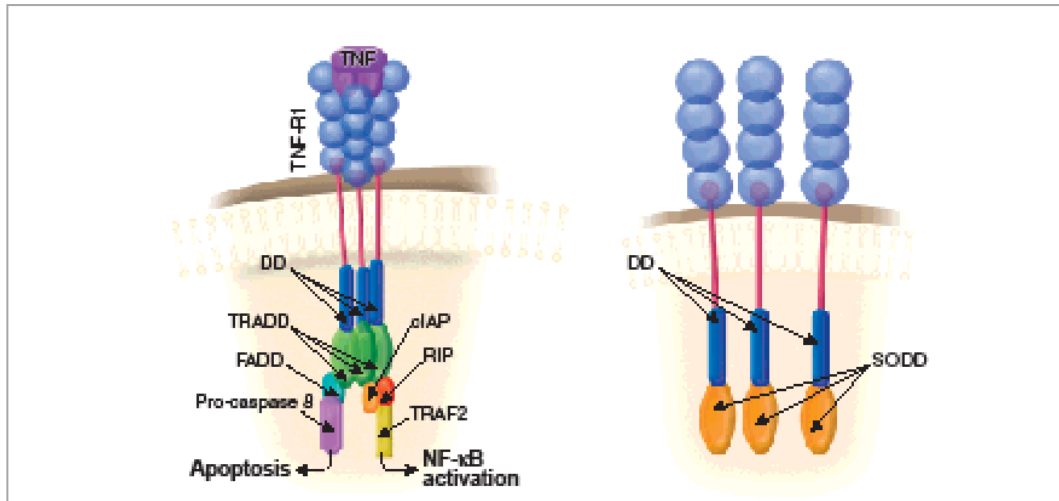


Figure 1.16: TNF trimer binding to TNF-R1 resulting in recruitment of signaling proteins into the receptor complex, which can then lead to either apoptotic or proliferative pathways¹⁸³.

As with other adipokines, TNF- α expression positively correlates to BMI and adiposity levels, additionally TNF- α is associated with development of obesity mediated insulin resistance⁵⁹. TNF- α has been shown to be a potent and significant factor in development of glomerulonephritis and renal injury, demonstrated by systemic administration of TNF- α which induced glomerular damage in rabbits¹⁸⁴. These findings were supported by TNF- α deficient glomerulonephritic mice which exhibited reduced proteinuria, decreased immune cell infiltration and diminished renal scarring¹⁸⁴.

1.7.4 Markers of anti-inflammation

1.7.4.1 Interleukin-10

IL-10 is an important anti-inflammatory and immunosuppressive cytokine responsible for the termination of inflammatory responses. It is recognised to inhibit the activation and function of T cells, monocytes and macrophages alongside regulation of numerous immune cells, by modulating the growth, differentiation and cytokine production of B cells, T cells, mast cells and natural killer cells¹⁸⁵. Similarly to adiponectin which also displays anti-inflammatory properties, in the presence of visceral obesity, plasma concentrations and adipose tissue mRNA expression of IL-10 are decreased¹⁸⁶, highlighting the pro-inflammatory state observed in subjects with central obesity. A dysregulation in cytokine network balance of IL-6, IL-10 and TNF- α is associated with the chronic systemic inflammatory condition observed in patients with CVD and ESRD¹⁸⁷.

1.7.4.2 Inducible nitric oxide synthase and nitric oxide

A member of the nitric oxide synthase family of soluble cytosol enzymes, iNOS is involved in the immune and cardiovascular system of mammalian species. It is responsible for oxidation of L-arginine in the presence of NADPH and molecular oxygen to produce nitric oxide gas (NO), an important biological signaling molecule involved in modulation of numerous physiological and pathological immune system processes¹⁸⁸.

Present in macrophages, natural killer cells, endothelial and epithelial cells, iNOS is activated by stimulation from IFN- γ or LPS-TLR4/CD14 complex formation to generate NO. This action drives numerous phenotypic effects, but primarily NO possesses a powerful immunoregulatory function. NO contributes to both pro and anti-inflammatory effects through the modulation of mRNA expression and production of cytokines, chemokines, growth factors and inhibition of antibody production and proliferation of B and T cells¹⁸⁸. Overstimulation of iNOS and NO production can have detrimental effects in a biological system. The chemical molecular structure of NO leads to a free radical form, which in the presence of a superoxide anion O_2^- molecule (a natural oxidative occurrence of molecular oxygen) forms a highly reactive oxidising peroxynitrite anion ($ONOO^-$) which is classed as a reactive oxygen species (ROS)¹⁸⁹.

If the antioxidant counter-response to ROS production is imbalanced or decreased, an over production of ROS can result in oxidative cellular toxicity triggering programmed cell death and apoptosis. Peroxynitrite damages DNA by double-strand breakage and base pair removal, but can also disrupt cellular function and increase synthesis of additional ROS through amino acid oxidation, inhibition of anti-oxidant enzymes and lipid peroxidation¹⁸⁹. Lipid peroxidation is the molecular oxidation of unsaturated lipids and fatty acids via a free radical molecule, leading to the formation of a lipid radical and eventual lipid peroxide molecule, another ROS, further perpetuating the oxidative stress cycle¹⁸⁹. NO has been observed to be an important vasodilatory signaling molecule in the kidney, involved in the regulation of sodium reabsorption and renal vasculature blood flow and pressure homeostasis¹⁹⁰. It is thought to reduce blood pressure in the kidneys via inhibition of renin production and increased sodium excretion¹⁹¹. In a rodent model of glomerulonephritis, expression of iNOS, eNOS and peroxynitrite were demonstrated to contribute to NO free radical induced renal tissue injury¹⁹².

Disruption of iNOS expression and production in obese iNOS knockout mice was reported to improve glucose tolerance and normalise insulin sensitivity in obese subjects, suggesting that iNOS is also involved in development of obesity related insulin resistance¹⁹³.

1.7.4.3 Peroxisome proliferating activated receptor- γ

Peroxisome proliferating activated receptor- γ (PPAR- γ) is a nuclear receptor and ligand-activated transcription factor expressed in practically all tissue, and is highly expressed in adipose tissue¹⁹⁴. It plays a role in numerous pathological metabolic processes such as insulin resistance, diabetes mellitus type II and obesity. Activation of PPAR- γ has been identified as a key pathway in the regulation of adipogenesis, lipid uptake, lipid metabolism and differentiation of pre-adipocytes. This has been demonstrated by over expression of PPAR- γ mRNA which induced lipid droplet accumulation in differentiated pre-adipocyte and fibroblast cells¹⁹⁵. Insulin sensitising agents, for example thiazolidinedione (TZD), have been shown to be PPAR- γ ligands. TZD binding results in decreased adipocyte lipolysis and a subsequent reduction of circulating fatty acids. Additionally PPAR γ -TZD binding regulates the expression of insulin modulator proteins and promotes adipose tissue remodeling in an attempt to re-direct lipid storage to subcutaneous instead of visceral adipose depots¹⁹⁶. Additionally PPAR- γ activation has demonstrated anti-inflammatory properties. PPAR- γ ligand binding was observed to inhibit the release of pro-inflammatory cytokines from monocytes and macrophages, modulate the expression of chemokines and endothelin, and reduce synthesis of IFN- γ by T cells in inflamed vasculature associated with atherosclerosis and CVD¹⁹⁷.

1.7.5 Lipid sensing receptors

1.7.5.1 Cluster of differentiation-14

Cluster of differentiation-14 (CD14) is a component gene of the innate immune system. It is found as a soluble membrane bound glycoprotein which is involved in monocyte differentiation and is expressed on the cell surfaces of monocytes, macrophages and neutrophils¹⁹⁸. CD14 receptor binds the lipid component of LPS, which can also be bound by free fatty acids. However it is suggested that CD14-LPS binding does not initiate a transmembrane signal alone, but rather that CD14 works as a protein anchor for additional signal transducers, i.e. toll-like receptors (TLRs), as part of an LPS-activation cluster¹⁹⁹, shown in Figure 1.17, p49.

Activation of this LPS-activation cluster modulates immune cell recruitment and synthesis of cytokines. In CD14 knockout mice, obese animals compared to wild type displayed lower adiposity, reduced blood pressure, down-regulated sympathetic activity and improved glucose homeostasis, this indicates that CD14 activation may play a role in the development of cardiovascular and metabolic conditions associated with obesity²⁰⁰. Renal CD14 expression has also been demonstrated to correlate with the impairment of kidney volume and progression of renal disease²⁰¹.

1.7.5.2 Toll-like receptor 4

TLR4 is a gene and member of the toll-like receptor family expressed by most tissues in the body and plays an important role in the inflammation and immune response pathways. It is a receptor for LPS which is a component of the outer membrane of gram-negative bacteria. When stimulated the TLR4 receptor complex activates inflammatory and immune molecular cascades involving the cellular transcription factors myeloid differentiation factor 88 (MyD88) and NF- κ B, resulting in an up-regulation of pro-inflammatory cytokines, cell mediated immunity and apoptosis²⁰²; Figure 1.17 (p49) shows the TLR4 activation pathway. Similarly to the TLR protein anchor CD14, TLR4 can also be stimulated by the lipid component of LPS found in circulating NEFAs which are elevated in obese subjects. Adipose tissue has also been implicated in the activation of the TLR4 pathway, with enlarged adipose stores responsible for the up-regulation of downstream NF- κ B transcription and subsequent pro-inflammatory cytokine generation²⁰³. Activation of TLR4 in the kidney is linked to the promotion of tubular damage and the progression of renal injury. In an experimental model using knockout TLR4 mice, the subjects exhibited reduced renal fibrosis by collagen deposition from growth factor stimulation²⁰⁴.

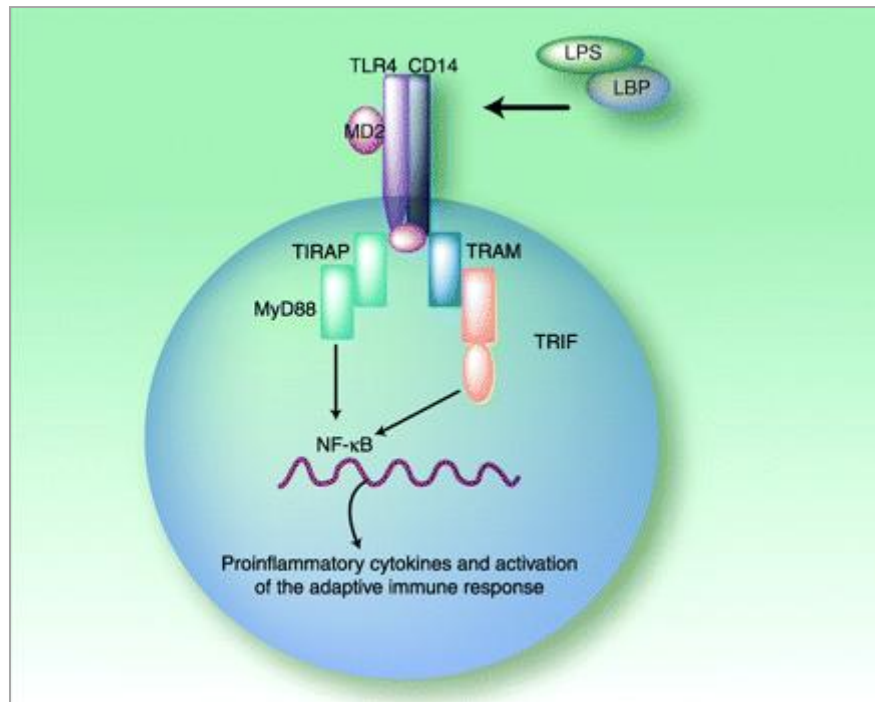


Figure 1.17: Summary of cellular membrane bound toll-like receptor 4 (TLR4) and cluster of differentiation-14 (CD14) lipopolysaccharide (LPS) activation cluster pathway. Lipid binding protein (LBP) presents LPS or lipid component of free fatty acid to receptor stimulating nuclear transcription factor NF-κB. Activation of TLR4 pathway results in up-regulation of pro-inflammatory cytokines and stimulation of immune response²⁰⁵.

1.7.6 Cell adhesion molecules

1.7.6.1 Intercellular adhesion molecule 1

ICAM-1 is a cell surface glycoprotein belonging to the immunoglobulin superfamily of proteins, that is expressed on vascular endothelial cells and non-vascular immune cells²⁰⁶. It plays a role in the inflammation and cytokine cascade, acting as a co-stimulatory molecule on APCs to activate T-cells. Endothelium bound ICAM-1 molecules function as migratory pathways for activated leukocytes to sites of injury, stress and inflammation²⁰⁶. ICAM-1 is induced by numerous cytokines and transcription factors including TNF-α, IFN-γ and NFκB, inhibition of ICAM-1 can be regulated by glucocorticoid action²⁰⁶. A study on diabetic nephropathy in rodents demonstrated that ICAM-1 mediated macrophage and leukocyte infiltration in renal tissue and ICAM-1 knockout mice had significantly decreased glomerular hypertrophy, proteinuria, mesangial matrix expansion and FSGS associated collagen deposition²⁰⁷, suggesting that ICAM-1 facilitates kidney inflammation and damage.

1.7.6.2 Vascular cell adhesion molecule-1

Vascular cell adhesion molecule-1 (VCAM-1) is an immunoglobulin-like cell adhesion molecule similar to ICAM-1. After stimulation of endothelial cells by circulating cytokines, expression of VCAM-1 is up-regulated. VCAM-1 mediates the adhesion of immune cells, for example, monocytes and macrophages to vascular endothelium for migration of adhered immune cells or signal transduction at the sites of tissue stress or injury²⁰⁸. Overstimulation of VCAM-1 has been attributed to endothelium dysfunction and the development of atherosclerotic lesions and subsequent vascular damage. Obese subjects with enlarged visceral but not subcutaneous adipose depots displayed both elevated plasma concentrations and up-regulated mRNA VCAM-1 expression; also these parameters positively correlated with BMI²⁰⁹. In healthy human kidney, VCAM-1 is expressed to a small extent, which is significantly increased in tubular cells of diseased renal tissue²¹⁰.

1.7.7 Cellular proliferation and apoptosis

1.7.7.1 Caspase-3

Caspase-3 is a member of the cysteine-aspartic acid protease family of enzymes; it has been implicated in key processes involved in effecting an apoptotic response by specific cleavage of cytoskeletal cellular proteins, a process initiated via apoptotic stimuli and cascaded by activation of the initiator and effector caspases resulting in degradation of DNA²¹¹. Apoptosis and programmed cell death are morphologically distinctive from necrotic cell death, and are believed to be responsible for regulation of cellular turnover and cellular homeostasis. Dysregulation of apoptosis is thought to contribute to the development of many pathological conditions; decreased apoptosis is linked to cancer, cellular hyperproliferation, auto-immune development and other chronic inflammatory disorders, whereas increased apoptosis may contribute to neuronal damage and neurodegenerative disease²¹². In rodent studies using an immune model of glomerulonephritis, up-regulation of apoptosis in renal cells was caspase-3 dependent, demonstrated by increases of caspase-3 activity, mRNA and protein expression. Increased renal cell apoptosis has been linked with renal scarring, FSGS, interstitial tubular fibrosis and tubular atrophy²¹³.

1.7.7.2 Proliferating cell nuclear antigen

Proliferating cell nuclear antigen (PCNA) is a protein involved in DNA replication and repair, which is a component of the cell cycle control apparatus. It is a homotrimeric protein which acts as a clamp and can slide along the double stranded helical molecule of DNA enabling localisation of proteins to specific areas of DNA²¹⁴. This PCNA clamp protein localisation mechanism allows for DNA polymerase enzymes to access the DNA strands for replication and for nucleotide excision or repair in response to damaged or mutated DNA²¹⁴. A balance of proliferative and apoptotic cellular processes control the natural cellular turnover, however a proliferative imbalance or over-expression of PCNA is associated with the renal nephropathies mesangioproliferative glomerulonephritis and glomerulosclerosis²¹⁵.

1.7.8 Renal molecules

1.7.8.1 Erythropoietin receptor

Erythropoietin receptor (EPOR) is the specific cell surface receptor for erythropoietin (EPO), the cytokine red cell progenitor and growth factor involved in erythropoiesis. The EPO and EPOR regulatory system is controlled via a feedback loop mechanism (shown in Figure 1.18, p52), where during periods of abnormal oxygen tension i.e. hypoxia or anaemia, it stimulates generation of EPO by endothelial cells of the kidney peritubular vasculature. This leads to increased circulating EPO and eventual correction in oxygen tension from EPO-EPOR binding and erythropoiesis²¹⁶.

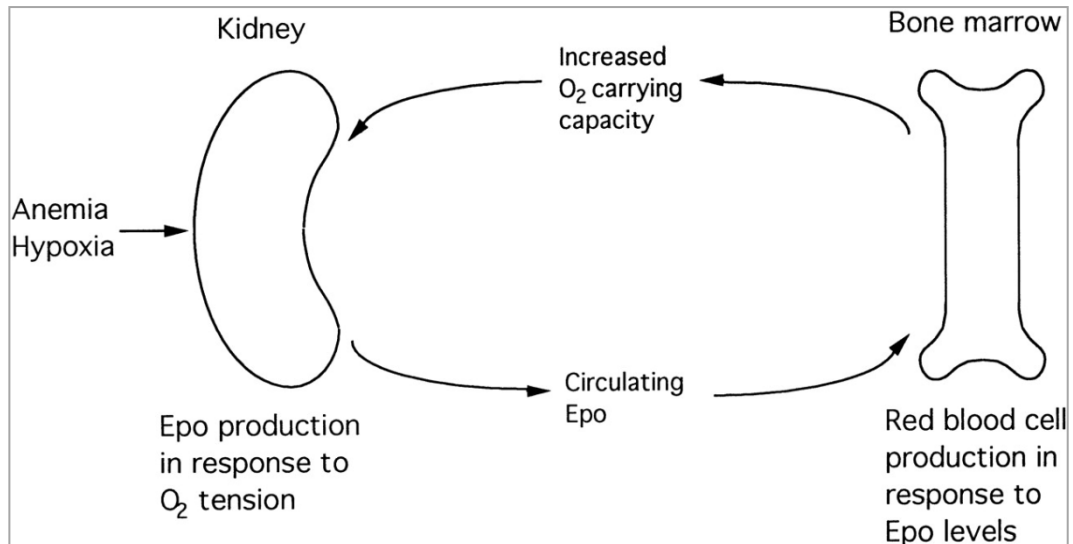


Figure 1.18: Regulation of erythropoiesis by negative feedback loop mechanism. Erythropoietin (EPO) is produced by the kidney resulting in increased circulating EPO in response to detection of abnormal oxygen tension²¹⁶.

It has been demonstrated that EPO-EPOR up-regulation reduces apoptotic processes and decreased caspase activity in renal tissue, and EPO injection protects against renal dysfunction and reduced morphological damage²¹⁷. Conversely, a severe elevation in EPOR gene expression has been linked to the progression of chronic renal disease²¹⁸. This heightened up-regulation may be a compensatory response to EPO-EPOR resistance which is attributed to cytokine derived inflammation, seen in patients with chronic kidney disease and heart failure²¹⁹.

1.7.8.2 Renin

Renin is a 37kDa enzyme produced by the granular cells of the renal juxtaglomerular apparatus in response to certain stimuli for activation of the RAAS. Mice lacking the renin gene displayed a lean and insulin sensitive phenotype; in addition these mice were resistant to diet induced obesity regardless of changes to dietary intake and physical activity, a result explained by the authors as an increase in metabolic rate²²⁰. This is further evidence to suggest that the RAAS plays an important role in obesity development, highlighting the potential of renin blockade as a potential therapeutic target in obesity treatment.

1.7.9 Gene, cytokine and protein summary

Obesity and related metabolic comorbidities are associated with a stimulation and up-regulation of pro-inflammatory and immune cytokines, proteins and other cellular communicators. Cytokines, proteins and signaling molecules involved in immune responses are not stored in intracellular compartments but newly synthesised by expression and transcription of mRNA in specific cells and released as a direct response to inflammatory stimuli²²¹. Hence these signaling molecules and cytokines are widely used as biomarkers to analyse the inflammatory and immune status of certain tissues or organisms under various interventions or conditions²²². However with regards to using cytokines as biomarkers, cytokines are pleiotropic molecules, meaning they are not limited to one specific function and thus classed as 'redundant', since a number of cytokines can perform the same biological function²²¹. Cytokines also induce other cytokines through complex inter-linked cascades and network pathways, sometimes referred to as cytokine crosstalk²²³.

Evidence in the literature suggests that the kidneys are especially sensitive to obesity, and an over-stimulated immune response in kidney tissue mediates renal injury and impaired renal function. Figure 1.19 (p54) is a summary of the relationships and pathways involved in the inflammation cascade network, alterations in renal function, increased adiposity and presence of metabolic comorbidities. In regards to inflammatory profiles and gender, there is a definite paucity of information in relation to sexual dimorphism and to date, any potential difference is unknown.

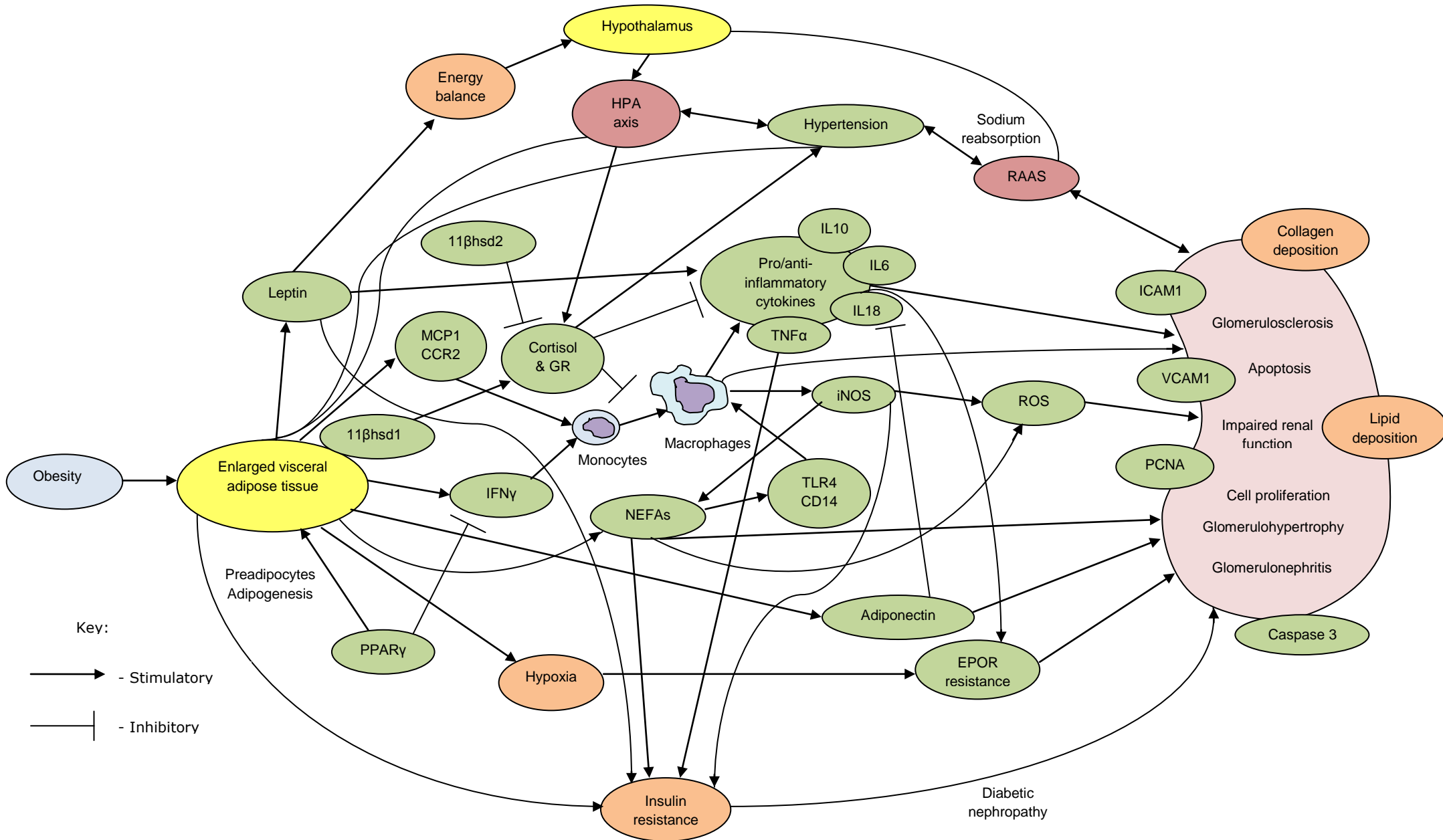


Figure 1.19: Summary of mechanism pathways involved in obesity activated inflammation and subsequent renal nephropathy¹¹³⁻²⁰⁴.

1.8 The sheep as an experimental model for obesity

Due to ethical reasons, it is not possible to manipulate humans using highly invasive physiological or experimental procedures. Large human epidemiological studies are widely used in some aspects of obesity research, for example a 2010 national UK study investigating childhood obesity recruited over one million subjects throughout UK schools²²⁴. However, there is a need to validate these data and elucidate the molecular biological mechanisms behind obesity and its associated comorbidities. Therefore it is important to use animals as translational tools, which display and have comparable characteristics when manipulated with specific key challenges or interventions, in this instance, an animal model of obesity. Sheep are important animals in biomedical research and possess comparable physiological features to humans, which is significant for the investigation of cardiovascular, respiratory, endocrine, renal and reproductive physiological systems. Sheep offspring are comparable in number, i.e. single, twin or triplet offspring, rather than large litter sizes. Newborn sheep are comparable in birth weight to human newborns ($\approx 4.5\text{kg}$); and are also born with fully developed organ systems and a mature HPA axis²²⁵. The metanephros (mature ovine kidney) develops over the early-mid gestation period, from gestation day 27 to gestation day 110, and at birth newborn sheep possess a fully mature renal system²²⁶. Sheep studies investigating the exposure of restricted maternal nutrition during periods of early gestation encompassing the period of nephrogenesis have identified a sensitivity of ovine kidney development to changes in maternal diet. These effects include the development of hypertension, elevated renal mRNA expression of GR and reduced nephron number²²⁶.

However, sheep are ruminants and as such possess a more complex digestive system resulting in different dietary requirements and glucose utilization compared to humans. Yet despite this, credible models of ovine obesity have been developed using programs of manipulation in maternal diet, post-natal feeding and post-weaning activity. This developmental pathway of obesity, i.e. a number of factors rather than solely over-consumption, is comparable to the one observed in human society. Secondly, these models also lead to development of obesity-related metabolic complications observed in humans such as hypertension, hyperleptinaemia, impaired inflammatory renal profile and insulin sensitivity^{226,227,228}.

The development of obesity observed in these models shows central visceral and ectopic perirenal and pericardial adipose tissue enlargement, which is believed to contribute to the development of a low grade chronic inflammatory state and obesity mediated metabolic comorbidities²²⁹. In 2005 a British Heart Foundation funded obesity study was performed by the Academic Child Health group at Nottingham University. This study investigated sheep exposed to restricted maternal nutrition during early gestation, post natal overfeeding and limited physical activity (17 sheep per 50m²) to promote obesity, which generated three experimental groups; lean control (C), obese (O) and nutrient restricted obese (NR)^{227,230}. At 1 year of age the O and NR sheep were \approx 35% heavier than the control sheep (C=58.58 \pm 2.46kg; O=88.71 \pm 2.67kg; NR=85.83 \pm 4.57kg), and in more detailed analysis kidney mass was \approx 30% (C=117.27 \pm 9.20g; O=155.70 \pm 6.68g; NR=164.86 \pm 7.16g) and PAT mass was \approx 500% (C=553.88 \pm 93.48g; O=2692.14 \pm 294.33g; NR=2783.23 \pm 197.92g) larger in the two obese groups compared to the lean animals²³⁰. In addition mean blood pressures were increased in the obese groups^{227,230} (C=91.5 \pm 1.75; O=102.3 \pm 2.65; NR=102.5 \pm 2.6mmHg). Also in determination of the inflammatory response and macrophage signaling in obesity, mRNA analysis showed an elevation in CCR2 (2-fold) expression in PAT and a reduction in renal MCP-1 and CCR2 (2.5-fold) mRNA expression in comparison of obese and lean sheep²²⁷. These findings supported the hypothesis that obesity modulates physiological changes in the kidney, possibly through adaptations in PAT and haemodynamic parameters, although gender was not investigated during this previous study.

Finally, sheep being larger animals than rats or mice allows for insertion of sampling or monitoring devices, manipulation of foetal development and higher yields in terms of amount of body fluids and organ tissues harvested after euthanasia etc. Although the husbandry time and expense of larger animals is increased compared to smaller rodent experiments²³¹.

1.9 Main hypothesis and aims

The introduction chapter has discussed the ideas behind obesity and how increased adiposity mediates a chronic inflammatory status and the mechanisms contributing to impaired renal function. Alongside gender, these aspects have so far been discussed as independent variables. Although the scientific literature suffers from a dearth of gender specific investigations in relation to obesity or inflammation and renal disease, clinical evidence suggests a sexual dimorphism exists which could have real implications in the treatment of obesity modulated morbidity.

The primary hypothesis behind this study was that the development and presence of onset obesity in an ovine model, promotes an amplified inflammatory state, mediated by physiological adaptations in ectopic adipose tissue depots. This heightened inflammatory milieu then contributes to structural renal impairment, dysfunction and damage. It was also possible that in agreement with epidemiological data, that gender may display dimorphic responses to the presence of obesity and related inflammation and the potential progression in kidney disease.

The following chapters were designed to answer the above hypothesis;

1. Description of gender differences observed in morphometric measurements and alterations in adipose tissue physiology and systemic metabolism induced by exposure to a postnatal obesogenic environment.
2. Determination of obesogenic PAT alterations on subsequent PAT inflammatory and metabolic genotype.
3. Identification of the renal morphology and physiology of each gender and their respective gene regulation and renal inflammatory genotype induced by exposure to a postnatal obesogenic environment.

Chapter 2 - Materials and methods

Chapter 2 will explain the basic scientific theory and implementation of the study models and experimental procedures used throughout this study.

2.1 Procedural & legislative declaration

All animal experimentation carried out in this study (2.2.1-2.2.5, p59-63) was conducted in accordance with the UK Home Office and the UK Animals (Scientific Procedures) Act (1986) by Professor M.E Symonds and Dr D. Gardner and performed by Dr S. Sebert. Additionally, all experimental procedures were completed under licence and with ethical approval from the University of Nottingham. All chemicals, reagents and laboratory procedures were assessed and implemented in compliance with the UK Health and Safety Executive's Control of Substances Hazardous to Health (COSHH, SI No. 1657, 1988) and Risk Assessment guidelines.

All laboratory-based techniques & protocols were conducted within the Academic Child Health department, School of Clinical Sciences, Division of Human Development, University of Nottingham, Queen's Medical Centre and the School of Veterinary Medicine and Science, Sutton Bonington Campus, University of Nottingham. The methodological procedures used in the study were either as recommended by the manufacturers and suppliers, or optimised within the Academic Child Health department by myself, Dr S. Sebert, Dr L. Chan, Dr M. Hyatt and Mr M. Pope.

All materials were purchased from Sigma-Aldrich (Poole, Dorset, UK) unless otherwise specified.

2.2 Study design

This study was conducted using sheep from the 2007 Early Nutrition Programming Project (EARNEST, FP6, #FOOD-CT-2005-007036²³²), which aimed to investigate the effects of maternal nutrition *in utero* and post-natal activity in the development of obesity and metabolic related disease later in adult life.

Experimental treatments in animals occurred at two critical stages of development. These were:

- Prenatal – Mothers were fed a low- or high-calorie intake during the last third of gestation (110 days to term) - as detailed below.
- Post Weaning – 3 month old offspring were placed in high or low physical activity environments until 17 months of age to encourage the development of lean and obese animals, respectively²²⁸.

2.2.1 Animals, diets and environments

Twenty Bluefaced Leicester cross Swaledale ewes of similar body weights and ages were selected and bred at the University of Nottingham's Joint Animal Breeding Unit, Sutton Bonington Campus. Twin bearing was confirmed by ultrasound scanning at 75 dGA. Ten pregnant ewes were randomly assigned into a nutritional restricted group (N) and received 60% of normal daily energy requirement ($0.46 \text{ MJ/kg}^{0.75}$ body weight at 110 dGA and $0.72 \text{ MJ/kg}^{0.75}$ body weight at 140 dGA) for pregnant sheep during the last third of pregnancy. Ten were allocated in fed to appetite group (A) and consumed 150% of energy requirements ($1.15 \text{ MJ/kg}^{0.75}$ body weight at 110 dGA and $1.80 \text{ MJ/kg}^{0.75}$ body weight at 140 dGA). 100% of nutrition and energy requirements for pregnant ewes was based on recommendations from the AFRC 1993 manual of 'Energy and Protein Requirements of Ruminants'²³³, and the amount and composition of nutrition, metabolisable energy and protein supplied to each sheep was calculated using maternal body weight, gestational age and expected energy utilisation for maintenance. After birth, the offspring for both groups (N: n=20 and A: n=20) were raised and fed by their mothers as twins for the 3 month lactation period. The mothers were fed to requirements during this stage. At weaning, twins were then separated into two experimental groups to determine the effect of physical activity on the development of obesity. Twins were either allocated into a restricted activity area (barn), an obesogenic environment (O) with a stocking rate of 6 sheep per 19m^2 , or an unrestrained activity area (field), lean environment (L) with a stocking rate of 6 sheep per 1125 m^2 .

During this phase, all sheep were fed the same diet, a mixture of hay (8.9 MJ/kg) and high concentrate pellets (12.6 MJ/kg) (Manor Farm Feeds, Oakham, UK) containing 100% recommended of energy requirements. For each animal, daily energy intake was assessed through weighed intake and food refusal. Diets were also supplemented with vitamins and minerals and all sheep had unlimited access to water.

Physical activity was measured using uniaxial accelerometers (Actiwatch, Linton Instrumentation, Diss, UK) of the two groups in periods of 30 seconds over a 24 hour period whilst in their respective manipulated activity environments. Accelerometry probes were placed on collars around the necks of the animals for a 24 hour period, with activity measurements recorded 32 times per second. The resulting readings were then subsequently uploaded to specialist software (Actigraph, FL, USA) for formatting and analysis. Accelerometry identified a two to three-fold increase in activity between the 'obese' and 'lean' stocked environments.

Throughout the study, specific physiological measurements were gathered from all animals; this involved moving the sheep to different holding pens for varying lengths of time before being returned to the original designated environment. Two weeks prior to completion of the study, all sheep were moved into individual indoor holding pens to conduct pre-mortem physiological measurements and plasma sampling.

During the experimental procedure, there were a small number of animal losses during the lactation and post-natal weaning stages. Figures 2.1-2.2 (p60), summarise the experimental animal models used, and the final group definitions and sample numbers. The final grouping of the experimental subjects for statistical analysis is discussed in 2.10, p101.

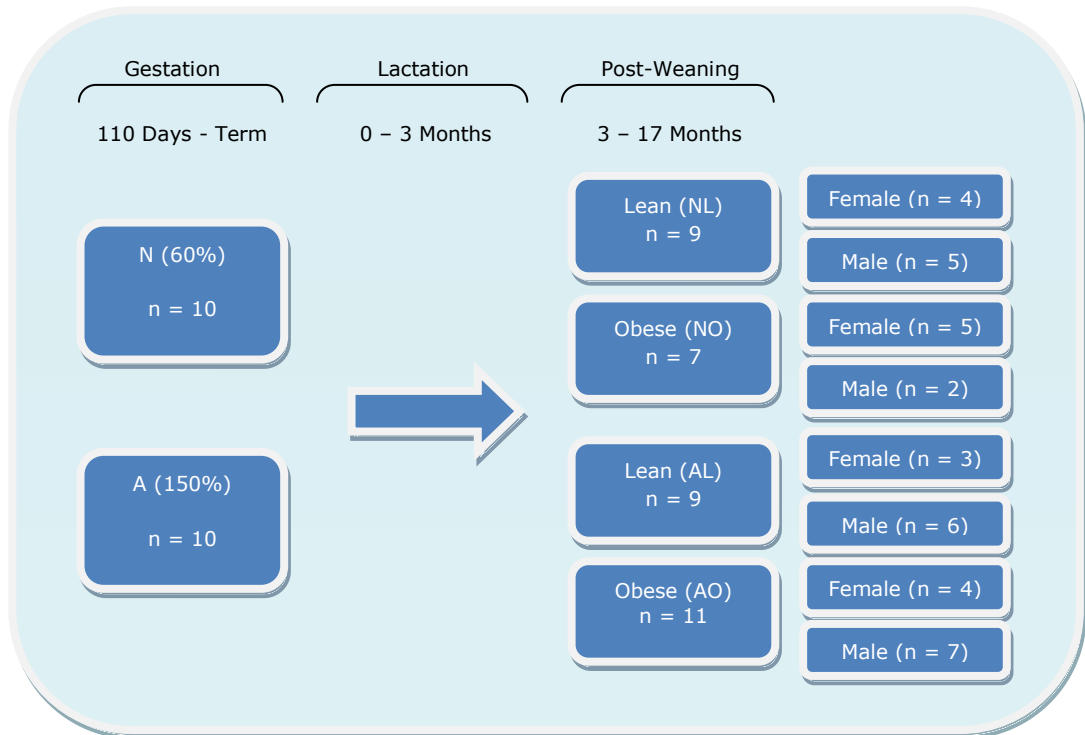


Figure 2.1: Initial experimental animal groups: N = nutrient restricted (60% of normal energy requirements), A = fed to appetite (150% of normal energy requirements), L = lean environment, O = obesogenic environment, and breakdown of groups into gender. Four animals between the NL and NO groups expired during the experimental procedure.

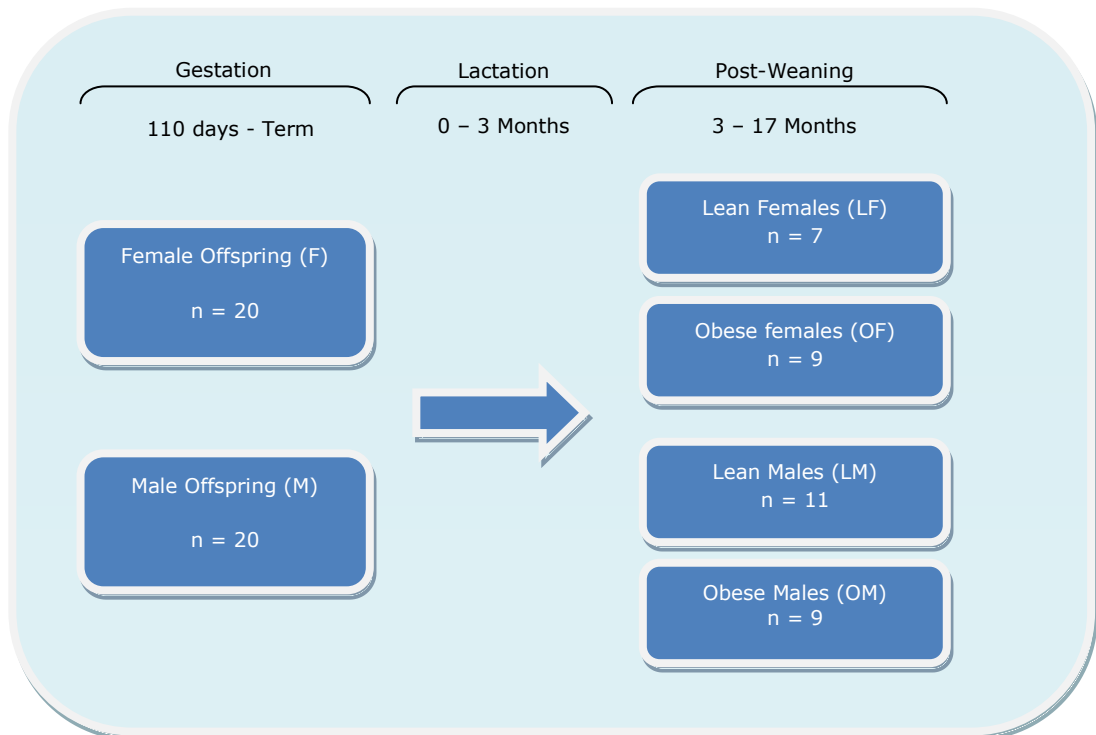


Figure 2.2: Final experimental animal groups: LF = lean females, OF = obese females, LM = lean males and OM = obese males. Four female animals expired during the experimental procedure.

2.2.2 Physiological measurements

Body weight measurements were determined every 3 days, including immediately at birth, during the first month and then once every week up until 3 months of age. Body weights were measured at specific time points until the completion of the study. All body weight measurements were determined by standard weighing scales. Both diastolic and systolic blood pressure measurements were determined at 16 months with a standard blood pressure measuring device during sedation.

2.2.3 Dual x-ray absorptiometry

Alongside these measurements, bone densities, fat mass and free fat mass were determined by dual x-ray absorptiometry²³⁴ (DXA) at 8 and 16 months of age. Overnight fasted sheep were sedated with an intramuscular injection of ketamine and xylazine and scanned for 15 minutes using a Lunar DPX-L bone densitometer (Lunar, Florida, USA). After scanning, animals were allowed to recover from sedation and were returned to the holding pens. To validate the DXA scan method, whole carcass chemical analysis was performed. Fourteen half carcasses were scanned by DXA before being macerated and dried. Nitrogen content and fat percentage analysis were determined on 250g of dried homogenised tissue using a FlashEA1112 nitrogen analyser (Thermo Scientific, Massachusetts, USA) and Gerhardt Soxtherm fat analyser (Wolflabs, York, UK).

2.2.4 Plasma sampling

At 6 and 16 months of age, overnight fasted sheep ($\approx 0800\text{h}$) were locally anaesthetised with lidocaine, and temporary jugular vein catheters were surgically implanted. Twenty four hours after surgery, sheep were subjected to intravenous glucose tolerance tests (GTT) by injecting a bolus. 5ml blood samples were withdrawn into ethylenediaminetetraacetic acid (EDTA) tubes at -10, -5, 10, 20, 30, 60, 90 and 120 minutes following 0.5g kg^{-1} glucose perfusion. A normal feeding regime was restored after the glucose tolerance test had been performed. After 48 hours, 5ml blood samples were withdrawn from overnight fasted animals into lithium heparin tubes for use in determination of circulatory leptin and cortisol levels at 0, 2, 4, 8 and 24 hour time points after being fed to requirement.

Following blood collection, both heparin and EDTA samples were rapidly centrifuged at 2500g for 10 minutes at 4°C to obtain plasma samples that were then stored at -80°C until analysis. Plasma leptin (Diasorin, Slough, UK) and cortisol (Diagnostic Products Corporation coat-a-count, Siemens, Camberley, UK) were determined by radioimmunoassay. Plasma insulin was measured by sheep insulin enzyme linked immunosorbent assay (ELISA) kit (Mercodia, Diagenics Ltd, Milton Keynes, UK).

2.2.5 Post mortem analysis

All animals were humanely euthanised between 0900h and 1100h by electrical stunning and exsanguination. All major tissues, glands, adipose depots and organs were weighed. Selected tissues sampled were partially dissected for histological analysis and fixed in 10% formalin. All remaining tissues were 'snap' frozen in liquid nitrogen and stored at -80°C.

2.3 Tissue analysis

Prior to all tissue and analytical molecular work, benches and instruments were cleaned with RNase Zap[®] (Ambion, California, USA), or 1% Virkon disinfectant (Antec International, Suffolk, UK) and 70% denatured ethanol (Ecolabs, Surrey, UK). Additionally, all experimental work was performed on ice, using autoclaved and sterile equipment including filter pipette tips, whilst wearing gloves. This was to eliminate possible contamination and ensure and preserve the integrity of all samples throughout the performed experimental procedures. The selected tissues were removed from -80°C storage and transferred to dry ice for sampling. The desired amount of renal cortical tissue or PAT was dissected for use in the relative assay and placed in labelled containers for later use. All samples were returned to -80°C storage until needed.

2.4 Ribonucleic acid extraction

Total Ribonucleic acid (RNA) extraction from tissue can be achieved using an adapted version of the single step acidified phenol-chloroform homogenisation method²³⁵ alongside an RNA extraction kit. By lysing the desired samples and homogenising in a phenol and guanidine thiocyanate mono-phase solution, this causes the denaturing and dissolution of all proteins and inhibition of any RNase activity²³⁶. Addition of chloroform leads to the formation of three phase layers, with proteins dissolved in the organic bottom phase, DNA dissolved in the interphase and RNA dissolved exclusively in the top aqueous phase^{235,236}. After separation, the aqueous RNA solution should be treated with ethanol to provide appropriate binding conditions to the RNA centrifuge column where total RNA ($\geq 100\mu\text{g}$) binds to the membrane. A series of washing steps with ethanol and guanidium salt-based buffers to remove any contaminants is performed before the final elution of RNA using nuclease-free water. Extracted RNA yields are unknown and can contain proteinaceous impurities, it is therefore necessary to determine the concentration and purity of extracted samples. One method by which this is achieved is through spectrophotometry. Nucleic acids absorb UV light at a wavelength of 260nm and thus RNA concentration can be estimated through relative wavelength absorption. As protein absorbs UV light at 280nm, protein contamination of the sample can also be measured through a ratio of absorption between wavelengths 260nm:280nm²³⁷; the recommended absorbance ratio for RNA is between 1.8 and 2.0²³⁸.

2.4.1 RNA extraction procedure

Cortical ($\approx 0.15\text{g}$) or PAT ($\approx 1.0\text{g}$) tissue samples were individually added to 1ml of TRI[®] Reagent. The samples were homogenised at 3000rpm using a Dispomix homogeniser (Medic Tools, Zurich, Switzerland) and then centrifuged for 1 minute at 550g. PAT samples were incubated for 2 minutes in a water bath at 37°C to break down the lipid content. Following this, the supernatant was transferred to a sterile 1.5ml eppendorf tube. 200 μl of analytical-grade chloroform (Fisher Scientific, Leicestershire, UK) was added, vortexed and left at room temperature for 10 minutes to allow for phase separation.

Following incubation, the samples were centrifuged at 12000g for 15 minutes at 4°C after which the top aqueous layer ($\approx 600\mu\text{l}$) was pipetted into a genomic deoxyribonucleic acid (gDNA) column and centrifuged at 8000g for 30 seconds at room temperature, to remove any remaining gDNA contamination. The remaining RNA was transferred into a sterile 2ml eppendorf tube and 700 μl of ethanol was added to the solution.

RNA was extracted from each individual sample using the RNeasy Plus Mini extraction kit (Qiagen, West Sussex, UK) by transferring the solution to a RNeasy minispin column and centrifuging at 8000g for 15 seconds at room temperature, discarding any flow-through, with all RNA being retained in the column. 700 μl of RW1 buffer was added to the column and centrifuged at 8000g for 15 seconds at room temperature, discarding the flow-through. 500 μl of RPE buffer was then added and centrifuged at 8000g for 2 minutes at room temperature, discarding the flow-through. The minispin column was then transferred to a sterile 2ml collection tube and centrifuged at 8000g for 1 minute to eliminate any chance of RPE buffer carry-over, which could interfere with future RNA applications. The minispin column was then transferred to a sterile 1.5ml collection tube; 30 μl of RNase-free water was added and centrifuged at 8000g for 1 minute. This final step was repeated to obtain higher concentrations of RNA. RNA concentration and purity measurements were determined using a Nanodrop[®]ND-1000 (Nanodrop Technologies, Wilmington, USA) spectrophotometer. To avoid freeze-thawing stock RNA which is attributed to RNA degradation²³⁸, 10 μl aliquots of each extracted RNA stock were then diluted to 1 $\mu\text{g}/\mu\text{l}$ to normalise samples ready for quantitative RT-PCR. All extracted RNA samples were stored at -80°C until further use.

2.4.2 Polymerase chain reaction

The concept and development of hot-start polymerase chain reaction (PCR) was a huge breakthrough in DNA analysis, and allowed the isolation and amplification of a specific region of a small known quantity of DNA sequence using a pair of complimentary oligonucleotide forward and reverse primers in an enzymatic reaction²³⁹. This reaction contains the target DNA, primers, deoxyribonucleoside triphosphates (dNTPs), thermostable enzyme (Taq Polymerase), and suitable pH and ion buffer.

Amplification of the target sequence occurs by repeated cycles of heat denaturation of the double stranded DNA, annealing primers to the complimentary sequence and extension of the annealed primers by enzymatic reaction. After each full cycle, the product of DNA is doubled, leading to an exponential increase of target DNA, approximately 2^n , where n is the number of cycles²⁴⁰. Figure 2.3 shows the basic PCR process and the exponential amplification of the target DNA sequence.

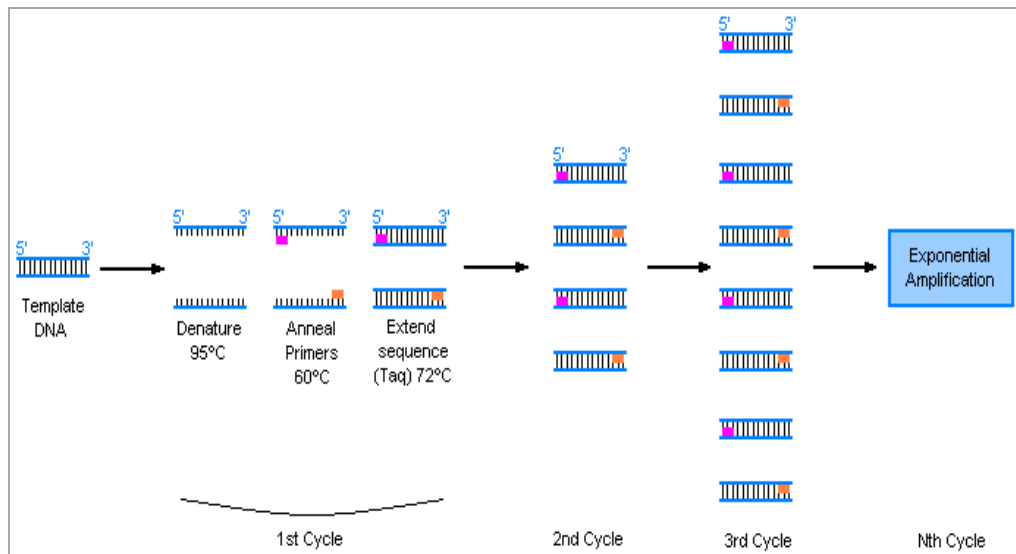


Figure 2.3: Basic theory of polymerase chain reaction. Template DNA is amplified exponentially in an enzymatic reaction of temperature controlled cycles by complimentary oligonucleotide primers.

Primer design is probably the most important aspect when working with PCR analysis, as elongation and amplification will only occur on the DNA sequence to which the complimentary primers have annealed. Poorly designed primers can lead to a decreased product yield, through interaction between each other to form primer dimers and hairpins or through dissimilar annealing and melting temperatures, which is affected by primer length and sequence content²³⁹. Table 2.1 (p68) shows the general parameter guidelines for optimal PCR primer design.

Parameter	Optimal Values
Primer Length	18-30 bases
Melting Temperature (T_m)	55-72°C
Percentage guanine/cytosine (GC) content	40-60%
No self-complimentarity (hairpin structures)	≤ 3 continuous bases
No-complimentarity to other primer (primer dimers)	≤ 3 continuous bases
Distance between two primers on target sequence	<2000 bases apart
T_m difference between forward and reverse primer set	≤ 5°C
No long runs with the same base	< 4 continuous bases

Table 2.1: *General parameter guidelines for optimal polymerase chain reaction primer design*²³⁹.

2.4.3 Reverse transcription PCR

PCR has the ability to amplify low-abundance messenger ribonucleic acid (mRNA) obtained from nucleated tissue samples, which can then be quantified by agarose gel electrophoresis and chemiluminescence, or spectrophotometry²⁴¹. As the principle of PCR is based on amplifying a double stranded molecule such as DNA, for single stranded RNA to work within the reaction, it must first be transcribed into double stranded complimentary DNA (cDNA) using a DNA primer and a reverse transcriptase enzyme; a process known as reverse transcriptase PCR (RT-PCR).

Using template mRNA, a DNA primer sequence anneals to its complimentary sequence of mRNA where elongation and transcription occurs by enzymatic reaction, thus creating a cDNA molecule ready for standard PCR to convert to a double stranded molecule and further amplification. Figure 2.4 (p69) shows a diagram of the basic principles of RT-PCR.

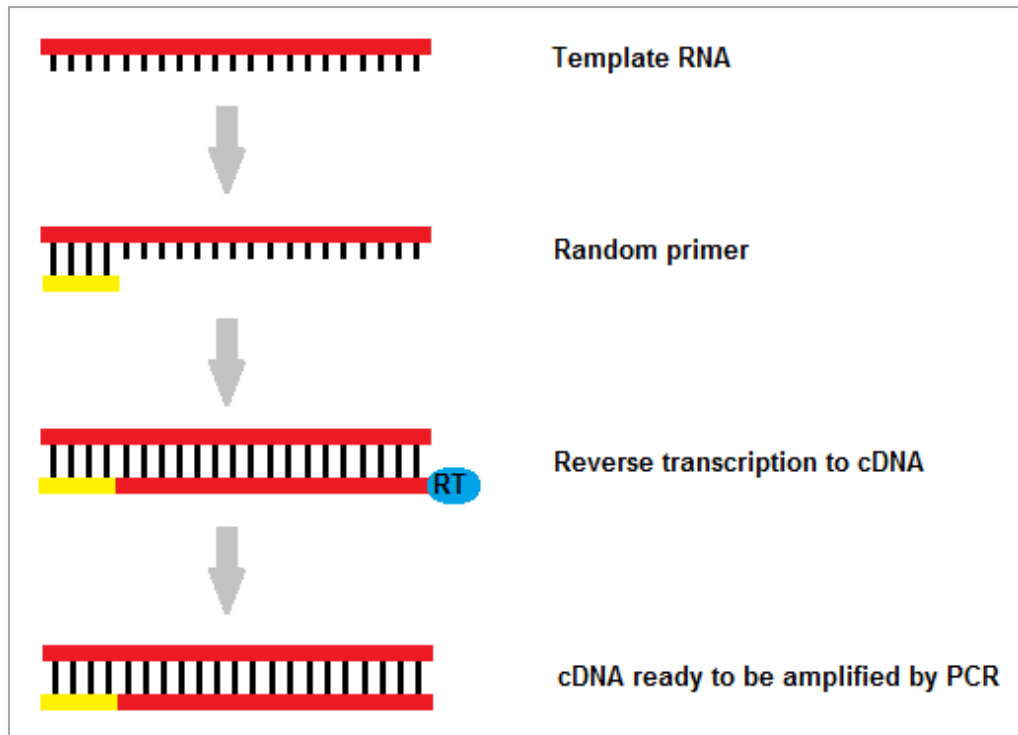


Figure 2.4: Diagram of reverse transcription polymerase chain reaction. A random primer binds to single stranded mRNA and sequence is elongated by a transcriptase enzyme to create cDNA. Template of double stranded cDNA is then amplified by classic PCR.

2.4.4 Quantitative PCR

Through advancements in PCR technology, nucleic acid analysis can now be achieved in real-time, i.e. detection and quantification of a sequence of DNA or mRNA can occur at the same time *in vitro* without additional steps of analysis such as gel electrophoresis or northern blotting, thus reducing time taken, expenditure and the probability of contamination²⁴². Quantitative PCR (Q-PCR) also removes the need to use hazardous fluorescent nucleic acid reagent dyes, such as ethidium bromide. Q-PCR detects and quantifies a PCR product by measuring a signal of fluorescence which is emitted by a fluorogenic chemical reagent when bound to DNA or cDNA. The intensity of fluorescent signal correlates to the amount of DNA bound to the fluorogenic tag, i.e. the greater the intensity of signal, the higher the concentration of DNA present. As these dyes emit a basal level of fluorescence, the detector unit within the Q-PCR instrument will only detect the fluorescent signal after a certain level of background fluorescent has been crossed, also referred to as the cycle threshold (c_t) or crossing point (c_p). The cycle threshold is the parameter used for quantification and correlates to the initial amount of target template.²⁴³

As the amplification of the targeted sequence within the PCR reaction is exponential, the instrument graphically represents this increase in fluorescent signal as a sigmoidal curve, from which the linear section of the curve can be compared to signals from other samples run within the same experiment, see Figure 2.5.

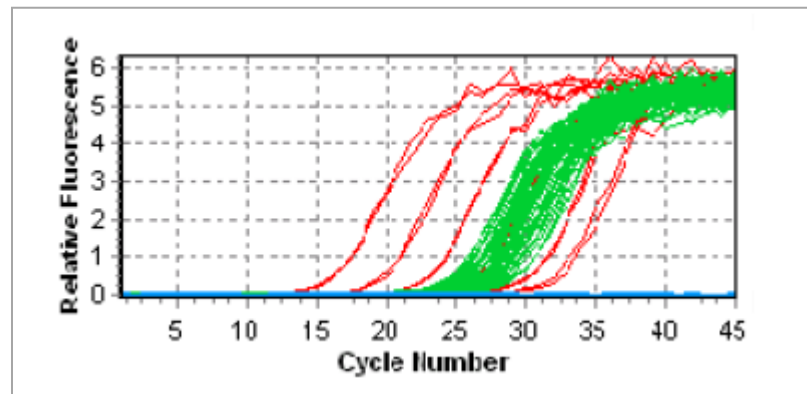


Figure 2.5: Typical 'sigmoidal' curves in Q-PCR. Fluorescent signal crosses threshold and increases exponentially until plateau from expenditure of reagents or cycle number. Red lines represent external standards, green are unknown samples and blue represent negative controls.

This method of analysis allows quantitation of cDNA concentration by standard curve method, where serial dilutions of a known concentration of target cDNA are amplified using the target sequence primers and then used to interpolate the concentration of an unknown from a standard curve. By plotting the log concentration of standards against cycle number when cycle threshold is reached on a graph, and thus calculating a straight line equation, shown in Figure 2.6 (p71), the efficiency of the reaction (E) and correlation coefficient (R^2) can be determined. This additionally acts as a positive control and verification of the experiment. Efficiency is calculated by the following formula, **Efficiency of PCR reaction = $10^{(-1/\text{gradient})} - 1$** ²⁴⁴; which is a derived from the basic equation describing PCR amplification²⁴⁵.

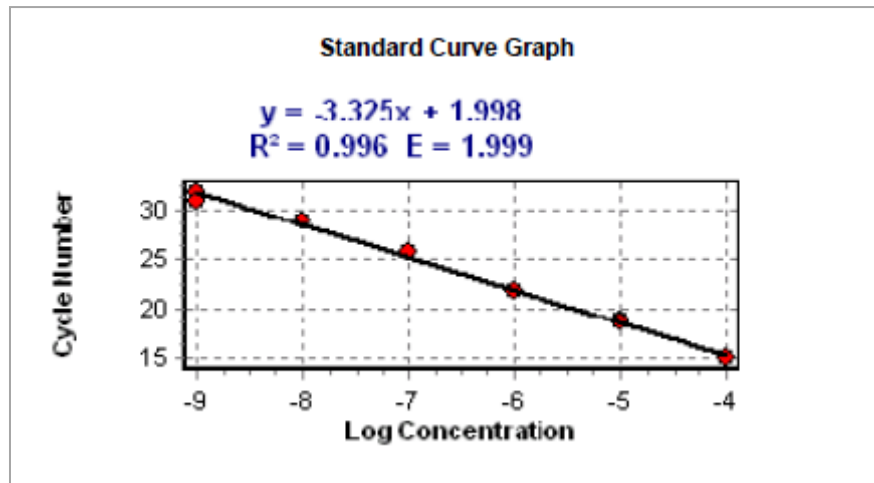


Figure 2.6: Standard curve from Q-PCR. Cycle number at cycle threshold is plotted against logarithm of known dilution series to produce linearised graph of exponential PCR reaction. Correlation coefficient (R^2) and reaction efficiency (E) are then calculated.

To quantify gene expression, it is vital to normalise samples for any variation in starting RNA abundance. By analysing the expression of a gene which is expressed at relatively constant high levels across all cells in many or all known conditions, usually a gene needed for cell function, it is possible to normalise mRNA expression levels for a target tissue. Comparison of the expression of the 'reference gene' against the gene of interest from the same sample makes it possible to quantify expression of the target gene. Using a mathematical model of a ratio of change in cycle threshold of reference control against the change in cycle threshold of target gene, relative gene expression can be calculated. Using the $2^{-\Delta c_t}$ ($2^{-\Delta c_t}$) method presented by PE Applied Biosystems²⁴⁶, where $\Delta c_t = [\text{average } c_t \text{ of target gene} - \text{average } c_t \text{ of reference gene (of the same sample)}]$, this method assumes that the efficiency of the PCR reaction is 100%, i.e. the cDNA strands replicate entirely within each cycle, hence 2^1 . This assumption of efficiency is verified by the standard curve, whereby general accepted efficiency limits range from 90-105%²⁴⁴.

As with standard PCR, primer design is a key component to specific region amplification of a sequence. However, fluorescent dyes such as SYBR green do not only fluoresce when bound to the desired double stranded DNA molecule, but also to non-specific bound dye-DNA complexes, for example, primer dimers. Thus, it is important to analyse the PCR product qualitatively to ensure the PCR product is the sequence targeted.

This is verified by performing a melt-curve, which records the temperature at which the PCR product(s) denature by measuring decrease in fluorescent signal. Melting temperatures are influenced by length and sequence base composition, and an expected melt curve for a specific product should produce one peak, see Figure 2.7. Further qualitative analysis can be performed by DNA sequencing after the product has been extracted by gel electrophoresis.

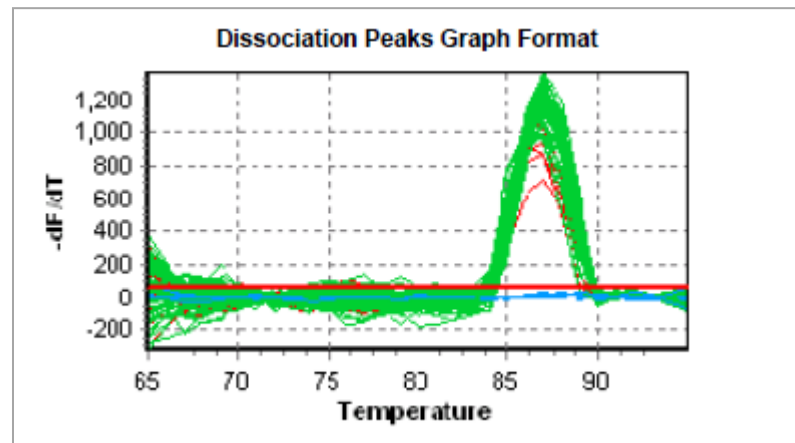


Figure 2.7: Typical melt curve from Q-PCR. The single peak indicates specificity of product amplified.

2.4.4.1 Reference genes in Q-PCR

The use of reference genes as internal controls and for RNA quantification is a common method, but it is vital that the selected reference gene(s) are validated when used in a particular tissue or with a specific experimental model²⁴⁷. A good reference gene by definition should have very little variation in expression throughout sample sets and be expressed relatively higher than any genes of interest²⁴⁸. Existing proposals in gene normalisation suggest that to accurately measure mRNA expression levels, the geometric mean of multiple reference genes should be utilised^{247,249}, however it is still important that any reference genes used match the criteria necessary to be a good reference gene. In an attempt to validate various reference genes, the genes ribosomal 18s (r18s), beta-actin (ACTB) & Tyrosine 3-monooxygenase/tryptophan 5-monooxygenase activation protein (YWHAZ), which have all been validated as reference genes in previous studies^{249,250,251}, were analysed to quantify expression in the specific tissue and animal model used in this project. Of the three genes analysed, only r18s yielded acceptable levels of expression and variation between samples to be a suitable candidate reference gene, see Figure 2.8, p73, a finding supported by other RT-PCR studies^{252,253}.

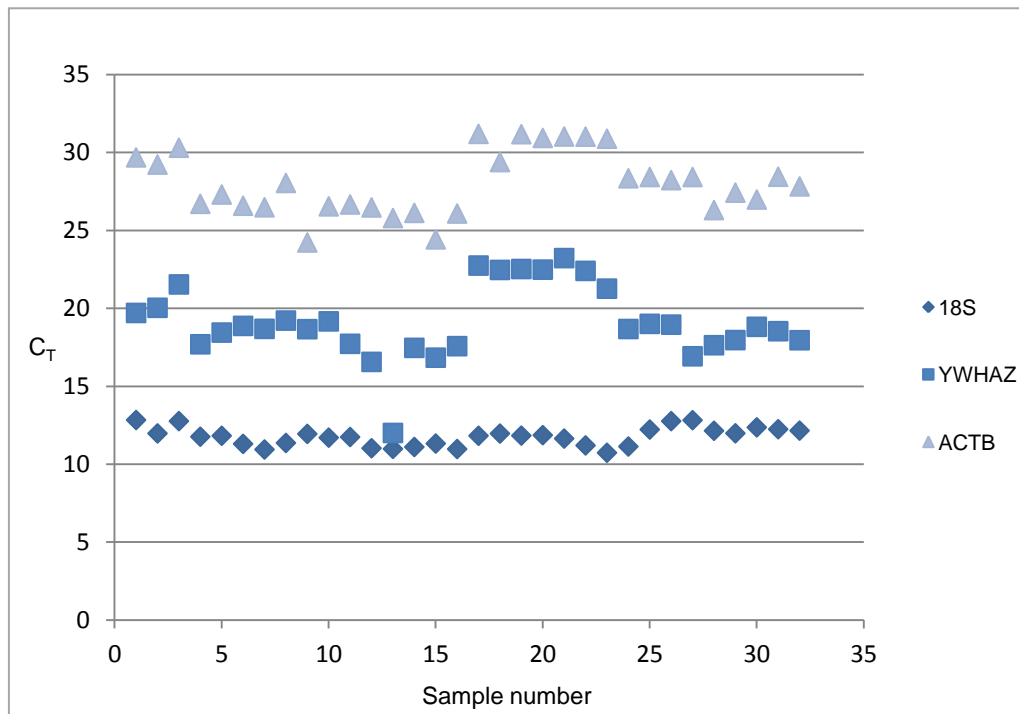


Figure 2.8: Comparison of three genes *r18s*, *YWHAZ* and *ACTB*. Crossing threshold of each gene was determined against 32 samples to validate use as mRNA reference gene.

As *YWHAZ* and *ACTB* displayed high variation and low expression, using them as controls in a multiple reference gene normalisation would reduce the effectiveness of such calculations and therefore only a single reference gene, i.e. *r18s* was used for normalisation in the QPCR analyses of renal tissue.

Due to intergroup variation of *r18s* mRNA expression in PAT samples, QPCR analysis performed on PAT was normalised using multiple reference genes, shown in Table 2.2, p75. Each reference gene was run against the study samples, and crossing threshold values for each reference gene were processed through geNorm software v3.5 (Primer Design Ltd, Southampton, UK). The geNorm software uses an algorithm of the geometric mean and pairwise variation of each gene compared to all other genes analysed, to calculate a stability value (M) for each gene and selects the two most stable genes, i.e. the two genes with the lowest M value for normalisation^{247,249}. The geNorm software then calculates a normalisation factor for each sample. Relative target gene values are divided by the normalisation factor to determine the gene of interest's expression. Figure 2.9, p74 shows the geNorm output from the four reference genes used in PAT mRNA analysis; a lower M values confirms higher stability.

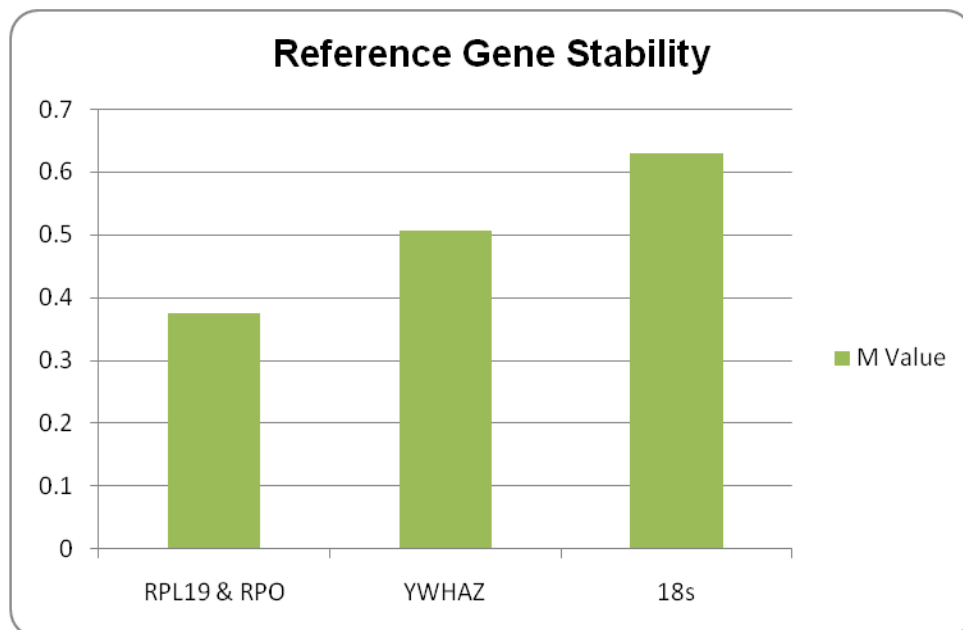


Figure 2.9: Graphical output from *geNorm* software in analysis of four reference genes. A lower *M* value represents a higher stability. A combination of *RPL19* and *RPO* were determined to have the highest stability of the reference genes analysed, and were used to calculate *PAT* sample gene expression.

2.4.5 Development of oligonucleotide primers for Q-PCR

Primers were designed using Beacon Designer 4.0 software (Premier Biosoft, Palo Alto, USA) using the sheep genome sequence from the National Centre for Biotechnology Information (NCBI) online database. The primer design software ensures amplification with greater specificity to the gene of interest by designing primers that flank exon boundaries in the intron sequence, and creates primers with similar optimum annealing temperatures, guanine-cytosine base pair content and length to achieve the most favourable reaction conditions. All designed primers were checked against the sequence and genome of interest using the NCBI nucleotide BLAST database to ensure amplification of the correct sequence. Primers were developed by and acquired from Sigma Aldrich or previously optimised by Dr S Sebert, Dr M Hyatt and Dr D Sharkey within the Academic Child Health Laboratory, Queen's Medical Centre, Nottingham, UK and stored in nuclease free water at a stock concentration of 100µmol/l. Tables 2.2, 2.3 and 2.4 (p75-77) detail all primer sequences used in mRNA quantification.

Reference Gene	Publication or NCBI seq.	Oligonucleotide Sequence (5'-3')
18s ribosomal RNA (r18s)	Williams P.J, et al (2007)	For - GATGCGGCGGCGTTATTCC
		Rev - CTCCTGGTGGTGCCCTCC
L19 ribosomal protein (RPL19)	Garcia-Crespo D, et al (2006)	For - CCGGGAATGGACAGTCACA
		Rev - CAACTCCCGCCAGCAGAT
Large ribosomal protein (RPO)	Robinson T.L, et al (2007)	For - CAACCCTGAAGTGCTTGACAT
		Rev - AGGCAGATGGATCAGCCA
tyrosine 3-monooxygenase/tryptophan 5-monooxygenase activation protein (YWHAZ)	Garcia-Crespo D, et al (2006)	For - TGTAGGAGCCCGTAGGTCATCT
		Rev - TTCTCTGTATTCTCGAGCCATCT

Table 2.2: Reference gene primer sequences for mRNA quantification.

Target Gene	Publication or NCBI seq.	Oligonucleotide Sequence (5'-3')
11 β hydroxysteroid dehydrogenase 1 (11βHSD1)	NM_001009395.1	For - GGCCAGATCCCTGTCTGAT
		Rev - AGCGGGATACCACCTTCTTT
11 β hydroxysteroid dehydrogenase 2 (11βHSD2)	Dodic M, et al (2002)	For - AGCAGGAGACATGCCGTTTC
		Rev - GCAATGCCAAGGCTGCTT
Adiponectin (ADI)	NC_007299.4	For - ATCAAACCTCTGGAACCTCTATCTAC
		Rev - TTGCATTGCAGGCTCAAG
Adiponectin receptor 2 (ADIPOR2)	NC_007303.4	For - GGCAAGTGTGACATCTGGTTTC
		Rev - GAAACGGAACCTCTGGAGGTT
Chemokine (C-C motif) receptor 2 (CCR2)	Sharkey D, et al (2009)	For - TGTCATGCTGTGTTTGCTT
		Rev - CCCAAGATGCTCCTCATAA
Cluster of differentiation-14 (CD14)	NM_001077209.1	For - TCAAGGCTCTGCGGTTCCGG
		Rev - GCAGGCCAGTGGCTTCCAG
Glucocorticoid receptor (GR)	Williams P.J, et al (2007)	For - ACTGCCCCAAGTGAAAACAGA
		Rev - ATGAACAGAAATGGCAGACATT
Intercellular adhesion molecule-1 (ICAM-1)	NM_001009731.1	For - ATGGACTACTGTGACCGTGAATG
		Rev - GGCAGCAGAGCAGGAGAAGTTG
Interferon-γ (IFN-γ)	NM_001009803.1	For - TGCAGATCCAGCGCAAAGCCA
		Rev - TGCTCTCCGGCCTCGAAAGAGA
Interleukin-6 (IL-6)	Sharkey D, et al (2009)	For - ACCACTCCAGCCACACAC
		Rev - GCCGCAGCTACTTCATCC
Interleukin-10 (IL-10)	NM_001009327.1	For - GTGCTCTGTTGCCTGGTCTTC
		Rev - GCTGTTCAAGTTGGTCTTCATTTG
Interleukin-18 (IL-18)	Sharkey D, et al (2009)	For - AACGACCAAGTTCTCTTCATTA
		Rev - GAACAGTCAGAATCAGGCATA
Inducible nitric oxide synthase (iNOS)	AF223942.1	For - TTGAGCGAGTGGTGGATGGC
		Rev - TGAGTGAGCAAGGTGGCAGTC
Leptin (Ob)	NM_173928.2	For - GGGTCACTGGTTGGACTTCA
		Rev - ACTGGCGAGGATCTGTTGGTA
Leptin receptor (Ob-R)	NM_001009763.1	For - TGAAACCACTGCCTCCATCC
		Rev - TCCACTTAAACCATAGCGAATC
Monocyte chemoattractant protein-1 (MCP1)	Dunphy J, et al (2001)	For - GCTGTGATTTTCAAGACCATCC
		Rev - GGCGTCTGGACCCATTT
Toll-like receptor 4 (TLR4)	Sharkey D, et al (2009)	For - TGCTGGCTGCAAAAAGTCTG
		Rev - CCCTGTAGTGAAGGCAGAGC
Tumour necrosis factor-α (TNFα)	NM_001024860.1	For - CCGAGTCTGGGCAGGTCTAC
		Rev - GGGATGAGGAGGTTCTGAAGG
Vascular cell adhesion molecule-1 (VCAM-1)	NM_174484.1	For - TGCTGCTCAGGTTGGCGACTC
		Rev - AGCCCTCACTCCTCACATTCCC

Table 2.3: Inflammatory gene primer sequences for mRNA quantification.

Reference Gene	Publication or NCBI seq.	Oligonucleotide Sequence (5'-3')
Erythropoietin receptor (EPOR)	AY029232.1	For - CCAGGGAGGCCGAAAATG
		Rev - GGACAGTGATATTCTCACTGAAGCT
Peroxisome proliferator activated receptor gamma (PPARγ1)	NM_001100921.1	For - CGCATGCCACAGGCCGAGAA
		Rev - CCCGTCAAGATCGCCCTCGC
Renin	NM_001009299.1	For - GCAGACACCGCCGCTTCAG
		Rev - GTCCACGCCTCGCTCCTTCAG

Table 2.4: Additional gene primer sequences for mRNA quantification.

2.4.6 RT-PCR procedure

Two sterile 0.2ml eppendorf tubes were labeled for each sample, one for the reverse transcription and one for a no-reverse transcription enzyme control to ensure transcription efficiency. A negative RNA template control, replaced with nuclease-free water, was also prepared. The reaction mix for each tube was as follows:

- 1.5 μ l of 1 μ g/ μ l of sample RNA
- 1 μ l of random primer Pd(N)₆ (Roche, Basel Switzerland)
- 7.5 μ l nuclease-free water (Ambion)

Samples were then centrifuged for 1 minute at 5000g and incubated for 10 minutes at 65°C in the Techne Touchgene Gradient thermal cycler (Techne Incorporated, New Jersey, USA) for primer hybridization and elongation.

During the above incubation, reverse transcriptase and control master mixes were prepared, using the method from Superscript II Reverse Transcriptase kit (Invitrogen Life Technologies, Paisley, UK) per sample tube as follows:

- 4 μ l 5x reaction buffer
- 2 μ l dithiothreitol (DTT)
- 1 μ l dNTPs
- 2.5 μ l nuclease-free water (3 μ l in no RT controls)
- 0.5 μ l Superscript[®] II enzyme (omitted from no RT controls)

10 μ l of either RT or no RT master mix was then added to the corresponding sample tube and centrifuged for 1 minute at 10000g. Samples were returned to the thermal cycler and run on the reverse transcription program for 45 minutes at 42°C. After reverse transcription the cDNA samples were stored in a freezer at -20°C.

2.4.7 Hot start PCR procedure

For primer optimization and the creation of cDNA Q-PCR standards, conventional PCR was performed. 0.2ml eppendorf tubes were labeled on ice and reaction mixture added per tube as follows:

- 2µl random cDNA template
- 10µl Thermo start PCR master mix (Abgene, Epsom, UK)
- 1µl 1:10 dilution of forward primer
- 1µl 1:10 dilution of reverse primer
- 6µl nuclease-free water

Negative controls containing no template cDNA and no primers were run concurrently to ensure the integrity of the prior RT-PCR reaction, and as quality controls against genomic DNA contamination. Tubes were centrifuged for 1 minute at 10000g then loaded into the Techne thermal cycler and ran on a 60°C hot start PCR program, the PCR program steps are shown in Table 2.5.

Process	Temperature (°C)	Duration (mins)
Initiation	105	4
Enzyme activation	96	15
Denaturing cDNA strands	94	0.5
Primer annealing	60	0.5
Primer Extension	72	1
Final Extension	72	7
Hold	4	∞

Table 2.5: Hot start PCR program conditions. Second phase of program repeats for 35 cycles.

2.4.8 Agarose gel electrophoresis & DNA extraction

PCR products can be analysed and resolved using a matrix such as agarose or polyacrylamide gel by electrophoresis. DNA molecules are negatively charged due to their phosphate ion backbones and can be separated according to the size of the DNA fragment by applying an electric field to the fragments; smaller fragments migrating further and quicker towards the positive electrode²⁵⁴. To visualise the DNA fragments, it is necessary to add an intercalating DNA dye to the separating medium, usually ethidium bromide, which fluoresces when exposed to ultra-violet light, consequently showing the presence of any DNA fragments as an intense band within the matrix.

By comparison of these unknown fragments with a positive control DNA fragment "ladder", it is possible to identify the size of the unknown bands. To remove the DNA from the agarose gel medium, it is necessary to extract the fragments which can be achieved using commercially available kits. The QIAquick[®] Spin extraction kit utilises high DNA affinity silica membrane columns and buffer washing steps to eliminate any possible contamination or agarose carry-over. The purified suspended DNA can then be eluted using either nuclease-free water or elution buffer.

2.4.8.1 Agarose gel electrophoresis & DNA extraction procedure

2% w/v of agarose electrophoresis grade (Invitrogen Life Technologies) was dissolved in 50ml of 1x TAE buffer, from a 50x stock solution of tris(hydroxymethyl)aminomethane base (tris), glacial acetic acid (Fisher Scientific), EDTA buffer, heated and mixed with 5µl of 10mg/ml ethidium bromide for visualization, and cooled to form a gel. PCR products were dyed with glycerol blue dye and passed through the gel alongside a DNA marker ladder (100bp Blue eXtendec, Bioron, Ludwigshafen, Germany) at 100v for 50 minutes. Gels and PCR products were visualised under a UV trans-illuminator CCD camera (Fuji film luminescent image analyser LAS-1000 v1.01). Fluorescent gel bands were cut out of the gel and extraction and purification of the PCR products was achieved using the QIAquick[®] gel extraction kit (Qiagen).

Dissected gel bands were weighed and re-dissolved in 1.5ml eppendorf tubes in 300µl GQ buffer per 100µg of gel at 50°C for 10 minutes. Once dissolved, 100µl isopropanol (Fisher Scientific) per 100µg of gel was added and the solution vortexed to aid DNA precipitation. This agarose-buffer mixture was then pipetted into a QIAquick spin column and centrifuged at 10000g for 1 minute, with any GQ buffer and isopropanol filtrate discarded. 500µl of GQ buffer was added to the spin column and centrifuged at 10000g for 1 minute to remove any remaining trace of agarose; again all filtrate was discarded. 700µl of PE buffer containing ethanol was added to the spin column, allowed to stand for 5 minutes and centrifuged at 10000g for 1 minute, with the filtrate discarded. The spin column was transferred to a fresh 2ml tube and centrifuged at 10000g for 1 minute to ensure removal of all residual PE buffer. The spin column was then transferred to a 1.5ml eppendorf tube and DNA was eluted by pipetting 30µl of elution buffer (EB buffer) directly onto the column membrane and centrifuging at 10000g for 1 minute.

Concentration and integrity measurements of the final DNA product were analysed using the nanodrop spectrophotometer. Samples from newly designed primer products were sent for DNA sequencing within the University of Nottingham's Centre for Genetics and Genomics (Queen's Medical Centre, Nottingham UK) and cross-referenced against the NCBI online database. All extracted and purified DNA samples were diluted to 1ng/μl aliquots and stored at -20°C until needed.

2.4.9 Q-PCR procedure

For each gene analysed, serial dilutions up to and including 1×10^{-9} from the 1ng/μl template cDNA gene standard were created and run in the Q-PCR experiment with the unknown samples to verify the efficiency of the experiment. For gene expression analysis, all unknown samples were measured with housekeeping gene r18s to normalise all unknown cDNA samples.

Samples and standards were loaded into a 96 well PCR plate (Abgene) in 15μl aliquots from a Q-PCR master mix, protocol for each individual well as follows:

- 4.5μl 1:10 nuclease-free water dilution of sample or standard
- 7.5μl of SYBR[®] green (Thermo Scientific) containing Taq DNA polymerase, magnesium chloride, dNTP mix in optimised buffer
- 1.5μl 1:40 dilution of forward primer
- 1.5μl 1:40 dilution of reverse primer

Samples and standards were run in duplicate to calculate the coefficient of variation within each experiment. Negative controls for no template cDNA and no primers were also run for each gene analysed.

Once prepared, PCR plates were heat sealed using an Abgene plate sealer and thermal seals (Alpha Laboratories, Hampshire, UK) and placed in the Quantica[®] Q-PCR instrument (Techne) or the StepOne Plus Real Time PCR System (Applied Biosystems). Q-PCR program steps are shown in Table 2.6, p81.

Process	Temperature	Duration
Initial denaturing of cDNA strand	95°C	15 minutes
Denaturing cDNA strand	95°C	15 seconds
Annealing of primers*	58-62°C	30 seconds
<i>For 45 cycles</i>		
Melt curve analysis	65 to 95°C in 1°C increments	15 minutes
<i>For 31 cycles</i>		
Hold	95°C	10 minutes

Table 2.6: *QPCR program conditions. * denotes range of optimal temperatures for genes analysed.*

Q-PCR analysis was measured using the Quansoft® (Techne) or the StepOne™ v2.2 (Applied Biosystems) software packages and gene expression data converted to and analysed using the $2^{-\Delta ct}$ method for kidney or gene of interest expression against a genorm normalization factor for PAT.

2.5 Histology

Histology is the anatomical microscopic study of sectioned tissues enabling visualisation of the structure and cellular composition, which can be enhanced by various histological stains. It is necessary to chemically fix all tissue prior to histology to preserve it from degradation; this is achieved by fixing the tissue in formaldehyde which irreversibly cross-links proteins contained in the tissue to preserve the sample²⁵⁵. It is also essential to encase the tissue in a holding matrix to maintain the structural and cellular composition of the sample and allow sectioning for microscopic analysis. A suitable matrix must be able to flood and permeate throughout the sample without disturbing or damaging its structure which can then solidify to suspend the tissue. A widely used matrix in light microscopy is paraffin wax. As paraffin wax is immiscible in water, a dehydration step must be performed on any tissue before embedding in the wax, usually by treatment with a dehydrating agent and a hydrophobic clearing chemical, usually by immersing the samples in ethanol & xylene. Once embedded, tissue sections can be sliced using a microtome.

2.5.1 Histological tissue processing

Renal and PAT from each animal were treated with 10% formalin (10% v/v formaldehyde in 0.9% w/v sodium chloride/distilled water (Fisher Scientific) saline solution) for two hours. Segments of each sample were loaded into a Histosette II (Simport, Quebec, Canada) 30mm x 27mm x 5mm cassette and processed through six stages of ethanol dehydration followed by three stages of xylene (Fisher Scientific) for ethanol-clearing. Samples were then immersed in three stages of paraffin wax using the Shandon Excelsior™ tissue wax processor (Thermo Scientific) at 60°C, and allowed to solidify overnight. Once the tissue samples had been paraffin blocked, they were sectioned for 10 slides per sample at 5µm, using a sledge microtome (Anglia Scientific, Cambridge, UK), rinsed in 70% ethanol and floated in 45°C water to stretch out the slices by surface tension. Sections were transferred to Superfrost™ Plus slides (Menzel-Gläser Inc, Braunschweig, Germany), dried on a heat rack for 15 minutes and stored in a drying oven at 37°C for 24 hours.

2.5.2 Haematoxylin and eosin staining

Harris' haematoxylin is a basic aluminium salt dye used for nuclear staining in tissue. Haematoxylin is oxidised to haematein by the chemical oxidising agent mercuric oxide and binds to acidic structures, i.e. nucleic acids, with the addition of an aluminium salt mordant. It is used as a regressive dye and is reduced in intensity and "blued" off by washing with a weak alkali^{256,257}. Eosin Yellowish is used as a contrasting dye to haematoxylin for visualising the tissue architecture surrounding the nuclei. Eosin is an acidic dye which binds to basic structures, termed eosinophilic, staining proteinaceous material such as cytosol, muscle fibres, collagen and erythrocytes²⁵⁶. Differentiation of the eosinophilic formations occurs through washing with water.

Haematoxylin and eosin (H&E) staining is widely used in kidney histology to examine the renal structure and architecture of samples. The development or presence of disease and injury, in particular renal tubule and glomerular abnormalities^{258,259}, can be assessed by observational study and through quantitative analysis.

2.5.2.1 H&E staining procedure

One slide from each sample was blinded by assignation of a random identifier and placed in a slide rack. Slides were dewaxed by immersion in two consecutive xylene troughs for 3 minutes and rehydrated through two stages of 100% ethanol immersion and one stage of 70% ethanol/distilled water immersion, before a final wash with distilled water. The sections were nuclear-stained in a trough of Harris' haematoxylin (VWR Ltd, Lutterworth, UK) for 5 minutes and then rinsed in tap water for 5 minutes to remove all excess dye. The haematoxylin stain was regressed by immersion in an acid-alcohol (1% conc. hydrochloric acid in 70% ethanol) solution for 5 seconds, rinsed in tap water and "blued" off in alkaline Scott's tap water (a 0.2% sodium bicarbonate and 20% magnesium sulphate distilled water solution) for 1 minute. Slides were washed in tap water, transferred to a 1% Eosin Yellowish (VWR Ltd) counter stain for 3 minutes, and washed in tap water afterwards to remove any excess and to differentiate any eosinophilic staining. Sections were then dehydrated in two stages of 100% ethanol immersion for 2 minutes and ethanol cleared in two 3 minute immersions of xylene. Sections were mounted with coverslips (VWR) using DPX mounting medium (Fisher Scientific), and left to dry overnight.

2.5.2.2 Glomerular H&E analysis

H&E-stained slides were visualised through a Leica DRM microscope (Leica Microsystems, Wetzlar, Germany) at 10x magnification and photographed for analysis using a Hamamatsu digital camera (Hamamatsu, Hertfordshire, UK). Renal sections were generally observed and quantified for changes in glomerular cross-sectional area (excluding Bowman's space) and glomerular cell count. Blinded samples were assessed by a manually optimised and validated technique using Volocity[®] v5.2.0 image software (Perkin Elmer, Massachusetts, USA) in forty randomly- selected glomeruli per sample, based on an adapted glomerular area method as described by Henegar et al²⁶⁰.

2.5.2.3 Perirenal adipocyte H&E analysis

Stained slides were visualised as described in 2.5.2.2 on all complete adipocytes in the field of vision using one slide per lean animal and two slides per obese animal at 20x magnification. Individual adipocyte perimeters (μm) and areas (μm^2) were determined using Volocity image software.

2.5.3 Masson's trichrome staining

Trichrome staining is the general staining technique to differentiate between various connective tissues such as cytoplasm, muscle, collagenous tissue, fibrin and erythrocytes. The three-colour stain works by two acidic dyes with different molecular sizes penetrating and staining proteinaceous material depending on porosity, with the permeating larger molecular dye replacing any initial smaller molecular dye²⁵⁶. Treating the samples with phosphomolybdic acid (PMA) between the small and large molecular dyes, allows the PMA to compete with the small molecular dye removing any excess, behaving as a mediator for and prior to exposure of the larger molecular dye. The larger molecular dye then replaces the PMA²⁵⁶. A third basic nuclear dye is also used within this technique similarly to the H&E method. In Masson's trichrome, the smaller molecular dye is Acid Fuchsin (red/pink), the larger molecular dye is Light Green SF Yellowish (green/blue) and the nuclear stain is Harris' Haematoxylin (purple). These three stains demonstrate the presence of cytoplasm and keratin, collagen and the nuclei respectively.

Masson's trichrome is another histological technique used for kidney analysis. Collagen formation and thickening in renal architecture has been researched as a determinant of renal disease and repair in a number of studies^{261, 262}.

2.5.3.1 Masson's trichrome staining procedure

Similarly to the H&E staining method (p20), one slide per animal was randomly assigned a blind identifier, dewaxed and rehydrated in xylene, ethanol and distilled water baths. Slides were nuclear-stained in Harris' haematoxylin for 5 minutes, regressed and blued off as per the H&E method. Sections were next immersed in a 0.5% Acid Fuchsin (Nustain, University of Nottingham, UK) in 0.5% acetic acid solution for 1 minute and rinsed in tap water before being transferred to 1% PMA (Raymond Lamb, London, UK) solution for 5 minutes.

Slides were then stained in a 2% Light Green Yellowish SF in 2% acetic acid solution for 1 minute, washed in tap water and immersed in a 1% acetic acid solution to remove any excess green dye. Slides were lastly treated in ethanol and xylene troughs to dehydrate the tissue sections, mounted with coverslips using DPX mounting medium and dried overnight.

Masson trichrome stained renal samples were visualised and photographed at four random areas using 5x magnification and blindly assessed by three reviewers for collagen development using an adapted semi-quantitative grading method²⁶³. The grading scale used ranked the amount of positive green/blue staining present in each image i.e. rank 0 = 0%, rank 1 = ≤24.9%, rank 2 = 25-49.9%, rank 3 = 50-74.9%, rank 4 = 75-100%.

2.5.4 Immunohistochemistry

Immunohistochemistry (IHC) is a method of detecting and localising a specific antigen, i.e. a protein of interest, in histological sections through binding of labeled antibodies, which produces a signal upon formation with the target. Antibodies can be conjugated with a variety of signaling markers, including fluorescent dyes and enzymes and used in a direct or indirect method of staining, shown in Figure 2.10, p86. Direct staining involves a primary antibody conjugate that binds with the target antigen to produce a signal; indirect staining uses primary and secondary antibody conjugate complexes, which has the advantage of increased specificity²⁶⁴.

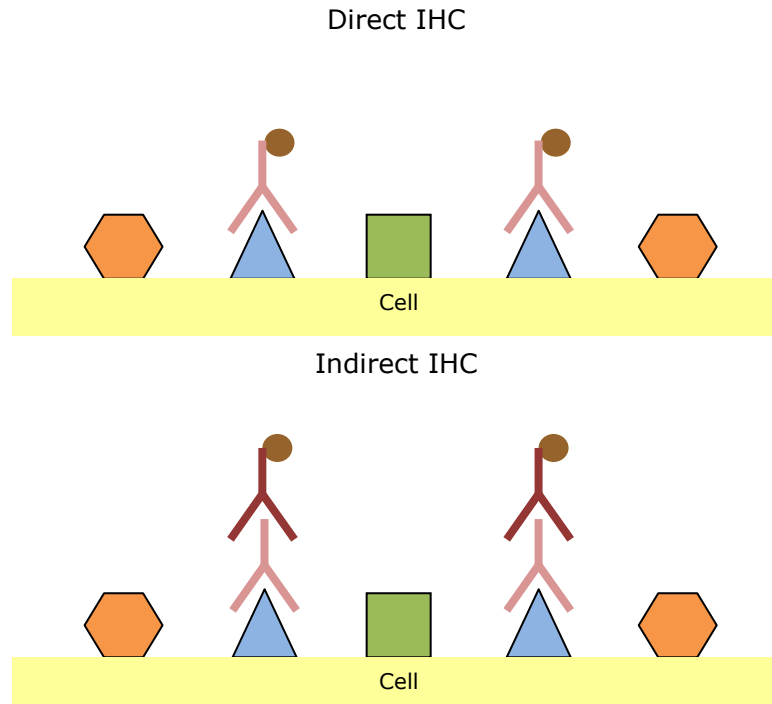


Figure 2.10: Antibody action in direct and indirect immunostaining method. Direct IHC uses a specific primary antibody conjugate to bind to target antigen, producing a signal for measurement, e.g. colour development. Indirect IHC uses a secondary antibody conjugate to bind to the primary antibody to form an antigen-primary-secondary antibody complex to produce the signal, an increased specificity method for antigen detection²⁶⁴.

A common method for indirect IHC is the use of a horseradish peroxidase (HRP) enzyme labeled secondary antibody, which develops a brown precipitate in the presence of 3,3 diaminobenzidine (DAB), a chromogenic substance, through catalytic conversion²⁶⁵. Prior to antibody exposure, it is important that all sections are dewaxed and rehydrated, similarly to histological staining, to allow all reagents access to the tissue. Furthermore the initial formalin fixation of the tissue results in the cross-linking of proteins, which in effect masks many antigenic sites. To break these protein cross-links, samples are treated to a heat-induced epitope retrieval (HIER) step²⁶⁶, usually heating with citrate buffer to unmask all hidden antigenic sites.

2.5.4.1 IHC procedure

One slide per animal and a negative control were labeled with a random identifier, placed in a slide rack and loaded into a Leica BondMax™ IHC slide processor (Leica Microsystems), and run on an automated software program (Vision Biosystems Bond version 3.4A) using Bond polymer refine detection reagents (Leica).

Samples were first treated with 1 minute xylene and 1 minute ethanol washes, before incubation at 95°C with epitope retrieval solution. Samples were then treated with Peroxide Block for 5 minutes at room temperature. All samples except the negative control were then exposed to 150µl of pre-optimised primary polyclonal anti-rabbit antibody (Abcam, Cambridge, UK) dilution (PCNA 1:4000, Abcam 18192; Caspase-3 1:50, Abcam 4051) for 30 minutes, and then exposed to 150µl of HRP conjugated secondary anti-mouse and rabbit antibody polymer for 8 minutes. Sections were subsequently exposed to 3,3 DAB for 10 minutes until brown precipitate had developed, and then nuclear stained with Harris' haematoxylin for 5 minutes for orientation. After each stage on the automated BondMax, slides were washed with Bondwash buffer and distilled water. Tissue sections were mounted with coverslips using DPX mounting medium and dried overnight.

Blinded sections were visualised at 10x magnification and photographed for analysis at ten random areas. Positive stained cell percentage, normalised against total cell number, was estimated using a manually validated technique on Volocity imaging software.

2.6 Plasma metabolite analysis

To help develop a metabolic profile for each of the animals used in the study, collected plasma from overnight fasted animals was analysed for circulating levels of glucose, NEFAs and triglycerides. The following sections describe the reaction principles of the target metabolites measured.

2.6.1 Glucose analysis

The glucose analysis measurement is based on an enzymatic colourimetric reaction adapted from Barham and Trinder²⁶⁷. Glucose, in the presence of oxygen and water, is oxidised by glucose oxidase to form hydrogen peroxide and gluconic acid. The hydrogen peroxide formed then undergoes catalysis by peroxidase to form a violet coloured complex with phenol and 4-aminophenazone, with absorbance measured at 500nm²⁶⁸ (Figure 2.11).

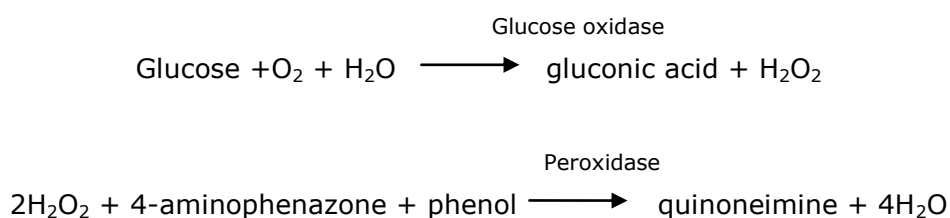


Figure 2.11: Principle enzymatic reaction involved in glucose analysis reaction^{267,268}.

2.6.2 Non-esterified fatty acids analysis

NEFAs can be measured by reaction with acyl-coenzyme-A synthetase which, when added to plasma in the presence of adenosine triphosphate (ATP), forms complex thiol esters of coenzyme-A and hydrogen peroxide²⁶⁹. Oxidation of the formed hydrogen peroxide by peroxidase with N-ethyl-N(2hydroxy-3-sulphopropyl)m-toluidine (TOOS) and 4-aminoantipyrine (4-AAP) forms a purple adduct which can be measured at 550nm, shown in Figure 2.12²⁷⁰.

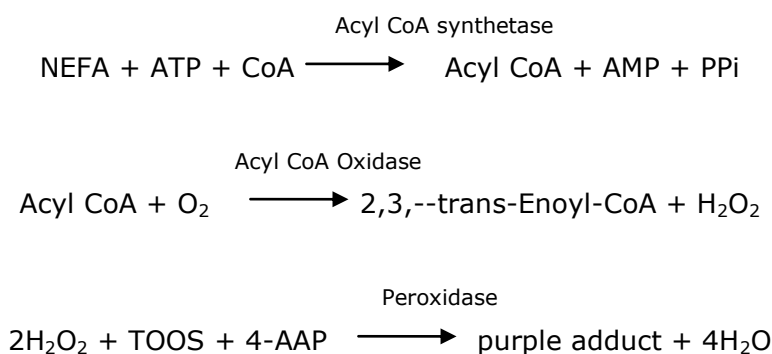


Figure 2.12: Principle enzymatic reaction involved in NEFA analysis reaction^{269,270}.

2.6.5 Plasma creatinine analysis

Creatinine concentrations in biological fluids can be determined by an enzymatic colourimetric reaction. Creatinine can be converted to creatine by creatininase and creatine converted to sarcosine by creatinase. Sarcosine is then oxidised by sarcosine oxidase to form a product which reacts with a probe to form a purple product²⁷², see Figure 2.14, with absorbance at 570nm.

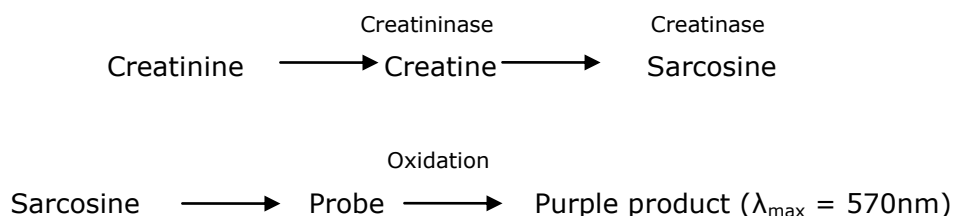


Figure 2.14: Enzymatic reaction involved in plasma creatinine analysis²⁷²

2.6.5.1 Plasma creatinine analysis procedure

Plasma creatinine analysis was performed using a creatinine assay kit (Abcam, ab65340) on overnight fasted plasma samples. Plasma samples were gently thawed on ice and 50µl of each sample or negative control was pipetted into a 96-well microplate ensuring no bubbles had formed. To create a standard curve, standards of 0, 2, 4, 6, 8 and 10µl were pipetted into the same plate and made up to 50µl with assay buffer. 50µl of reaction mix containing assay buffer, creatininase, creatinase, enzyme mix and probe was added to each well and the microplate was incubated at 37°C for 1 hour for colour development. Creatinine concentrations were then measured on a µQuant plate reader (BIO-TEK Instruments Inc. Vermont, USA) at 570nm using KC Junior analysis software (Biotek Ltd, Vermont, USA) and expressed as nmol per µl. All samples and standards were analysed in duplicate, and showed a variance coefficient of ≤10%.

2.6.6 Plasma cytokine analysis

Through performance of ELISA or immunoassays, it is possible to detect the presence and quantity of specific target antigens in plasma samples. ELISAs are based on a similar methodological premise as shown in Figure 2.10 (p86). Formation of a labelled-antibody antigen complex produces a fluorescent or electrochemical signal which can be measured. It is necessary to first coat the surface of each well in the detection microplate with a capture antibody, i.e. an antibody which binds to the target antigen. The second step involves incubating the plate with a blocking agent to block any non-specific binding sites, followed by introduction of the sample containing the target antigen.

Application of the antigen-specific primary antibody and secondary antibody enzyme-conjugate completes the full protein complex which when exposed to a chemical converter, produces a signal, shown in Figure 2.15. Gentle washing with buffered saline solution occurs after each stage to remove all excess reagents.

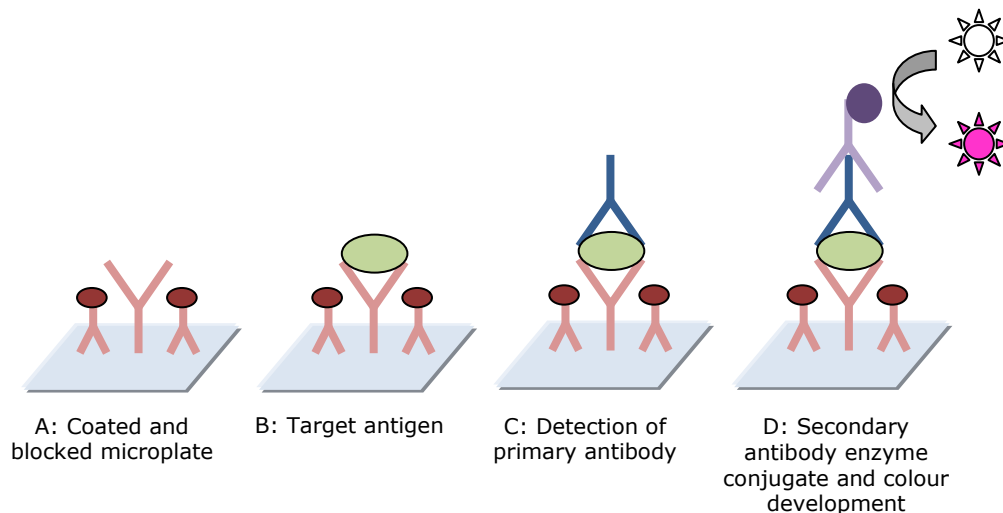


Figure 2.15: Stages of sandwich ELISA. A: Microplate is coated with capture antibody, and non-specific binding sites blocked with blocking agent. B: Sample containing target antigen introduced to well. C: Primary antibody applied to bind to target antigen. D: Secondary antibody with enzyme conjugate applied to primary antibody complex. Protein complex emits fluorescent signal after addition of chemical reagent.

2.6.6.1 Plasma cytokine analysis procedure

A 96 well microplate was coated with 100µl of capture antibody; 2µg/ml TNFα CC327 mouse monoclonal to cow antibody (Abcam 25797) diluted in sodium carbonate/sodium bicarbonate coating buffer or 8µg/ml IL-6 CC310 mouse monoclonal to cow antibody (GTX82951, Genetex, California, USA) diluted in distilled water, and incubated overnight at room temperature. After incubation, plate wells were washed five times with 500µl PBS and 0.05% Tween® 20 washing buffer and blocked for a minimum of 1 hour at room temperature with 300µl of 1% sodium casein/PBS blocking reagent. Plate wells were again washed five times with 500µl washing buffer, before loading with 100µl/well of samples or standards diluted in blocking buffer and incubated for 1 hour at room temperature.

After a repeated washing step, 100µl/well of secondary antibody was pipetted into the microplate; 1µg/ml TNFα CC328 mouse monoclonal to cow biotinylated antibody (Abcam 35284) or 1µl/ml anti-ovine IL-6 polyclonal rabbit serum diluted in blocking buffer, and incubated for 1 hour at room temperature. After another repeated washing step, the IL-6 ELISA method contained an additional step, whereby IL-6 plate wells were coated with 100µl/well of 1µl/3ml sheep anti rabbit IgG biotin (Abcam 97093) and incubated for 1 hour at room temperature. Plate wells were then washed five times in washing buffer, and coated with 100µl/well of 2µl/ml Streptavidin-HRP (GE Healthcare UK Ltd, Buckinghamshire, UK) diluted in blocking buffer/ 0.05% Tween and incubated for 45 minutes at room temperature. After a repeat washing step, plate wells were developed with 100µl/well of TMB substrate (10mg TMB in 1ml dimethylsulphoxide (DMSO) in 99ml sodium acetate/citric acid (BDH) pH6 solution, activated with 1.5µl hydrogen peroxide) and incubated for 30 minutes at room temperature. Plate development was stopped using 50µl of 1M sulphuric acid, and microplates read at 450nm using a spectrophotometer.

2.7 Triglyceride analysis

In 1957 Folch, Lees and Stanley published a method of lipid isolation and extraction from tissue²⁷³, which has been used to extract triglycerides from frozen kidney tissue in recent studies²⁷⁴. This method utilises interactions between a chloroform-methanol-saline (8:4:3) homogenisation solvent, which separates the solution into its lipid and non-lipid components by dissolution, centrifugation and filtration. The pure lipid components released upon homogenisation of the tissue are dissolved in the chloroform phase of the solvent, applying gravity filtration, and washing this mixture with saline removes any contaminants or solid tissue from the chloroform fraction. Removal of the filtrated solvent mix occurs under nitrogen steam, leaving the evaporated pure lipid component which can be stored or re-suspended in solvent, and the triglyceride concentration measured using a number of commercially available assay kits. The Randox triglyceride analysis kit uses a colourimetric reaction to determine triglyceride concentration by spectrophotometric absorbance at a specific wavelength. The kit contains enzymatic reagents which react with triglycerides to form quinoneimine as previously described in Figure 2.13 (p89), a coloured product measured at 500nm absorbance. Triglyceride concentrations for unknown samples are determined by interpolation of measured values from an internal control standard curve.

2.7.1 Triglyceride analysis procedure

500mg of renal cortical or *longissimus dorsi* (LD) muscle tissue from each animal was homogenised in a 50ml dispomix tube in 2ml of chloroform-methanol mixture (2:1 ratio) and gently centrifuged at 150g for 1 minute to ensure all homogenised tissue was exposed to the solvent. Samples were then agitated in an orbital shaker for 20 minutes at room temperature, before being passed through a funnel and 150mm Whatman filter paper (Scientific Laboratory Supplies, Nottinghamshire, UK) into a 15ml tube under gravity to recover the liquid phase. Tubes and filtration equipment were washed with 8ml of chloroform-methanol solvent, ensuring all available lipids were collected. Filtrated samples were next washed with 2ml 0.9% saline, vortexed for 5 seconds and centrifuged at 800g for 1 minute to separate the organic and aqueous phases of solution. The aqueous phase (top layer) of solution was discarded using a Pasteur pipette and 2ml of the remaining organic phase transferred to a 2ml eppendorf tube and evaporated under nitrogen steam using a Driblock DB-3 (Techne).

Evaporated lipid samples were then re-dissolved in 60µl tert-butanol (BDH) and 40µl Triton X-100, and stored in a spark-free fridge until further analysis. Analysis of triglycerides was performed with the Randox triglyceride assay kit using an adapted method from the manufacturer's instructions. 2µl of each sample, negative control or standard, and 200µl of supplied enzyme reagent were pipetted into a 96 well microplate (Grenier Bio-one, Gloucestershire, UK), ensuring no bubbles were formed and incubated at 37°C for 5 minutes for colour development. Triglyceride concentrations were then measured on a µQuant plate reader at 500nm and expressed as a ratio of triglyceride in micrograms (mg) per gram (g) of kidney tissue (mg/g). Each sample extraction and analysis was performed in duplicate, with a 5% coefficient of variance accepted between duplicate samples; analyses were repeated for samples outside this CV% value.

2.8 Thiobarbituric acid reactive substances analysis

Lipid peroxidation is the oxidative degradation of lipids and is a mechanism of cellular damage within plant and animal tissue. ROS, particularly free radicals, initiate a reaction with unsaturated lipids which ultimately form lipid peroxides²⁷⁵. Lipid peroxides are unstable molecules that decompose to form other compounds such as malondialdehyde (MDA), reported as a DNA mutagen and carcinogen²⁷⁶, and 4-hydroxynonenal (4-HNE). A number of commercially available Thiobarbituric acid reactive substances (TBARS) assay kits determine the end products of lipid peroxidation by measuring the colourimetric byproduct between thiobarbituric acid (TBA) and MDA, see Figure 2.16.

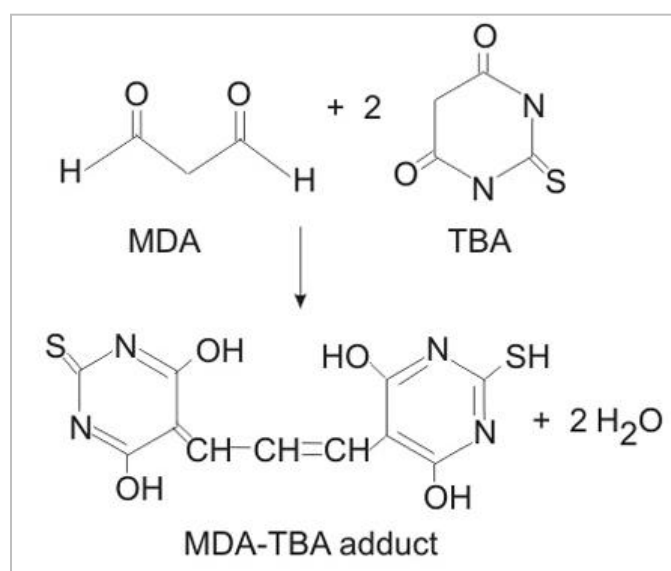


Figure 2.16: Malondialdehyde-thiobarbituric acid adduct formation²⁷⁵.

The Oxiselect™ TBARS Assay kit (Cell Biolabs Inc, CA, USA) determines lipid peroxidation through the formation of MDA-TBA adducts under acidic conditions at approximately 95°C. This reaction produces a pink chromagen which can be measured colourimetrically at 532nm. However, the specificity of the reaction has been questioned, as TBA and MDA can both react with additional compounds such as aldehydes, DNA and amino acids to form similar colourimetric products^{275,277,278}, and hence it is suggested the reaction measures TBARS rather than MDA concentration. Despite this, the method is still the most widely used analysis to determine lipid peroxidation^{275,278} and has recently been published within a renal oxidative-stress study²⁷⁹.

2.8.1 TBARS procedure

≈100mg of renal cortical tissue from each sample was resuspended and homogenised in 1ml of 1 x butylated hydrotoluene kit reagent (BHT) and phosphate buffered saline (PBS). Samples were initially centrifuged for 1 minute at 2000g at room temperature with the supernatant transferred to 1.5ml labeled eppendorf tubes. Centrifugation was repeated at 10000g for 5 minutes at 4°C and the supernatant transferred to clean 1.5ml tubes to ensure removal of any remaining cell debris. Samples were then stored at -20°C until use in the TBARS assay, or for total protein concentration analysis. Analysis of TBARS was performed using the Oxiselect™ TBARS assay kit as per the manufacturer's instructions; analysis of both standards and samples were performed in duplicate.

Ten MDA standards (500µl) were created ranging from 0mg/dl-195mg/dl using the MDA reagent supplied and distilled water. 100µl of standard, negative control or unknown sample was added to a fresh 1.5ml eppendorf tube; 100µl of sodium dodecyl sulphate (SDS) lysis solution was added to each tube and incubated at room temperature for 5 minutes. 250µl of TBA reagent was next added and tubes were incubated in a water bath at 95°C for 60 minutes, after which samples were removed and cooled on ice for a further 5 minutes. Samples were then centrifuged at 1200g for 15 minutes, with 300µl of supernatant transferred to a fresh eppendorf tube. 300µl of n-butanol was next added to the samples to prevent interference of haemoglobin and its derivatives. Samples were vortexed for 1-2 minutes and centrifuged for 5 minutes at 10000g at room temperature to allow for phase separation. The n-butanol layer, i.e. the top layer of the solution, was then decanted into another eppendorf tube for spectrophotometric analysis. 200µl of each sample and standard was then pipetted into a 96 well microplate and absorbance measured at 532nm. Unknown sample concentrations of MDA/TBARS were determined against the standard curve, and normalised against total protein concentration using the bicinchoninic acid (BCA) method (2.8.2.1, p97), results were expressed as TBARS µM / total protein concentration (µg/µl).

2.8.2 Bicinchoninic acid total protein determination

Total protein concentrations were determined using the BCA assay method. This assay relies on a colourimetric reaction between proteins, BCA and copper sulphate^{280,281}. Peptide bonds in proteins reduce Cu^{2+} to Cu^{1+} ions when incubated at temperature; BCA reagent then chelates to Cu^{1+} ions which forms a purple coloured compound²⁸⁰.

The colour development (from green to purple) is in proportion to the amount of protein present in the sample and absorbance can be measured at 562nm. Unknown concentrations can then be referenced against a standard curve.

2.8.2.1 BCA assay procedure

50ml of BCA reagent (reagent A) containing 1% bicinchoninic acid, 2% sodium carbonate, 0.16% sodium tartrate and 0.4% sodium hydroxide was made up to volume with distilled water and made to pH 11.25 with 10% sodium bicarbonate. 50ml of 4% copper sulphate solution (reagent B), was made up to volume with distilled water. Reagent C was then made by mixing reagent A and reagent B in a ratio of 100ml: 2ml and stored at 4°C until needed. To create the standards, eight concentrations of bovine serum albumin (BSA) ranging from 1.0-0.00 mg/ml were made up in 0.9% saline. 2.5µl of each unknown protein sample was diluted by 1:20 in 0.9% saline solution to make a final volume of 50µl.

10µl of each standard, negative control or unknown was pipetted into a 96-well microplate. 200µl of reagent C was then added to each well and incubated in an orbital shaker at 37°C for 30 minutes for colour development, after which absorbance was measured at 562nm. Each analysis was performed in duplicate, with a 5% coefficient of variance accepted between duplicate samples; analyses were repeated for samples outside this CV% value. A 20x multiplication factor was applied to all recorded absorbance results to account for the initial 1:20 dilution factor.

2.9 Western blotting

Western blotting or protein immunoblotting is a method to analyse protein size and expression in biological cell lysate samples²⁸². Tissue samples are homogenised and lysed to release the proteins into the sample and protein concentration measured. To denature, ionise and align the proteins, samples are heated with an ionic detergent, usually SDS and 2-mercaptoethanol to prevent additional protein disulphide bond cross-linking. Protein samples along with a protein marker ladder (Biorad Precision Plus Protein Standards, Biorad, California, USA) are then loaded onto a 2-D polyacrylamide gel and undergo electrophoresis. Proteins are separated along the polyacrylamide matrix towards the positive electrode according to their size and molecular charge. Once separated the proteins can be transferred from the gel matrix to an electrostatic membrane, either nitrocellulose or polyvinylidene fluoride (PVDF), using a semi dry electroblotting method. Membrane cut to the same size of the gel is laid directly onto the gel surface, which is then sandwiched between buffer soaked filter paper and placed into a semi-dry blotter. A small electric charge is then passed through the 'gel sandwich', drawing the proteins from the gel and onto the membrane, by a combination of capillary action and electrostatic attraction²⁸³. After blotting, the membrane is stained using a reversible protein dye to ensure completion of protein transfer. As described in the IHC (2.5.4, p86) and ELISA methods (2.6.6, p90), detection of protein in Western Blotting occurs by a similar mechanism. The membrane is first incubated in a blocking reagent to block any non-specific binding sites, before the target antigen-antibody protein complex is built through incubation in optimised primary and secondary antibody dilutions. Detection of the secondary antibody enzyme conjugate occurs by incubation in a chemiluminescent reagent, which emits a signal in proportion to the abundance of target antigen present. Chemiluminescent signal can be detected by exposure with a CCD camera and quantitation determined through analysis of protein band density using densitometry software.

2.9.1 Western blot protein extraction procedure

For each sample $\approx 0.2\text{g}$ cortical tissue was weighed into a dispomix tube and homogenised in 4ml CelLytic MT lysis reagent and 0.04ml protease inhibitor cocktail P8340 at 3000 rpm for 30 seconds. The homogenate was then transferred to a 2ml eppendorf tube and centrifuged for 10 minutes at 12000g to pellet all cell debris.

Protein supernatant was then transferred to a fresh 2ml eppendorf tube and protein concentration of each sample determined by BCA method. Samples were then stored at -20°C for further analysis.

2.9.2 Western blot polyacrylamide gel electrophoresis procedure

Extracted protein samples were diluted to 4.2mg/ml using CelLytic MT diluent before addition of 50µl protein association buffer (containing 50mM Tris, 10% glycerol, 2% SDS, 5% beta-mercaptoethanol and distilled water pH 6.8). Samples were made up to 84µl with glycerol-bromophenol dye (containing 0.01g bromophenol blue, 14.9g sodium hydroxide and 23.5ml distilled water) and incubated for 10 minutes at 100°C in a water bath.

A 12% polyacrylamide-resolving gel (containing 12ml 30% polyacrylamide (Severn Biotech, Worcestershire, UK), 9.9ml distilled water, 7.5ml 1.5M Tris pH 6.8, 0.3ml 10% SDS, 0.3ml 10% ammonium persulphate (APS) and 0.012ml N,N,N',N'-tetramethylethylenediamine (TEMED) (Acros Organics, New Jersey, USA)) was cast in a 18cm x 16cm Hoefer SE600 gel chamber (Hoefer Inc, Massachusetts, USA), by syringe injection, allowing a 3-4cm space for stacking gel and loading comb. Water-saturated butanol was poured onto the gel to level the resolving gel surface and prevent the gel from drying out, and allowed to polymerise for 1 hour at room temperature. The butanol was poured off and the set gel washed with distilled water. A 3% stacking gel (containing 1.7ml polyacrylamide, 6.8ml distilled water, 1.25ml 1.0M Tris pH 6.8, 0.1ml 10% SDS, 0.1ml 10% APS and 0.01ml TEMED) was injected in the gel chamber on top of the resolving gel. A loading comb was inserted in the stacking gel and allowed to polymerise for 1 hour at room temperature. After removal of the loading comb, gel wells were washed with distilled water and filled with 1x running buffer (containing 5mM tris, 50mM glycine (Fisher Scientific), 2% SDS and distilled water). 20µl of each sample, a non-immune mouse serum negative control and a protein marker ladder were randomly loaded in duplicate onto the gel, loading any empty wells with 20µl glycerol-bromophenol dye to ensure even running during electrophoresis. The gel chamber was attached to the upper and lower electrophoresis chambers, which were filled with 1x running buffer, and electrophoresis was run at 150v (40mA) for 2 hours.

2.9.3 Western blot semi-dry blotting procedure

A nitrocellulose membrane (Hybond-C Super, GE Healthcare) and six sheets of 1mm filter paper were cut to approximately the same size as the polyacrylamide gel. Filter paper was soaked in Towbin buffer (containing 25mM Tris, 192mM glycine, 20% v/v methanol, and distilled water, p.H 8.3). After electrophoresis the gel tank was disassembled and the gel carefully unloaded. The stacking gel was removed and the resolving gel was placed directly onto the nitrocellulose membrane, placing three sheets of filter paper either side of the gel and membrane to form a sandwich. Any air bubbles were carefully rolled out of the gel sandwich, which was then placed into a Hoefer semi-dry transfer unit TE77x and proteins transferred at 0.8mA per cm² at a maximum of 30v for 2 hours.

2.9.4 Western blot protein detection procedure

After protein transfer, the nitrocellulose membrane was washed in 100ml tris buffered saline with Tween[®] 20 (TTBS), and then soaked in 100ml 1:10 Ponceau S red stain dilution (containing 0.2g ponceau S, 3g trichloroacetic acid (Fisher Scientific), 3g sulphosalicylic acid (Acros Organics) and distilled water), to visualise protein band location. The protein marker ladder was highlighted with a rabbit primary antigen/antibody pen (Alpha Diagnostic, Texas, USA), before removing Ponceau S stain from the membrane with distilled water and TTBS. The membrane was then blocked overnight at 4°C in 100ml 10% Marvel dried milk powder ensuring complete dissolution, to prevent any speckling on the membrane. The membrane was blocked for an additional 30 minutes at room temperature before being rinsed twice in 100ml TTBS. Next, the membrane was agitated in 10ml 1:50 TTBS/3% Marvel dilution of mouse monoclonal to TLR4 primary antibody (Abcam 22048) for 1 hour at room temperature, after which the membrane was washed in 100ml TTBS for 3 x 10 minutes. The membrane was agitated in 10ml 1:2000 TTBS/ 3% Marvel dilution of rabbit polyclonal to mouse IgG HRP conjugate secondary antibody (Abcam 6728) or 1:2000 protein G HRP conjugate secondary antibody (Biorad) for 1 hour at room temperature, followed by four 15 minutes washes in 100ml TTBS and a further two 30 minute washes in TBS. Additionally, a negative control using a primary binding solution of 1:1000 non-immune mouse serum was conjugated with 1:2000 rabbit polyclonal to mouse secondary antibody.

For chemiluminescent visualisation, 3ml of hydrogen peroxide and 3ml luminol (Immobilon Western Chemiluminescent HRP Substrate, Millipore, Massachusetts, USA) were applied directly onto the membrane and agitated for 5 minutes, before being drained and covered in cling wrap. Protein bands were visualised using a CCD digital camera, exposing the membrane for 5 minutes under visible light (EPI) and chemiluminescence.

Protein band densities were analysed using Aida Densitometry v2.0 software (Raytek Scientific Ltd, Sheffield). Efficiency of protein transfer from polyacrylamide gel to nitrocellulose membrane was assessed by washing the polyacrylamide gel in Coomassie Brilliant Blue dye for 1 hour, to visualise any remaining protein bands.

2.10 Statistical analysis

Prior to any statistical analysis, coefficient of variance between each duplicate individual sample was calculated for the assays and experiments performed using Microsoft Office Excel 2007 software spreadsheet package (Microsoft Corporation, Berkshire, UK). A coefficient of variance $\leq 5\%$ confirmed low variance, thus supporting the reproducibility of the respective assay. Data points that fulfilled this criterion were included in further statistical analyses. Statistical analysis of data was performed using SPSS v18.0 statistical software for Windows package. All data were subjected to the Kolmogorov-Smirnov normality test for parametric or non-parametric distribution, where $p \geq 0.05$ determined normality. Comparable groups (i.e. groups with at least one of the same variable) were assessed using either analysis of variance (ANOVA) for parametric data or Kruskal-Wallis one-way analysis of variance for non-parametric data, with multiple group *post hoc* Bonferroni or Dunn's correction tests applied respectively. All statistical graphs were produced using software package GraphPad Prism v5.00 (GraphPad Software, California, USA), and for consistency, data presented as mean average \pm standard error of the mean (SEM). Details of any additional statistical tests used are provided in the relevant results chapters.

In analysis of all 8 groups, i.e. groupings by maternal nutrition, obesity and gender (NLf, ALf, NLm, ALm, NOf, AOf, NOM and AOm, see Figure 2.1, p105), there were no statistical differences between the maternal nutrition intervention groups; this applied to all the experiments performed as described in this chapter. These results did however indicate that gender and post-natal obesity displayed an overriding influence within the study groups. To examine the effect of gender and post-natal obesity throughout this study, the maternal nutrition groups were combined, thus the groups analysed were lean females (LF, n=7), lean males (LM, n=11), obese females (OF, n=9) and obese males (OM, n=9), shown in Figure 2.2, p105.

To reduce the probability of performing a type I or type II statistical error, i.e. by erroneously rejecting or accepting the null hypothesis respectively, power calculations were performed using Minitab v16 statistical software (Minitab Ltd, Warwickshire, UK). Minitab power calculations determine the recommended sample sizes per group depending on an expected difference and standard deviation between each group. Sample size was calculated at 80% power, a value generally accepted in the literature as standard.

The recommended sample size to detect a 20% difference between groups with a 10% standard deviation was 6 samples per group with a statistical power of $\geq 80\%$ to yield a significant result of $p < 0.05$. However, to detect a smaller difference with similar standard deviations at the same power and significance, as may have been present between the maternal nutrition groups, it is recommended that sample sizes are increased to ≈ 100 per group.

Chapter 3 – The effect of gender and obesity on systemic metabolism and adipose tissue physiology

3.1 Introduction and aims

Surveying the scientific literature has identified the association of obesity development leading to an alteration in adipose tissue expansion and enlargement, and also a change in adipose tissue location, which may be influenced by gender^{37,38}. This responsiveness between adaptations in adipose tissue profile is postulated to play a role in mediating a chronic low grade inflammatory phenotype, to which the kidneys are particularly sensitive resulting in structural and functional renal impairment. This chapter therefore aimed to investigate whether the exposure to an obesogenic environment of restricted physical activity encourages the development of central obesity by switching the deposition location from peripheral to intra-abdominal adipose tissue. These adaptations could result in an elevated inflammatory systemic profile, via increased circulatory hormones, cytokines and metabolic molecules. Promotion of an inflammatory phenotype can then contribute to an increased risk in CVD and related end organ damage⁶⁹.

Therefore, this chapter details the effect of a reduced activity obesogenic environment and how this environment encourages the development of adipose tissue size and its locale, and the subsequent impact on systemic and PAT physiological alterations in sheep, with additional gender analysis.

3.1.1 Hypothesis

The hypothesis for Chapter 3 was that sheep exposed to a restricted area of physical activity develop increased deposits of adipose tissue and impaired metabolic status. Additionally, development of intra-abdominal and subcutaneous fat depots may depend on gender.

3.2 Materials and methods

A complete description of all the methods used in this chapter can be located in Chapter 2. The experimental model used in my study which is referenced in the subsequent results chapters is reviewed in Figure 3.1. All reported animal experimentations, i.e. DXA measurements, tissue weights, plasma measurements and dissections were performed and supervised by Dr S.Seibert and Dr L.Chan. Leptin and cortisol plasma analyses were performed by Miss N.Dellschaft and Dr S.Seibert. Where appropriate, any sample or analytical omissions are explained in the relevant results section. In addition, description of statistical tests utilised are provided in this results chapter or are detailed in Chapter 2.

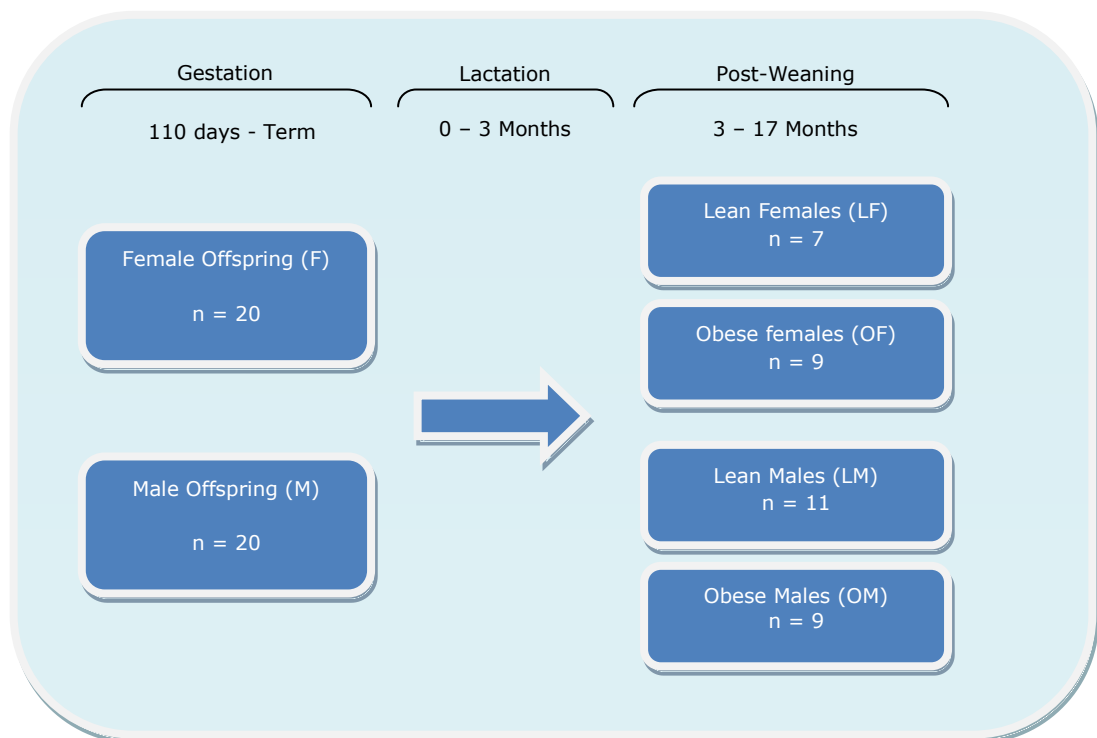


Figure 3.1: Review of experimental animal model used throughout my thesis: LF = lean female, OF = obese female, LM = lean male and OM = obese male sheep. Four female animals expired during the experimental procedure.

3.3 The ovine model of obesity and maternal nutrition

Previous work from the University of Nottingham Academic Child Health Department on models of ovine obesity, have utilised models derived from a combination of maternal nutrition restriction and postnatal activity manipulation²²⁸. The nutritional intervention has targeted the *in utero* period of ovine embryo- and organogenesis, i.e. the early to mid-gestation period (dGA 30-80)²²⁷. In analysis of physiological renal and adipose tissue adaptations, this study identified that restriction of maternal nutrition during this period alters inflammatory and metabolic gene-protein responses in renal and perirenal adipose tissue in comparison of lean, obese and nutrition restricted obese subjects^{227,284}. Additionally the nutrient restricted obese group displayed advanced signs of metabolic dysfunction characterised by increased renal oxidative stress, apoptosis and proliferation in addition to elevated renal lipid and collagen depositions²³⁰.

However, my study utilised a restricted maternal nutrition period targeting a late gestation *in utero* window (i.e. dGA 110-130). As previously mentioned, this development period is after nephrogenesis²²⁶, meaning that the renal and urinary systems are fully matured prior to the applied nutritional intervention, thus resulting in no discernible effect in these systems. This is the probable explanation why no significant differences were observed between the maternal nutrition intervention groups for both phenotype and genotype, and as discussed in Chapter 2, comparisons of gender and obesity were the overriding influences in all analyses.

3.4 Results

3.4.1 The effects of an obesogenic environment and gender and their contribution to body weight and adipose tissue deposition

During the post-weaning period (≈ 3 months) to the time of euthanasia (≈ 17 months), both lean and obesogenic environment animals were allowed access to the same amount of food and water. Obese males showed significantly higher energy intake than the lean males, a response not observed in the females. Obese males additionally displayed greater energy intake than the obese females. However, analysis of energy intake per kg of body weight showed no significant differences between either obesity or gender groups, see Table 3.1.

Group	LF (n=7)	OF (n=9)	LM (n=11)	OM (n=9)	Gender	Obesity
Energy intake (MJ/24h)	17.02 \pm 1.16	22.91 \pm 1.16 ^a	16.27 \pm 1.42 ^{**}	30.35 \pm 1.79 ^{b**}	S	S
Relative Energy intake (MJ/kg/24h)	0.35 \pm 0.02	0.38 \pm 0.02	0.29 \pm 0.02	0.36 \pm 0.02	NS	NS

Table 3.1: Energy intake (MJ/kg/24 hours) throughout post-natal environment intervention of lean female (LF), obese female (OF), lean male (LM) and obese male (OM) sheep. Values are means \pm SEM. NS = no significant differences, S = significance where only one of two comparable groups display significance; statistical difference is denoted by ^{ab}, ** = $p < 0.005$ (ANOVA).

Conversely, activity measurements for the animals highlighted a significant difference in increased activity between the lean and obesogenic environment males, a trend also displayed by the females, shown in Figure 3.2, p108. In the lean males and both female groups, no activity data was recorded for one animal, most likely due to a fault with the accelerometer. These omissions may have reduced the power of the applied statistical test (ANOVA), thus providing a possible explanation as to the lack of statistical significance in comparison of the two experimental female groups.

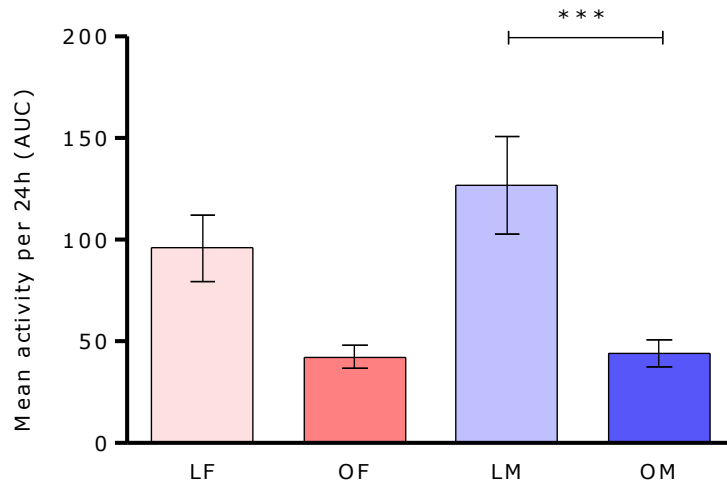


Figure 3.2: Area under curve (AUC) of mean activity per 24 hour period of lean female (LF; $n=6$), obese female (OF; $n=8$), lean male (LM; $n=10$) and obese male (OM; $n=9$) sheep. Values are mean \pm SEM. Statistical difference is denoted by *** = $p < 0.001$ (ANOVA).

From the individual values of energy uptake and mean physical activity, it was possible to determine relative values for food intake percentage and physical activity percentage. These values were then used to calculate an energy uptake to physical activity ratio using the lean group as a reference. This energy balance ratio was determined by $((\text{food intake \%}/\text{physical activity \%})/(\text{food intake}_{\text{ref}} \%/\text{physical activity}_{\text{ref}} \%)) - 1$, where the average relative ratio for lean animals was considered to be 0. A positive value for energy balance represents a net gain of energy, and a negative value represents a net loss of energy, see Figure 3.3, p109.

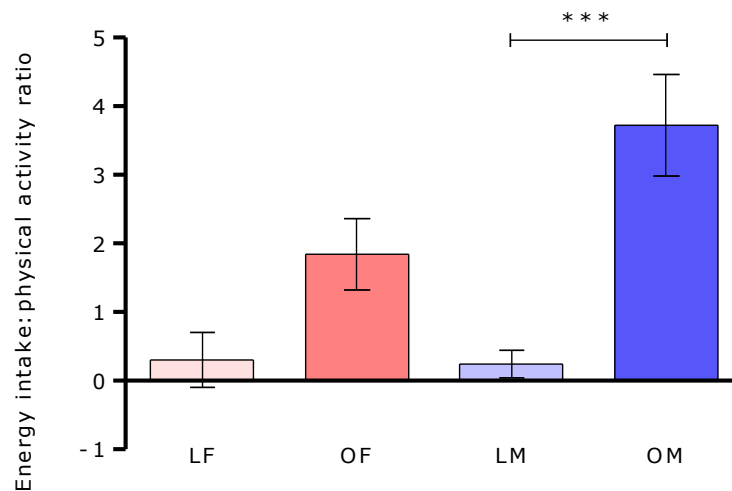


Figure 3.3: Ratio of energy intake to physical activity of lean female (LF; $n=6$), obese female (OF; $n=8$), lean male (LM; $n=10$) and obese male (OM; $n=9$) sheep. Values are mean \pm SEM. Statistical difference is denoted by *** = $p<0.001$ (ANOVA).

Obese males exhibited a significant increase in the ratio of energy intake to physical activity in comparison to lean males, a trend also displayed between obese females and obese males ($p=0.078$). No significant differences were observed in comparison of the female groups, but similarly to the mean activity results, obese females appeared to display a trend towards increased energy intake and physical activity ratio, and any statistically significant result was potentially dampened through a reduction in sample number as previously discussed.

The obesogenic environment intervention of reduced activity and subsequent change in energy balance contributed towards the development of larger sheep. As BMI is a weight formula specifically for humans, body weight measurements were used to determine an overweight or obese condition. Body weights (kg) showed a statistical significant increase in comparison of lean to obese animals in both genders, with an approximate increase of 25-50% in body weight. Additionally obese males exhibited higher body weight compared to obese females, a result not seen in the lean animals, see Table 3.2, p110. An estimation of total fat mass by DXA scan further allowed a comparison of lean and obese animals which identified a significant rise in total fat mass (kg) shown in Table 3.2 (p110). In addition relative fat mass percentage was calculated (total estimated fat mass/ body weight). Relative fat mass percentage showed a significant, two-fold increase between lean and obese animals for both genders.

Females exhibited slightly higher relative fat mass percentage in both lean and obese groups compared to their male counterparts, however these results were not statistically significant, Table 3.2. Total fat mass was increased with obesity, as were body weights corrected for total fat mass (kg). These results showed that obese males were significantly larger when compared to lean males and obese females, a result not observed between female groups, Table 3.2. To ascertain as to whether the increased corrected body weight observed in obese males was due to amplified lean mass development, analysis of lean mass (kg) identified a significant difference with gender but not obesity, and although not statistically significant, lean males exhibited a 25% increase in lean mass compared to lean females. Finally analysis of lean to total fat mass ratio showed a decrease in lean mass ratio in the presence of obesity but not with gender, Table 3.2.

Group	LF (n=7)	OF (n=9)	LM (n=11)	OM (n=9)	Gender	Obesity
Body weight (kg)	49.50±1.04	61.56±2.07 ^a	56.38±2.59	83.84±1.82 ^b	S	**
Total fat mass (kg)	3.85±0.48	8.11±0.74	3.61±0.44	9.67±0.88	NS	**
Relative fat mass (%)	8.42±1.12	14.31±1.26	6.77±0.66	12.93±1.06	NS	**
Body weight corrected for fat mass (kg)	45.30±0.75	52.20±1.84 ^a	52.50±2.13**	73.00±1.81 ^{b**}	S	S
Lean mass (kg)	39.72±0.87	44.03±1.22 ^a	49.09±1.89	62.41±1.30 ^b	S	NS
Lean mass: total fat mass ratio (kg)	11.40±1.59	5.83±0.57	15.31±1.62	6.93±0.67	NS	*

Table 3.2: Body weight parameter measurements of lean female (LF), obese female (OF), lean male (LM) and obese male (OM) sheep. Values are mean ± SEM. NS = no significant difference, S = significance where only one of two comparable groups display significance; statistical differences are denoted by * = $p < 0.05$; ^{ab}, ** = $p < 0.005$; *** = $p < 0.001$, (ANOVA). Body weight corrected for fat mass, Lean mass and Lean mass:total fat mass ratio analyses treated with Kruskal-Wallis statistical test.

As expected, exposure in an obesogenic environment promoted total fat mass. To determine how an obesogenic environment impacted on adipose tissue development and deposition, fat mass was further analysed with regard to its different depots and relative composition of total fat mass, calculated in Table 3.3.

Group	LF (n=7)	OF (n=9)	LM (n=11)	OM (n=9)	Gender	Obesity
Subcutaneous (kg)	3.12±0.38	5.33±0.48	3.06±0.36***	7.07±0.70***	NS	*
Omental (kg)	0.33±0.06	1.62±0.17	0.26±0.05***	1.54±0.16***	NS	*
Perirenal (PAT) (kg)	0.31±0.04	1.06±0.13	0.22±0.02	0.96±0.11	NS	***
Relative subcutaneous (%)	81.45±1.15	65.97±1.31	85.17±0.76	72.98±1.46	NS	**
Relative omental (%)	8.11±0.93	19.73±0.88 ^a	6.63±0.64	16.03±0.96 ^b	S	***
Relative PAT (%)	8.05±0.44	12.90±0.64 ^a	6.83±0.26	9.90±0.67 ^b	S	***

Table 3.3: Adipose tissue depot measurements of lean female (LF), obese female (OF), lean male (LM) and obese male (OM) sheep. Values are mean ± SEM. NS = no significant difference, S = significance where only one of two comparable groups display significance; statistical differences are denoted by ^{ab}, * = $p < 0.05$; ** = $p < 0.005$; *** = $p < 0.001$ (ANOVA). Omental (kg) and relative subcutaneous analyses treated with Kruskal-Wallis statistical test.

In response to obesity, all adipose tissue depots showed a significant increase in size. Obese males showed a greater development of subcutaneous and omental adipose tissue deposition compared to lean males ($p < 0.001$), in comparison to the presence of obesity in the female groups ($p < 0.05$). No further gender effects were observed. Relative adipose tissue deposition (%) showed a similar effect to the presence of obesity, expressed by an increased relative percentage in both obese groups compared to lean. Additionally, obese females also exhibited increased relative PAT and omental adipose tissue depots compared to obese males.

3.4.1.1 The effect of an obesogenic environment and gender on perirenal adipose tissue and adipocyte development

As PAT depot size was increased in both genders from exposure to an obesogenic environment, histological analysis of PAT adipocytes was performed, as described in 2.5.2, p83. Figure 3.4 shows representative microscopic slides of lean and obese samples for both genders.

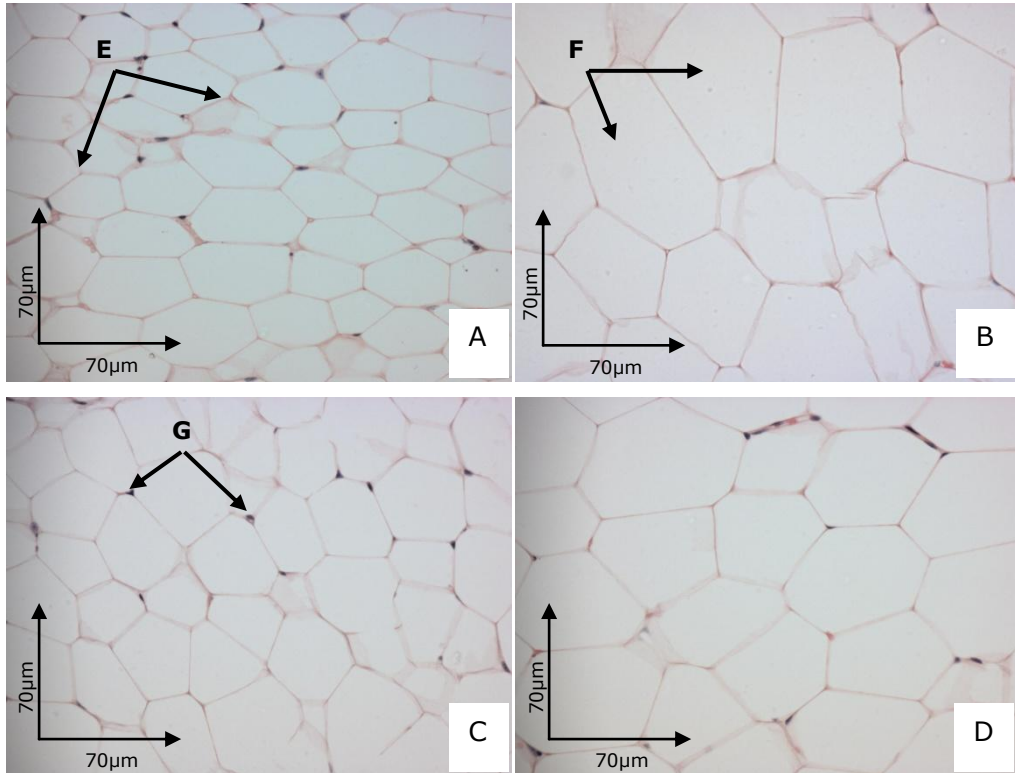


Figure 3.4: Representative microscopic slides of haematoxylin and eosin stained perirenal adipose tissue (PAT) of lean female (A), obese female (B), lean male (C) and obese male (D) sheep. Adipocyte membranes (pink stained boundaries marked by arrow E) in obese groups are enlarged and more polygonal in shape, thus contain more lipid area (white non-stained region; arrow F). Blue stained nuclei in obese samples appear pushed to periphery of adipocyte membrane (arrow G). Slides are displayed at 20x magnification.

PAT adipocytes appeared larger in the obese samples, as demonstrated by an enlarged white coloured lipid area and expanded adipocyte membrane, with no apparent effect of gender. None of the microscopic samples from lean or obese animals displayed an increased infiltration of nucleated cellular structures or any development of crown-like structures. Therefore, any quantification of this measurement was impossible to perform. Visual software analysis of microscopic slides identified a significant increase of adipocyte perimeter (μm) and adipocyte area (μm^2) between lean and obese for both genders ($p < 0.001$), as shown in Figure 3.5 and 3.6, p113.

One obese female and one lean male PAT sample had not been loaded into a paraffin histology cassette at time of dissection, and thus were omitted from the PAT histology analysis.

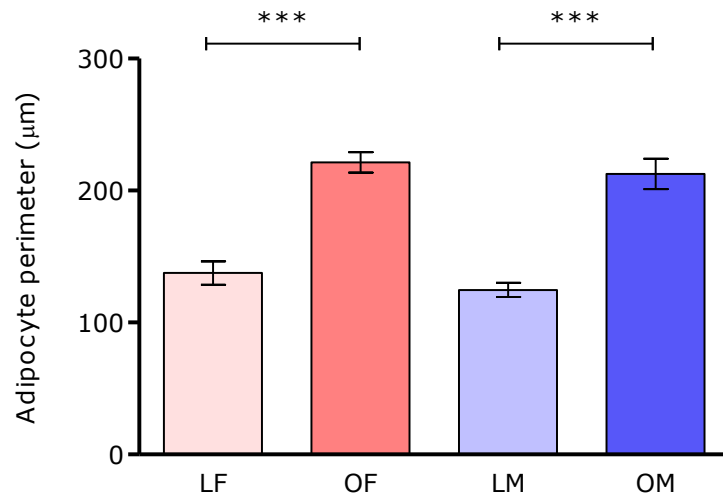


Figure 3.5: Adipocyte perimeter (μm) of perirenal adipocytes of lean female (LF; $n=7$), obese female (OF; $n=8$), lean male (LM; $n=10$) and obese male (OM; $n=9$) sheep. Values are mean \pm SEM. Statistical difference is denoted by *** = $p < 0.001$ (ANOVA).

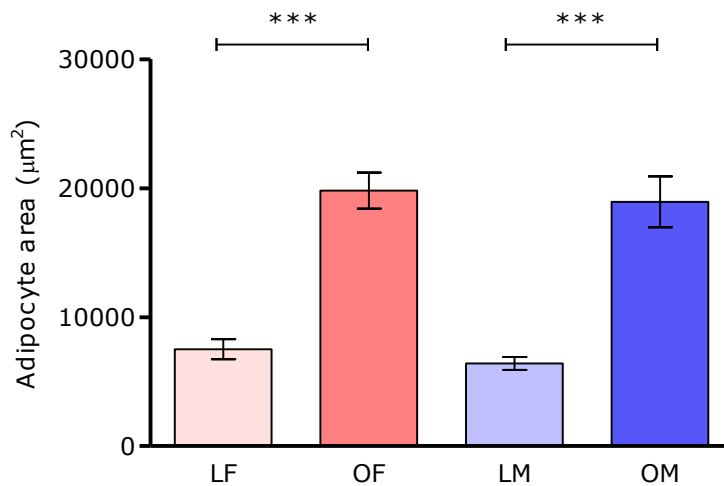


Figure 3.6: Adipocyte area (μm^2) of perirenal adipocytes of lean female (LF; $n=7$), obese female (OF; $n=8$), lean male (LM; $n=10$) and obese male (OM; $n=9$) sheep. Values are mean \pm SEM. Statistical difference is denoted by *** = $p < 0.001$ (ANOVA).

Correlation of PAT size (g) against perirenal adipocyte area (μm^2) identified a positive correlation, with a p value of <0.0001 and r^2 of 0.85, see Figure 3.7.

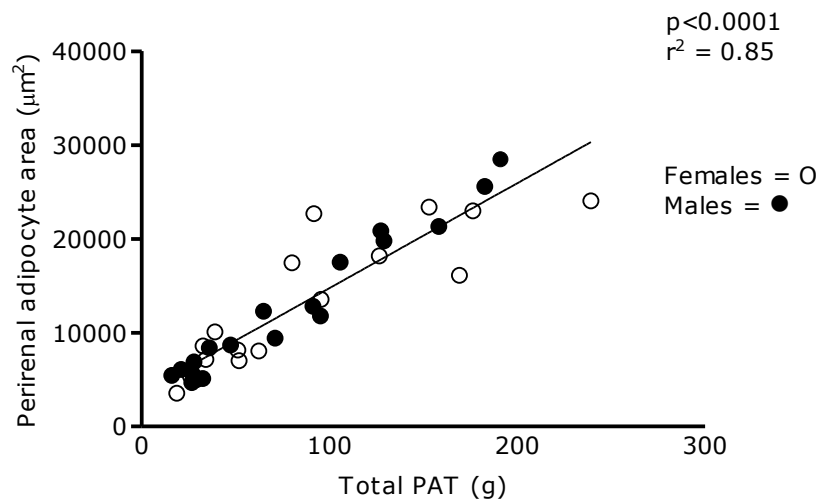


Figure 3.7: Relationship between PAT mass (g) and perirenal adipocyte area (μm^2) of total sheep (n=34). Correlation analysis showed a statistical significance where $p < 0.0001$ and $r^2 = 0.85$ (Pearson's correlation coefficient).

As adipocyte area measurements were mean average values for total adipocyte number, analysis of individual adipocyte frequencies were performed to elucidate if adipocyte size was affected by gender or its exposure to obesity. Using an F-test to compare the variance in a population, comparison between adipocyte area distributions identified a significant difference in lean females and lean males, ($p=0.0002$).

As shown in Figure 3.8 (p115), lean female PAT appears to consist of larger adipocytes in comparison to lean males despite overall mean adipocyte area showing no difference between groups, Figure 3.6 (p113). Performing the same variance test between obese females and obese males showed no significant difference, see Figure 3.9, p115.

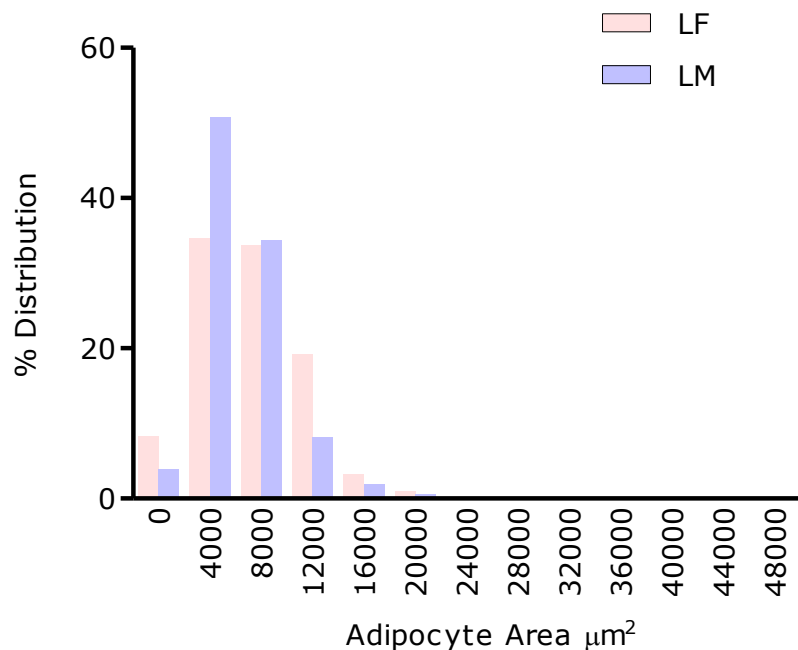


Figure 3.8: Frequency distribution (%) of perirenal adipocyte area for lean female (LF; n=311) and lean male (LM; n=465) sheep. Variance of distribution between groups by F-test showed significance, where $p=0.0002$.

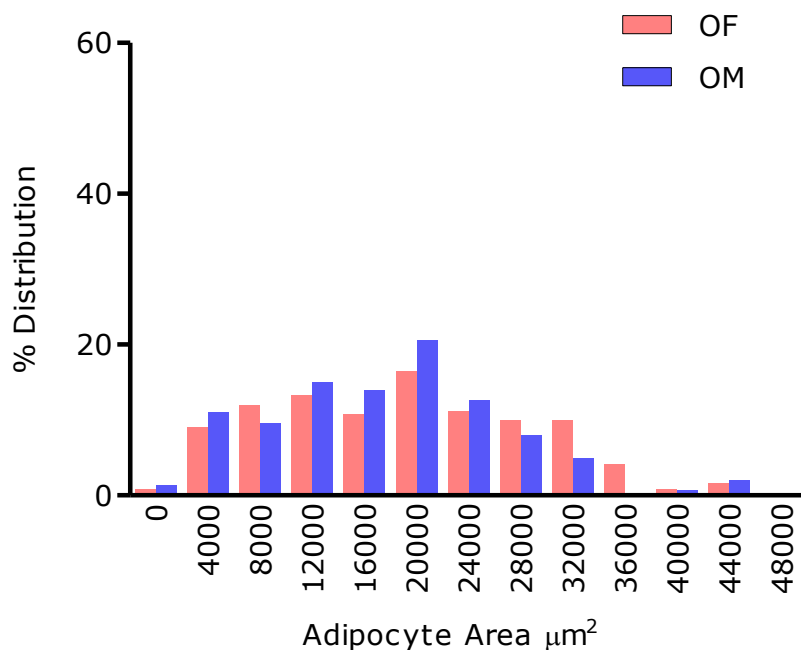


Figure 3.9: Frequency distribution (%) of perirenal adipocyte area for obese female (OF; n=242) and obese male (OM; n=301) sheep. Variance of distribution between groups showed no statistical significance.

3.4.2 The effect of increased adiposity on plasma hormones and metabolites

GTT insulin baseline analysis measured following an overnight fast identified elevated plasma insulin levels in obese males compared to lean males, a result not observed in females (Figure 3.10). Although appearing to exhibit a trend of elevated GTT insulin baseline levels compared to lean females, obese females were not statistically significant.

No GTT insulin baseline data was recorded for two animals in the obese female and obese male group, and one animal in the lean male group. This was possibly due to catheter malfunction resulting in a failure to collect plasma from the affected animals. Additionally one obese female displayed abnormally high readings of plasma insulin (≈ 15 fold greater) and was omitted from subsequent insulin results. As previously postulated, these omissions may have reduced the power of the applied statistical test and thus reduced any potential statistical significance from the subsequent analysis.

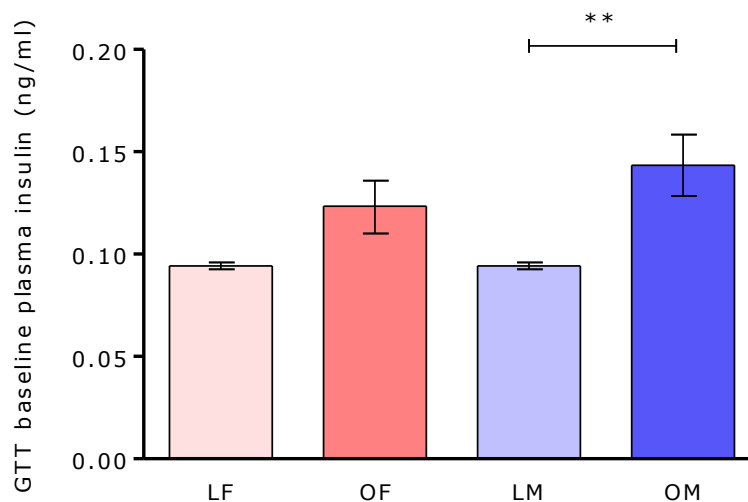


Figure 3.10: GTT plasma insulin baseline (ng/ml) of lean female (LF; $n=7$), obese female (OF; $n=6$), lean male (LM; $n=10$) and obese male (OM; $n=7$) sheep. Values are mean \pm SEM. Statistical difference is denoted by ** = $p < 0.005$ (Kruskal-Wallis).

Following intravenous glucose administration, time course measurement ng/ml (Figure 3.11, p117 and Figure 3.12, p118) and subsequent GTT insulin area under the curve (AUC) (Figure 3.13, p118) analysis displayed the same trend as the GTT insulin baseline measurements.

Obese males again exhibited elevated plasma insulin after glucose administration at all time points yet these data were not statistically significant. However, obese males did display greater total insulin AUC compared to lean males, shown in Figure 3.13.

Obese females displayed a trend of elevated plasma insulin following glucose administration, which were statistically significant between the lean and obese groups at 10 and 20 minutes after glucose infusion (Figure 3.11). Plasma insulin level converged after 120 minutes. Obese female sample numbers were reduced by three, as per the GTT insulin baseline omissions.

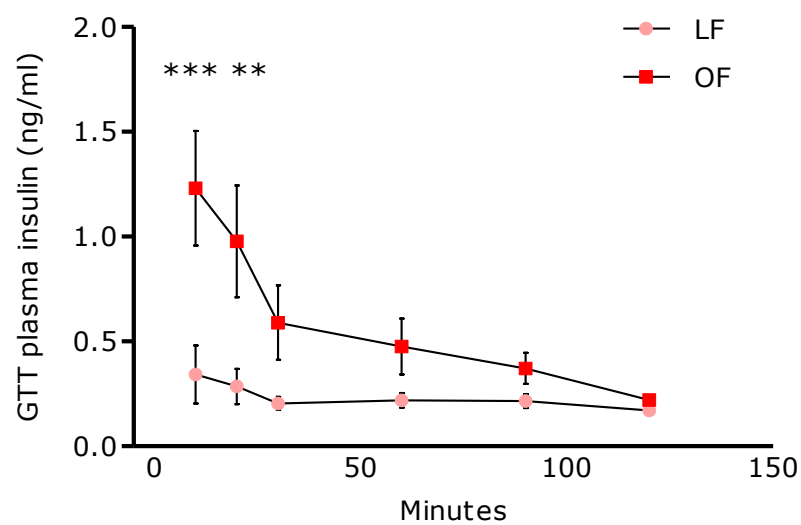


Figure 3.11: GTT plasma insulin time course measurements of lean female (LF; n=7) and obese female (OF; n=6) sheep. Values are mean \pm SEM. Statistical difference is denoted by ** = $p < 0.005$ between LF and OF at time point 20m; *** = $p < 0.001$ between LF and OF at time point 10m (Two-way ANOVA with repeated measures).

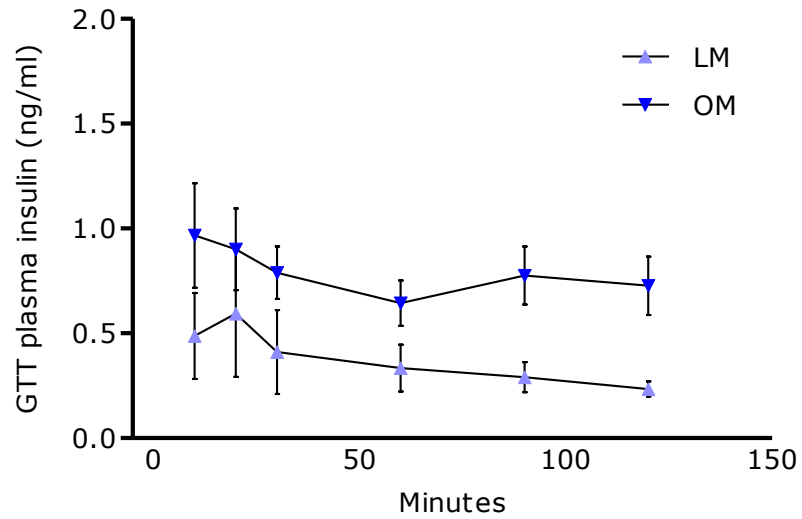


Figure 3.12: GTT plasma insulin time course measurements of lean male (LM; n=10) and obese male (OM; n=7) sheep. Values are mean \pm SEM.

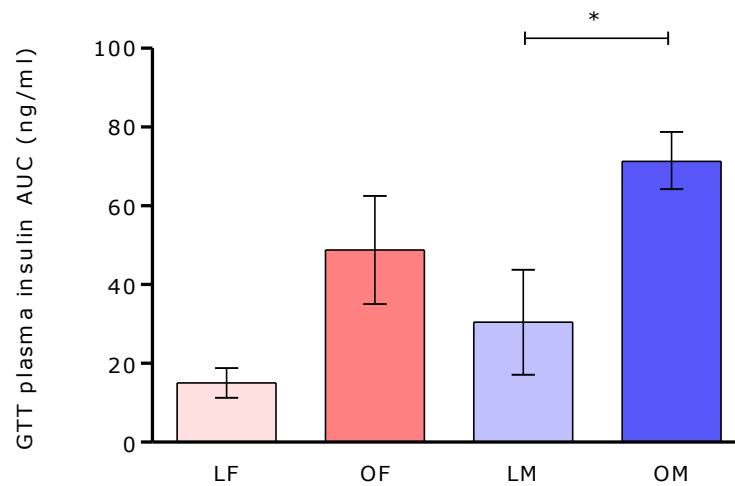


Figure 3.13: GTT plasma insulin AUC (ng/ml) of lean female (LF; n=7), obese female (OF; n=6), lean male (LM; n=10) and obese male (OM; n=7) sheep. Values are mean \pm SEM. Statistical difference is denoted by * = $p < 0.05$ (Kruskal-Wallis).

A positive correlation was determined by Pearson's correlation coefficient ($r^2 = 0.46$, $p = 0.003$) in correlation analysis of total fat mass and GTT plasma insulin AUC in males only (Figure 3.15, p119), where females did not display this trend (Figure 3.14, p119).

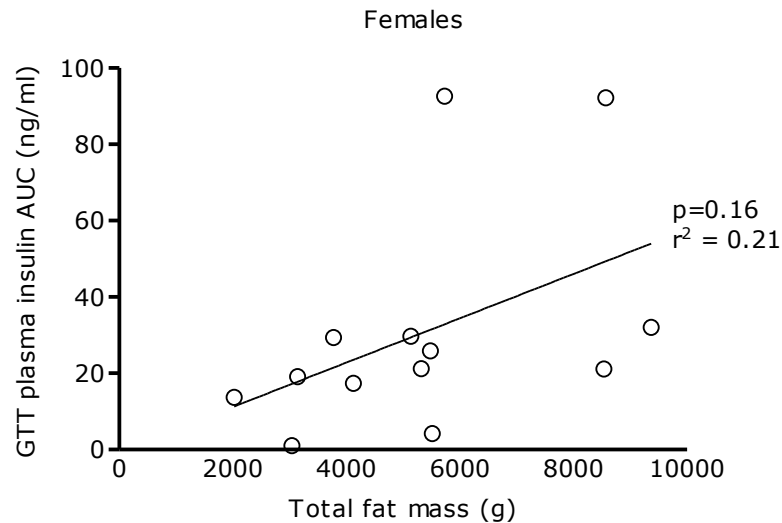


Figure 3.14: Relationship between total fat mass (g) and plasma insulin AUC (ng/ml) of female (n=12) sheep. Correlation analysis showed no statistical significance where $p=0.16$ and $r^2 = 0.21$ (Pearson's correlation coefficient).

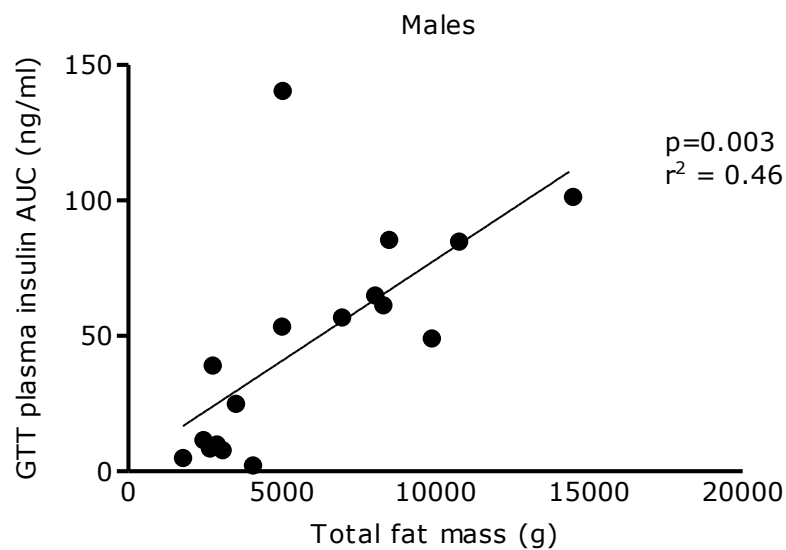


Figure 3.15: Relationship between total fat mass (g) and plasma insulin AUC (ng/ml) of male (n=17) sheep. Correlation analysis showed statistical significance where $p=0.003$ and $r^2 = 0.46$ (Pearson's correlation coefficient).

Baseline plasma leptin measurements (ng/ml) (Figure 3.16, p120) showed no statistical significance in gender or obesity groups. Obesity groups exhibited a trend, where comparison of lean females to obese females gave a p value of 0.112 and lean males to obese males gave a p value of 0.081.

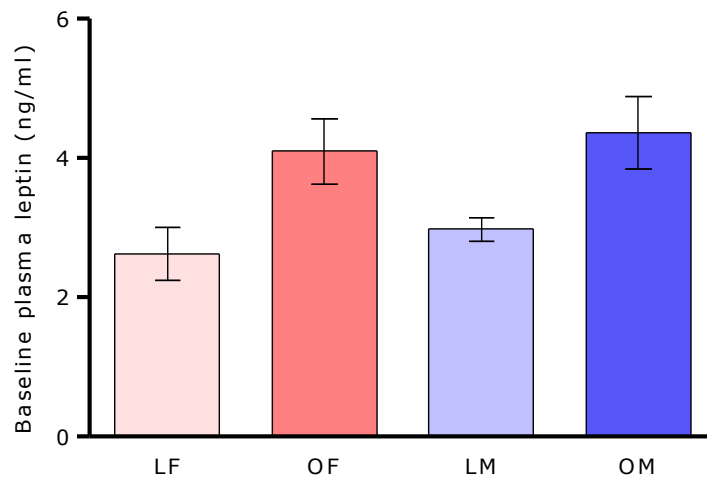


Figure 3.16: Baseline plasma leptin (ng/ml) of lean female (LF; n=7), obese female (OF; n=9), lean male (LM; n=11) and obese male (OM; n=9) sheep. Values are mean \pm SEM.

Following feeding, plasma samples were collected at various time points to determine circulatory levels of leptin. Time course measurements and subsequent AUC analysis identified a statistically significant elevation in plasma leptin between lean and obese groups, shown in Figures 3.17, 3.18 and 3.19 (p121-122). Gender appeared to have no effect on plasma leptin.

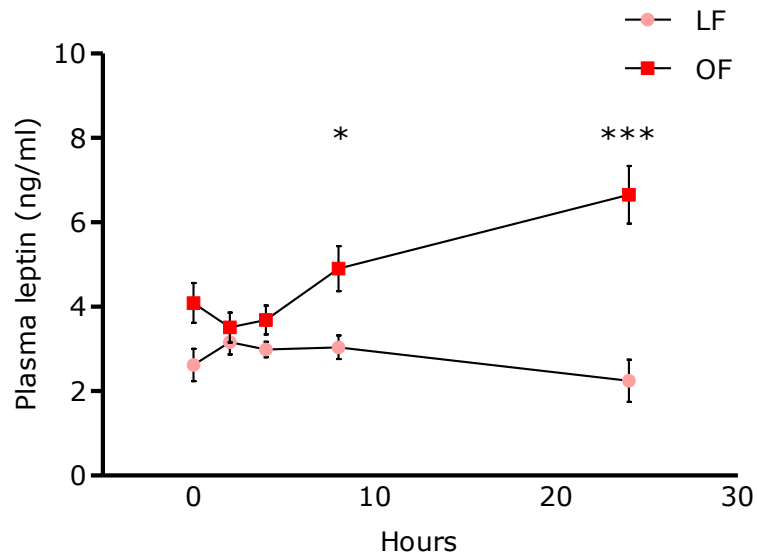


Figure 3.17: Plasma leptin time course measurements after feeding for lean female (LF; $n=7$) and obese female (OF; $n=9$) sheep. Values are mean \pm SEM. Statistical differences are denoted by * = $p < 0.05$ between LF-OF at time point 8h; *** = $p < 0.001$ between LF-OF at time point 24h (Two-way ANOVA with repeated measures).

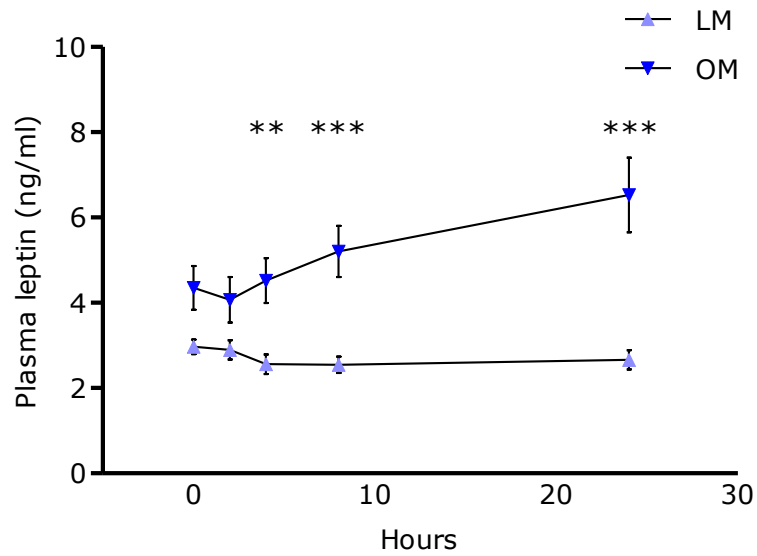


Figure 3.18: Plasma leptin time course measurements after feeding for lean male (LM; $n=11$) and obese male (OM; $n=9$) sheep. Values are mean \pm SEM. Statistical differences are denoted by ** = $p < 0.01$ between LM-OM at time point 4h, *** = $p < 0.001$ between LM-OM at time point 8h and 24h (Two-way ANOVA with repeated measures).

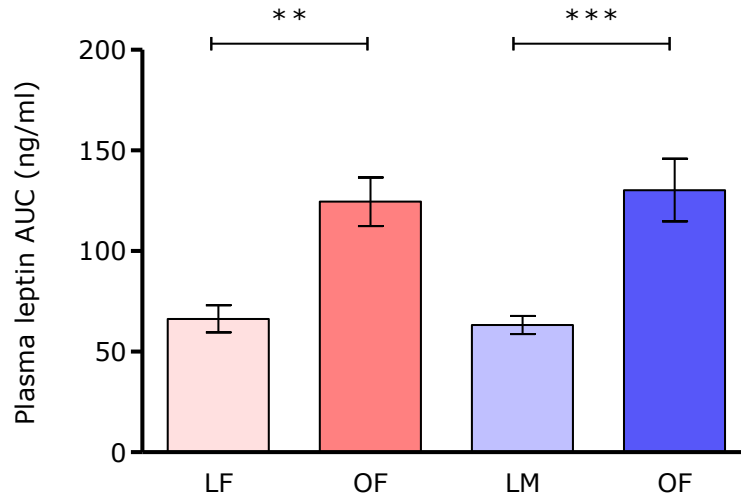


Figure 3.19: Plasma leptin AUC (ng/ml) of lean female (LF; n=7), obese female (OF; n=9), lean male (LM; n=11) and obese male (OM; n=9) sheep. Values are mean \pm SEM. Statistical differences are denoted by ** = $p < 0.005$; *** = $p < 0.001$ (ANOVA).

Correlation analysis of total fat mass (g) against plasma leptin AUC (ng/ml) identified a positive correlation with a p value of < 0.0001 and r^2 of 0.64, see Figure 3.20.

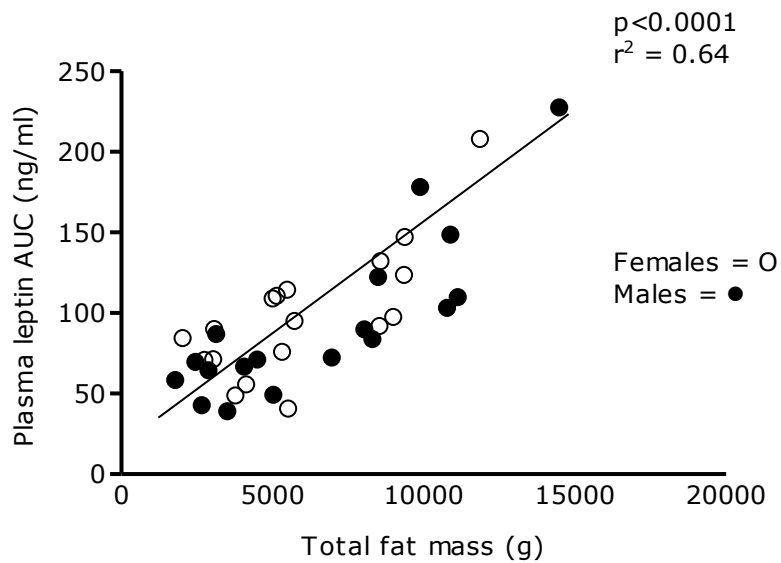


Figure 3.20: Relationship between total fat mass (g) and plasma leptin AUC (ng/ml) of total sheep (n=36). Correlation analysis showed a statistical significance where $p < 0.0001$ and $r^2 = 0.64$ (Pearson's correlation coefficient).

No statistical significance was observed in correlation analysis between GTT plasma insulin AUC and plasma leptin AUC shown in Figure 3.21, p123.

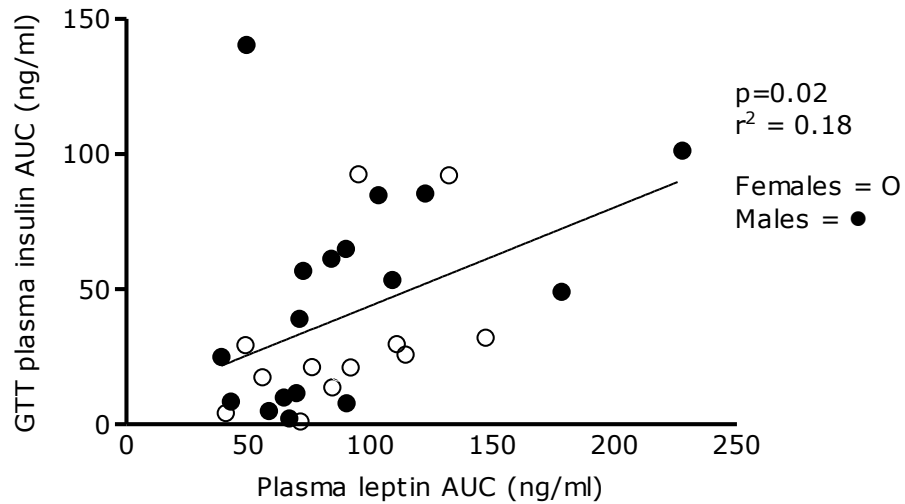


Figure 3.21: Relationship between GTT plasma insulin AUC (ng/ml) and plasma leptin AUC (ng/ml) of total sheep (n=30). Correlation analysis showed no significant difference where $p=0.02$ and $r^2 = 0.18$ (Pearson's correlation coefficient).

Baseline plasma cortisol (nmol/l) measurements (Figure 3.22) showed a significant elevation between obese females compared to obese males, a result not displayed between the lean groups. The effect of obesity in the female group exhibited a trend towards elevated baseline plasma cortisol ($p=0.058$) although this result was not statistically significant. Obesity in males had no effect in comparison to their lean counterparts.

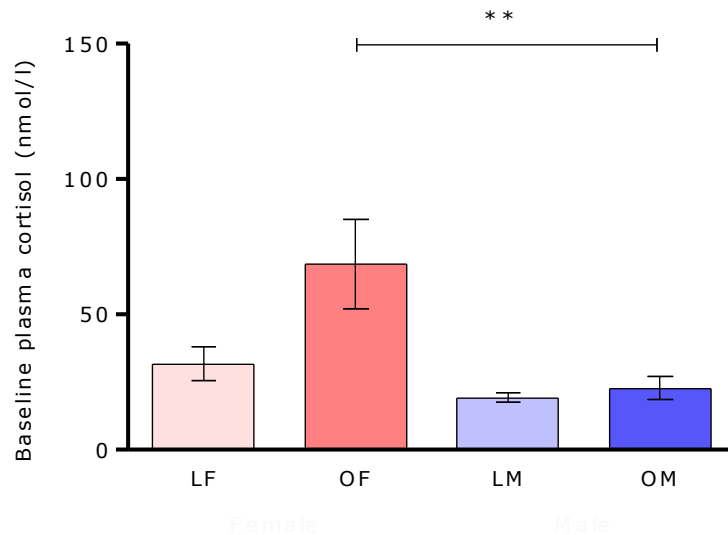


Figure 3.22: Baseline plasma cortisol (nmol/l) of lean female (LF; n=7), obese female (OF; n=9), lean male (LM; n=11) and obese male (OM; n=9) sheep. Values are mean \pm SEM. Statistical difference is denoted by ** = $p < 0.005$ (ANOVA).

Similarly to baseline plasma cortisol levels, following feeding, plasma cortisol time course measurements (Figures 3.23-3.24, p125) and AUC (Figure 3.25, p125) analysis identified elevated levels in the obese female group only. Obese females displayed significantly increased plasma cortisol levels in comparison to both lean females and obese males, where $p < 0.005$. Again obesity in males appeared to have no effect in comparison to lean males.

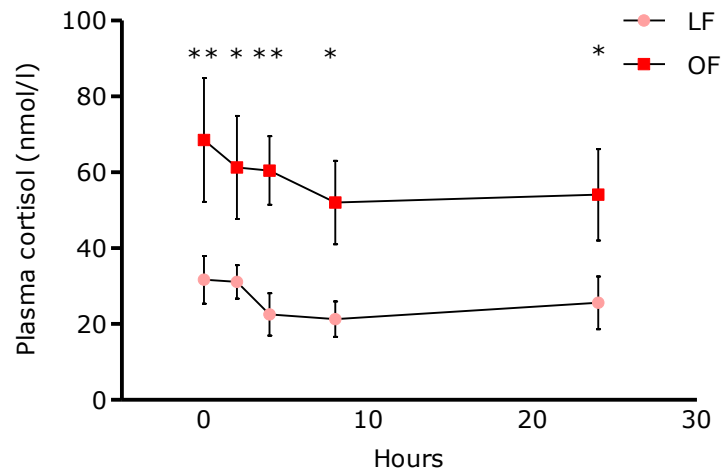


Figure 3.23: Plasma cortisol time course measurements after feeding for lean female (LF; $n=7$) and obese female (OF; $n=9$) sheep. Values are mean \pm SEM. Statistical differences are denoted by * = $p < 0.05$ between LF-OF at time point 0h, 8h and 24h; ** = $p < 0.01$ between LF-OF at time point 0h and 4h (Two-way ANOVA with repeated measures).

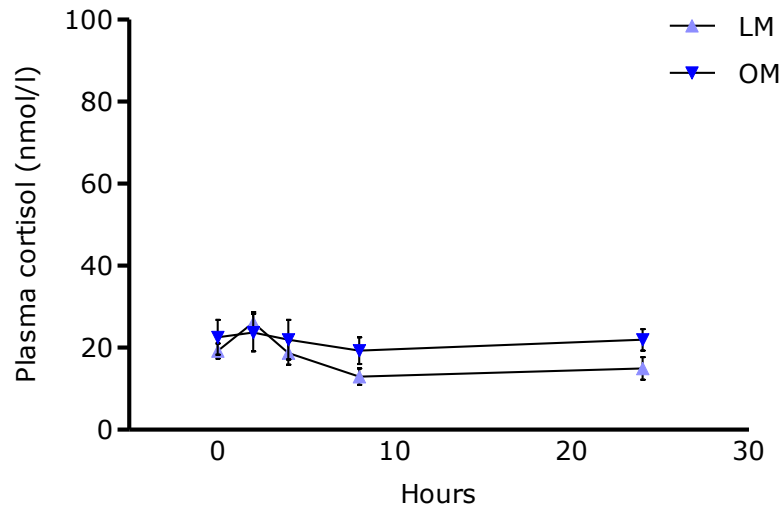


Figure 3.24: Plasma cortisol time course measurements after feeding for lean male (LF; n=11) and obese male (OF; n=9) sheep. Values are mean \pm SEM.

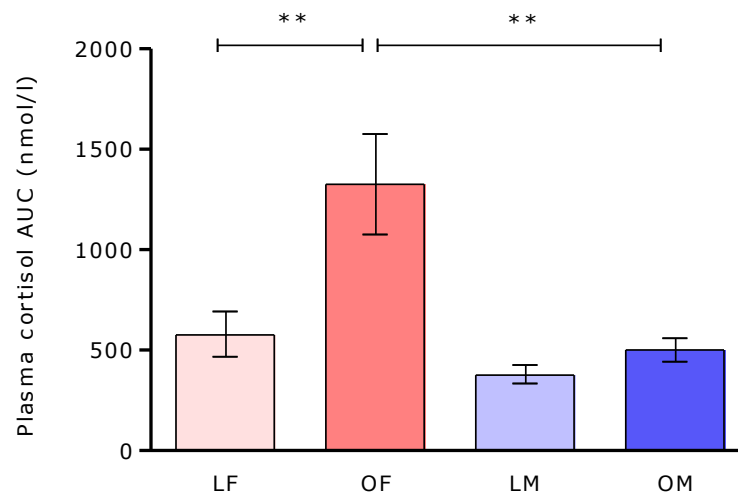


Figure 3.25: Plasma cortisol AUC (nmol/l) of lean female (LF; n=7), obese female (OF; n=9), lean male (LM; n=11) and obese male (OM; n=9) sheep. Values are mean \pm SEM. Statistical difference is denoted by ** = $p < 0.005$ (ANOVA).

Correlation analysis between plasma cortisol AUC (nmol/l) and omental and PAT depots identified a positive correlation in females where Pearson's correlation coefficient showed $p = 0.0003$ and $r^2 = 0.63$ shown in Figure 3.26, p126. This relationship was not demonstrated in analysis of the males, see Figure 3.27, p126.

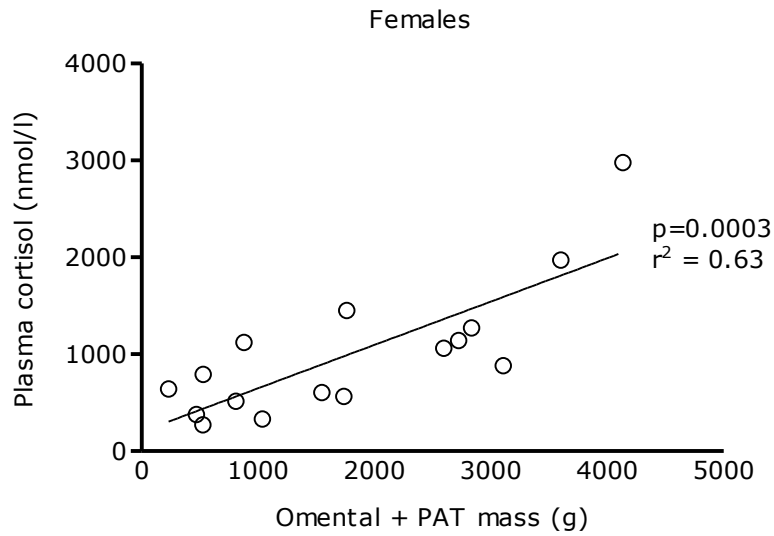


Figure 3.26: Relationship between omental + PAT mass (g) and plasma cortisol AUC (nmol/l) of female sheep (n=16). Correlation analysis showed a statistical significance where $p=0.0003$ and $r^2 = 0.63$ (Pearson's correlation coefficient).

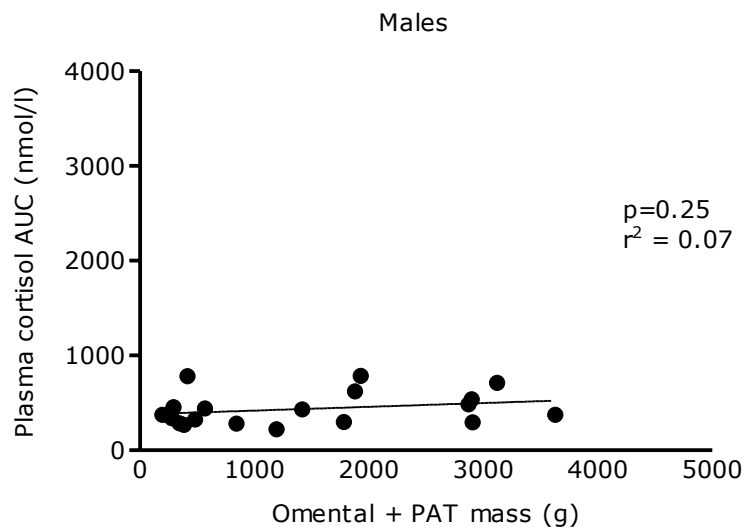


Figure 3.27: Relationship between omental + PAT mass (g) and plasma cortisol AUC (nmol/l) of male sheep (n=20). Correlation analysis showed no statistical significance where $p=0.25$ and $r^2 = 0.07$ (Pearson's correlation coefficient).

To further assess circulatory metabolic status, additional plasma metabolite concentration analyses of glucose, NEFAs and triglycerides were performed. These measurements identified no significant differences related to either gender or obesity shown in Table 3.4.

Group	LF (n=7)	OF (n=9)	LM (n=11)	OM (n=9)	Gender	Obesity
Glucose (mmol/l)	3.04±0.18	3.08±0.14	2.94±0.10	3.03±0.11	NS	NS
NEFAs (mmol/l)	0.43±0.06	0.49±0.06	0.40±0.03	0.50±0.06	NS	NS
Triglycerides (mmol/l)	0.35±0.06	0.31±0.03	0.40±0.05	0.38±0.07	NS	NS

Table 3.4: Plasma metabolite measurements for glucose, non-esterified fatty acids (NEFAs) and triglycerides (mmol/l) of lean female (LF), obese female (OF), lean male (LM) and obese male (OM) sheep. NS = no significant difference (ANOVA). Plasma glucose analysis treated with Kruskal-Wallis statistical test.

3.4.2.1 The effect of increased adiposity on triglyceride accumulation in muscle

In determination of triglyceride accumulation (mg per g *LD* muscle tissue), analysis of *LD* muscle samples identified a significant increase ($p < 0.05$) in obese males compared to lean males, a result not seen in females. Statistical analysis of muscle triglyceride accumulation of lean to obese females provided a p value of $p = 0.112$. Gender analysis of the lean and obesogenic groups identified no significant differences, shown in Figure 3.28.

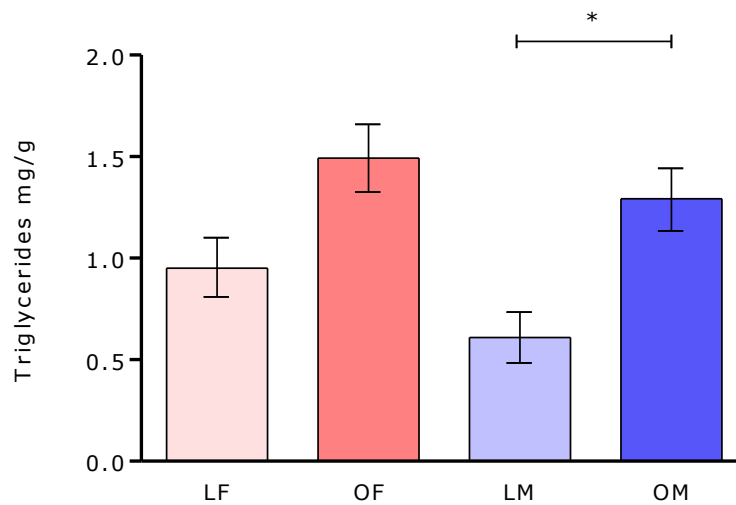


Figure 3.28: Triglyceride deposition in mg per g longissimus dorsi (*LD*) muscle of lean female (LF; $n=7$), obese female (OF; $n=9$), lean male (LM; $n=11$) and obese male (OM; $n=9$) sheep. Values are mean \pm SEM. Statistical difference is denoted by * = $p < 0.05$ (Kruskal-Wallis).

Pearson's correlation coefficient analysis of muscle triglycerides and plasma insulin (Figure 3.29, p129) displayed no statistical correlation, $p = 0.20$ and $r^2 = 0.06$.

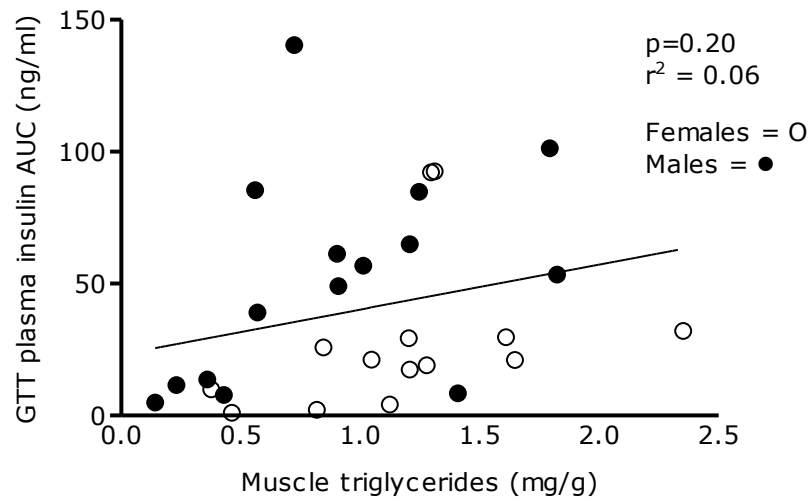


Figure 3.29: Relationship between GTT plasma insulin AUC (ng/ml) and muscle triglycerides (mg/g) of total sheep (n=30). Correlation analysis showed no statistical significance where $p=0.20$ and $r^2 = 0.06$ (Pearson's correlation coefficient).

3.5 Discussion

3.5.1 An obesogenic environment and obesity development

In my study, the exposure to an obesogenic environment, i.e. an area of higher stocking rates of sheep (6 sheep per 19m² compared to 6 sheep per 1125m²) led to a reduction in physical activity, with no alteration to the amount of relative energy consumed. This reduction in physical activity and subsequent imbalanced ratio of energy intake to physical activity contributed to increased body weights between the 'lean' and 'obese' environment animals. However, the lean female sheep were slightly less active than their male counterparts and although not statistically significant, nevertheless showed a resulting smaller energy intake ratio imbalance in comparison to males. From human behavioural studies, in general, females usually display reduced physical activity in comparison to their male counterparts; this is attributed to a number of lifestyle and psychological factors²⁸⁵. Shown by the obesogenic model used in this study, it is unknown as to why the lean female animals exhibited a slight, albeit non-significant reduction in physical activity to the lean males, although this subtle difference was removed between the obese animals. In contrast, many rodent models of physical activity induced obesity have demonstrated a gender dimorphic response where females display on average a 20-50% higher activity rate than males²⁸⁶. It is proposed that sex hormones may be mediating this gender dimorphic activity response observed in rodents. Gorzek et al reported that ovariectomy in female mice led to reduced physical activity, a trend which was reversed by the administration of 17 β -oestradiol²⁸⁷. Yet in the human population, activity levels in postmenopausal females negatively correlate with elevated serum oestradiol concentrations²⁸⁸ suggesting in humans that sex hormones may have the reverse effect on physical activity compared to rodents. It is therefore possible that in sheep that sex hormones influence physical activity similarly to that observed in humans rather than rodent models.

Despite the fact only males showed a significant reduction in physical activity with obesity, both females and males exhibited increased body weights of 25% and 50% respectively after exposure to an obesogenic environment, albeit with males showing a much greater response.

In the obese males, this observed body weight increase was attributed to an increase in both fat mass and lean mass offering an explanation for the increased energy balance. In a human MRI scan study, males displayed higher muscle and skeletal mass compared to females²⁸⁹. The study also demonstrated that the resting metabolic rate of skeletal muscle tissue was 54.4 kJ/kg and adipose tissue 18.8 kJ/kg²⁸⁹ and hence a higher proportion of muscle mass would require higher amounts of energy. One hypothesis during the experimental analysis of these morphometric body measurements was that the increase in lean mass observed in the obese male sheep, may have been due to increased triglyceride and lipid accumulation in the muscle tissue. It is widely established that the presence of obesity contributes to increased triglyceride accumulation in skeletal muscle tissue²⁹⁰, a finding supported in this study where obese males showed elevated muscle triglycerides compared to their lean counterparts. However, obese males did not show elevated muscle triglycerides in comparison to the obese females, suggesting that the obese male lean mass increase was not due to increased muscle triglycerides, and a more probable explanation for the observed difference was an increase in skeletal muscle mass. In obese females the body weight increase was completely attributable to raised fat mass.

Both genders showed a significant increase in total fat mass after exposure to an obesogenic environment. However as expected, lean and obese female animals were relatively fatter than the males, results which are in agreement with human epidemiological data^{11,12}. Relative total fat mass percentage identified a two-fold increase with obesity. In obese humans, it is estimated that total body fat mass percentage is approximately >32% and >25% for females and males respectively²⁹¹. Yet in this sheep study despite the two-fold increase in body fat percentage, obese females had only \approx 15% and obese males \approx 13% of relative fat mass. In comparison to another sheep obesity study, exposure of animals to an obesogenic environment of both increased food intake and restricted physical activity, resulted in body fat percentages to increase from \approx 15% to \approx 30%²³⁴. However the animals in the comparative study were reared for a shorter period (13 months) and consumed increased amounts of food.

The relative fat mass results for this particular study model of obesity through restricted physical activity only, implies the development of a moderate obese condition in the sheep exposed to an obesogenic environment.

3.5.2 Changes in adipose tissue deposition, location and physiology

A more detailed analysis of the adipose tissue location and deposition indicated both genders exposed to such an environment exhibited increased adipose tissue mass in subcutaneous and central depots (PAT and omental). Obese males possessed more omental and subcutaneous adipose tissue mass compared to obese females. Human epidemiological data tends to suggest that in obesity, males develop increased central adipose tissue and females develop more peripheral adipose depots, i.e. gluteal and subcutaneous adipose depots^{11,12}.

It appeared not to be the case in this sheep study, although the males may have exhibited higher increases of omental and subcutaneous adipose tissue due to a higher energy ratio imbalance and more a pronounced reduction in physical activity. Furthermore, development of adipose tissue in females occurs during critical physiological periods, and can be affected by changes in sexual maturity, parity and at menopause²⁹². Taking this into consideration, the female sheep in my study were relatively young and allowing for a longer rearing period of these animals may alter the observed results in adipose depot locations.

Alternatively a reason for these discrepancies may be the higher inaccuracies of indirect methods used in some human body fat measurements, such as skin-fold thickness against a more direct and accurate DXA scanning method. In analysis of relative adipose deposition, in response to an obesogenic environment, relative subcutaneous depot percentage was reduced due to an overriding increase in central adipose tissue deposition. This was the case for both genders, and obese females even showed higher relative PAT and omental adipose tissue percentage in comparison to obese males, a finding which reinforces the notion that females in general have a higher body fat percentage composition²⁹³.

Microscopic analysis of perirenal adipocytes identified adipocyte enlargement between the obese and lean sheep. Subsequent quantitative analysis identified a three-fold difference in mean adipocyte area in the obese compared to lean animals, where gender showed no effect.

In human adipocyte studies, obese individuals, both males and females, were shown to have increased ectopic and intra-abdominal adipose tissue depot mass, results which were due to parallel adipocyte enlargement hypertrophy rather than adipocyte hyperplasia^{294,295}.

In my study, the strong correlation ($r^2=0.85$) between adipocyte area and PAT mass would suggest that adipocyte hypertrophy is largely responsible for the increase in PAT mass size. Although experimental attempts were made to determine possible adipocyte hyperplasia of each PAT mass sample via individual adipocyte cell counting, no validated counting method could be produced to translate two dimensional samples to a three dimensional tissue depot. Therefore it was not possible to determine any potential effect of obesity on increased perirenal adipocyte number. Population distribution analysis of perirenal adipocytes identified that lean males tended to have smaller adipocytes than lean females, but after exposure to an obesogenic environment and resulting adipocyte enlargement, this difference was removed. These results may reflect the fact that females generally have a higher body fat percentage, and thus require a higher storage capacity for triglycerides and lipids. Alternatively this may reflect a difference in the male PAT depot capabilities, and male central adipocytes may have a larger storage capacity for triglycerides and lipids, potentially encouraging the increased central deposition observed in male obesity. It is possible that with a longer exposure to obesity, the male animals could display a greater increase in perirenal adipocyte enlargement than the female animals. In human studies, subcutaneous adipocytes were demonstrated to be larger and have an increased triglyceride storage capacity than intra-abdominal adipocytes in females or males. Additionally these subcutaneous depots were shown to be more active, and thus play a greater role in the metabolic profile of females³⁸.

Several human studies suggest that in adipose tissue mass enlargement, the non-fat cell fraction of adipose tissue increases. This includes elevated immune cell and macrophage infiltration, preadipocyte infiltration and endothelial cell deposition^{65,66,67} which can result in changes to adipose tissue physiology and signs of tissue damage, for example the increased development of crown-like structures²⁹⁶. In general observations of the analysed microscopic samples, no increased cellular bodies or any crown-like structures were observed. Again, this may be due to analysing two-dimensional samples in relation to a three-dimensional tissue depot, and thus any effect of these parameters was therefore not detected.

Also the magnification capabilities of the equipment were limited to 40x, a magnification power which did not allow for identification of the individual nucleated cell bodies present.

Alternatively, Sharkey et al reported the increased occurrence of PAT crown-like structures and adipocyte cell death in the presence of severe obesity in sheep. These findings were conjoined by elevated mRNA expression in cluster of differentiation 68 (CD68), a marker of macrophage infiltration²²⁷. Perhaps then, the moderate nature of the developed obese condition, age of the animals and length of exposure period in these sheep may give explanation to the general observations made

3.5.3 Metabolic adaptations with obesity and gender

My study also analysed a number of circulatory hormones and metabolites which human studies been shown to increase in the presence of an obese condition. In response to moderate obesity, the main finding in this chapter identified an increase of baseline plasma cortisol in obese females compared to obese males which persisted after feeding, but without effect between any other groups. Plasma cortisol AUC measurements further reinforced the baseline plasma cortisol results, as obese females showed elevated plasma cortisol compared to both lean females and obese males. Elevation of plasma glucocorticoids is an established measure of the level of physiological, social or psychological stress²⁹⁷, these results therefore suggest that the development of a moderate obese condition in females results in a higher stress response in sheep. Different species have shown varying results in regards to gender and stress response, for example rat studies have demonstrated a higher stress response in females²⁹⁸, but in adult humans, aged matched males are reported to show increased plasma cortisol in varying stress responses in comparison to females²⁹⁹. It is likely that the variations displayed in the referenced studies are attributable to the type and age of the species studied, and also the type of stress imposed on the test subjects

Research into the relationship between fat mass and cortisol has demonstrated that hypercortisolism is a feature in human obesity, both systemically and intracellularly¹³⁶. It is generally understood that with obesity, cortisol production is enhanced but cortisol clearance is also raised, and thus circulating plasma concentration is not affected¹³⁷. A human gender-obesity study identified a positive correlation between raised cortisol clearance rate and increased total body fat in females only, which suggested that female adipose tissue contained a functioning binding mechanism for cortisol i.e. GR which was not shown in males³⁰⁰.

Although no cortisol clearance rates were determined in these sheep, the correlation in PAT mass and plasma cortisol shown by the females suggests a gender disparity in obesity with cortisol and possible glucocorticoid function, a finding further discussed in Chapter 4 and 5. Generally it is thought chronic exposure to raised plasma cortisol and repeated activation of the HPA contributes to the pathogenesis and development of abdominal obesity³⁰¹. This mechanism may have aided in the central fat deposition observed in the female sheep, which was contrary to the surveyed human data in relation to gender adiposity dimorphism^{37,38}. Additionally, amplified plasma and tissue cortisol levels are believed to suppress inflammation via immune cell function inhibition¹⁴³, and as a consequence may provide protection against the chronic low-grade inflammation often exhibited by obese subjects⁷¹.

The sex differences observed in HPA axis activation and resulting stress response is thought to be partly due to the circulating gonadal sex steroid hormone milieu. Through cognate central nervous system (CNS) receptor binding, it is believed oestrogen can amplify HPA function, whereas testosterone via the same mechanism has the opposite effect and suppresses HPA function³⁰². Again, unfortunately no circulatory sex hormone levels were determined for the study animals, but Austin et al reported elevated serum oestrone and oestradiol in adult females in response to obesity³⁰³. It is possible then, that the development of moderate obesity exhibited in this study consequently elevates oestrogen HPA enhancement action in the obese females, potentially mediated by central or ectopic adipose depots. This results in increased plasma cortisol, an outcome not observed in the obese males which conversely may be due to the HPA suppressive functionality of testosterone.

Fasting insulin concentrations are known to be elevated in obese subjects in comparison to lean counterparts, a relationship often associated with development of central obesity⁵¹. In my study, plasma insulin did not appear to be affected by intravenous administration of glucose. Although obese males exhibited initial raised baseline plasma insulin levels, during the GTT only lean and obese females displayed time course differences, which were observed immediately after glucose infusion, and during the remaining GTT time points, insulin levels were not significantly different. This may be due to the relative insulin insensitivity and reduced glucose utilization observed in sheep³⁰⁴.

Overall only obese males presented elevated plasma insulin at baseline and AUC levels, a metabolic alteration not displayed by females with obesity. This suggests that perhaps the male sheep are more sensitive to developing hyperinsulinaemia in the presence of moderate obesity. Chronic exposure of hyperinsulinaemia, otherwise termed insulin resistance, is believed to be a precursor of diabetes mellitus type II. Insulin resistance can also result in additional weight gain and obesity development, hypertension and dyslipidaemia. Epidemiological data suggests that the prevalence of diabetes mellitus type II and abnormalities in glucose metabolism is higher in males compared to females, and females also exhibit a decreased susceptibility to NEFA induced peripheral insulin resistance³⁰⁵.

These gender differences in insulin sensitivity are often attributed to the actions of sex hormones. Differences which are especially evident during the period of menopause where a reduction in oestrogen and increase in testosterone levels contributes to a loss of peripheral adipose tissue and increase in visceral fat mass in females leading to an increase in insulin resistance¹³. The exact mechanism behind this sex hormone mediated reduction in development of insulin resistance observed in females is currently unknown.

As expected, this study demonstrated that moderate obesity results in hyperleptinaemia, but gender had no effect on this outcome. Baseline levels of plasma leptin showed a slight trend towards increased concentration in both genders. These levels were then shown to be significant with obesity directly after feeding and with AUC analysis. Elevated plasma leptin is linked to adiposity and central nervous system regulation of appetite reduction and enhanced energy expenditure³⁰⁶. Additional studies have demonstrated positive correlations between hyperleptinaemia and hyperlipidaemia, insulin resistance and hypertension independent of total adiposity³⁰⁶.

In vitro administration of insulin and glucocorticoids were also shown to contribute to elevated plasma leptin in sheep³⁰⁷, results that suggested that insulin and glucocorticoids may play a role in regulation of white adipocyte leptin mRNA expression. This may explain the possible mechanisms mediating the hyperleptinaemic conditions observed in the obesogenic animals within the present study. This study showed no positive correlations between plasma leptin and insulin but a positive correlation between total fat mass and plasma leptin.

It is possible that the moderate nature of the obese condition displayed in these sheep has contributed to onset hyperleptinaemia in an attempt to control appetite, energy expenditure and further weight gain. Prolonged exposure to this hyperleptinaemic condition and a more severe obesity challenge could amplify the detrimental effects often linked with elevated plasma leptin.

In analysis of circulating glucose, NEFAs and triglycerides in this study, no differences were observed in any group and thus neither gender nor obesity had any effect. This may be due to the moderate nature of obesity development; alternatively these results may be because of the altered utilization and synthesis of these metabolites in sheep^{304,308}. In human epidemiological studies, obesity is often associated with the development of hyperglycaemia and dyslipidaemia^{121,309,310}.

3.5.4 Lipid deposition, peroxidation and lipotoxicity with gender and obesity

Despite there being no effect of gender or obesity in circulatory plasma NEFAs and triglycerides in this study, analysis of lipid accumulation in muscle tissue identified an increase in lipid deposition in obese males compared to their lean counterparts. This trend was also reflected in the female group. Muscle triglyceride accumulation has been suggested to contribute to the pathogenesis of insulin resistance²⁹⁰, a pathway especially enhanced in the presence of obesity and diabetes mellitus type II. The postulated mechanism behind this relationship is a functional impairment of mitochondria in obesity resulting in fatty acid metabolism dysfunction, a defect which leads to diminished usage of NEFAs and an increased esterification and storage of lipids within skeletal muscle tissue³¹¹. This fatty acid metabolic impairment is thought to be related to the development of reduced insulin sensitivity and impairment of glucose metabolism associated with insulin resistance^{124,125,311}. Although in this study, plasma insulin and muscle triglyceride composition measurements do not correlate directly in individuals, obese males exhibited both elevated plasma insulin and increased muscle triglyceride deposition. A result which suggests that even in moderate exposure to obesity, the male sheep are prone to a greater risk of insulin resistance; possibly through a raised capacity to store triglycerides in lean mass, which was increased with obesity in the males.

3.5.5 Conclusion and summary

In conclusion, this study has demonstrated that sheep exposed to a post-natal obesogenic environment through a reduction in physical activity develop a moderate obese condition. In general the obesogenic animals exhibited increased body weights and higher adipose tissue deposition, of which adipose tissue accumulation occurred in central fat depots. In more detailed analysis, the treated animals also displayed differing systemic, physiological and phenotypic characteristics in relation to gender. Obese males appeared to exhibit a more pronounced response to moderate obesity compared to obese females, as summarised in Figure 3.30, p139. These findings may in part help to elucidate some of the mechanisms involved in the gender disparity observed in human epidemiological obesity studies, particularly the anatomical distribution of adipose tissue and its associated risk with metabolic syndrome development demonstrated by obese males. In addition to these findings it is postulated that sex hormones significantly contribute to these gender dimorphic mechanisms, a potential target for future studies³⁰².

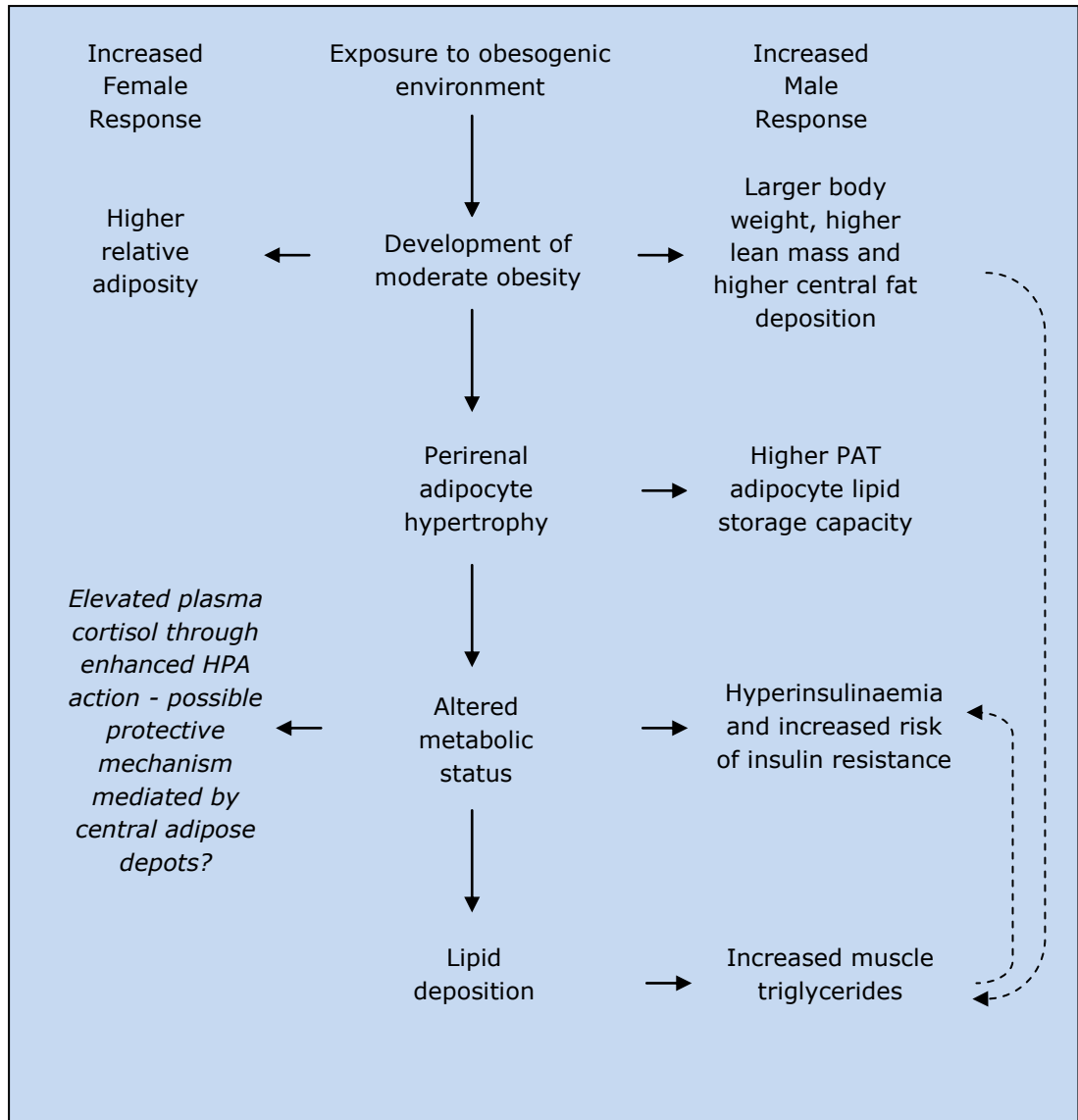


Figure 3.30: Summary of findings in effect of gender and obesity on systemic metabolism and adipose tissue physiology. HPA – Hypothalamic pituitary adrenal axis.

Chapter 4 – The effects of gender and obesity on the perirenal adipose tissue inflammatory genotype

4.1 Introduction and aims

My thesis has already discussed the effect of exposure to an obesogenic environment on adipose tissue deposition, physiology and systemic metabolism, and how gender impacts on these outcomes (see Chapter 3). Evidence in the scientific literature suggests that the alterations so far observed in this study in development of central obesity and resulting metabolic adaptations⁵⁰, are biological contributors to the chronic low-grade inflammation often exhibited by obese subjects^{63,64}. Therefore the focus for this chapter was investigating the presence of moderate obesity and resulting metabolic and adipose tissue phenotype adaptations resulted in an amplified inflammatory genotype, specifically in perirenal adipose tissue. It was also postulated that due to the gender dimorphism that existed in the present study, that gender may play a role in the inflammatory genotype and status of perirenal adipose tissue.

4.1.1 Hypothesis

The hypothesis for Chapter 4 was that the metabolic and physiological adaptations mediated by moderate obesity and gender contribute to an elevated inflammatory state in PAT.

To elucidate any potential mechanism behind this, mRNA transcription analysis of the PAT depot was performed on genes involved in metabolic, glucocorticoid and inflammatory pathways which may display adaptive regulation in exposure to moderate obesity and its resulting effects.

4.2 Materials and methods

A complete description of all the methods used in this chapter can be located in Chapter 2. Development and optimisation of the mRNA primers was performed by Dr S.Seibert, Dr L.Chan, Dr M.Hyatt and myself. Normalisation and expression values for the mRNA gene results were calculated with GeNorm™ software against two reference genes (RPO and RPL19). Where appropriate, any sample or analytical omissions are explained in the relevant results section. In addition, description of statistical tests utilised are provided in this results chapter or can be found in Chapter 2.

4.3 Results

4.3.1 The effect of moderate obesity and gender on the metabolic genotype in perirenal adipose tissue

Metabolite analysis identified elevated plasma leptin in response to moderate obesity in both genders. In analysis of leptin and leptin receptor mRNA in PAT, no significant differences were exhibited in response to either gender or obesity in either leptin or its receptor, shown in Table 4.1. During the experimental analysis, one obese male PAT sample could not be located in the -80°C storage freezer, thus this sample was omitted from all the mRNA PAT analysis performed.

Group	LF (n=7)	OF (n=9)	LM (n=11)	OM (n=8)	Gender	Obesity
Leptin	0.14±0.06	0.27±0.06	0.18±0.10	0.25±0.04	NS	NS
Leptin Receptor	0.22±0.02	0.27±0.06	0.24±0.07	0.18±0.05	NS	NS

Table 4.1: *Leptin and leptin receptor GeNorm mRNA gene expression values of lean female (LF), obese female (OF), lean male (LM) and obese male (OM) sheep in PAT. Values are mean ± SEM. NS = no significant difference (Kruskal-Wallis).*

In contrast, PAT mRNA analysis of adiponectin identified a significant up-regulation of mRNA expression between the obese males and obese females. No further statistical significance was demonstrated in comparison of the remaining gender and obesogenic groups, although statistical analysis did identify a subtle up-regulation trend in comparison of lean males to obese males where $p=0.09$, see Table 4.2, p142. Similarly, PAT mRNA expression analysis of adiponectin receptor exhibited no significant differences in response to either gender or obesity, although comparison of lean females to obese females exhibited a subtle trend of up-regulation where $p=0.06$ and lean males to obese males did display a down-regulation trend where $p=0.09$.

Group	LF (n=7)	OF (n=9)	LM (n=11)	OM (n=8)	Gender	Obesity
Adiponectin	0.10±0.02	0.09±0.03 ^a	0.26±0.14	0.46±0.09 ^b	S	NS
Adiponectin Receptor	0.27±0.05	0.50±0.07	0.41±0.05	0.36±0.06	NS	NS

Table 4.2: Adiponectin and adiponectin receptor GeNorm mRNA gene expression values of lean female (LF), obese female (OF), lean male (LM) and obese male (OM) sheep in PAT. Values are mean ± SEM. NS = no significant difference, S = significance where only one of two comparable groups display significance; statistical difference is denoted by ^{ab} = $p < 0.005$ (Kruskal-Wallis).

4.3.2 The effect of moderate obesity and gender on the glucocorticoid genotype in perirenal adipose tissue

The differences in plasma cortisol response observed between the study groups led to an investigative focus on the glucocorticoid pathway and the adipose tissue gene transcription response. GR PAT mRNA expression analysis identified a significant up-regulation of expression between the lean female and obese female groups, a difference not exhibited in comparison of the male groups. Additionally, obese females also displayed up-regulated GR expression in comparison to obese males, shown in Figure 4.1, a result which was not demonstrated by the lean groups.

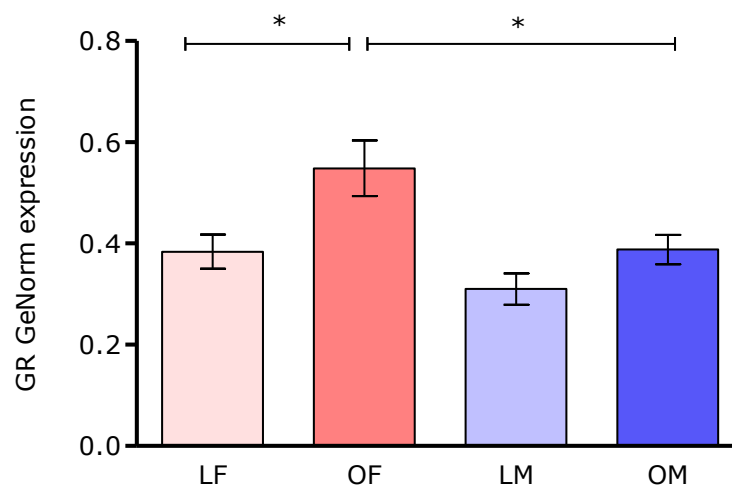


Figure 4.1: Glucocorticoid receptor (GR) GeNorm mRNA expression values of lean female (LF; n=7), obese female (OF; n=9), lean male (LM; n=11) and obese male (OM; n=8) sheep in PAT. Values are mean ± SEM. Statistical difference is denoted by * = $p < 0.05$ (ANOVA).

Analysis of PAT 11 β HSD1 mRNA expression demonstrated a significant down-regulation in expression between obese males and obese females. No other significant differences were exhibited in comparison of obesity and gender, shown in Figure 4.2.

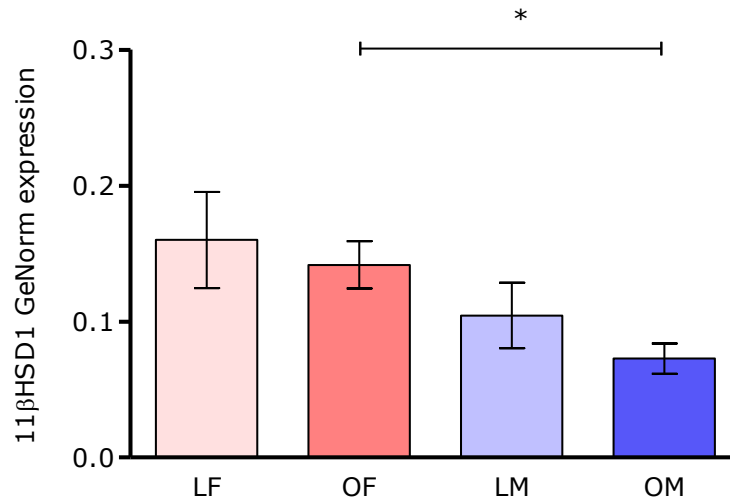


Figure 4.2: 11 β -hydroxysteroid dehydrogenase type 1 (11 β HSD1) GeNorm mRNA expression values of lean female (LF; n=7), obese female (OF; n=9), lean male (LM; n=11) and obese male (OM; n=8) sheep in PAT. Values are mean \pm SEM. Statistical difference is denoted by * = $p < 0.05$ (Kruskal-Wallis).

PAT mRNA expression analysis of the 11 β HSD2 enzyme isoform displayed an opposite trend to 11 β HSD1, where lean males showed a significant up-regulation of mRNA expression in comparison to lean females, shown in Figure 4.3, p144. Again, no other significant differences were exhibited in comparison of the remaining obesity and gender groups.

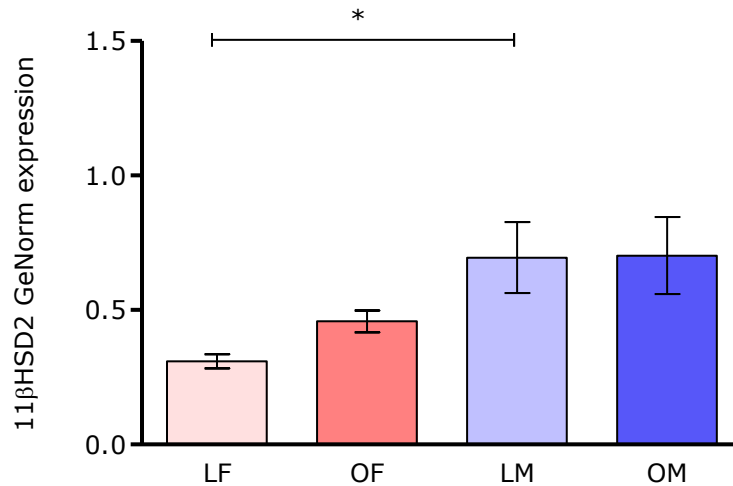


Figure 4.3: *11β-hydroxysteroid dehydrogenase type 2 (11βHSD2) GeNorm mRNA expression values of lean female (LF; n=7), obese female (OF; n=9), lean male (LM; n=11) and obese male (OM; n=8) sheep in PAT. Values are mean ± SEM. Statistical difference is denoted by * = p<0.05 (Kruskal-Wallis).*

4.3.3 The effect of moderate obesity and gender on the inflammatory genotype in perirenal adipose tissue

To determine the effects of moderate obesity and gender on PAT mediated inflammation, mRNA transcription analysis was performed on certain key genes involved in obesity linked inflammatory conditions. PAT mRNA expression analysis of IL-6 identified a significant down-regulation in lean females of IL-6 expression in comparison to lean males, shown in Figure 4.4, p145. No additional differences were observed in analysis of the remaining comparable gender and obesogenic groups.

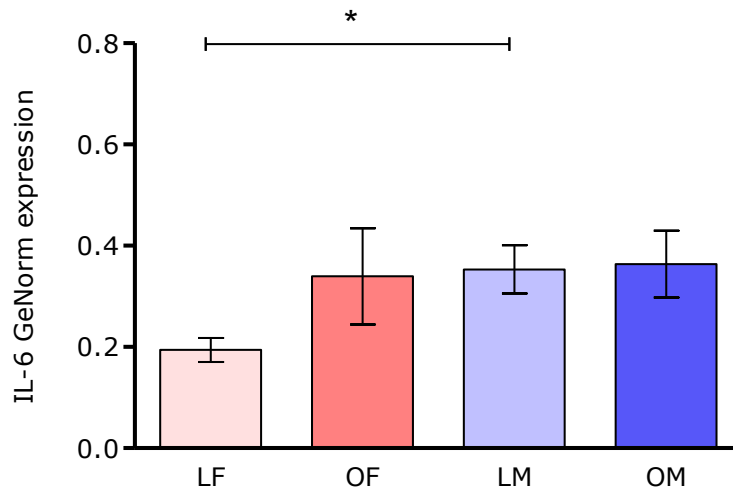


Figure 4.4: Interleukin-6 (IL-6) GeNorm mRNA expression values of lean female (LF; $n=7$), obese female (OF; $n=9$), lean male (LM; $n=11$) and obese male (OM; $n=8$) sheep in PAT. Values are mean \pm SEM. Statistical difference is denoted by * = $p < 0.05$ (Kruskal-Wallis).

Analysis of PAT mRNA expression of MCP-1 identified a significant up-regulation of expression in obese males compared to lean males, and although this trend was also exhibited in comparison of the female groups, this result was not statistically significant, shown in Figure 4.5. Additionally, comparison of gender groups showed no significant differences.

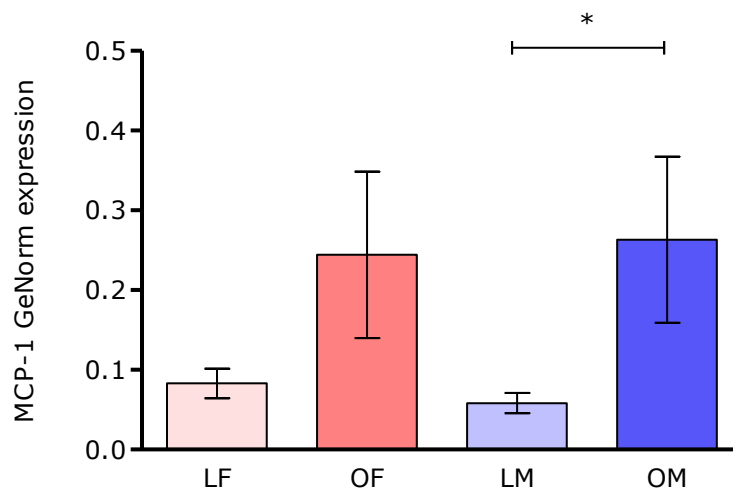


Figure 4.5: Monocyte chemoattractant protein-1 (MCP-1) GeNorm mRNA expression values of lean female (LF; $n=7$), obese female (OF; $n=9$), lean male (LM; $n=11$) and obese male (OM; $n=8$) sheep in PAT. Values are mean \pm SEM. Statistical difference is denoted by * = $p < 0.05$ (Kruskal-Wallis).

This pattern of significantly elevated mRNA expression exhibited by the obese in comparison to lean males was also reflected in analysis of PAT mRNA TLR4 expression, shown in Figure 4.6. Obese females indicated a subtle increased response in mRNA TLR4 expression in comparison to lean, but again this result was not statistically significant. No further significant differences were demonstrated in comparison of the gender groups.

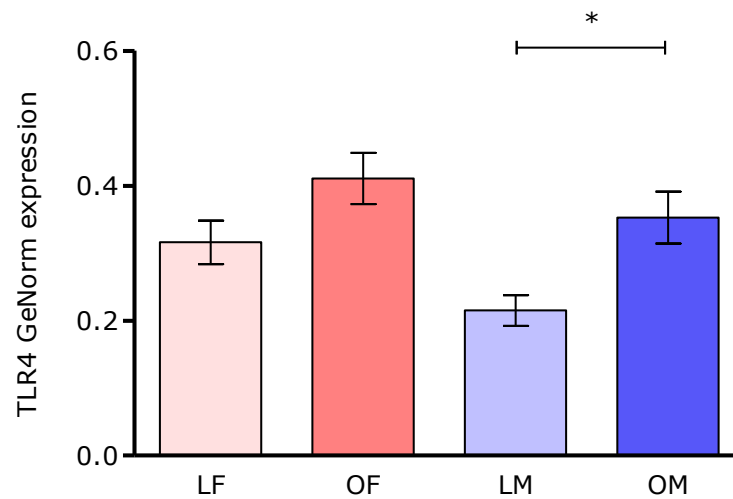


Figure 4.6: Toll-like receptor 4 (TLR4) GeNorm mRNA expression values of lean female (LF; n=7), obese female (OF; n=9), lean male (LM; n=11) and obese male (OM; n=8) sheep in PAT. Values are mean ± SEM. Statistical difference is denoted by * = $p < 0.05$ (ANOVA).

4.4 Discussion

4.4.1 Metabolic gene expression of PAT in response to moderate obesity

Prior to tissue sampling the study animals demonstrated plasma hyperleptinaemia (Chapter 3, Figures 3.16-3.18, p121-122), a condition linked to total fat mass¹⁶⁸. It was therefore hypothesised that perhaps, leptin adipose tissue mRNA expression may be up-regulated in the obesogenic animals, providing a mechanistic source for the plasma leptin elevation observed in the obese animals. In response to the elevated plasma leptin, it was also hypothesised that mRNA leptin receptor expression may be down-regulated, and thus providing a mechanism of leptin resistance often observed in obese subjects¹⁶⁹. However, leptin mRNA expression results in PAT identified that transcription was not affected, a result also observed in leptin receptor. Leptin transcription and subsequent protein synthesis are demonstrably affected by energy intake, a pathway that is decreased with fasting and increased with feeding³¹². An additional rodent study has demonstrated a reduction in leptin expression from white adipose tissue after exogenous intravenous leptin administration³¹³. It is possible the leptin and leptin receptor mRNA results reflect these mechanisms. The animals were euthanised after an overnight fasting period, so potentially the mRNA transcript instance at the time of tissue harvest was during a period of reduced energy intake and thus PAT leptin expression was consequently down-regulated. Alternatively, as the obese males and females displayed hyperleptinaemia, leptin mRNA transcript may have been down-regulated as a compensatory mechanism towards the increased systemic plasma elevation. Human and primate studies in leptin expression have identified adipose depot and gender specific differences, where leptin mRNA expression levels were demonstrated as higher in subcutaneous in comparison to omental fat depots, an effect heightened in females³¹⁴. A ruminant based study further reinforced these findings as sheep and goat leptin mRNA was again demonstrated as higher in subcutaneous adipose depots compared to visceral tissues³⁰⁷. As no study to date has focused on PAT in comparative adipose depot genotypes, potentially the PAT transcription profile may differ in comparison to other adipose tissue depots. Perhaps different adipose depots contribute to certain signaling pathways more than others, a possible explanation for the observed leptin mRNA expression results.

Conversely, the leptin and leptin receptor mRNA transcription levels may be reflective of the moderate obese condition present in the test subjects, and perhaps a more severe or prolonged exposure to obesity would regulate chronic leptin and leptin receptor mRNA up and down-regulation respectively, as associated with obesity mediated leptin resistance¹⁶⁹.

No plasma adiponectin analysis was performed for this study as no commercially reliable plasma adiponectin kit was available for sheep. However adiponectin mRNA expression did show an up-regulation in obese males compared to obese females, although no differences were observed between the lean groups or as a direct effect of obesity. Adiponectin receptor mRNA expression demonstrated no differences in expression from either gender or obesity. Human adiponectin studies have demonstrated a strong positive correlation between plasma adiponectin and adiponectin mRNA expression in white adipose tissue, this correlation was weakened in the presence of obesity, as adiponectin expression was down-regulated in obese subjects³¹⁵. Gender was also shown to have an effect in the human study, despite females possessing higher relative body fat which is linked to reduced plasma adiponectin¹⁶³, females actually exhibited increased plasma adiponectin compared to males³¹⁵. As the current study demonstrated reverse trends, it is possible that plasma hyperinsulinaemia may be the mediating factor behind this elevation in adiponectin mRNA observed in the obese males. Several studies have identified that adiponectin plays a role in insulin mediated glucose uptake, and perhaps the elevation in plasma insulin and potential increased risk of insulin resistance development displayed by the obese males, results in a compensatory up-regulation in adiponectin mRNA to increase insulin sensitization. However, *in vivo* and *in vitro* studies of insulin action has demonstrated the direct effect of down-regulating adiponectin in white adipose tissue, and therefore perhaps the over-expression of adiponectin exhibited in the present study is being mediated by an unknown insulin-sensitising agent³¹⁶. It is possible this mechanism is being mediated by testosterone, as one study reported a strong correlation between low serum testosterone concentration and promotion of insulin resistance via impaired mitochondrial function in males³¹⁷. Additionally enhancement of insulin-sensitivity via adiponectin action is postulated to occur via direct action on insulin receptor substrate and IL-6 molecule pathways through activation of an unidentified adiponectin receptor³¹⁸, a potential explanation as to why no differences in mRNA adiponectin receptor expression were observed in the current study.

Unfortunately without plasma adiponectin measurements for the current study subjects, it is impossible to confirm the proposed hypothesis.

Over-expression of adiponectin in white adipose tissue has been linked with promotion of an anti-inflammatory condition, reduction in adiposity and attenuated oxidative DNA damage³¹⁹. In the current study, perhaps the pronounced morphometric and metabolic response exhibited in the male sheep has also resulted in a more pronounced genotype response in the ectopic adipose depots, especially the inflammatory network and associated glucocorticoid genes which is discussed in the following sub-chapter.

4.4.2 Glucocorticoid and inflammatory gene expression of PAT in response to moderate obesity

One of the key findings in Chapter 3 was raised plasma cortisol in females in response to obesity. My study has also demonstrated an increase in GR mRNA expression in PAT in obese females. Obesity is recognised to affect glucocorticoid metabolism in humans and rodents, which has been shown by an up-regulation in GR and 11 β HSD1 gene expression in visceral adipose tissue, and by enhanced glucocorticoid signaling through increased cortisol secretion³²⁰. A human study conducted by Veilleux et al, reported an elevation of 11 β HSD1 mRNA expression in omental compared to subcutaneous adipose tissue in females³²¹. These findings were in conjunction with raised 11 β HSD1 protein abundance and increased plasma cortisol levels, which were positively correlated to visceral obesity³²¹. 11 β HSD1 has been shown to convert inactive cortisone to cortisol in mature adipocytes, an effect amplifying local glucocorticoid action in obese rodents and humans³²². Over-expression of 11 β HSD1 is also associated with an over-expression of GR- α in murine adipose tissue³²³. Wake et al demonstrated that expression of 11 β HSD1 mRNA correlated with 11 β HSD1 enzyme activity in human adipose tissue³²⁴. As discussed in Chapter 3, human females have shown increased oestrogen concentration with obesity³⁰³, and rodent models of elevated circulating oestrogen in females were shown to mediate an enhanced HPA function³⁰². Taking these findings into account, the elevation in PAT GR mRNA expression displayed in the obese females only, may be a compensatory response in central fat to raised plasma cortisol mediated via elevated circulatory oestrogens. 17 β -oestradiol concentrations have been reported to augment both basal and stimulated ACTH secretion in rodent and ovine animal models³²⁵, and such a mechanism could be responsible for the observed raise in plasma cortisol.

Consequently increased GR gene expression leads to an up-regulation in 11 β HSD1 mRNA expression³²², and amplified activity of the 11 β HSD1 gene may further contribute to an increase in both circulatory and intra-adipose tissue cortisol.

11 β HSD2 gene expression in human and ovine adipose tissue is a relatively recent discovery and its precise role in adipose tissue physiology is unknown³²⁶. Levels of adipose tissue 11 β HSD2 mRNA expression were shown to correlate with BMI, however this was only in subcutaneous adipose depots of male rodents³²⁷. As the function of the 11 β HSD2 enzyme is to convert inactive cortisol to cortisone, the higher levels of gene expression observed in male PAT are predicted to increase 11 β HSD2 activity. This may allow for greater amounts of cortisol to be deactivated and stored in male PAT as cortisone, which limits available systemic and intracellular cortisol compared to females. To date no study has been performed on 11 β HSD2 activity and cortisone storage capacity in PAT with respect to gender.

Intracellular glucocorticoid binding to GR is a pathway involved in the inhibition of cytokine transcription and production¹²⁹, as this pathway appeared to be increased in the obese females, my hypothesis was that PAT inflammatory gene expression would be down-regulated in the females compared to males with obesity. Both MCP-1 and TLR4 mRNA expression in PAT showed a similar pattern whereby obese males demonstrated an up-regulation in these inflammatory genes compared to their lean counterparts. Although the obese females exhibited a trend in elevated gene expression, the results were not significant. This suggests that perhaps the potential increased activation of GR through raised circulatory cortisol and amplified GR expression observed in the obese females may be responsible for a modest inhibition of MCP-1 and TLR4 expression in PAT of obese females. Over-expression of MCP-1 in murine adipose tissue is linked to raised plasma MCP-1, increased adipose tissue macrophage infiltration and development of insulin resistance⁶⁴. Elevated TLR4 gene expression in adipose tissue contributes to adipocyte hypertrophy, insulin resistance and increased macrophage infiltration³²⁸. MCP-1 and TLR4 are both linked to development of insulin resistance. Thus the mRNA expression levels of these genes displayed by the obese males may explain their more pronounced hyperinsulinaemic condition.

As discussed in Chapter 3, no evidence of macrophage infiltration was observed in PAT from the obese subjects. However the displayed over-expression in PAT inflammatory genes in the obese males may be an early onset marker for this infiltration process.

Glucocorticoids have also been shown to down-regulate adiponectin³²⁹, a molecule demonstrated to possess anti-inflammatory properties¹⁶⁶. Adiponectin mRNA expression in PAT of my study showed an analogous response as the pro-inflammatory molecules, so perhaps the glucocorticoid-GR binding displayed in the obese females is suppressing both anti- and pro-inflammatory gene expression in PAT.

Atypical of this genotype pattern was expression levels for IL-6, which only displayed a difference in expression between the lean groups. As no effect was observed with obesity, it is unlikely that increased cortisol-GR binding altered PAT IL-6 expression. IL-6 gene and protein levels have however been shown to correlate to both total fat mass and exercise³³⁰. Perhaps the reduced levels of PAT IL-6 mRNA expression exhibited by the lean females are reflective of the subtle decrease in activity displayed by these animals which is offset with obesity.

4.4.3 Conclusion and summary

Following on from the conclusion in Chapter 3, in response to moderate obesity the males appear to show a more pronounced inflammatory genotype in PAT, which may be responsible for a greater risk in metabolic dysfunction, i.e. the development of hyperinsulinaemia and insulin resistance reported in the last chapter. Obesity in females may be inhibiting this same response by the glucocorticoid and GR binding pathway, supported by raised plasma cortisol, and up-regulation of GR and 11 β HSD1 gene expression in PAT. The key findings in Chapter 4 are summarised in Figure 4.7, p152. The findings reported in this chapter can help in understanding the dimorphic gender response in clinical morbidity trends, particularly in relation to obesity and its comorbidities¹³. Again there is a strong suggestion that sex hormones are key mediators behind these observed sex differences, further strengthening the case for future investigations in the role of sex hormones in obesity mediated inflammation.

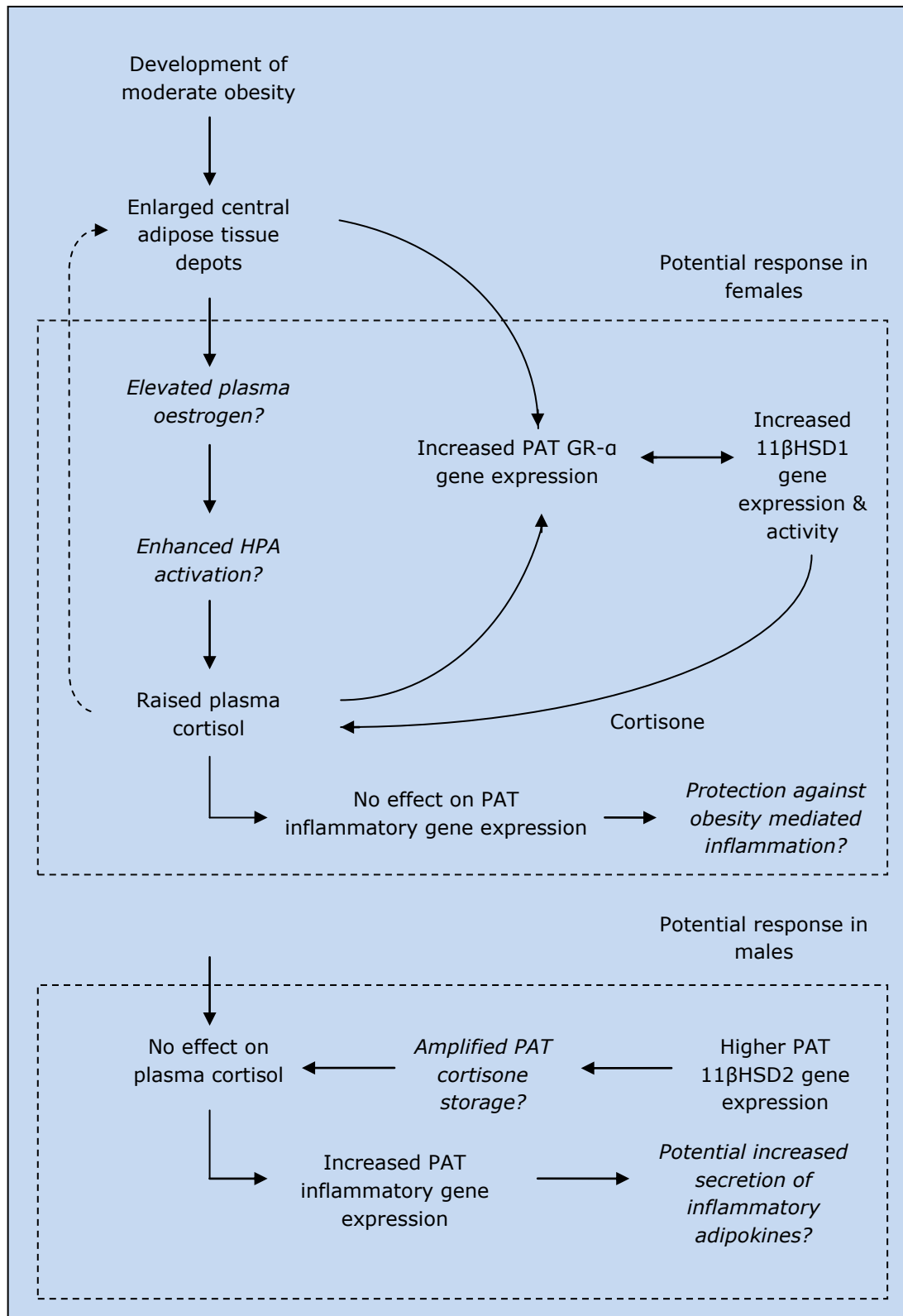


Figure 4.7: Summary of findings in effect of gender and obesity on perirenal adipose tissue (PAT) inflammatory genotype. 11βHSD1/2 – 11beta hydroxysteroid dehydrogenase type-1/2; GR-α – Glucocorticoid receptor-α; HPA – Hypothalamic pituitary adrenal axis.

Chapter 5 – The effects of gender and obesity on renal physiology, function and inflammation

5.1 Introduction and aims

The previous results sections have discussed how development of moderate obesity leads to the development of adaptations in metabolism, adipose tissue and PAT inflammation. However, these responses have displayed a sexual dimorphism which suggested that females showed a reduced inflammatory status compared to males. In the introduction section, obesity was identified as a risk factor for both structural and functional impairment of renal tissue via obesity associated metabolic dysfunction, elevated adipose tissue inflammation and impairment of haemodynamic parameters^{62,102}. The investigative focus for this chapter was that the presence of moderate obesity and resulting metabolic and adipose tissue inflammatory status would lead to haemodynamic alterations contributing to structural impairment, dysfunction and possible early signs of renal injury in the test sheep. Additionally the observed gender differences in PAT inflammation and metabolism could also manifest themselves in determination of renal response to moderate obesity.

5.1.1 Hypothesis

Chapter 5 investigates the hypothesis that moderate obesity and the reported adipose tissue inflammation and metabolic adaptations observed with gender so far, impacts on renal morphology, physiology and function. Analysis of renal mRNA transcription of inflammatory and metabolic genes was undertaken to elucidate the genotype of the kidney. Histological, lipotoxicity and protein analysis was also performed to understand the renal phenotype in these animals.

5.2 Materials and methods

A complete description of all the methods used in this chapter can be located in Chapter 2. Development and optimisation of the mRNA primers was performed by Dr S.Seibert, Dr D.Sharkey, Mr M.Pope and myself. Normalisation and expression values for the mRNA gene results were calculated using the $2^{-\Delta Ct}$ method and normalised against one reference gene (r18s). Where appropriate, any sample or analytical omissions are explained in the relevant results section. In addition, description of statistical tests utilised are provided in this results chapter or can be found in Chapter 2.

5.3 Results

5.3.1 The effect of moderate obesity and gender on renal morphology, physiology and function.

Analysis of total kidney weight (g) in the study animals identified an increase in kidney weight in obese males compared to lean males, a result not observed between the female groups, shown in Table 5.1. Obese males also showed a significant difference in kidney weight in comparison to their obese female counterparts (Table 5.1). Additionally relative kidney (g kidney per kg body weight) only identified a significant difference in comparison of lean to obese males, where lean males had higher relative kidney weights.

Group	LF (n=7)	OF (n=9)	LM (n=11)	OM (n=9)	Gender	Obesity
Kidney weight (g)	117.8±9.38	116.5±5.04 ^a	110.7±5.05**	144.3±4.80 ^{b**}	S	S
Relative Kidney weight (g/kg)	2.39±0.24	1.89±0.06	1.98±0.07*	1.72±0.04*	NS	S

Table 5.1: Kidney weight (g) and relative kidney weight (g/kg body weight) of lean female (LF), obese female (OF), lean male (LM) and obese male (OM) sheep. Values are mean ± SEM. NS = no significant difference, S = significance where only one of two comparable groups display significance; statistical differences are denoted by ^{ab}, * = $p < 0.05$; ** = $p < 0.005$ (ANOVA). Relative kidney weight analysis treated with Kruskal-Wallis statistical test.

5.3.1.1 Glomerular physiology

To determine the impact of moderate obesity on renal morphology, an investigation on glomerular area (μm^2) and glomerular nucleated cell number was performed. This analysis showed a statistically significant increase in glomerular size and cell number between lean and obese males, a difference which was also displayed in comparison of obese males to females (Figures 5.2-5.3, p156-157). Correlation analysis between glomerular area and glomerular nucleated cell number showed a very strong correlation using Pearson's correlation coefficient, where $p < 0.0001$ and $r^2 = 0.82$ (see Figure 5.4, p157)

Two lean male kidney samples had not been loaded into a paraffin histology cassette at time of dissection, and thus were omitted from all relevant renal histology analysis. Representative kidney sections used in glomerular analysis are shown in Figure 5.1, p156.

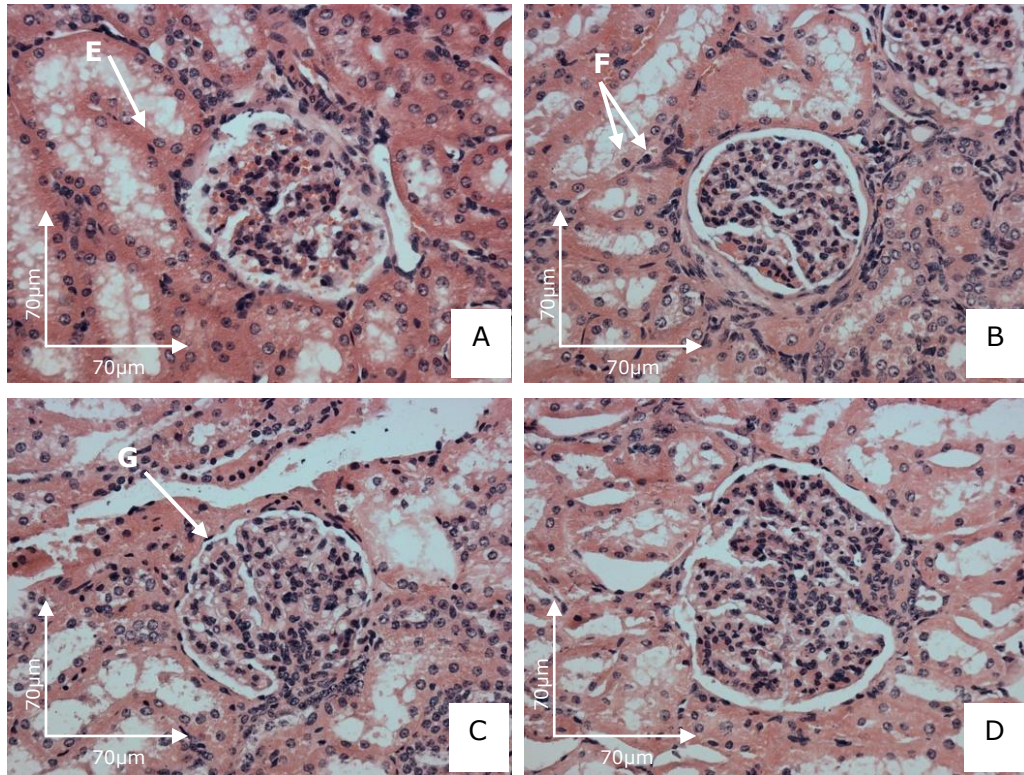


Figure 5.1: Representative haematoxylin & eosin (H&E) 5µm stained microscopic sections at 20x magnification; A – lean female, B – obese female, C – lean male and D – obese male sheep. The pink coloured stain represents connective tissue, red blood cells and non-nucleated cellular material shown by arrow E. Blue/black staining represents cellular nuclei (arrow F). The circular structures are the glomeruli (arrow G). In area and cell count analysis ≈ 40 glomeruli were analysed for each animal.

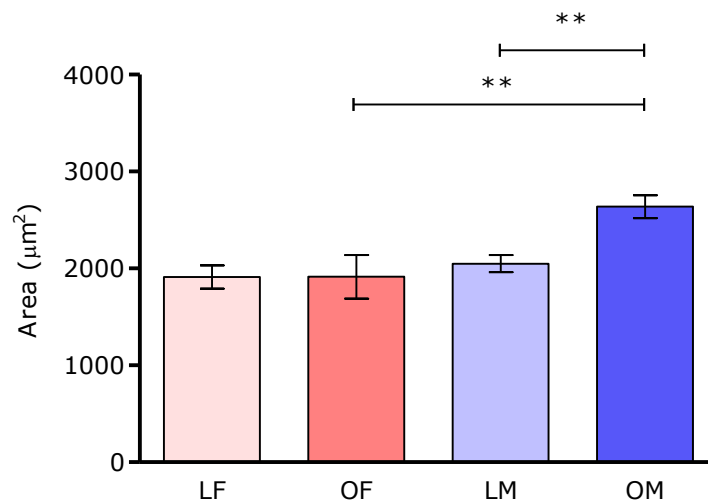


Figure 5.2: Glomerular area mean average (μm^2) of lean female (LF; $n=7$), obese female (OF; $n=9$), lean male (LM; $n=9$) and obese male (OM; $n=9$) sheep. Values are mean \pm SEM. Statistical difference is denoted by ** = $p < 0.005$ (ANOVA).

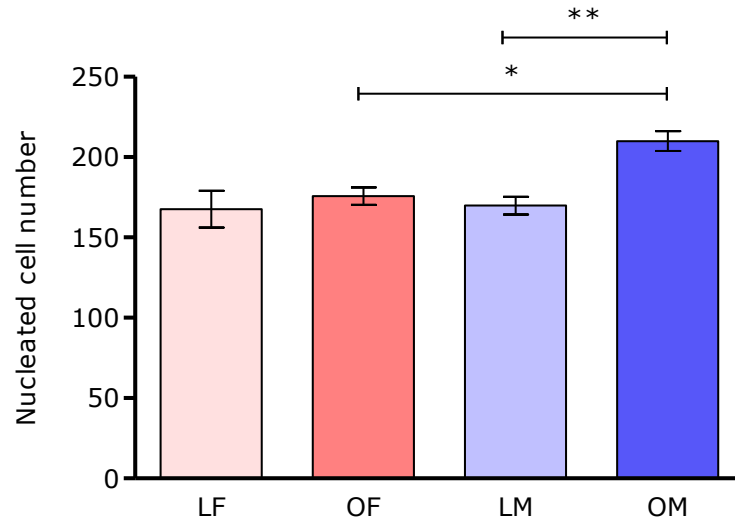


Figure 5.3: Glomerular nucleated cell number mean average of lean female (LF; $n=7$), obese female (OF; $n=9$), lean male (LM; $n=9$) and obese male (OM; $n=9$) sheep. Values are mean \pm SEM. Statistical difference is denoted by * = $p<0.05$; ** = $p<0.005$ (Kruskal-Wallis).

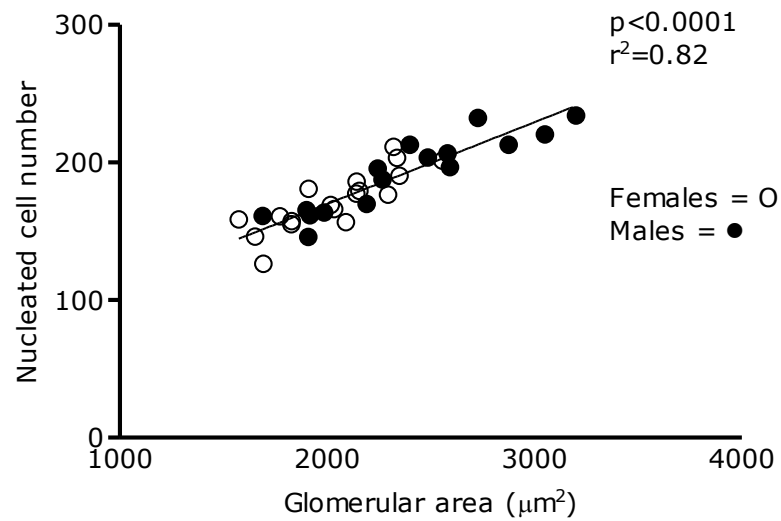


Figure 5.4: Relationship between glomerular area (μm^2) and glomerular nucleated cell number of total sheep ($n=34$). Correlation analysis showed a statistical significance where $p<0.0001$ and $r^2 = 0.82$ (Pearson's correlation coefficient).

5.3.1.2 Haemodynamic parameters

To elucidate either the mechanism or resulting effect by this increase of glomerular size and accompanying increase of glomerular nucleated cell infiltration, haemodynamic parameters were investigated. Table 5.2 shows results for heart rate, systolic, diastolic and mean blood pressure measurements. No data was collected for one lean male due to equipment failure and was omitted from the data analysis. Statistical analysis of all haemodynamic parameters showed no differences in comparison of either gender or obesity.

Group	LF (n=7)	OF (n=9)	LM (n=10)	OM (n=9)	Gender	Obesity
Heart rate (bpm)	86.22±11.5	81.01±5.02	62.07±3.78	81.58±6.18	NS	NS
Systolic blood pressure (mmHg)	126.9±8.91	134.1±4.88	132.3±4.36	138.2±4.60	NS	NS
Diastolic blood pressure (mmHg)	86.79±5.43	91.92±4.44	86.75±4.08	88.72±3.30	NS	NS
Mean blood pressure (mmHg)	106.8±7.09	113.0±4.55	109.5±4.09	113.5±3.58	NS	NS

Table 5.2: Heart rate (bpm), systolic, diastolic and mean blood pressure (mmHg) measurements for lean female (LF), obese female (OF), lean male (LM) and obese male (OM) sheep. Values are mean ± SEM. NS = no significant difference (ANOVA).

5.3.1.3 Glomerular cellular proliferation and apoptosis

As glomerular nucleated cell number increased with glomerular area, cellular turnover was analysed. Protein expression of markers involved in proliferation and apoptosis were measured using IHC; representative slides of caspase-3 and PCNA immunostaining are shown by images A-D in Figure 5.5-5.6, p159-160. In general histological observation of caspase-3 IHC, cells contained within the glomerulus appeared to show a reduced amount of positive staining compared to the rest of the microscopic section, a trend which was reversed in PCNA staining. Thus separate positive staining analysis was performed on total and glomerular regions.

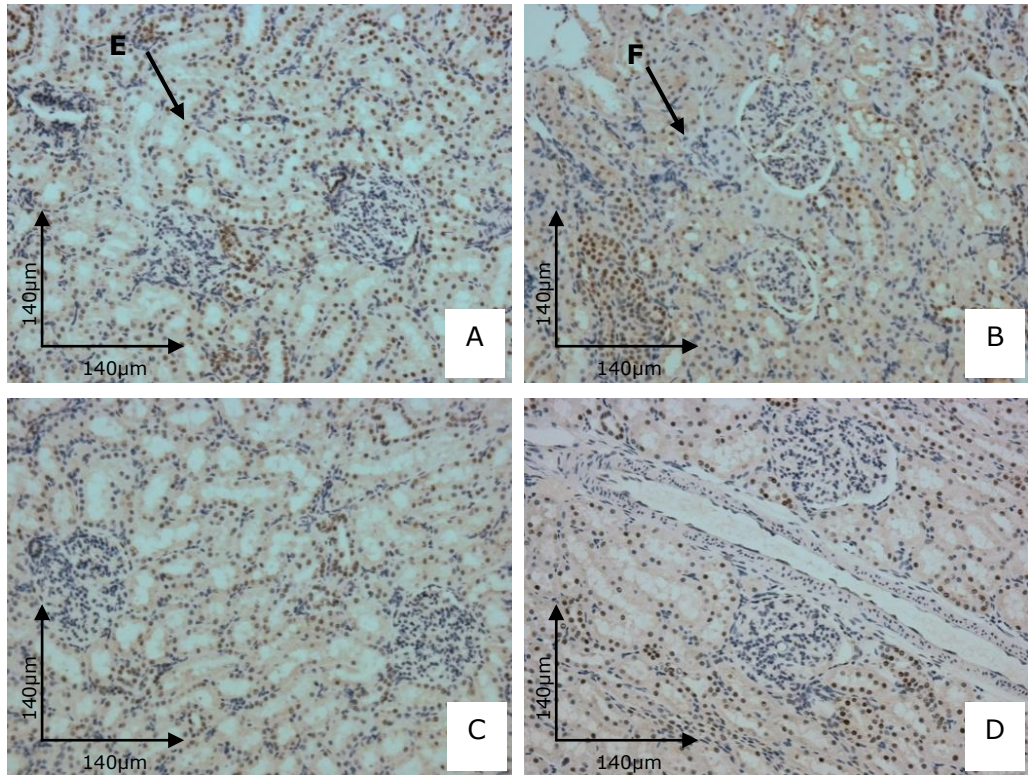


Figure 5.5: Representative caspase-3 (1:50 primary antibody dilution) immunohistochemistry 5µm stained microscopic sections at 10x magnification; A – lean female, B – obese female, C – lean male and D – obese male sheep. The brown coloured stain represents positively stained nuclei shown by arrow E. Blue staining represents negatively stained nuclei (arrow F).

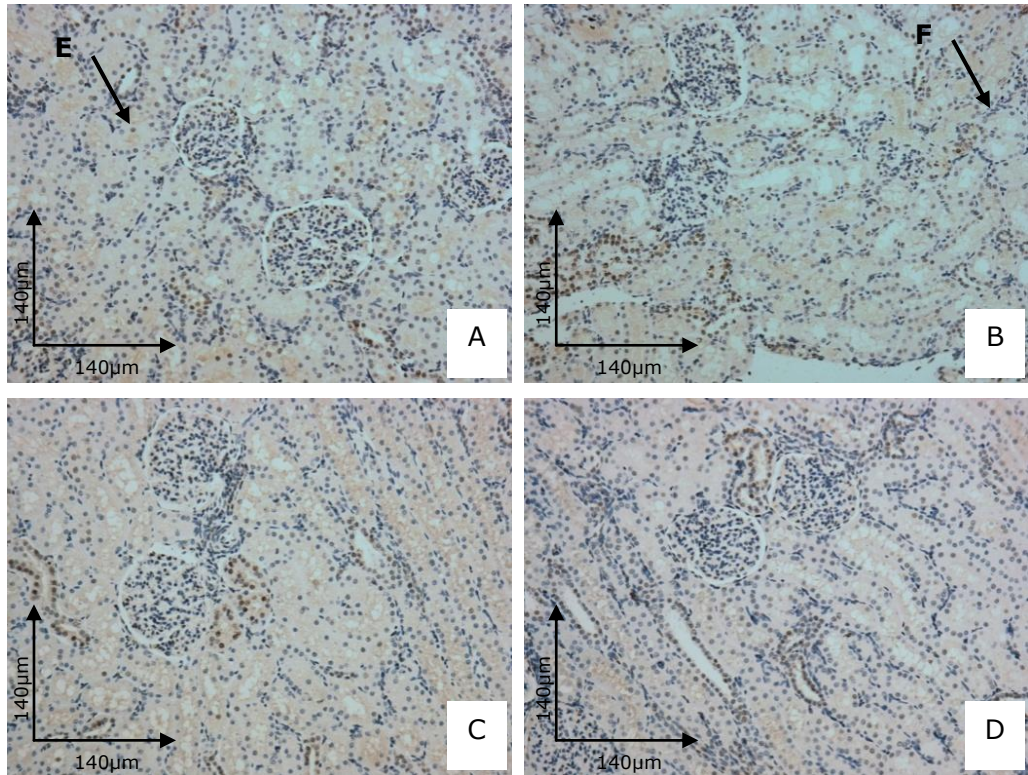


Figure 5.6: Representative proliferating cell nuclear antigen (PCNA, 1:4000 primary antibody dilution) immunohistochemistry 5µm stained microscopic sections at 10x magnification; A – lean female, B – obese female, C – lean male and D – obese male sheep. The brown coloured stain represents positively stained nuclei shown by arrow E. Blue staining represents negatively stained nuclei (arrow F).

Total caspase-3 positive staining displayed no significant differences with either gender or obesity, but in glomerular caspase-3 stain abundance, lean males showed an up-regulation in protein expression compared to their obese counterparts which was not observed in the females (Table 5.3, p161). Neither total nor glomerular PCNA protein abundance was affected with gender or obesity, shown in Table 5.3.

Group	LF (n=7)	OF (n=9)	LM (n=9)	OM (n=9)	Gender	Obesity
Total caspase-3 %	44.99±3.10	33.78±3.03	46.61±3.21	43.82±2.88	NS	NS
Glomerular caspase-3 %	9.07±1.64	8.55±3.06	18.21±3.82*	5.72±1.58*	NS	S
Total PCNA %	13.87±0.39	11.72±0.74	10.84±0.68	11.25±0.79	NS	NS
Glomerular PCNA %	20.21±2.96	14.21±1.86	16.41±2.34	17.23±2.41	NS	NS

Table 5.3: Total and glomerular staining % of caspase-3 and proliferating cell nuclear antigen (PCNA) of lean female (LF), obese female (OF), lean male (LM) and obese male (OM) sheep. Values are mean ± SEM. NS = no significant difference, S = significance where only one of two comparable groups display significance; statistical difference is denoted by * = $p < 0.05$ (ANOVA).

5.3.1.4 Renal triglyceride accumulation and oxidative stress

In contrast to *LD* muscle tissue, triglyceride accumulation analysis (mg per g kidney tissue) in renal tissue identified a significant increase ($p < 0.005$) of renal triglycerides in obese females compared to obese males. Comparison of all other comparative groups in renal triglyceride levels displayed no statistical significant differences, shown in Figure 5.7. One lean male kidney sample could not be located during -80°C freezer storage and was therefore omitted from renal lipotoxicity and oxidative stress analysis.

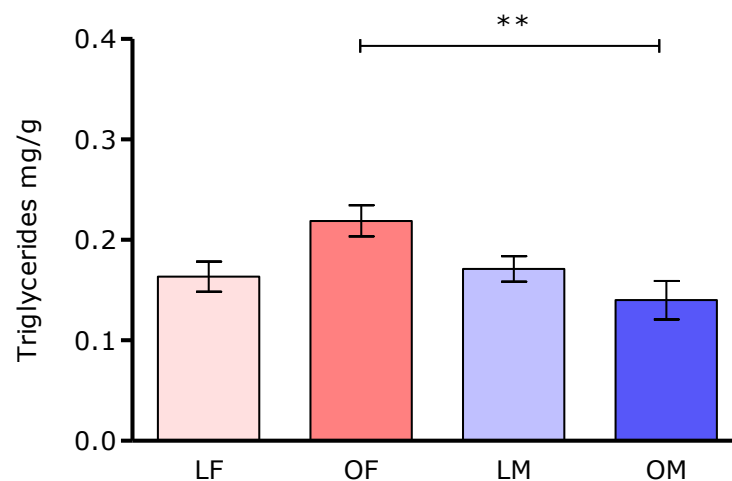


Figure 5.7: Triglyceride deposition in mg per g kidney of lean female (LF; $n=7$), obese female (OF; $n=9$), lean male (LM; $n=10$) and obese male (OM; $n=9$) sheep. Values are mean ± SEM. Statistical difference is denoted by ** = $p < 0.005$ (ANOVA).

To determine the lipid peroxidation status of renal tissue, TBARS (MDA μM /total protein $\mu\text{g}/\mu\text{l}$) analysis was performed. TBARS results showed no significant differences influenced by gender or in exposure to an obesogenic environment, see Figure 5.8.

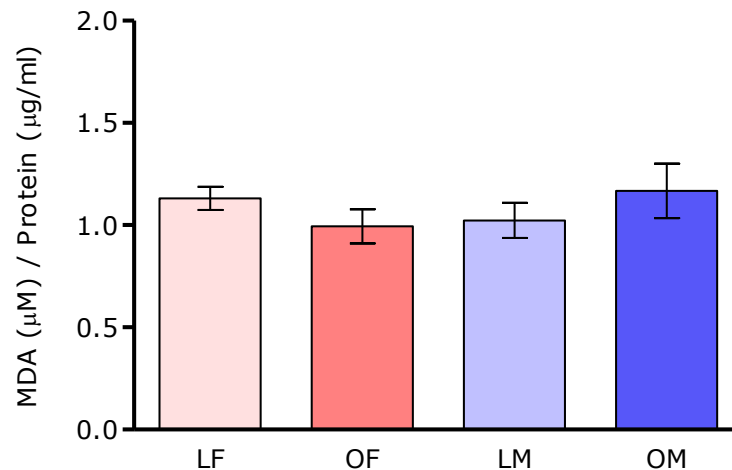


Figure 5.8: Renal thiobarbituric acid reactive substance (TBARS) measurements of lean female (LF; $n=7$), obese female (OF; $n=9$), lean male (LM; $n=10$) and obese male (OM; $n=9$) sheep. Values are mean \pm SEM.

5.3.1.5 Renal collagen deposition

Using Masson trichrome histological staining, collagen deposition was analysed using an adapted semi-quantitative grading system, see 2.5.3.1, p85. No signs of increased collagen deposition were observed in the samples (representative microscopic slides are shown in images A-D, Figure 5.9, p163), and no signs of increased collagen development was observed in the glomeruli in comparison between the study groups. Statistical analysis of the collagen deposition data identified no significant differences with either gender or obesity, shown in Table 5.4, p163. However, Masson trichrome staining did appear to be affected by the histological and sectional tissue processing. It is possible that xylene, alcohol and paraffin wax processing led to greater dehydration of some samples compared to others which resulted in increased stain binding as shown in images E-F, Figure 5.9, p163. Despite this discrepancy between samples, over-staining did not appear to lead to an over- or under-estimation in the final collagen index grading results.

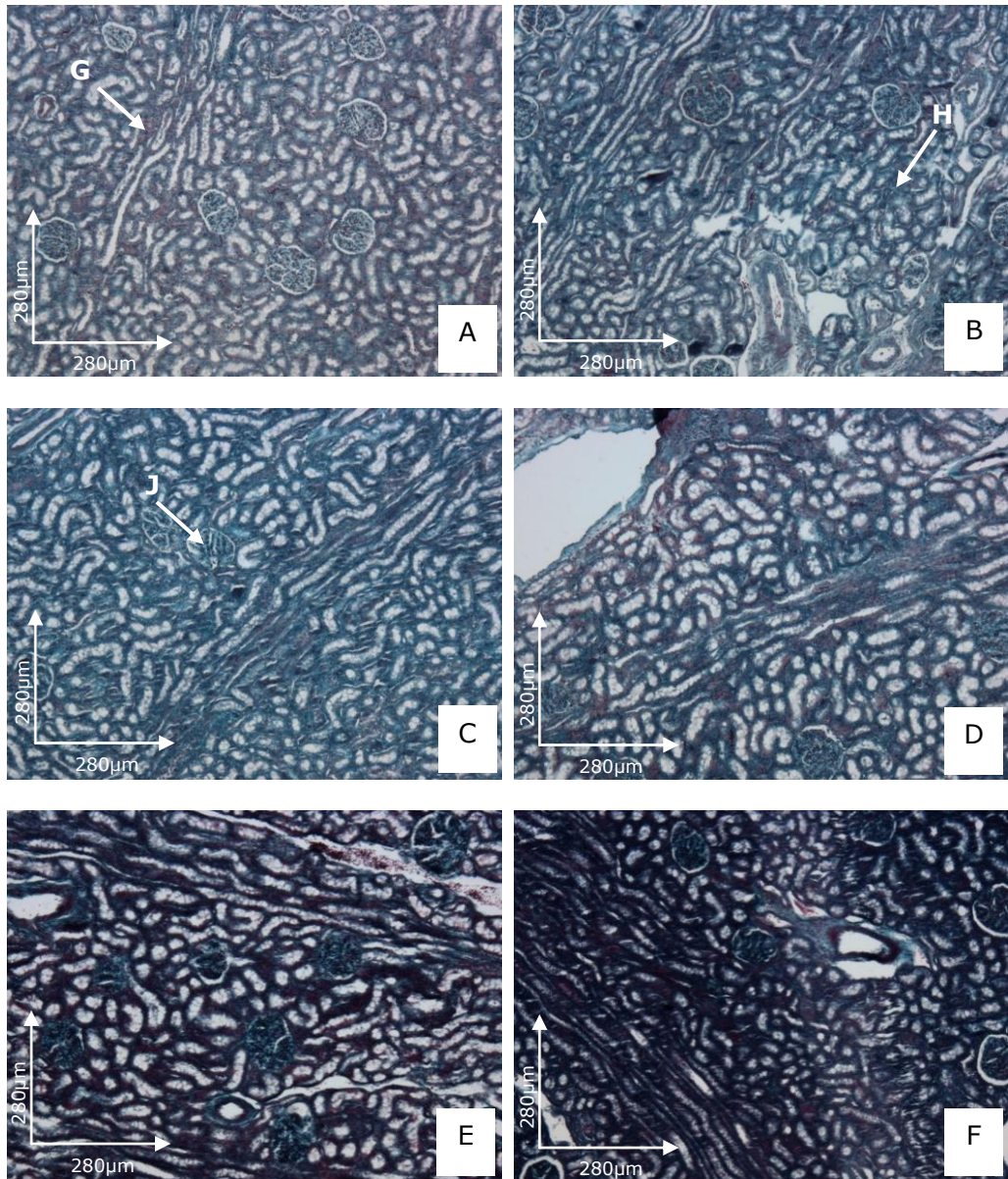


Figure 5.9: Representative Masson trichrome staining for collagen 5µm stained microscopic sections at 5x magnification; A – lean female, B – obese female, C – lean male and D – obese male sheep. The red coloured stain represents keratin and connective tissue (arrow G), green colour represents staining of collagen peptides (arrow H) and blue/black staining represents cellular nuclei (arrow J). Images E and F represent over-stained samples, possibly due to increased dehydration during tissue processing.

Group	LF (n=7)	OF (n=9)	LM (n=9)	OM (n=9)	Gender	Obesity
Collagen index	2.98±0.26	2.61±0.25	2.92±0.19	2.45±0.13	NS	NS

Table 5.4: Collagen index (arbitrary units) for lean female (LF), obese female (OF), lean male (LM) and obese male (OM) sheep. Values are mean ± SEM. NS = no significant difference (Kruskal-Wallis).

5.3.1.6 Plasma creatinine and renal function

To determine renal function, plasma creatinine (nmol/ μ l) was measured (Figure 5.10). Unfortunately no additional urine creatinine measurements were collected and no eGFR for sheep currently exists. Therefore as creatinine is a metabolite of creatine phosphate in muscle^{84,85}, plasma creatinine levels were corrected for lean muscle mass (nmol/ μ l per g of lean mass) shown in Figure 5.11, p165, to estimate potential creatinine clearance and subsequent renal function.

Statistical analysis of plasma creatinine identified a significant increase in lean males compared to lean females, a gender effect not observed in the obese animals, Figure 5.10. Additionally, obesity had no effect on plasma creatinine levels.

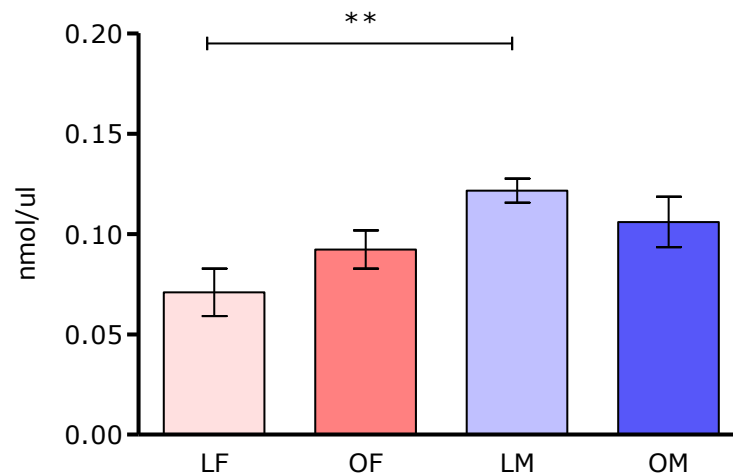


Figure 5.10: Plasma creatinine (nmol/ μ l) of lean female (LF; $n=7$), obese female (OF; $n=9$), lean male (LM; $n=11$) and obese male (OM; $n=9$) sheep. Values are mean \pm SEM. Statistical difference is denoted by ** = $p < 0.005$ (ANOVA).

After correcting plasma creatinine levels for lean mass, statistical analysis showed a significant decrease in the obese compared to lean males, a response not displayed by the females (Figure 5.11, p165). Linear regression analysis identified a negative correlation between lean mass and plasma creatinine where $p=0.004$ and $r^2=0.51$ (Figure 5.12, p166), a relationship which was not exhibited in females (Figure 5.13, p166). No further gender or obesity differences were observed.

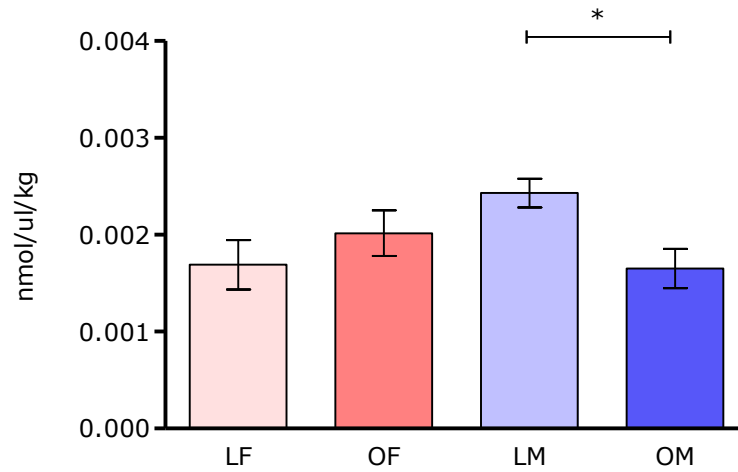


Figure 5.11: Plasma creatinine corrected for lean mass (nmol/μl/kg) of lean female (LF; n=7), obese female (OF; n=9), lean male (LM; n=11) and obese male (OM; n=9) sheep. Values are mean ± SEM. Statistical difference is denoted by * = $p < 0.05$ (ANOVA).

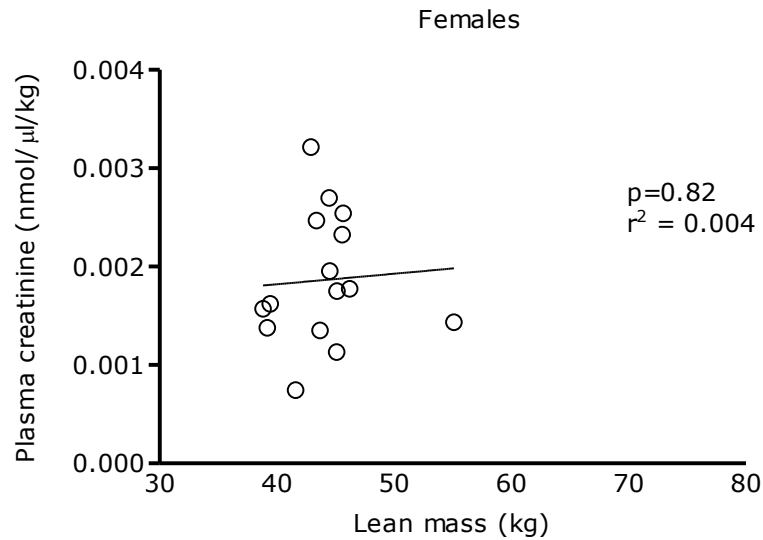


Figure 5.12: Relationship between lean mass (kg) and plasma creatinine corrected for lean mass (nmol/μl/kg) of female sheep (n=15). Correlation analysis showed no statistical significance where $p=0.82$ and $r^2 = 0.004$ (Pearson's correlation coefficient).

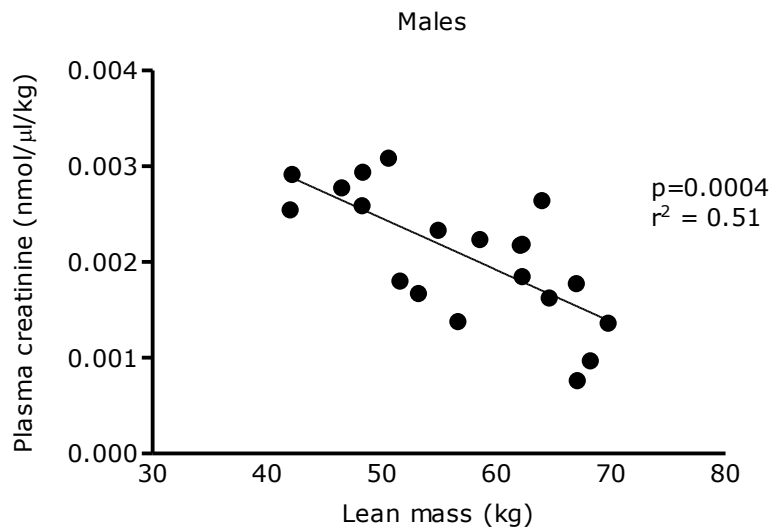


Figure 5.13: Relationship between lean mass (kg) and plasma creatinine corrected for lean mass (nmol/μl/kg) of male sheep (n=15). Correlation analysis showed a statistical significance where $p=0.0004$ and $r^2 = 0.51$ (Pearson's correlation coefficient).

5.3.2 The effect of moderate obesity and gender on the renal inflammatory genotype.

To determine the renal inflammatory genotype, gene expression analysis was performed on a number of key genes involved in obesity mediated renal inflammation as discussed in the introduction chapter. One lean male tissue sample could not be located in the -80°C storage freezer and thus is omitted from all renal gene expression analysis.

5.3.2.1 Glucocorticoid renal gene expression

Glucocorticoid analysis showed a statistically significant up-regulation in 11 β HSD2 renal gene expression of obese males compared to both lean males and obese females, shown in Figure 5.14.

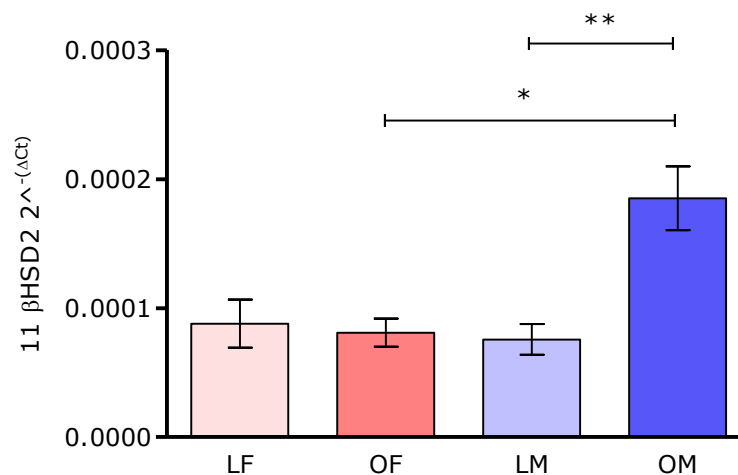


Figure 5.14: 11 β -hydroxysteroid dehydrogenase type 2 (11 β HSD2) $2^{-(\Delta Ct)}$ mRNA expression values of lean female (LF; n=7), obese female (OF; n=9), lean male (LM; n=10) and obese male (OM; n=9) sheep in renal tissue. Values are mean \pm SEM. Statistical difference is denoted by * = $p < 0.05$; ** = $p < 0.005$ (Kruskal-Wallis).

GR analysis showed the same significant trend where obese males showed over-expression in obese males in comparison to lean males and obese females, Figure 5.15, p168. No additional statistical differences were observed in either 11 β HSD1 or GR analysis.

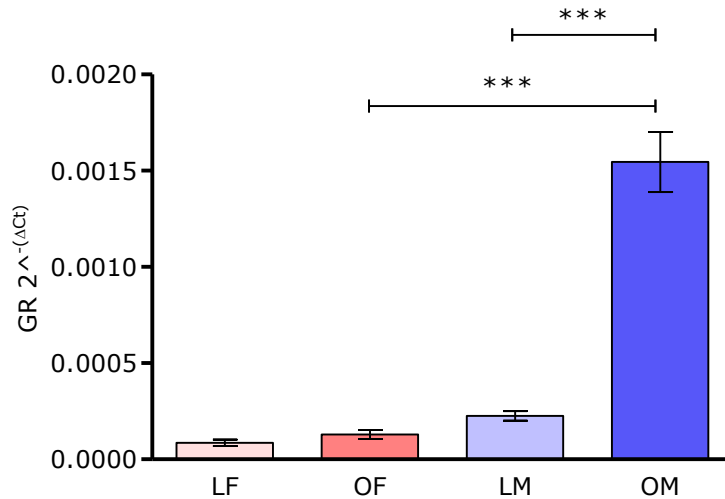


Figure 5.15: Glucocorticoid receptor (GR) $2^{-(\Delta Ct)}$ mRNA expression values of lean female (LF; $n=7$), obese female (OF; $n=9$), lean male (LM; $n=10$) and obese male (OM; $n=9$) sheep in renal tissue. Values are mean \pm SEM. Statistical difference is denoted by *** = $p < 0.001$ (ANOVA).

5.3.2.2 Pro-inflammatory renal cytokine expression

Gene expression analysis of pro-inflammatory cytokines identified no significant differences in renal IL-18 expression with gender of obesity (Table 5.5). However, renal IL-6 expression displayed an up-regulation in lean females compared to lean males, shown in Table 5.5.

Group	LF (n=7)	OF (n=9)	LM (n=10)	OM (n=9)	Gender	Obesity
IL-6 ($2^{-(\Delta Ct)}$)	2.07×10^{-5} $\pm 0.37 \times 10^{-5a}$	1.98×10^{-5} $\pm 0.23 \times 10^{-5}$	1.07×10^{-5} $\pm 0.14 \times 10^{-5b}$	1.13×10^{-5} $\pm 0.14 \times 10^{-5}$	S	NS
IL-18 ($2^{-(\Delta Ct)}$)	1.60×10^{-5} $\pm 0.44 \times 10^{-5}$	1.12×10^{-5} $\pm 0.20 \times 10^{-5}$	1.02×10^{-5} $\pm 0.04 \times 10^{-5}$	1.20×10^{-5} $\pm 0.24 \times 10^{-5}$	NS	NS

Table 5.5: Interleukin-6 (IL-6) and interleukin-18 (IL-18) $2^{-(\Delta Ct)}$ mRNA gene expression values of lean female (LF), obese female (OF), lean male (LM) and obese male (OM) sheep in renal tissue. Values are mean \pm SEM. NS = no significant difference, S = significance where only one of two comparable groups display significance; statistical difference is denoted by ^{ab} = $p < 0.05$ (ANOVA). IL-18 analysis treated with Kruskal-Wallis statistical test.

In response to gender and obesity, renal MCP-1 expression was not altered and no statistical differences were observed between any of the groups (Table 5.6, p169). Yet MCP-1 receptor (CCR2) showed mRNA over-expression with gender ($p < 0.005$) in both lean and obese groups and also in response to obesity in the male animals ($p < 0.001$), shown in Table 5.6, p169.

Group	LF (n=7)	OF (n=9)	LM (n=10)	OM (n=9)	Gender	Obesity
CCR2 ($2^{\Delta Ct}$)	0.78×10^{-5} $\pm 0.09 \times 10^{-5}$	1.11×10^{-5} $\pm 0.17 \times 10^{-5}$	3.98×10^{-5} $\pm 0.59 \times 10^{-5}^{***}$	7.42×10^{-5} $\pm 0.82 \times 10^{-5}^{***}$	**	S
MCP-1 ($2^{\Delta Ct}$)	2.53×10^{-5} $\pm 0.54 \times 10^{-5}$	1.98×10^{-5} $\pm 0.23 \times 10^{-5}$	1.81×10^{-5} $\pm 0.17 \times 10^{-5}$	2.77×10^{-5} $\pm 0.31 \times 10^{-5}$	NS	NS

Table 5.6: Chemokine C-C motif receptor 2 (CCR2) and monocyte chemoattractant protein-1 (MCP-1) $2^{\Delta Ct}$ mRNA gene expression values of lean female (LF), obese female (OF), lean male (LM) and obese male (OM) sheep in renal tissue. Values are mean \pm SEM. NS = no significant difference, S = significance where only one of two comparable groups display significance; statistical differences are denoted by ** = $p < 0.005$; *** = $p < 0.001$ (ANOVA). MCP-1 analysis treated with Kruskal-Wallis statistical test.

Figure 5.16 shows statistical analysis of renal IFN- γ expression where obese males exhibited elevated gene expression compared to obese females. Lean males displayed a trend of up-regulation compared to lean females where $p = 0.11$, but this result was not statistically significant. No differences were observed in response to obesity.

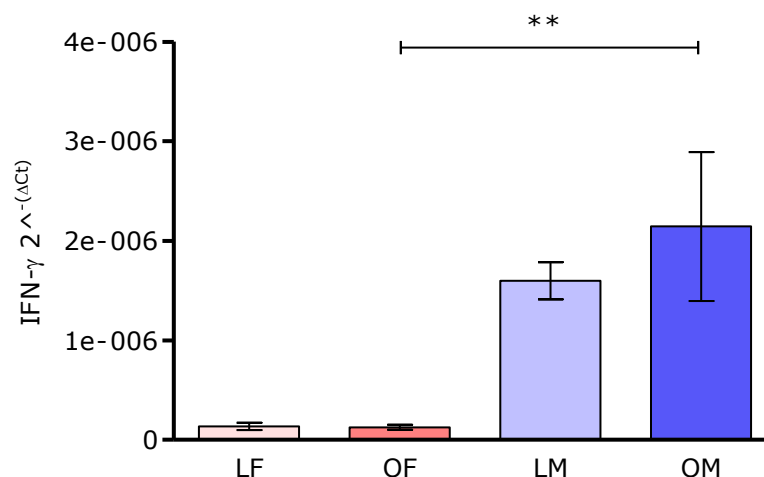


Figure 5.16: Interferon- γ (IFN- γ) $2^{\Delta Ct}$ mRNA expression values of lean female (LF; $n = 7$), obese female (OF; $n = 9$), lean male (LM; $n = 10$) and obese male (OM; $n = 9$) sheep in renal tissue. Values are mean \pm SEM. Statistical difference is denoted by ** = $p < 0.005$ (ANOVA).

Similarly, TNF- α renal gene expression also showed up-regulation in the obese males compared to obese females (Figure 5.17, p170). No additional significant differences or trends were exhibited in response to gender or obesity.

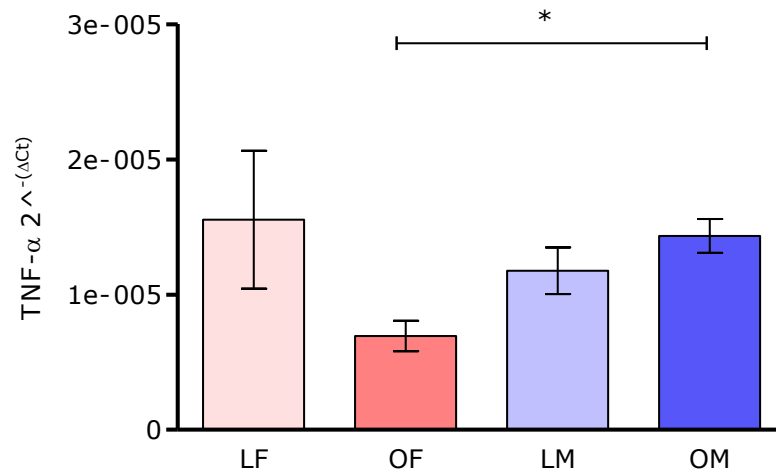


Figure 5.17: Tumour necrosis factor- α (TNF- α) $2^{-\Delta Ct}$ mRNA expression values of lean female (LF; $n=7$), obese female (OF; $n=9$), lean male (LM; $n=10$) and obese male (OM; $n=9$) sheep in renal tissue. Values are mean \pm SEM. Statistical difference is denoted by * = $p < 0.05$ (Kruskal-Wallis).

5.3.2.3 Anti-inflammatory renal gene expression

In response to gender and obesity, anti-inflammatory gene expression was up-regulated in obese males compared to obese females. This expression pattern was shown by all three of the anti-inflammatory genes analysed; IL-10, iNOS and PPAR- γ as shown in Table 5.7.

Group	LF (n=7)	OF (n=9)	LM (n=10)	OM (n=9)	Gender	Obesity
IL-10 ($2^{-\Delta Ct}$)	0.85×10^{-6} $\pm 0.25 \times 10^{-6}$	0.86×10^{-6} $\pm 0.02 \times 10^{-6a}$	2.71×10^{-6} $\pm 0.06 \times 10^{-6}$	3.07×10^{-6} $\pm 0.04 \times 10^{-6b}$	S	NS
iNOS ($2^{-\Delta Ct}$)	0.08×10^{-5} $\pm 0.02 \times 10^{-5}$	0.09×10^{-5} $\pm 0.02 \times 10^{-5a}$	0.16×10^{-5} $\pm 0.03 \times 10^{-5}$	0.23×10^{-5} $\pm 0.03 \times 10^{-5b}$	S	NS
PPAR-γ ($2^{-\Delta Ct}$)	0.16×10^{-5} $\pm 0.04 \times 10^{-5}$	0.16×10^{-5} $\pm 0.20 \times 10^{-5a}$	0.29×10^{-5} $\pm 0.02 \times 10^{-5}$	0.37×10^{-5} $\pm 0.08 \times 10^{-5b}$	S	NS

Table 5.7: Interleukin-10 (IL-10), inducible nitric oxide synthase (iNOS) and peroxisome proliferator activated receptor- γ (PPAR- γ) $2^{-\Delta Ct}$ mRNA gene expression values of lean female (LF), obese female (OF), lean male (LM) and obese male (OM) sheep in renal tissue. Values are mean \pm SEM. NS = no significant difference, S = significance where only one of two comparable groups display significance; statistical difference is denoted by ^{ab} = $p < 0.05$. iNOS analysis treated with ANOVA statistical test.

5.3.2.4 Lipid sensing receptor renal gene expression

As displayed by the anti-inflammatory molecules, renal gene expression of the lipid sensing receptors involved in the inflammation pathway showed a similar trend. Both CD14 and TLR4 exhibited increased gene expression in obese males compared to obese females (Figure 5.18-5.19 p172). In addition, TLR4 also showed up-regulation in mRNA expression in males with obesity, where conversely females did not show an equivalent response (Figure 5.19, p172).

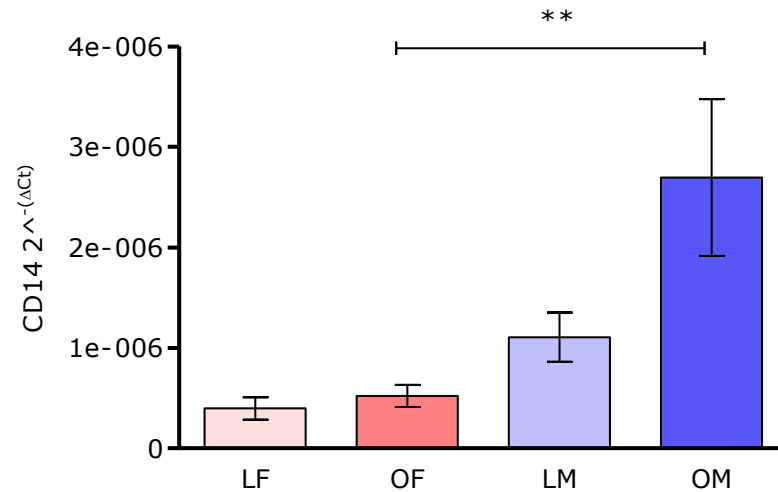


Figure 5.18: Cluster of differentiation 14 (CD14) $2^{-\Delta Ct}$ mRNA expression values of lean female (LF; $n=7$), obese female (OF; $n=9$), lean male (LM; $n=10$) and obese male (OM; $n=9$) sheep in renal tissue. Values are mean \pm SEM. Statistical difference is denoted by ** = $p < 0.005$ (ANOVA).

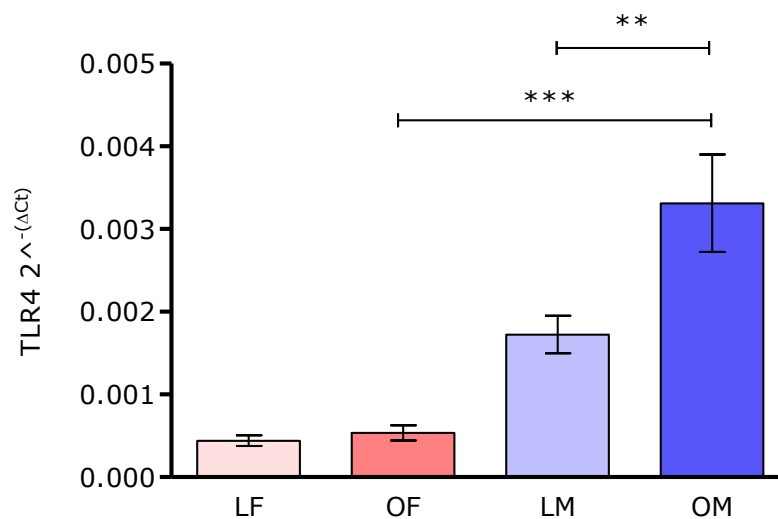


Figure 5.19: Toll-like receptor 4 (TLR4) $2^{-\Delta Ct}$ mRNA expression values of lean female (LF; $n=7$), obese female (OF; $n=9$), lean male (LM; $n=10$) and obese male (OM; $n=9$) sheep in renal tissue. Values are mean \pm SEM. Statistical difference is denoted by ** = $p < 0.005$; *** = $p < 0.001$ (ANOVA).

5.3.2.5 Cell adhesion molecule renal gene expression

Again renal gene expression of the cell adhesion molecules ICAM-1 and VCAM-1 exhibited an up-regulation between the obese males and obese females (Table 5.8). VCAM-1 also showed increased expression in the males with obesity, see Table 5.8.

Group	LF (n=7)	OF (n=9)	LM (n=10)	OM (n=9)	Gender	Obesity
ICAM-1 ($2^{-(\Delta Ct)}$)	1.69x10 ⁻⁵ ±0.60x10 ⁻⁵	1.23x10 ⁻⁵ ±0.15x10 ^{-5a}	2.56x10 ⁻⁵ ±0.34x10 ⁻⁵	4.20x10 ⁻⁵ ±0.72 x10 ^{5b}	S	NS
VCAM-1 ($2^{-(\Delta Ct)}$)	0.10x10 ⁻⁵ ±0.04x10 ⁻⁵	0.11x10 ⁻⁵ ±0.02x10 ^{-5a}	0.20x10 ⁻⁵ ±0.02x10 ^{-5**}	0.35x10 ⁻⁵ ±0.05x10 ^{-5b**}	S	S

Table 5.8: Intracellular cell adhesion molecule-1 (ICAM-1) and vascular cell adhesion molecule (VCAM-1) $2^{-(\Delta Ct)}$ mRNA gene expression values of lean female (LF), obese female (OF), lean male (LM) and obese male (OM) sheep in renal tissue. Values are mean ± SEM. NS = no significant difference, S = significance where only one of two comparable groups display significance; statistical differences are denoted by ^{ab}, ** = $p < 0.005$ (ANOVA).

5.3.2.6 Renal molecule gene expression

Analysis of EPOR identified this repeated expression pattern where obese males display an up-regulation compared to obese females, and once again males also showed increased expression in response to obesity (Table 5.9). However, renin gene expression analysis showed no statistical differences with either gender or obesity (Table 5.9).

Group	LF (n=7)	OF (n=9)	LM (n=10)	OM (n=9)	Gender	Obesity
EPOR ($2^{-(\Delta Ct)}$)	0.31x10 ⁻⁵ ±0.09x10 ⁻⁵	0.43x10 ⁻⁵ ±0.08x10 ^{-5a}	0.54x10 ⁻⁵ ±0.10x10 ^{-5**}	1.09x10 ⁻⁵ ±0.13x10 ^{-5b**}	S	S
Renin ($2^{-(\Delta Ct)}$)	0.39x10 ⁻⁵ ±0.19x10 ⁻⁵	0.26x10 ⁻⁵ ±0.03x10 ⁻⁵	0.29x10 ⁻⁵ ±0.05x10 ⁻⁵	0.40x10 ⁻⁵ ±0.10x10 ⁻⁵	NS	NS

Table 5.9: EPOR (erythropoietin receptor) and renin $2^{-(\Delta Ct)}$ mRNA expression values of lean female (LF; n=7), obese female (OF; n=9), lean male (LM; n=10) and obese male (OM; n=9) sheep in renal tissue. Values are mean ± SEM. Statistical differences are denoted by ** = $p < 0.005$; ^{ab} = $p < 0.001$ (ANOVA). Renin analysis treated with Kruskal-Wallis statistical test.

5.3.3 The effect of moderate obesity and gender on inflammatory protein expression

To compliment the collated renal gene expression data, protein expression analysis was performed on TLR4 protein using Western blotting and IHC in kidney tissue. Additionally, to determine how renal gene expression impacts on systemic circulatory inflammation, IL-6 and TNF- α plasma concentrations were analysed using an ELISA technique. These methods are described in Chapter 2.

5.3.3.1 Renal TLR4 protein expression

Figure 5.20 shows a Western blotting trial on random protein samples using a TLR4 primary antibody; a faint protein band was displayed at the expected protein size location (≈ 100 kDa). To ensure the visible bands were not due to non-specific binding, a negative control blot was performed using non-immune mouse serum in place of the TLR4 primary antibody, shown in Figure 5.21, p174. Unfortunately the same protein bands appeared in the blot; therefore it was likely that the protein bands were non-specific products binding to the secondary antibody.

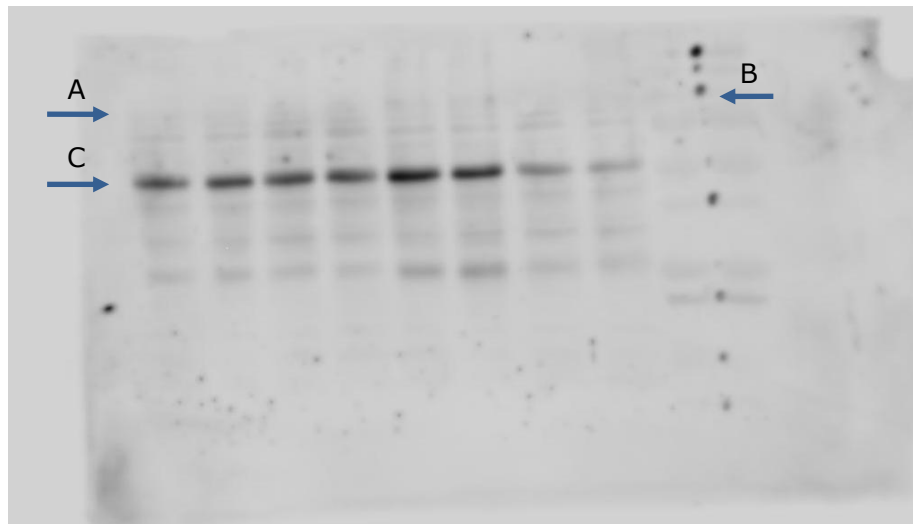


Figure 5.20: Representative Western blot image for toll-like receptor 4 (TLR4) a 100kDa protein; 1:500 TLR4 mouse primary antibody dilution; 1:2000 rabbit anti-mouse secondary antibody dilution on 20 μ g random protein samples. Arrow A identifies the faint protein band at approximately 100kDa, referenced against protein standard lane identified by arrow B. The main protein band (≈ 50 kDa) identified by arrow C is unknown.

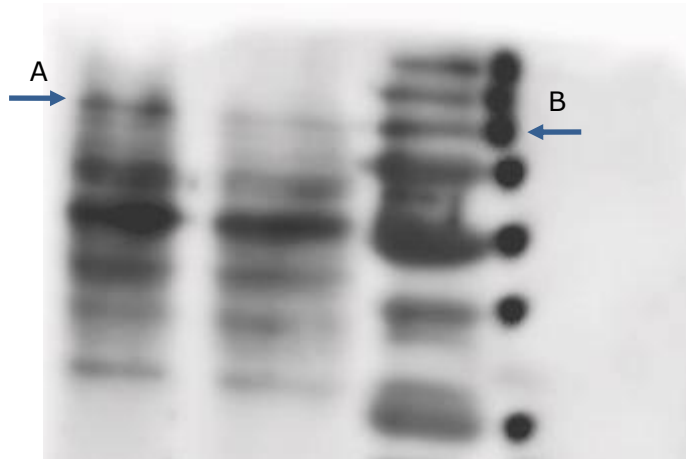


Figure 5.21: Representative Western blot image for toll-like receptor 4 (TLR4) negative control; 1:1000 non-immune mouse serum dilution; 1:2000 rabbit anti-mouse secondary antibody dilution on 20µg random protein samples. Faint 100kDa band is still present in negative control identified by arrow A. Protein standard lane identified by arrow B.

In an attempt to resolve this problem, an alternative secondary antibody was used (Protein G). However, using this secondary antibody produced no protein bands and the blot was blank. Due to time constraints, no additional secondary antibodies could be purchased and trialed.

IHC analysis using the same TLR4 primary again displayed non-specific binding highlighted in image A Figure 5.22. All background tissue stained brown in comparison to a negative control (image B Figure 5.22), rather than the expected target areas (i.e. cellular membranes).

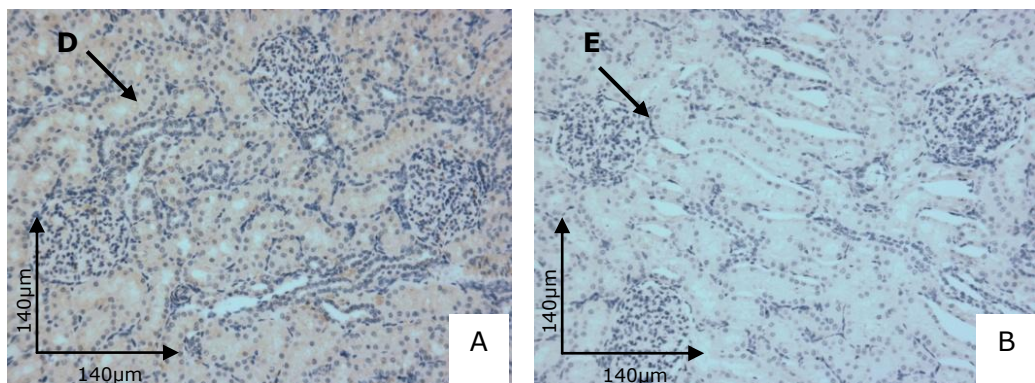


Figure 5.22: Representative toll-like receptor 4 (TLR4) immunohistochemistry 5µm stained microscopic sections at 10x magnification; A – 1:100 primary antibody dilution, B – negative control. The brown coloured stain represents positively stained area which appeared to be due to non-specific binding shown by arrow D. Blue staining represents negatively stained nuclei (arrow E).

5.3.3.2 Systemic IL-6 and TNF- α protein concentrations

After spectroscopic analysis, sample plasma measurements for IL-6 and TNF- α showed similar concentration as the negative control (blocking buffer only). This result may be for a number of reasons and one possibility may be because of cytokine half-life. Rabbit models of LPS induced inflammation have demonstrated that IL-6 and TNF- α plasma clearance after synthesis is around 6-7 minutes³³¹. Although the plasma samples were stored at -80°C after collection, it is possible that any cytokine molecules have degenerated in the short time period after collection. Alternatively the target cytokine molecules may have degraded during the freeze/thaw process which occurred prior to analysis. It is probable that plasma cytokine analysis must be performed immediately after collection or by *in vivo* techniques.

5.4 Discussion

5.4.1 Alterations in renal and glomerular physiology and function with moderate obesity

Renal size has been shown to increase with early stage obesity in dogs, this adaptation was coupled with increased glomerular area, hypertension, enlargement and thickening of the mesangial matrix, and raised glomerular nucleated cell number attributed to elevated PCNA protein expression²⁶⁰. This study however did not investigate gender. In my study, the development of moderate obesity has led to increased kidney size in the males only. Alongside this change, the obese males also showed enlarged glomerular area and increased glomerular nucleated cell number, alterations which were not observed in obese females. Additionally glomerular caspase 3 protein expression was also decreased with obesity in the males, a possible sign of reduced apoptosis which has been linked to the development of glomerular proliferative nephritis in humans²¹⁵. Despite this observed response with obesity in males, no changes were seen in the haemodynamic parameters and these animals were not hypertensive. However these measurements were made whilst the animals were sedated and at only one time point; anaesthesia in sheep can result in hypotension and bradycardia³³², which may have influenced the haemodynamic measurements recorded. Alternatively, the absence of hypertension may have been due to the onset and moderate nature of the developed obese condition, and perhaps the observed renal adaptations in these animals are precursors which contribute towards obesity associated hypertension. It is possible that males are at an increased risk to obesity associated renal adaptations responsible for increases in blood pressure, and prolonged exposure to an obesogenic environment may reflect this hypothesis.

Several studies have shown that glomerular hypertrophy and increased glomerular volume is a factor of pathogenesis in FSGS and glomerular scarring⁷⁵. Yet collagen deposition analysis in my study showed no differences with obesity or gender. Hyperinsulinaemia has also been linked with glomerular hypertrophy and sclerotic damage, a condition exhibited in the obese male animals³³³. This suggests again that the alterations observed with obesity in the males are early markers of renal adaptations which may be enhanced and more progressive with a prolonged period of exposure to obesity.

Although glomerular hypertrophy is often linked with increased capillary pressures and subsequent hypertension⁷⁵, the absence of elevated blood pressures in this model shows that development of glomerular hypertrophy can be independent from changes in blood pressure. The exact mechanism behind the displayed glomerular hypertrophy is unknown, but glomerular expansion could occur through increased glomerular cell infiltration. Conversely this glomerular hypercellularity may be an effect of the glomerular hypertrophy, a mechanism attributed to development of human proliferative glomerulonephritis³³⁴. Jennette et al proposed that glomerular hypertrophy without hypertension is a compensatory mechanism driven by a reduction in functioning nephrons⁷⁵. Additionally, compensatory glomerular hypertrophy is associated with higher numbers of endothelial and mesangial cells demonstrated in early glomerular alterations of prehypertensive rats³³⁵. Within this study however, nephron number analysis was not performed as no validated and accurately reproducible method of nephron counting was available, but this postulated mechanism may be mediating the glomerular hypertrophy observed with obesity in the male sheep.

The accompanying glomerular hypercellularity in the obese males, was shown to strongly correlate ($r^2 = 0.82$), to glomerular area. This suggests that during glomerular enlargement, cellular hyperplasia occurs rather than cellular hypertrophy, another indication of proliferative glomerulonephritis. Unfortunately due to limitations in microscopic power, identification of the increased nucleated cells present was not achievable but increased infiltration happened throughout the entire glomerular diameter including the outer capillary tufts and mesangial matrix. Distinction of these cells may be accomplished through flow cytometry analysis or more precise histological techniques which could be a target for future studies.

With regards to renal function, the increased plasma creatinine concentrations displayed by the lean males was attributed to the increased lean mass observed in these animals. However, obese males had higher lean mass measurements compared to the lean males and obese females, yet this elevation in plasma creatinine was not observed after statistical analysis was performed. It was therefore hypothesised that plasma creatinine clearance may be increased in males in response to obesity, indicating a functional adaptation in the kidney and possible contributory pathway involved in the observed glomerular alterations.

The estimated plasma creatinine clearance measurements showed that obesity in males resulted in reduced plasma creatinine despite having increased lean mass. This finding was reinforced by the negative correlation where males with increased lean mass showed an elevation in estimated plasma creatinine clearance, a relationship not displayed by the females. GFR has been shown to be raised with obesity in the human population³³⁶ but after normalization of GFR measurements with lean instead of total fat mass, this increase in GFR is removed³³⁶. My study however shows that the normalization of plasma creatinine concentrations with lean mass in obese males demonstrates an increase in plasma creatinine clearance, a finding which may indicate glomerular hyperfiltration in males with obesity. It is possible raised synthesis of creatinine from increased muscle development and subsequent elevation in plasma creatinine concentration prompts adaptive hyperfiltration by enlargement of the glomeruli and accompanying glomerular hypercellularity. Bak et al demonstrated that renal enlargement and glomerular hypertrophy precede hyperfiltration in a diabetic rat model³³⁷, structural and functional adaptations that have long been associated with an increased risk in the development of glomerulosclerosis and eventual ESRD¹⁰². As with compensatory glomerular hypertrophy, renal hyperfiltration is postulated to occur as a compensatory mechanism from a reduction in nephron number³³⁸. Decreased nephron number is thought to occur via the actions of maladaptive metabolic, haemodynamic and nephropathic abnormalities attributed to the presence of obesity³³⁹. These include increased capillary pressure, glomerular scarring and nephritis which drive tissue injury, damage and eventual glomerular loss³³⁹.

Although in my study no sign of actual kidney damage or haemodynamic impairment was apparent, this may imply that if nephron reduction has occurred that an alternate mechanism may be responsible. One proposal is that these renal adaptations observed in obesity are not maladaptive but represent coordinated and regulated alterations which are proportionate to the metabolic and excretory needs of obese individuals³³⁹. This may explain the absence of hypertension displayed by the obese males in my study. However, as a huge body of evidence suggests that obesity contributes to hypertension^{91,92}, it is probable that prolonged exposure to obesity and the associated renal modifications will lead to hypertension and related kidney injury.

Such a hypothesis would suggest that males therefore show an increased risk to the development of obesity mediated kidney disease, a finding in agreement with human epidemiological data¹¹⁰. As discussed in the introduction chapter, the gender disparity observed in the progression of human renal disease has to date been attributed to differences in diet, glomerular haemodynamics, kidney and glomerular size¹¹⁰. It is also believed that oestrogens and oestrogen receptors in renal tissue may slow the progression rate of kidney disease¹¹⁰.

5.4.2 Changes in renal inflammatory gene transcription

In contrast to glucocorticoid gene expression in PAT, renal mRNA expression demonstrated an opposite trend where males showed an up-regulation in response to obesity. Females showed no effect of obesity with regards to renal GR or 11 β HSD2 expression. This is surprising taking into consideration the plasma cortisol concentrations discussed in Chapter 3 which were raised with obesity in females. Perhaps the elevated plasma cortisol levels in the obese females contribute to no changes in basal GR and 11 β HSD2 mRNA expression in renal tissue in response to obesity. It maybe that the increased renal glucocorticoid mRNA levels expressed in the obese males is a compensatory mechanism to redress the reduction in plasma cortisol in comparison to the obese females. Rat studies have shown raised renal 11 β HSD2 expression and activity is responsible for increased conversion of cortisol to cortisone and subsequent impairment in mineralocorticoid-like effects in the kidney³⁴⁰. It is possible the elevated renal 11 β HSD2 gene expression exhibited by the obese males is converting plasma cortisol to cortisone similarly to that hypothesised in PAT tissue (see Chapter 4), resulting in lower plasma cortisol concentrations. This mechanism may result in a compensatory increase in renal GR mRNA expression to maintain cortisol and GR binding in the kidney. Alternatively the glucocorticoid expression pattern displayed in the obese male renal tissue may reflect a dysregulation in GR α :GR β ratio and thus males in response to obesity show an increased insensitivity to glucocorticoid action¹⁶¹, which may explain the reduction in plasma cortisol also demonstrated.

One of the functions of glucocorticoid binding is an immunosuppressive action on chemokine/cytokine transcription and expression¹⁴⁴. Further expression analysis of renal genes involved in both pro- and anti-inflammation demonstrated this familiar pattern where males demonstrated an up-regulation in transcription of these genes in comparison to females with response to obesity. If glucocorticoid binding in males was up-regulated with obesity and thus hypothesising that increased GR expression leads to elevated GR function, one would expect to see immunosuppressive action on the additional inflammatory network genes analysed. However, this was not the case, and it was obese females that displayed a possible down-regulation in renal pro- and anti-inflammatory gene transcription. This implied immunosuppression observed in the females with obesity may be mediated by increased plasma cortisol via GR binding in kidney, but also potentially directed by the glucocorticoid expression adaptations exhibited by PAT.

With the exception of a few inflammatory renal genes analysed (i.e. IL-6, IL-18 and MCP-1) the obese males consistently displayed an over-expression compared to their female counterparts. A regular trend of increased expression was also displayed in the males in response to obesity. As this expression pattern appears in a variety of molecules involved in a broad range of the inflammatory processes. It appears that in males, the presence of obesity leads to a potential elevation in basal mRNA levels in kidney in the majority of the inflammatory network cascade. Such a genetic response and widespread alteration in mRNA transcription is likely to be mediated via a transcription control mechanism, and it may be that kidney tissue with obesity in males undergoes epigenetic changes. DNA methylation and histone modification can be responsible for adaptations in mRNA expression³⁴¹. An epigenetic obesity study by Wang et al, demonstrated that methylation patterns in two inflammatory genes synthesised by leukocytes from lean and obese adolescents were differentially methylated, a result that was postulated to impact on immune function and subsequent pathogenesis of obesity³⁴². Alternatively perhaps the consistent down-regulation in obese female renal inflammatory gene expression is due to epigenetic programming which leads to gene silencing³⁴¹. Although epigenetic research with regards to obesity is relatively innovative, further investigation into epigenetic alterations in my study may help elucidate the mechanisms involved in the extensive dimorphic inflammatory gene response shown by males and females with obesity.

An alternative hypothesis for the exhibited consistent up-regulation of renal inflammatory gene expression in obese males was that perhaps due to the nature of the cytokine network, i.e. pleiotropic molecules involved in inter-linked cross-talk synthesis, that up-regulation of one inflammatory mediator leads to the up-regulation of the entire pro- and anti-inflammatory gene positive feedback network. This increased expression maybe controlled via one molecule, for example the transcription factor NF- κ B which has been postulated as the master regulator in inflammation and innate immunity³⁴³. However, to pinpoint the initiating molecule behind this cross-talk up-regulation would be difficult, but may be elucidated via genome wide association analysis.

Again it appears that the obese males show a more pronounced response to moderate obesity. Perhaps this observed elevated basal inflammatory mRNA state is a primed transcriptional condition which may contribute to the gender disparity clinically manifested in progression rates of renal disease¹¹⁰. Additionally this primed inflammatory state may also be instrumental to the adaptations in renal morphology in obese males demonstrated in this chapter. For instance increased renal expression of IFN- γ augments macrophage activation and recruitment, leading to tissue inflammation and glomerular hypertrophy. So it is possible that the elevated mRNA expression could be driving the observed renal alterations in obese males. However, without corroborating protein expression data, it is impossible to determine if the elevations in renal gene transcription is coupled with the appropriate protein response. In addition, the displayed glomerular hypercellularity in males with obesity may involve increased immune cell infiltration, another potential mechanism behind the amplified inflammatory gene expression. Although to confirm this, mRNA expression analysis would need to be performed on entire glomeruli of these animals.

Gene expression analysis of renin showed no differences in response to gender or obesity, which may reflect the absence of any change in haemodynamic measurements. This result may also suggest that the RAAS is not over-stimulated in a moderate obese condition, although as males have shown a more pronounced response to obesity, perhaps a longer exposure period alongside the discussed developed conditions may consequently produce obesity induced RAAS stimulation and associated glomerulopathy¹⁰⁸.

The exception to the renal gene expression pattern displayed with gender was the mRNA expression of IL-6. Lean females expressed higher levels of renal IL-6 than lean males, the only cytokine expression result where a difference was displayed with gender between the lean groups. It is unknown why this difference in renal IL-6 expression was demonstrated, although this disparity was removed with obesity.

5.4.3 Development of renal lipid deposition

Renal triglyceride analysis identified increased accumulation in obese females compared to obese males. In comparison to lean females, no increased renal triglyceride accumulation was observed, suggesting that perhaps obese males have reduced renal triglyceride accumulation compared to obese females. Renal triglyceride accumulation is attributed to hyperlipidaemia, where excess plasma triglycerides and NEFAs filtered by the kidney are deposited in the renal tubules leading to lipotoxicity. During this study, one hypothesis for this apparent decrease in renal triglyceride deposition exhibited by the obese males was that renal lipid peroxidation in obese males was increased thus reducing the amount of renal triglyceride deposition. Yet in analysis of renal lipid peroxidation, these results showed no differences with effect of gender or obesity.

Perhaps the moderate nature and relative short exposure time to the obesogenic environment was not severe enough to lead to renal lipotoxicity as expected in the observed obese groups. As discussed in Chapter 3, the obese males exhibited a higher lean mass, it is therefore possible that obese males have a higher storage capacity of triglycerides from greater skeletal muscle mass and larger perirenal adipocyte expansion capacity, thus reducing the mechanism of lipid deposition in other organ systems and tissues. Alternatively a possible explanation for the absence of any significant increase of renal triglyceride deposition in both obese groups may be due to the absence of elevated circulatory plasma NEFAs and triglycerides, demonstrated in this sheep model of moderate obesity.

The TBARS assay measures thiobarbituric acid reactive substances, and although the gold standard analytical techniques to determine lipid peroxidation in obesity mediated oxidative stress²⁷⁹, the technique itself often overestimates MDA levels due to unselective binding²⁷⁶. Consequently if a more selective analytical technique of oxidative stress i.e. determination of OONO⁻ levels was utilised, significantly different results may have been observed.

5.4.4 Conclusions and summary

Similar to the conclusions reached in the previous two results chapters, obesity in males has resulted in an exaggerated response. Expression of inflammatory genes in kidney tissue was up-regulated in the majority of analysed molecules. As discussed, this entire inflammatory network over-expression implicates a potential alteration in transcription control mechanism, with a focus on epigenetic changes. This heightened inflammatory transcription observed in obese males is another indication of the increased risk toward obesity mediated inflammation. Exposure to moderate obesity has also led to renal morphological adaptations and functional impairment associated with nephropathy in obese males. Although no signs of actual tissue damage were apparent, these onset markers are a further suggestion that males are at an increased risk of obesity associated renal disease. Conversely females appear to show a dampened inflammatory renal response and no changes in renal morphology with obesity, which may imply a protective immunosuppression via cortisol and glucocorticoid binding in obese females. The findings of Chapter 5 are summarised in Figure 5.23, p186.

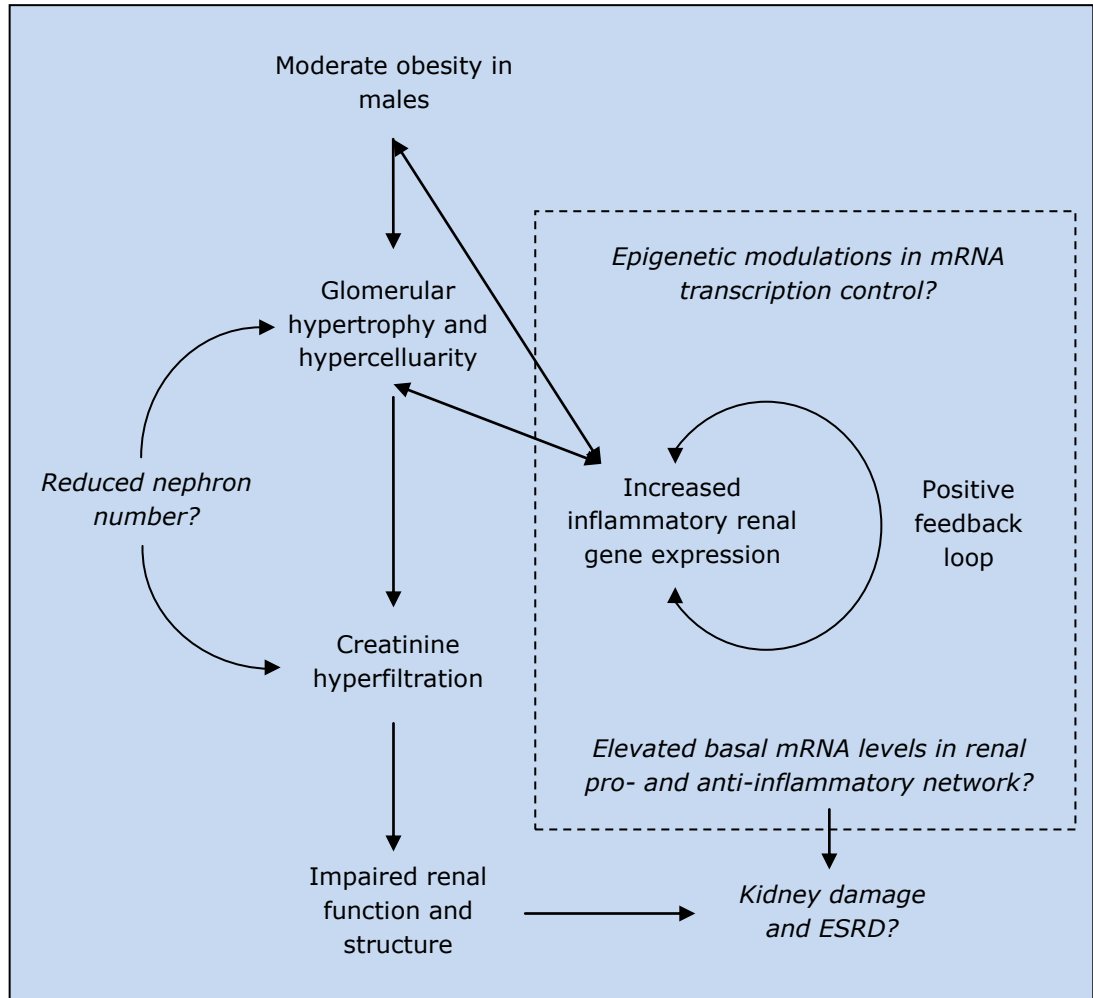


Figure 5.23: Summary diagram of male response to obesity and its effect on renal morphology and inflammatory gene expression. None of these renal adaptations were displayed by females in response to obesity. ESRD – End stage renal disease.

Chapter 6 – Conclusion

6.1 General aims

My study aimed to investigate the effects of obesity and gender on adipose tissue mediated inflammation and its contribution to renal disease. This was achieved by assessing the metabolic status, morphology and physiology of kidney and adipose tissue depots of male and female sheep exposed to a lean or obesogenic environment. Furthermore, this study had a particular focus on inflammatory gene expression in PAT and renal tissue. Chapter 6 summarises the key findings ascertained during this thesis.

6.1.1 Development of moderate obesity

Surveying the scientific literature identified a sexual dimorphism especially with regards to adipose tissue deposition in development of obesity. Males were often linked with increased central and intra-abdominal fat with obesity³⁷, whereas females displayed a greater peripheral accumulation of adipose tissue, mainly in the gluteal region³⁸. After exposure to an obesogenic environment both genders demonstrated increased body weights and in addition, males also showed enlarged lean mass.

Restriction of physical activity lead to both males and females exhibiting increased central and subcutaneous fat mass which in PAT was shown to be largely due to adipocyte hypertrophy. This development of adipose tissue observed in my study was a moderate increase in comparison to other ovine obesity studies²³⁴, yet regardless of this and in agreement with epidemiological data, females were still relatively fatter than males³⁸. Although in contrast to human epidemiological evidence, these animals did not display differences in adipose tissue location with gender.

6.1.2 Gender disparity in obesity mediated inflammation

Despite the morphological homogeneity displayed by males and females in adipose tissue development in this obesity model, there were inconsistencies between gender with respect to metabolic and inflammatory status. With obesity, both genders displayed metabolic impairments where males showed hyperinsulinaemia and females displayed hypercortisolism. Both these systemic conditions may in part contribute to the renal and PAT inflammatory gene expression exhibited by the obese animals. Insulin resistance has long been established to contribute to the chronic low grade inflammation often associated with obesity¹⁰⁰. In contrast, cortisol is known to suppress the immune system¹⁴², a pathway potentially accountable for the reduced renal and PAT inflammatory gene expression observed in the obese females. Although it is widely accepted that the gender differences observed in susceptibility to complex diseases are likely to be endocrinological³⁴⁴, it is possible sex hormones may mediate epigenetic modifications in DNA and histones which can regulate the risk of disease development³⁴⁴.

6.1.3 Summary

Figure 6.1, p189 shows the activated metabolic, renal and PAT gene expression pathways of females exposed to an obesogenic environment identified in my study. In comparison to males, the female pathway network shows a greatly reduced activation and resulting adaptations in renal physiology and function. Obese males (Figure 6.2, p190), however, displayed a comprehensive augmented renal and PAT inflammatory gene response with an indication of renal hyperfiltration, glomerular hypertrophy and glomerular hypercellularity, conditions which could lead to eventual renal damage and failure³³⁷.

In summary, females appear to show an increased protective response to obesity mediated inflammation and associated renal disease compared to males.

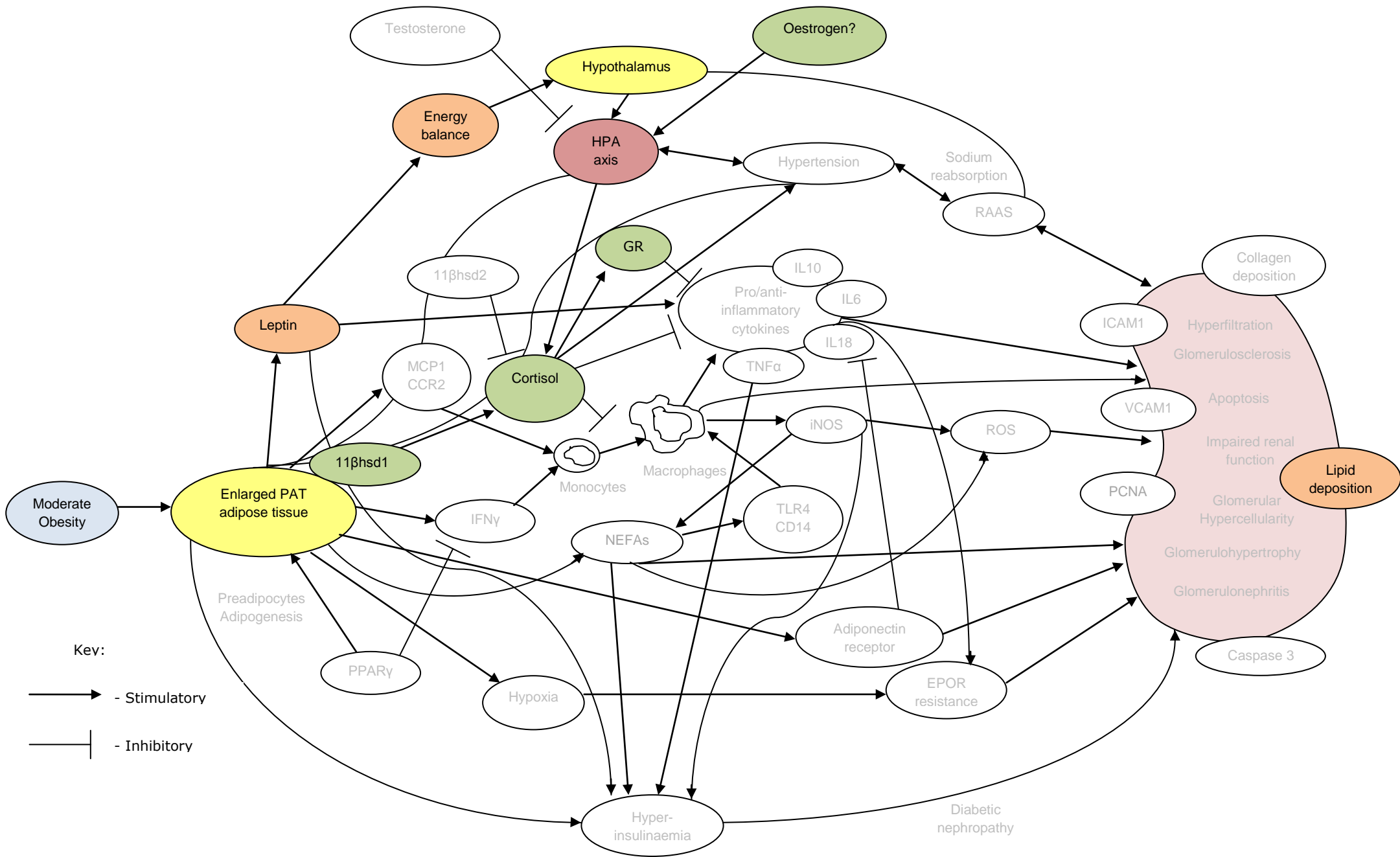


Figure 6.1: Obesity induced inflammatory gene expression and metabolic pathways in PAT and renal tissue exhibited by females in my study.

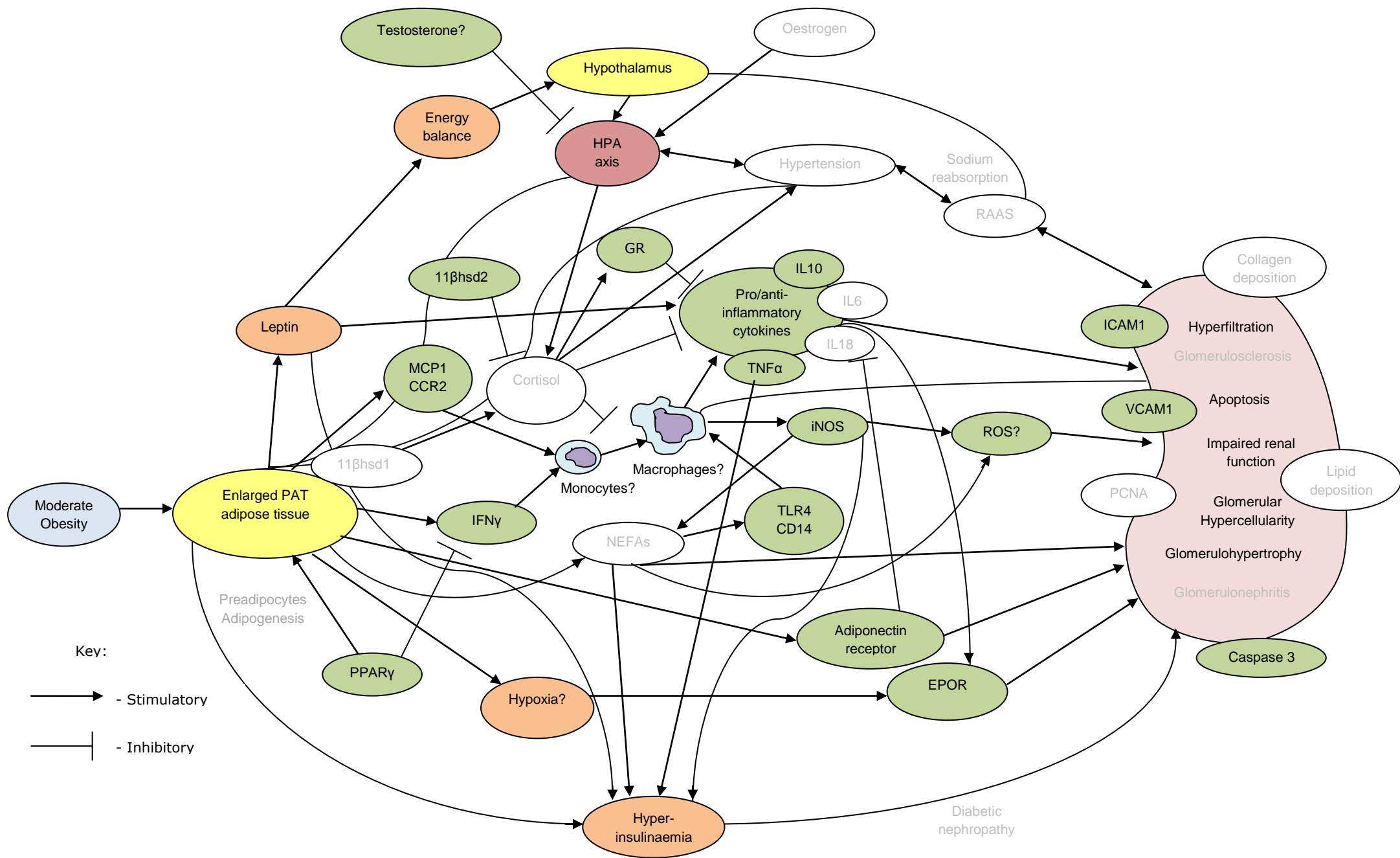


Figure 6.2: Obesity induced inflammatory gene expression and metabolic pathways in PAT and renal tissue exhibited by males in my study.

6.2 Study limitations

6.2.1 Sheep model of obesity

Using an ovine model of obesity in translational research poses its own limitations. As discussed, ruminants possess different dietary requirements to that of humans. In particular, sheep show reduced glucose utilization and insulin sensitivity, two important metabolic molecules involved in the pathogenesis of obesity and diabetic nephropathy. This obesity model however, was an investigation into how reduced activity rather than dietary manipulation induces increased fat deposition during the post-natal period. As demonstrated in Chapter 3, exposure to this reduced physical activity environment led to increased fat mass in the 'obesogenic' animals. In addition, the alterations in adipose tissue physiology, morphology, metabolism and inflammation observed indicate that impaired glucose utilization exhibited by ruminants has not undermined the experimental model of obesity used throughout this thesis.

6.2.2 Maternal nutritional intervention

Part of my study aimed to investigate the effect of maternal foetal programming through nutritional intervention and post-natal reduced physical activity on obesity and renal inflammation with gender. Unfortunately a gender imbalance occurred within the proposed study groups during the prenatal period. Moreover, four female animals died prematurely, and these events decreased the statistical power to investigate the intended groups. Throughout analysis, it was quickly identified that obesity and gender were the overriding factors in determination of any statistical differences, and whilst the nutritional intervention may have affected the results, no significant differences were observed in comparison of these groups. As described in Chapter 2, power calculations performed on the maternal nutrition groups suggested that sample numbers of ≈ 100 per group would be required to determine the effects of this intervention.

6.2.3 Histological analysis

Due to a lack of histological expertise it is possible that during analysis of the microscopic sections that some markers of renal or adipose tissue damage were overlooked in observational scrutiny. For example initial signs of glomerular scarring which indicates glomerulosclerosis, can be extremely difficult to determine, likewise CLS in adipose tissue. Certain microscopic sections appeared to display increased stain intensity in comparison with simultaneously processed samples. Other sections displayed artifacts that were not features of the sample. One explanation for this is the difference in response to histological treatment and processing, which appeared to dehydrate some samples more than others. Drier samples when stained developed a greater intensity of stain which may have impaired any statistical analysis. However, statistical differences were only observed with glomerular and adipocyte area, which were not affected by histological staining inconsistencies.

6.2.4 Gene expression

To date the sheep genome is not recorded in its entirety. This resulted in a limitation of which genes could be analysed in determination of mRNA expression. For example, NF- κ B is believed to be a master transcription control in the inflammatory network³⁴³, yet attempts to design primers to analyse its gene expression were unsuccessful because of the incomplete sheep genome information available. This restriction affected the examination of several other genes of interest, in particular angiotensin II and lipid binding protein which were also not successfully analysed.

6.2.5 Protein expression

The inflammatory protein expression work performed in my study provided no satisfactory data. Commercially available ovine antibodies for markers of inflammation are relatively novel in comparison to the antibodies available for rodents and humans. Although the purchased TLR4 antibody was anticipated to work in sheep tissue, the experimental analysis was ineffectual. It was likely that the failed protein expression analysis was due to problems with the secondary antibody as discussed in Chapter 5. With a greater time allowance it may have been possible to optimise the TLR4 protein expression in both the Western blot and IHC analysis by trialing different secondary antibodies. Additionally, as commercially existing sheep antibodies are limited and untested, perhaps it would be necessary to produce the required antibodies during operation of the experimental animal model.

6.3 Future work and perspectives

In order to elucidate the findings in this thesis, it would be necessary to complete further investigations using both the applied model of ovine moderate obesity and modified versions of this. Several suggestions are discussed in the following sub-chapters.

6.3.1 Physiology and inflammatory profile of other adipose depots

As demonstrated in Chapter 3, all adipose tissue depots showed increased mass with development of moderate obesity. However, only PAT was investigated with regards to inflammatory gene profile and tissue physiology. Summary Table 1.3 (p18) identifies the different inflammatory responses shown with gender and adipose tissue location. To determine if the inflammatory response is homogeneous between the different adipose tissue depots, and if the PAT observed sexual dimorphic inflammation also exists in these depots, it would be necessary to perform similar analyses on both central and subcutaneous fat tissue. Histological analysis of these different depots could also highlight any development of obesity mediated inflammatory pathology that was not observed in PAT.

6.3.2 Epigenetic factors

It was proposed in my study that the elevation in basal renal inflammatory gene expression exhibited by the obese males may have been due to epigenetic changes in gene transcription. To further understand these mechanisms, DNA methylation and histone modification analysis could be completed on renal DNA samples from the study sheep to determine the role of epigenetic alterations in the inflammatory gene profile of kidney tissue with obesity.

6.3.3 Sex hormone analysis

The disparity in response with gender observed throughout my thesis was mainly attributed to differences in sex hormones. To confirm this, future work would target endogenous concentrations of oestrogens and androgens in a comparable study of moderate obesity. Further analysis could investigate how exogenous administration of these hormones affects adipose tissue deposition, glucocorticoid response and renal inflammatory gene expression. Additionally gonadectomy experiment models could be utilised to determine the absence of these hormones on the displayed outcomes addressed in my work.

6.3.4 Original project proposal

Initially my study aimed to investigate inflammation and end-organ damage with obesity and sepsis. The aim was to study obesity mediated inflammation on the kidney using the EARNEST ovine model and following these analyses to replicate this experimental obesity model but induce a septic condition in the study animals. This hoped to identify if obesity mediated an inflammatory state and subsequent renal pathogenesis which may be attenuated by the introduction of a known inflammatory condition, i.e. sepsis. However during my research it was quickly realised that replication of the ovine obesity model would be impossible within my study period. Additionally the gender disparity observed throughout my initial experimental analysis warranted a more detailed examination. Therefore further investigation is required to determine if this sexual dimorphic renal inflammation observed in moderate obesity exists in the presence of a septic condition, with particular interest in the glucocorticoid network response.

6.4 Final remarks

This study has demonstrated how development in moderate obesity contributes to adaptations in adipose tissue physiology, metabolic status and modifications in renal and PAT inflammatory gene expression. Additionally, gender has been shown to impact on these responses. The findings in this study could in part help clarify the mechanisms involved in the reported differences between males and females in the human population. Particularly with regards to the progression of renal nephropathies often associated with the presence of obesity¹¹⁰.

References

- 1 NICE, Obesity: the prevention, identification, assessment of overweight and obesity in adults and children. *National Institute for Health and Clinical Excellence* (2006).
- 2 WHO, Obesity and overweight. *World Health Organisation Fact Sheet No. 311* (2011).
- 3 WHO, Global database on body mass index. *World Health Organisation* (2008).
- 4 NHS, Statistics on obesity, physical activity and diet: England, 2010. *The information centre for health and social care* (2010).
- 5 Government, HM, Healthy lives, healthy people: Our strategy for public health in England. *Department of Health* (2011).
- 6 Martinez, J. A., Body-weight regulation: causes of obesity. *Proc Nutr Soc* **59** (3), 337 (2000).
- 7 McMillen, I. C. and Robinson, J. S., Developmental origins of the metabolic syndrome: prediction, plasticity, and programming. *Physiol Rev* **85** (2), 571 (2005).
- 8 Hales, C. N. and Barker, D. J., The thrifty phenotype hypothesis. *Br Med Bull* **60**, 5 (2001).
- 9 Kopelman, P. G., Obesity as a medical problem. *Nature* **404** (6778), 635 (2000); Lawrence, V. J. and Kopelman, P. G., Medical consequences of obesity. *Clin Dermatol* **22** (4), 296 (2004).
- 10 WHO, Definition, diagnosis, and classification of diabetes mellitus and its complications. *Report of a WHO consultation Geneva* (World Health Organization) (1999).
- 11 Lemieux, S. et al., Sex differences in the relation of visceral adipose tissue accumulation to total body fatness. *Am J Clin Nutr* **58** (4), 463 (1993).
- 12 Enzi, G. et al., Subcutaneous and visceral fat distribution according to sex, age, and overweight, evaluated by computed tomography. *Am J Clin Nutr* **44** (6), 739 (1986).
- 13 Turgeon, J. L. et al., Complex actions of sex steroids in adipose tissue, the cardiovascular system, and brain: Insights from basic science and clinical studies. *Endocr Rev* **27** (6), 575 (2006).
- 14 Rappelli, A., Hypertension and obesity after the menopause. *J Hypertens Suppl* **20** (2), S26 (2002).
- 15 Garg, A., Regional adiposity and insulin resistance. *J Clin Endocrinol Metab* **89** (9), 4206 (2004).

- ¹⁶ Ravelli, G. P., Stein, Z. A., and Susser, M. W., Obesity in young men after famine exposure in utero and early infancy. *N Engl J Med* **295** (7), 349 (1976).
- ¹⁷ Ravelli, A. C. et al., Obesity at the age of 50 y in men and women exposed to famine prenatally. *Am J Clin Nutr* **70** (5), 811 (1999).
- ¹⁸ de Rooij, S. R. et al., Glucose tolerance at age 58 and the decline of glucose tolerance in comparison with age 50 in people prenatally exposed to the Dutch famine. *Diabetologia* **49** (4), 637 (2006).
- ¹⁹ Roseboom, T., de Rooij, S., and Painter, R., The Dutch famine and its long-term consequences for adult health. *Early Hum Dev* **82** (8), 485 (2006).
- ²⁰ Lopuhaa, C. E. et al., Atopy, lung function, and obstructive airways disease after prenatal exposure to famine. *Thorax* **55** (7), 555 (2000).
- ²¹ Bispham, J. et al., Maternal endocrine adaptation throughout pregnancy to nutritional manipulation: consequences for maternal plasma leptin and cortisol and the programming of fetal adipose tissue development. *Endocrinology* **144** (8), 3575 (2003).
- ²² Guo, F. and Jen, K. L., High-fat feeding during pregnancy and lactation affects offspring metabolism in rats. *Physiol Behav* **57** (4), 681 (1995).
- ²³ Samuelsson, A. M. et al., Diet-induced obesity in female mice leads to offspring hyperphagia, adiposity, hypertension, and insulin resistance: a novel murine model of developmental programming. *Hypertension* **51** (2), 383 (2008).
- ²⁴ Howie, G. J., Sloboda, D. M., Kamal, T., and Vickers, M. H., Maternal nutritional history predicts obesity in adult offspring independent of postnatal diet. *J Physiol* **587** (Pt 4), 905 (2009).
- ²⁵ Gardner, D. S. et al., Programming of glucose-insulin metabolism in adult sheep after maternal undernutrition. *Am J Physiol Regul Integr Comp Physiol* **289** (4), R947 (2005).
- ²⁶ Kershaw, E. E. and Flier, J. S., Adipose tissue as an endocrine organ. *J Clin Endocrinol Metab* **89** (6), 2548 (2004).
- ²⁷ Klaus, S., Ely, M., Encke, D., and Heldmaier, G., Functional assessment of white and brown adipocyte development and energy metabolism in cell culture. Dissociation of terminal differentiation and thermogenesis in brown adipocytes. *J Cell Sci* **108** (Pt 10), 3171 (1995).
- ²⁸ Klaus, S., Functional differentiation of white and brown adipocytes. *Bioessays* **19** (3), 215 (1997).
- ²⁹ Lean, M. E., Brown adipose tissue in humans. *Proc Nutr Soc* **48** (2), 243 (1989).
- ³⁰ Virtanen, K. A. et al., Functional brown adipose tissue in healthy adults. *N Engl J Med* **360** (15), 1518 (2009).

- 31 Seale, P. et al., PRDM16 controls a brown fat/skeletal muscle switch. *Nature* **454** (7207), 961 (2008).
- 32 Wang, P., Mariman, E., Renes, J., and Keijer, J., The secretory function of adipocytes in the physiology of white adipose tissue. *J Cell Physiol* **216** (1), 3 (2008).
- 33 Arner, P., Differences in lipolysis between human subcutaneous and omental adipose tissues. *Ann Med* **27** (4), 435 (1995).
- 34 Spalding, K. L. et al., Dynamics of fat cell turnover in humans. *Nature* **453** (7196), 783 (2008).
- 35 Bjorntorp, P., Karlsson, M., and Pettersson, P., Expansion of adipose tissue storage capacity at different ages in rats. *Metabolism* **31** (4), 366 (1982).
- 36 Sniderman, A. D. et al., Why might South Asians be so susceptible to central obesity and its atherogenic consequences? The adipose tissue overflow hypothesis. *Int J Epidemiol* **36** (1), 220 (2007).
- 37 Tchoukalova, Y. D. et al., Subcutaneous adipocyte size and body fat distribution. *Am J Clin Nutr* **87** (1), 56 (2008).
- 38 Tchernof, A. et al., Regional differences in adipose tissue metabolism in women: minor effect of obesity and body fat distribution. *Diabetes* **55** (5), 1353 (2006).
- 39 Drolet, R. et al., Hypertrophy and hyperplasia of abdominal adipose tissues in women. *Int J Obes (Lond)* **32** (2), 283 (2008).
- 40 Ahima, R. S., Central actions of adipocyte hormones. *Trends Endocrinol Metab* **16** (7), 307 (2005).
- 41 Skurk, T., Alberti-Huber, C., Herder, C., and Hauner, H., Relationship between adipocyte size and adipokine expression and secretion. *J Clin Endocrinol Metab* **92** (3), 1023 (2007).
- 42 Trayhurn, P. and Wood, I. S., Signalling role of adipose tissue: adipokines and inflammation in obesity. *Biochem Soc Trans* **33** (Pt 5), 1078 (2005).
- 43 Wellen, K. E. and Hotamisligil, G. S., Obesity-induced inflammatory changes in adipose tissue. *J Clin Invest* **112** (12), 1785 (2003).
- 44 Opie, L. H. and Walfish, P. G., Plasma free fatty acid concentrations in obesity. *N Engl J Med* **268**, 757 (1963).
- 45 Boden, G. et al., Mechanisms of fatty acid-induced inhibition of glucose uptake. *J Clin Invest* **93** (6), 2438 (1994).
- 46 Apovian, C. M. et al., Adipose macrophage infiltration is associated with insulin resistance and vascular endothelial dysfunction in obese subjects. *Arterioscler Thromb Vasc Biol* **28** (9), 1654 (2008).

- 47 Riemens, S. C., Sluiter, W. J., and Dullaart, R. P., Enhanced escape of non-esterified fatty acids from tissue uptake: its role in impaired insulin-induced lowering of total rate of appearance in obesity and Type II diabetes mellitus. *Diabetologia* **43** (4), 416 (2000).
- 48 Hajer, G. R., van Haeften, T. W., and Visseren, F. L., Adipose tissue dysfunction in obesity, diabetes, and vascular diseases. *Eur Heart J* **29** (24), 2959 (2008).
- 49 Kahn, B. B. and Flier, J. S., Obesity and insulin resistance. *J Clin Invest* **106** (4), 473 (2000).
- 50 Kahn, S. E., Hull, R. L., and Utzschneider, K. M., Mechanisms linking obesity to insulin resistance and type 2 diabetes. *Nature* **444** (7121), 840 (2006).
- 51 Goodpaster, B. H. et al., Effects of weight loss on regional fat distribution and insulin sensitivity in obesity. *Diabetes* **48** (4), 839 (1999).
- 52 Biology, Beta Cell, Insulin-mediated glucose uptake, Available at <http://www.betacell.org/content/articles/articlepanel.php?aid=1&pid=3>, (2005).
- 53 Aderem, A. and Ulevitch, R. J., Toll-like receptors in the induction of the innate immune response. *Nature* **406** (6797), 782 (2000).
- 54 Karopka, T., Fluck, J., Mevissen, H. T., and Glass, A., The Autoimmune Disease Database: a dynamically compiled literature-derived database. *BMC Bioinformatics* **7**, 325 (2006).
- 55 Madigan, Michael T., *Brock biology of microorganisms*. (Benjamin Cummings, San Francisco).
- 56 Baron, Samuel and National Center for Biotechnology, Information, *Medical microbiology [electronic resource]*. (University of Texas Medical Branch at Galveston, [Galveston, Tex.], 1996).
- 57 Pickens, Charles O., *Cell apoptotic signalling pathways*. (Nova Biomedical Books, New York, 2007).
- 58 Vachharajani, V., Influence of obesity on sepsis. *Pathophysiology* **15** (2), 123 (2008).
- 59 Hotamisligil, G. S., Shargill, N. S., and Spiegelman, B. M., Adipose expression of tumor necrosis factor-alpha: direct role in obesity-linked insulin resistance. *Science* **259** (5091), 87 (1993).
- 60 Hotamisligil, G. S., Inflammatory pathways and insulin action. *Int J Obes Relat Metab Disord* **27 Suppl 3**, S53 (2003).
- 61 Roytblat, L. et al., Raised interleukin-6 levels in obese patients. *Obes Res* **8** (9), 673 (2000).
- 62 Eder, K., Baffy, N., Falus, A., and Fulop, A. K., The major inflammatory mediator interleukin-6 and obesity. *Inflamm Res* **58** (11), 727 (2009).

- 63 Juge-Aubry, C. E. et al., Adipose tissue is a regulated source of interleukin-10. *Cytokine* **29** (6), 270 (2005).
- 64 Kanda, H. et al., MCP-1 contributes to macrophage infiltration into adipose tissue, insulin resistance, and hepatic steatosis in obesity. *J Clin Invest* **116** (6), 1494 (2006).
- 65 Cinti, S. et al., Adipocyte death defines macrophage localization and function in adipose tissue of obese mice and humans. *J Lipid Res* **46** (11), 2347 (2005).
- 66 Fain, J. N., Release of inflammatory mediators by human adipose tissue is enhanced in obesity and primarily by the nonfat cells: a review. *Mediators Inflamm* **2010**, 513948.
- 67 Ye, J., Adipose Tissue Vascularization: Its Role in Chronic Inflammation. *Curr Diab Rep*.
- 68 Harle, P. and Straub, R. H., Leptin is a link between adipose tissue and inflammation. *Ann N Y Acad Sci* **1069**, 454 (2006).
- 69 Mangge, H. et al., Inflammation, adiponectin, obesity and cardiovascular risk. *Curr Med Chem* **17** (36), 4511.
- 70 Beasley, L. E. et al., Inflammation and race and gender differences in computerized tomography-measured adipose depots. *Obesity (Silver Spring)* **17** (5), 1062 (2009).
- 71 Fain, J. N. et al., Comparison of the release of adipokines by adipose tissue, adipose tissue matrix, and adipocytes from visceral and subcutaneous abdominal adipose tissues of obese humans. *Endocrinology* **145** (5), 2273 (2004).
- 72 Alvehus, M. et al., The human visceral fat depot has a unique inflammatory profile. *Obesity (Silver Spring)* **18** (5), 879.
- 73 Rocha, V. Z. and Libby, P., Obesity, inflammation, and atherosclerosis. *Nat Rev Cardiol* **6** (6), 399 (2009).
- 74 Greenberg, Arthur and National Kidney, Federation, *Primer on kidney diseases*. (Academic Press, San Diego ;London, 1994).
- 75 Jennette, J. Charles and Heptinstall, Robert H., *Heptinstall's pathology of the kidney*. (Lippincott Williams & Wilkins, Philadelphia, PA, 2007).
- 76 Vize, Peter D., Woolf, Adrian S., and Bard, Jonathan B. L., *The kidney : from normal development to congenital abnormalities*. (Academic, San Diego, Calif. ; London, 2003).⁷⁷ Kuehnel, Wolfgang and Frotscher, M., *Color atlas of human anatomy*. (Thieme, Stuttgart ;New York, 2009).
- 78 Gallant, Trevor, Nephron structure, Available at http://kvhs.nbed.nb.ca/gallant/biology/nephron_structure.jpg, (2011).

- 79 Cummings, Benjamin, Gross anatomy of the urinary system, Available at
at
<http://legacy.owensboro.kctcs.edu/gcaplan/anat2/notes/Image136.gif>,
(2001).
- 80 Bullock, John, Boyle, Joseph, and Wang, Michael B., *Physiology*.
(Lippincott Williams & Wilkins, Philadelphia ;London, 2001).
- 81 O'Callaghan, C. A. and dawsonera, *The renal system at a glance*.
(Wiley-Blackwell, Oxford, 2009).
- 82 O'Callaghan, C. A., *The renal system at a glance*. (Blackwell Pub.,
Oxford, 2006).
- 83 Jelkmann, W., Regulation of erythropoietin production. *J Physiol* **589**
(Pt 6), 1251.
- 84 Stevens, L. A., Coresh, J., Greene, T., and Levey, A. S., Assessing
kidney function--measured and estimated glomerular filtration rate. *N
Engl J Med* **354** (23), 2473 (2006).
- 85 Linnetz, E. and Graves, T., Glomerular filtration rate in general small
animal practice. *Compend Contin Educ Vet* **32** (10), E1.
- 86 Levey, A. S. et al., A more accurate method to estimate glomerular
filtration rate from serum creatinine: a new prediction equation.
Modification of Diet in Renal Disease Study Group. *Ann Intern Med*
130 (6), 461 (1999).
- 87 Filler, G. et al., The Cockcroft-Gault formula should not be used in
children. *Kidney Int* **67** (6), 2321 (2005).
- 88 Cockcroft, D. W. and Gault, M. H., Prediction of creatinine clearance
from serum creatinine. *Nephron* **16** (1), 31 (1976); Gault, M. H.,
Longerich, L. L., Harnett, J. D., and Wesolowski, C., Predicting
glomerular function from adjusted serum creatinine. *Nephron* **62** (3),
249 (1992).
- 89 Bosma, R. J. et al., Body mass index is associated with altered renal
hemodynamics in non-obese healthy subjects. *Kidney Int* **65** (1), 259
(2004).
- 90 Thomas, F. et al., Cardiovascular mortality in overweight subjects: the
key role of associated risk factors. *Hypertension* **46** (4), 654 (2005).
- 91 Julius, S., Valentini, M., and Palatini, P., Overweight and hypertension :
a 2-way street? *Hypertension* **35** (3), 807 (2000).
- 92 Narkiewicz, K., Obesity and hypertension--the issue is more complex
than we thought. *Nephrol Dial Transplant* **21** (2), 264 (2006).
- 93 Luft, F. C. and Haller, H., Hypertension-induced renal injury: is
mechanically mediated interstitial inflammation involved? *Nephrol Dial
Transplant* **10** (1), 9 (1995).

- 94 Cai, Y. I. et al., Collagen distribution in focal and segmental glomerulosclerosis: an immunofluorescence and ultrastructural immunogold study. *J Pathol* **179** (2), 188 (1996).
- 95 Kambham, N. et al., Obesity-related glomerulopathy: an emerging epidemic. *Kidney Int* **59** (4), 1498 (2001).
- 96 Davy, K. P. and Hall, J. E., Obesity and hypertension: two epidemics or one? *Am J Physiol Regul Integr Comp Physiol* **286** (5), R803 (2004).
- 97 Abitbol, Carolyn L., Obesity-related nephropathy in children. *Paediatric Health* **3** (2), 141 (2009).
- 98 Mathieu, P. et al., Visceral obesity: the link among inflammation, hypertension, and cardiovascular disease. *Hypertension* **53** (4), 577 (2009).
- 99 Mokdad, A. H. et al., Prevalence of obesity, diabetes, and obesity-related health risk factors, 2001. *JAMA* **289** (1), 76 (2003).
- 100 Dandona, P., Aljada, A., and Bandyopadhyay, A., Inflammation: the link between insulin resistance, obesity and diabetes. *Trends Immunol* **25** (1), 4 (2004).
- 101 Mogensen, C. E., Christensen, C. K., and Vittinghus, E., The stages in diabetic renal disease. With emphasis on the stage of incipient diabetic nephropathy. *Diabetes* **32 Suppl 2**, 64 (1983).
- 102 Qian, Y. et al., From fibrosis to sclerosis: mechanisms of glomerulosclerosis in diabetic nephropathy. *Diabetes* **57** (6), 1439 (2008).
- 103 WHO, Diabetes. *World Health Organisation Fact Sheet No. 312* (2011).
- 104 Hall, J. E., The kidney, hypertension, and obesity. *Hypertension* **41** (3 Pt 2), 625 (2003).
- 105 Harrison-Bernard, L. M., The renal renin-angiotensin system. *Adv Physiol Educ* **33** (4), 270 (2009).
- 106 Loscalzo, Joseph, *Harrison's cardiovascular medicine*. (McGraw-Hill Medical, New York).
- 107 Booth, R. E., Johnson, J. P., and Stockand, J. D., Aldosterone. *Adv Physiol Educ* **26** (1-4), 8 (2002).
- 108 Sarzani, R., Salvi, F., Dessi-Fulgheri, P., and Rappelli, A., Renin-angiotensin system, natriuretic peptides, obesity, metabolic syndrome, and hypertension: an integrated view in humans. *J Hypertens* **26** (5), 831 (2008).
- 109 Fleming, Bill, Function of the adrenal glands, Available at <http://www.endocrinesurgery.net.au/adrenal-function/>, (2011).
- 110 Silbiger, S. and Neugarten, J., Gender and human chronic renal disease. *Gen Med* **5 Suppl A**, S3 (2008).

- 111 Kwan, G. et al., Effects of sex hormones on mesangial cell proliferation and collagen synthesis. *Kidney Int* **50** (4), 1173 (1996).
- 112 Schunkert, H. et al., Effects of estrogen replacement therapy on the renin-angiotensin system in postmenopausal women. *Circulation* **95** (1), 39 (1997).
- 113 Fischer, M., Baessler, A., and Schunkert, H., Renin angiotensin system and gender differences in the cardiovascular system. *Cardiovasc Res* **53** (3), 672 (2002).
- 114 Ingelfinger, J. R. et al., Intrarenal angiotensinogen: localization and regulation. *Pediatr Nephrol* **4** (4), 424 (1990).
- 115 Ellison, K. E., Ingelfinger, J. R., Pivor, M., and Dzau, V. J., Androgen regulation of rat renal angiotensinogen messenger RNA expression. *J Clin Invest* **83** (6), 1941 (1989).
- 116 Gnanalingham, M. et al., Maternal dexamethasone administration and the maturation of perirenal adipose tissue of the neonatal sheep. *Organogenesis* **4** (3), 188 (2008).
- 117 Montani, J. P. et al., Ectopic fat storage in heart, blood vessels and kidneys in the pathogenesis of cardiovascular diseases. *Int J Obes Relat Metab Disord* **28 Suppl 4**, S58 (2004).
- 118 Lamacchia, O. et al., Para- and perirenal fat thickness is an independent predictor of chronic kidney disease, increased renal resistance index and hyperuricaemia in type-2 diabetic patients. *Nephrol Dial Transplant* **26** (3), 892.
- 119 Zhao, H. L. et al., Fat redistribution and adipocyte transformation in uninephrectomized rats. *Kidney Int* **74** (4), 467 (2008).
- 120 Dulloo, A. G., Antic, V., and Montani, J. P., Ectopic fat stores: housekeepers that can overflow into weapons of lean body mass destruction. *Int J Obes Relat Metab Disord* **28 Suppl 4**, S1 (2004).
- 121 Smith, Ulf, Visceral fat, like epicardial fat, is an ectopic fat depot which reflects cardiometabolic risk in obesity. *Journal of the International Official Chair on Cardiometabolic Risk* **1** (2), 17 (2008).
- 122 van Herpen, N. A. and Schrauwen-Hinderling, V. B., Lipid accumulation in non-adipose tissue and lipotoxicity. *Physiol Behav* **94** (2), 231 (2008).
- 123 Schaffer, J. E., Lipotoxicity: when tissues overeat. *Curr Opin Lipidol* **14** (3), 281 (2003).
- 124 Griffin, M. E. et al., Free fatty acid-induced insulin resistance is associated with activation of protein kinase C theta and alterations in the insulin signaling cascade. *Diabetes* **48** (6), 1270 (1999).
- 125 Yu, C. et al., Mechanism by which fatty acids inhibit insulin activation of insulin receptor substrate-1 (IRS-1)-associated phosphatidylinositol 3-kinase activity in muscle. *J Biol Chem* **277** (52), 50230 (2002).

- 126 Nolasco, F. et al., Interstitial foam cells in the nephrotic syndrome belong to the monocyte/macrophage lineage. *Proc Eur Dial Transplant Assoc Eur Ren Assoc* **21**, 666 (1985).
- 127 Weinberg, J. M., Lipotoxicity. *Kidney Int* **70** (9), 1560 (2006).
- 128 Taves, M. D., Gomez-Sanchez, C. E., and Soma, K. K., Extra-adrenal glucocorticoids and mineralocorticoids: evidence for local synthesis, regulation, and function. *Am J Physiol Endocrinol Metab*.
- 129 Labeur, M. and Holsboer, F., Molecular mechanisms of glucocorticoid receptor signaling. *Medicina (B Aires)* **70** (5), 457.
- 130 Lullmann, Heinz, Hein, Lutz, and Mohr, Klaus, *Color atlas of pharmacology*. (Thieme, Stuttgart).
- 131 Stimson, R. H. et al., Effects of proportions of dietary macronutrients on glucocorticoid metabolism in diet-induced obesity in rats. *PLoS One* **5** (1), e8779.
- 132 Syed, A. A. and Weaver, J. U., Glucocorticoid sensitivity: the hypothalamic-pituitary-adrenal-tissue axis. *Obes Res* **13** (7), 1131 (2005).
- 133 Duclos, M. et al., Increased cortisol bioavailability, abdominal obesity, and the metabolic syndrome in obese women. *Obes Res* **13** (7), 1157 (2005).
- 134 Stewart, P. M. et al., Cortisol metabolism in human obesity: impaired cortisone-->cortisol conversion in subjects with central adiposity. *J Clin Endocrinol Metab* **84** (3), 1022 (1999).
- 135 Dallman, M. F. et al., Feast and famine: critical role of glucocorticoids with insulin in daily energy flow. *Front Neuroendocrinol* **14** (4), 303 (1993).
- 136 Salehi, M., Ferenczi, A., and Zumoff, B., Obesity and cortisol status. *Horm Metab Res* **37** (4), 193 (2005).
- 137 Bjorntorp, P. and Rosmond, R., Obesity and cortisol. *Nutrition* **16** (10), 924 (2000).
- 138 Livingstone, D. E. et al., Understanding the role of glucocorticoids in obesity: tissue-specific alterations of corticosterone metabolism in obese Zucker rats. *Endocrinology* **141** (2), 560 (2000).
- 139 Tomlinson, J. W. et al., 11beta-hydroxysteroid dehydrogenase type 1: a tissue-specific regulator of glucocorticoid response. *Endocr Rev* **25** (5), 831 (2004).
- 140 Melander, O. et al., Association between a variant in the 11 beta-hydroxysteroid dehydrogenase type 2 gene and primary hypertension. *J Hum Hypertens* **14** (12), 819 (2000).
- 141 Baybutt, H. N. and Holsboer, F., Inhibition of macrophage differentiation and function by cortisol. *Endocrinology* **127** (1), 476 (1990).

- 142 Billing, A. M., Fack, F., Turner, J. D., and Muller, C. P., Cortisol is a potent modulator of lipopolysaccharide-induced interferon signaling in macrophages. *Innate Immun.*
- 143 Auphan, N. et al., Immunosuppression by glucocorticoids: inhibition of NF-kappa B activity through induction of I kappa B synthesis. *Science* **270** (5234), 286 (1995).
- 144 Singh, N., Mechanisms of glucocorticoid-mediated anti-inflammatory and immunosuppressive action. *Paediatric and perinatal drug therapy* **6** (2), 107 (2004).
- 145 Slominski, A., A nervous breakdown in the skin: stress and the epidermal barrier. *J Clin Invest* **117** (11), 3166 (2007).
- 146 Griffiths, Anthony J. F., *Introduction to genetic analysis*. (W. H. Freeman, New York, NY ;[Basingstoke], 2008).
- 147 Guan, H. et al., Adipose tissue gene expression profiling reveals distinct molecular pathways that define visceral adiposity in offspring of maternal protein-restricted rats. *Am J Physiol Endocrinol Metab* **288** (4), E663 (2005).
- 148 Patterson, L. T. and Potter, S. S., Profiling gene expression in kidney development. *Nephron Exp Nephrol* **98** (4), e109 (2004).
- 149 McTernan, P. G. et al., Increased resistin gene and protein expression in human abdominal adipose tissue. *J Clin Endocrinol Metab* **87** (5), 2407 (2002).
- 150 NHGRI, National Human Genome Research Institute, Gene Expression, Available at http://www.genome.gov/Pages/Hyperion//DIR/VIP/Glossary/Illustration/gene_expression.shtml, (2002).
- 151 Krozowski, Z. et al., The type I and type II 11beta-hydroxysteroid dehydrogenase enzymes. *J Steroid Biochem Mol Biol* **69** (1-6), 391 (1999).
- 152 Thomas, M. P. and Potter, B. V., Crystal structures of 11beta-hydroxysteroid dehydrogenase type 1 and their use in drug discovery. *Future Med Chem* **3** (3), 367.
- 153 Mariniello, B. et al., Adipose tissue 11beta-hydroxysteroid dehydrogenase type 1 expression in obesity and Cushing's syndrome. *Eur J Endocrinol* **155** (3), 435 (2006).
- 154 Kotelevtsev, Y. et al., 11beta-hydroxysteroid dehydrogenase type 1 knockout mice show attenuated glucocorticoid-inducible responses and resist hyperglycemia on obesity or stress. *Proc Natl Acad Sci U S A* **94** (26), 14924 (1997).
- 155 Quinkler, M. et al., Expression of renal 11beta-hydroxysteroid dehydrogenase type 2 is decreased in patients with impaired renal function. *Eur J Endocrinol* **153** (2), 291 (2005).

- 156 Lavery, G. G. et al., Association studies between the HSD11B2 gene (encoding human 11beta-hydroxysteroid dehydrogenase type 2), type 1 diabetes mellitus and diabetic nephropathy. *Eur J Endocrinol* **146** (4), 553 (2002).
- 157 Kotelevtsev, Y. et al., Hypertension in mice lacking 11beta-hydroxysteroid dehydrogenase type 2. *J Clin Invest* **103** (5), 683 (1999).
- 158 Mussig, K. et al., 11beta-hydroxysteroid dehydrogenase 2 activity is elevated in severe obesity and negatively associated with insulin sensitivity. *Obesity (Silver Spring)* **16** (6), 1256 (2008).
- 159 Pujols, L. et al., Expression of glucocorticoid receptor alpha- and beta-isoforms in human cells and tissues. *Am J Physiol Cell Physiol* **283** (4), C1324 (2002).
- 160 Sternberg, E. M., Neural regulation of innate immunity: a coordinated nonspecific host response to pathogens. *Nat Rev Immunol* **6** (4), 318 (2006).
- 161 Boullu-Ciocca, S. et al., Expression of the mRNAs coding for the glucocorticoid receptor isoforms in obesity. *Obes Res* **11** (8), 925 (2003).
- 162 Kadowaki, T. and Yamauchi, T., Adiponectin and adiponectin receptors. *Endocr Rev* **26** (3), 439 (2005).
- 163 Haluzik, M., Parizkova, J., and Haluzik, M. M., Adiponectin and its role in the obesity-induced insulin resistance and related complications. *Physiol Res* **53** (2), 123 (2004).
- 164 Yamauchi, T. et al., The fat-derived hormone adiponectin reverses insulin resistance associated with both lipodystrophy and obesity. *Nat Med* **7** (8), 941 (2001).
- 165 Iwashima, Y. et al., Adiponectin and renal function, and implication as a risk of cardiovascular disease. *Am J Cardiol* **98** (12), 1603 (2006).
- 166 Ouchi, N. et al., Adipocyte-derived plasma protein, adiponectin, suppresses lipid accumulation and class A scavenger receptor expression in human monocyte-derived macrophages. *Circulation* **103** (8), 1057 (2001).
- 167 Jequier, E., Leptin signaling, adiposity, and energy balance. *Ann N Y Acad Sci* **967**, 379 (2002).
- 168 Ingalls, A. M., Dickie, M. M., and Snell, G. D., Obese, a new mutation in the house mouse. *J Hered* **41** (12), 317 (1950).
- 169 Kennedy, A. et al., The metabolic significance of leptin in humans: gender-based differences in relationship to adiposity, insulin sensitivity, and energy expenditure. *J Clin Endocrinol Metab* **82** (4), 1293 (1997).
- 170 Cole, S. A. et al., Genetics of leptin expression in baboons. *Int J Obes Relat Metab Disord* **27** (7), 778 (2003).

- 171 Bjorbaek, C. and Kahn, B. B., Leptin signaling in the central nervous system and the periphery. *Recent Prog Horm Res* **59**, 305 (2004).
- 172 Fantuzzi, G. and Faggioni, R., Leptin in the regulation of immunity, inflammation, and hematopoiesis. *J Leukoc Biol* **68** (4), 437 (2000).
- 173 Schroder, K., Hertzog, P. J., Ravasi, T., and Hume, D. A., Interferon-gamma: an overview of signals, mechanisms and functions. *J Leukoc Biol* **75** (2), 163 (2004).
- 174 Ikezumi, Y., Atkins, R. C., and Nikolic-Paterson, D. J., Interferon-gamma augments acute macrophage-mediated renal injury via a glucocorticoid-sensitive mechanism. *J Am Soc Nephrol* **14** (4), 888 (2003).
- 175 Heinrich, P. C. et al., Principles of interleukin (IL)-6-type cytokine signalling and its regulation. *Biochem J* **374** (Pt 1), 1 (2003).
- 176 Pecoits-Filho, R., Lindholm, B., Axelsson, J., and Stenvinkel, P., Update on interleukin-6 and its role in chronic renal failure. *Nephrol Dial Transplant* **18** (6), 1042 (2003).
- 177 Akira, S., The role of IL-18 in innate immunity. *Curr Opin Immunol* **12** (1), 59 (2000).
- 178 Netea, M. G. et al., Deficiency of interleukin-18 in mice leads to hyperphagia, obesity and insulin resistance. *Nat Med* **12** (6), 650 (2006).
- 179 Washburn, K. K. et al., Urinary interleukin-18 is an acute kidney injury biomarker in critically ill children. *Nephrol Dial Transplant* **23** (2), 566 (2008).
- 180 Tesch, G. H., MCP-1/CCL2: a new diagnostic marker and therapeutic target for progressive renal injury in diabetic nephropathy. *Am J Physiol Renal Physiol* **294** (4), F697 (2008).
- 181 Idriss, H. T. and Naismith, J. H., TNF alpha and the TNF receptor superfamily: structure-function relationship(s). *Microsc Res Tech* **50** (3), 184 (2000).
- 182 Lee, N. K. and Lee, S. Y., Modulation of life and death by the tumor necrosis factor receptor-associated factors (TRAFs). *J Biochem Mol Biol* **35** (1), 61 (2002).
- 183 Harrington, J. R., SODD-silencer of death domains. *Stem Cells* **18** (5), 388 (2000).
- 184 Vielhauer, V., Stavrakis, G., and Mayadas, T. N., Renal cell-expressed TNF receptor 2, not receptor 1, is essential for the development of glomerulonephritis. *J Clin Invest* **115** (5), 1199 (2005).
- 185 Moore, K. W., de Waal Malefyt, R., Coffman, R. L., and O'Garra, A., Interleukin-10 and the interleukin-10 receptor. *Annu Rev Immunol* **19**, 683 (2001).

- 186 Manigrasso, M. R. et al., Association between circulating adiponectin and interleukin-10 levels in android obesity: effects of weight loss. *J Clin Endocrinol Metab* **90** (10), 5876 (2005).
- 187 Stenvinkel, P. et al., IL-10, IL-6, and TNF-alpha: central factors in the altered cytokine network of uremia--the good, the bad, and the ugly. *Kidney Int* **67** (4), 1216 (2005).
- 188 Bogdan, C., Nitric oxide and the immune response. *Nat Immunol* **2** (10), 907 (2001).
- 189 Pacher, P., Beckman, J. S., and Liaudet, L., Nitric oxide and peroxynitrite in health and disease. *Physiol Rev* **87** (1), 315 (2007).
- 190 Marin, E. and Sessa, W. C., Role of endothelial-derived nitric oxide in hypertension and renal disease. *Curr Opin Nephrol Hypertens* **16** (2), 105 (2007).
- 191 Herrera, M. and Garvin, J. L., Recent advances in the regulation of nitric oxide in the kidney. *Hypertension* **45** (6), 1062 (2005).
- 192 Heeringa, P. et al., Expression of iNOS, eNOS, and peroxynitrite-modified proteins in experimental anti-myeloperoxidase associated crescentic glomerulonephritis. *Kidney Int* **53** (2), 382 (1998).
- 193 Perreault, M. and Marette, A., Targeted disruption of inducible nitric oxide synthase protects against obesity-linked insulin resistance in muscle. *Nat Med* **7** (10), 1138 (2001).
- 194 Heikkinen, S., Auwerx, J., and Argmann, C. A., PPARgamma in human and mouse physiology. *Biochim Biophys Acta* **1771** (8), 999 (2007).
- 195 Rosen, E. D. and Spiegelman, B. M., PPARgamma : a nuclear regulator of metabolism, differentiation, and cell growth. *J Biol Chem* **276** (41), 37731 (2001).
- 196 Berger, J. P., Role of PPARgamma, transcriptional cofactors, and adiponectin in the regulation of nutrient metabolism, adipogenesis and insulin action: view from the chair. *Int J Obes (Lond)* **29 Suppl 1**, S3 (2005).
- 197 Marx, N., PPARgamma and vascular inflammation: adding another piece to the puzzle. *Circ Res* **91** (5), 373 (2002).
- 198 Qiu, X. T. et al., Molecular cloning, mapping, and tissue expression of the porcine cluster of differentiation 14 (CD14) gene. *Biochem Genet* **45** (5-6), 459 (2007).
- 199 Triantafilou, M. and Triantafilou, K., Lipopolysaccharide recognition: CD14, TLRs and the LPS-activation cluster. *Trends Immunol* **23** (6), 301 (2002).
- 200 Roncon-Albuquerque, R., Jr. et al., Attenuation of the cardiovascular and metabolic complications of obesity in CD14 knockout mice. *Life Sci* **83** (13-14), 502 (2008).

- 201 Zhou, J. et al., Renal CD14 expression correlates with the progression
of cystic kidney disease. *Kidney Int* **78** (6), 550.
- 202 Akira, S. and Takeda, K., Toll-like receptor signalling. *Nat Rev
Immunol* **4** (7), 499 (2004).
- 203 Vitseva, O. I. et al., Inducible Toll-like receptor and NF-kappaB
regulatory pathway expression in human adipose tissue. *Obesity
(Silver Spring)* **16** (5), 932 (2008).
- 204 Pulskens, W. P. et al., TLR4 promotes fibrosis but attenuates tubular
damage in progressive renal injury. *J Am Soc Nephrol* **21** (8), 1299.
- 205 Paulos, C. M. et al., Toll-like receptors in tumor immunotherapy. *Clin
Cancer Res* **13** (18 Pt 1), 5280 (2007).
- 206 van de Stolpe, A. and van der Saag, P. T., Intercellular adhesion
molecule-1. *J Mol Med* **74** (1), 13 (1996).
- 207 Okada, S. et al., Intercellular adhesion molecule-1-deficient mice are
resistant against renal injury after induction of diabetes. *Diabetes* **52**
(10), 2586 (2003).
- 208 Carlos, T. M. et al., Vascular cell adhesion molecule-1 mediates
lymphocyte adherence to cytokine-activated cultured human
endothelial cells. *Blood* **76** (5), 965 (1990).
- 209 Bosanska, L. et al., The influence of obesity and different fat depots on
adipose tissue gene expression and protein levels of cell adhesion
molecules. *Physiol Res* **59** (1), 79.
- 210 Seron, D., Cameron, J. S., and Haskard, D. O., Expression of VCAM-1
in the normal and diseased kidney. *Nephrol Dial Transplant* **6** (12),
917 (1991).
- 211 Riedl, S. J. and Shi, Y., Molecular mechanisms of caspase regulation
during apoptosis. *Nat Rev Mol Cell Biol* **5** (11), 897 (2004).
- 212 Zangemeister-Wittke, U. and Simon, H. U., Apoptosis--regulation and
clinical implications. *Cell Death Differ* **8** (5), 537 (2001).
- 213 Yang, B. et al., Caspase-3 and apoptosis in experimental chronic renal
scarring. *Kidney Int* **60** (5), 1765 (2001).
- 214 Essers, J. et al., Nuclear dynamics of PCNA in DNA replication and
repair. *Mol Cell Biol* **25** (21), 9350 (2005).
- 215 Soto, H. et al., Apoptosis in proliferative glomerulonephritis: decreased
apoptosis expression in lupus nephritis. *Nephrol Dial Transplant* **12** (2),
273 (1997).
- 216 Ebert, B. L. and Bunn, H. F., Regulation of the erythropoietin gene.
Blood **94** (6), 1864 (1999).
- 217 Rossert, J. and Eckardt, K. U., Erythropoietin receptors: their role
beyond erythropoiesis. *Nephrol Dial Transplant* **20** (6), 1025 (2005).

- 218 Ikegaya, N., Hishida, A., and Yamamoto, T., High expression of erythropoietin receptor in human chronic progressive glomerulonephritis. *Kidney Int* **56** (3), 1159 (1999).
- 219 van der Putten, K., Braam, B., Jie, K. E., and Gaillard, C. A., Mechanisms of Disease: erythropoietin resistance in patients with both heart and kidney failure. *Nat Clin Pract Nephrol* **4** (1), 47 (2008).
- 220 Takahashi, N. et al., Increased energy expenditure, dietary fat wasting, and resistance to diet-induced obesity in mice lacking renin. *Cell Metab* **6** (6), 506 (2007).
- 221 Blackwell, T. S. and Christman, J. W., Sepsis and cytokines: current status. *Br J Anaesth* **77** (1), 110 (1996).
- 222 Ferreira, M. A., Cytokine expression in allergic inflammation: systematic review of in vivo challenge studies. *Mediators Inflamm* **12** (5), 259 (2003).
- 223 House, Robert V. and Descotes, Jacques, *Cytokines in human health : immunotoxicology, pathology, and therapeutic applications*. (Humana ; Quantum [distributor], Totowa, N.J.Paisley, 2007).
- 224 NHS, National child measurement programme: England, 2009/2010 school year. *The health and social care information centre Department of Health* (2010).
- 225 Symonds, M. E., Stephenson, T., Gardner, D. S., and Budge, H., Long-term effects of nutritional programming of the embryo and fetus: mechanisms and critical windows. *Reprod Fertil Dev* **19** (1), 53 (2007).
- 226 Williams, P. J. et al., Hypertension and impaired renal function accompany juvenile obesity: the effect of prenatal diet. *Kidney Int* **72** (3), 279 (2007).
- 227 Sharkey, D. et al., Maternal nutrient restriction during pregnancy differentially alters the unfolded protein response in adipose and renal tissue of obese juvenile offspring. *FASEB J* **23** (5), 1314 (2009).
- 228 Sebert, S. P. et al., Maternal nutrient restriction between early and midgestation and its impact upon appetite regulation after juvenile obesity. *Endocrinology* **150** (2), 634 (2009).
- 229 Hyatt, M. A., Keisler, D. H., Budge, H., and Symonds, M. E., Maternal parity and its effect on adipose tissue deposition and endocrine sensitivity in the postnatal sheep. *J Endocrinol* **204** (2), 173.
- 230 Fainberg, Hernan, Alterations induced by juvenile obesity on the renal tissue of nutrient restricted offspring. *UoN Academic Child Health Department* (2010).
- 231 Mcmillan, C, The sheep - an ideal model for biomedical research? *The Australian and New Zealand council for the care of animals in research and training* **14** (2), 1 (2001).
- 232 Consortium, Metabolic Programming, The Early Nutrition Programming Project, Available at <http://www.metabolic-programming.org>, (2005).

- 233 Agricultural, Food Research Council. Technical Committee on Responses to, Nutrients, Alderman, G., and Cottrill, B. R., *Energy and protein requirements of ruminants*. (CAB International, Wallingford, 1993).
- 234 Rhodes, P. et al., Adult-onset obesity reveals prenatal programming of glucose-insulin sensitivity in male sheep nutrient restricted during late gestation. *PLoS One* **4** (10), e7393 (2009).
- 235 Chomczynski, P. and Sacchi, N., Single-step method of RNA isolation by acid guanidinium thiocyanate-phenol-chloroform extraction. *Anal Biochem* **162** (1), 156 (1987).
- 236 Chomczynski, P., A reagent for the single-step simultaneous isolation of RNA, DNA and proteins from cell and tissue samples. *Biotechniques* **15** (3), 532 (1993).
- 237 Glasel, J. A., Validity of nucleic acid purities monitored by 260nm/280nm absorbance ratios. *Biotechniques* **18** (1), 62 (1995).
- 238 Wilson, Keith and Walker, John, *Principles and techniques of biochemistry and molecular biology*. (Cambridge University Press, Cambridge).
- 239 Butler, John M., *Forensic DNA typing : biology & technology behind STR markers*. (Academic Press, London, 2001).
- 240 Saiki, R. K. et al., Primer-directed enzymatic amplification of DNA with a thermostable DNA polymerase. *Science* **239** (4839), 487 (1988).
- 241 Ahn, S. J., Costa, J., and Emanuel, J. R., PicoGreen quantitation of DNA: effective evaluation of samples pre- or post-PCR. *Nucleic Acids Res* **24** (13), 2623 (1996).
- 242 Kochanowski, Bernd and Reischl, Udo, *Quantitative PCR protocols*. (Humana Press, Totowa, N.J., 1999).
- 243 Bustin, Stephen A., *A-Z of quantitative PCR*. (International University Line, La Jolla, Calif., 2004).
- 244 Pfaffl, M. W., A new mathematical model for relative quantification in real-time RT-PCR. *Nucleic Acids Res* **29** (9), e45 (2001).
- 245 Rutledge, R. G. and Cote, C., Mathematics of quantitative kinetic PCR and the application of standard curves. *Nucleic Acids Res* **31** (16), e93 (2003).
- 246 Livak, K. J. and Schmittgen, T. D., Analysis of relative gene expression data using real-time quantitative PCR and the 2(-Delta Delta C(T)) Method. *Methods* **25** (4), 402 (2001).
- 247 Bustin, S. A. et al., The MIQE guidelines: minimum information for publication of quantitative real-time PCR experiments. *Clin Chem* **55** (4), 611 (2009).

- 248 Silver, N., Best, S., Jiang, J., and Thein, S. L., Selection of housekeeping genes for gene expression studies in human reticulocytes using real-time PCR. *BMC Mol Biol* **7**, 33 (2006).
- 249 Vandesompele, J. et al., Accurate normalization of real-time quantitative RT-PCR data by geometric averaging of multiple internal control genes. *Genome Biol* **3** (7), RESEARCH0034 (2002).
- 250 Jain, M., Nijhawan, A., Tyagi, A. K., and Khurana, J. P., Validation of housekeeping genes as internal control for studying gene expression in rice by quantitative real-time PCR. *Biochem Biophys Res Commun* **345** (2), 646 (2006).
- 251 Biederman, J., Yee, J., and Cortes, P., Validation of internal control genes for gene expression analysis in diabetic glomerulosclerosis. *Kidney Int* **66** (6), 2308 (2004).
- 252 Goidin, D. et al., Ribosomal 18S RNA prevails over glyceraldehyde-3-phosphate dehydrogenase and beta-actin genes as internal standard for quantitative comparison of mRNA levels in invasive and noninvasive human melanoma cell subpopulations. *Anal Biochem* **295** (1), 17 (2001).
- 253 Flouriot, G. et al., An S1 nuclease mapping method for detection of low abundance transcripts. *Anal Biochem* **237** (1), 159 (1996).
- 254 Lodish, Harvey F., *Molecular cell biology*. (W.H. Freeman, New York, 2008).
- 255 Werner, M., Chott, A., Fabiano, A., and Battifora, H., Effect of formalin tissue fixation and processing on immunohistochemistry. *Am J Surg Pathol* **24** (7), 1016 (2000).
- 256 Bancroft, John D. and Gamble, Marilyn, *Theory and practice of histological techniques*. (Churchill Livingstone, Edinburgh, 2007).
- 257 Kiernan, J. A., *Histological and histochemical methods : theory and practice*. (Arnold, London, 2002).
- 258 Aprahamian, T. et al., The peroxisome proliferator-activated receptor gamma agonist rosiglitazone ameliorates murine lupus by induction of adiponectin. *J Immunol* **182** (1), 340 (2009).
- 259 Jennette, J. Charles and Heptinstall, Robert H., *Heptinstall's pathology of the kidney : editors, J. Charles Jennette ... [et al.]*. (Lippincott Williams & Wilkins, Philadelphia, PA, 2007).
- 260 Henegar, J. R. et al., Functional and structural changes in the kidney in the early stages of obesity. *J Am Soc Nephrol* **12** (6), 1211 (2001).
- 261 Sugimoto, H., Grahovac, G., Zeisberg, M., and Kalluri, R., Renal fibrosis and glomerulosclerosis in a new mouse model of diabetic nephropathy and its regression by bone morphogenic protein-7 and advanced glycation end product inhibitors. *Diabetes* **56** (7), 1825 (2007).

- 262 Cochrane, A. L. et al., Renal structural and functional repair in a mouse model of reversal of ureteral obstruction. *J Am Soc Nephrol* **16** (12), 3623 (2005).
- 263 Wintour, E. M. et al., Reduced nephron number in adult sheep, hypertensive as a result of prenatal glucocorticoid treatment. *J Physiol* **549** (Pt 3), 929 (2003).
- 264 Ramos-Vara, J. A., Technical aspects of immunohistochemistry. *Vet Pathol* **42** (4), 405 (2005).
- 265 Graham, R. C., Jr. and Karnovsky, M. J., The early stages of absorption of injected horseradish peroxidase in the proximal tubules of mouse kidney: ultrastructural cytochemistry by a new technique. *J Histochem Cytochem* **14** (4), 291 (1966).
- 266 Shi, S. R., Key, M. E., and Kalra, K. L., Antigen retrieval in formalin-fixed, paraffin-embedded tissues: an enhancement method for immunohistochemical staining based on microwave oven heating of tissue sections. *J Histochem Cytochem* **39** (6), 741 (1991).
- 267 Barham, D. and Trinder, P., An improved colour reagent for the determination of blood glucose by the oxidase system. *Analyst* **97** (151), 142 (1972).
- 268 Laboratories, Randox, Glucose (gluc-pap) godpap manual, Available at <http://www.cegepsheerbrooke.qc.ca/~fournire/Biolaboratoire/Glucose/GlucMan.pdf>, (2007).
- 269 Hosaka, K., Kikuchi, T., Mitsuhide, N., and Kawaguchi, A., A new colorimetric method for the determination of free fatty acids with acyl-CoA synthetase and acyl-CoA oxidase. *J Biochem* **89** (6), 1799 (1981).
- 270 Laboratories, Randox, Triglycerides (trigs) gpopap manual method, Available at <http://www.cegepsheerbrooke.qc.ca/~fournire/Biolaboratoire/Cholesterol/TriMan.pdf>, (2007).
- 271 Laboratories, Randox, NEFA non-esterified fatty acids manual, Available at <http://www.eugene-chen.com.tw/download/FA115.pdf>, (2007).
- 272 Abcam, Creatinine Assay Kit, Available at <http://www.abcam.com/index.html?pageconfig=protocols&pid=1010&intAbID=65340&strTab=protocols&mode=prot>, (2010).
- 273 Folch, J., Lees, M., and Sloane Stanley, G. H., A simple method for the isolation and purification of total lipides from animal tissues. *J Biol Chem* **226** (1), 497 (1957).
- 274 Bobulescu, I. A. et al., Reduction of renal triglyceride accumulation: effects on proximal tubule Na⁺/H⁺ exchange and urinary acidification. *Am J Physiol Renal Physiol* **297** (5), F1419 (2009).

- 275 Held, P, An introduction to reactive oxygen species - measurement of ROS in cells, Available at http://www.biotek.com/assets/tech_resources/ROS_White_Paper.pdf, (2010).
- 276 Marnett, L. J., Oxy radicals, lipid peroxidation and DNA damage. *Toxicology* **181-182**, 219 (2002).
- 277 Draper, H. H., Csallany, A. S., and Hadley, M., Urinary aldehydes as indicators of lipid peroxidation in vivo. *Free Radic Biol Med* **29** (11), 1071 (2000).
- 278 Biolabs, Cell, Oxiselect™ TBARS Assay Kit, Available at <http://www.cellbiolabs.com/sites/default/files/STA-330-tbars-assay-kit.pdf>, (2010).
- 279 Song, Y. R. et al., Activation of hypoxia-inducible factor attenuates renal injury in rat remnant kidney. *Nephrol Dial Transplant* **25** (1), 77.
- 280 Sigma-Aldrich, Bicinchoninic acid protein assay kit, Available at <http://www.sigmaaldrich.com/etc/medialib/docs/Sigma/Bulletin/bca1bul.Par.0001.File.tmp/bca1bul.pdf>, (2011).
- 281 Smith, Paul, USA Patent No. 4839295 (1989).
- 282 Burnette, W. N., "Western blotting": electrophoretic transfer of proteins from sodium dodecyl sulfate--polyacrylamide gels to unmodified nitrocellulose and radiographic detection with antibody and radioiodinated protein A. *Anal Biochem* **112** (2), 195 (1981).
- 283 Towbin, H., Staehelin, T., and Gordon, J., Electrophoretic transfer of proteins from polyacrylamide gels to nitrocellulose sheets: procedure and some applications. *Proc Natl Acad Sci U S A* **76** (9), 4350 (1979).
- 284 Sharkey, D., Gardner, D. S., Symonds, M. E., and Budge, H., Maternal nutrient restriction during early fetal kidney development attenuates the renal innate inflammatory response in obese young adult offspring. *Am J Physiol Renal Physiol* **297** (5), F1199 (2009).
- 285 Finch, H, Physical activity 'what we think' - Qualitative research among women aged 16-24. *Health Education Authority Social and community planning research*, 1 (1998).
- 286 Lightfoot, J. T., Sex hormones' regulation of rodent physical activity: a review. *Int J Biol Sci* **4** (3), 126 (2008).
- 287 Gorzek, J. F. et al., Estradiol and tamoxifen reverse ovariectomy-induced physical inactivity in mice. *Med Sci Sports Exerc* **39** (2), 248 (2007).
- 288 Chan, M. F. et al., Usual physical activity and endogenous sex hormones in postmenopausal women: the European prospective investigation into cancer-norfolk population study. *Cancer Epidemiol Biomarkers Prev* **16** (5), 900 (2007).

- 289 Heymsfield, S. B. et al., Body-size dependence of resting energy expenditure can be attributed to nonenergetic homogeneity of fat-free mass. *Am J Physiol Endocrinol Metab* **282** (1), E132 (2002).
- 290 Kelley, D. E., Goodpaster, B. H., and Storlien, L., Muscle triglyceride and insulin resistance. *Annu Rev Nutr* **22**, 325 (2002).
- 291 Kopelman, Peter G., Caterson, Ian D., and Dietz, William H., *Clinical obesity in adults and children*. (Wiley-Blackwell, Chichester).
- 292 Kanadys, W. M. and Oleszczuk, J., [Pathophysiological aspects of adipose tissue development in women]. *Ginekol Pol* **70** (6), 456 (1999).
- 293 Romanski, S. A., Nelson, R. M., and Jensen, M. D., Meal fatty acid uptake in adipose tissue: gender effects in nonobese humans. *Am J Physiol Endocrinol Metab* **279** (2), E455 (2000).
- 294 Koska, J. et al., Increased fat accumulation in liver may link insulin resistance with subcutaneous abdominal adipocyte enlargement, visceral adiposity, and hypo adiponectinemia in obese individuals. *Am J Clin Nutr* **87** (2), 295 (2008).
- 295 Marin, P. et al., The morphology and metabolism of intraabdominal adipose tissue in men. *Metabolism* **41** (11), 1242 (1992).
- 296 Altintas, M. M. et al., Mast cells, macrophages, and crown-like structures distinguish subcutaneous from visceral fat in mice. *J Lipid Res* **52** (3), 480.
- 297 Giussani, D. A., Fletcher, A. J., and Gardner, D. S., Sex differences in the ovine fetal cortisol response to stress. *Pediatr Res* **69** (2), 118.
- 298 Rivier, C., Gender, sex steroids, corticotropin-releasing factor, nitric oxide, and the HPA response to stress. *Pharmacol Biochem Behav* **64** (4), 739 (1999).
- 299 Roca, C. A. et al., Sex-related differences in stimulated hypothalamic-pituitary-adrenal axis during induced gonadal suppression. *J Clin Endocrinol Metab* **90** (7), 4224 (2005).
- 300 Strain, G. W. et al., Sex difference in the influence of obesity on the 24 hr mean plasma concentration of cortisol. *Metabolism* **31** (3), 209 (1982).
- 301 Bjorntorp, P., Do stress reactions cause abdominal obesity and comorbidities? *Obes Rev* **2** (2), 73 (2001).
- 302 Handa, R. J., Burgess, L. H., Kerr, J. E., and O'Keefe, J. A., Gonadal steroid hormone receptors and sex differences in the hypothalamo-pituitary-adrenal axis. *Horm Behav* **28** (4), 464 (1994).
- 303 Austin, H. et al., Endometrial cancer, obesity, and body fat distribution. *Cancer Res* **51** (2), 568 (1991).
- 304 Annison, E. F. and White, R. R., Glucose utilization in sheep. *Biochem J* **80**, 162 (1961).

- 305 Frias, J. P. et al., Decreased susceptibility to fatty acid-induced peripheral tissue insulin resistance in women. *Diabetes* **50** (6), 1344 (2001); Kuhl, J. et al., Characterisation of subjects with early abnormalities of glucose tolerance in the Stockholm Diabetes Prevention Programme: the impact of sex and type 2 diabetes heredity. *Diabetologia* **48** (1), 35 (2005).
- 306 Ren, J., Leptin and hyperleptinemia - from friend to foe for cardiovascular function. *J Endocrinol* **181** (1), 1 (2004).
- 307 Chilliard, Y. et al., Leptin in ruminants. Gene expression in adipose tissue and mammary gland, and regulation of plasma concentration. *Domest Anim Endocrinol* **21** (4), 271 (2001).
- 308 Bickerstaffe, R. and Annison, E. F., Triglyceride synthesis by the small-intestinal epithelium of the pig, sheep and chicken. *Biochem J* **111** (4), 419 (1969).
- 309 Bo, S. et al., Contributors to the obesity and hyperglycemia epidemics. A prospective study in a population-based cohort. *Int J Obes (Lond)*.
- 310 Carr, M. C. and Brunzell, J. D., Abdominal obesity and dyslipidemia in the metabolic syndrome: importance of type 2 diabetes and familial combined hyperlipidemia in coronary artery disease risk. *J Clin Endocrinol Metab* **89** (6), 2601 (2004).
- 311 Kelley, D. E. and Goodpaster, B. H., Skeletal muscle triglyceride. An aspect of regional adiposity and insulin resistance. *Diabetes Care* **24** (5), 933 (2001).
- 312 Fruhbeck, G., Jebb, S. A., and Prentice, A. M., Leptin: physiology and pathophysiology. *Clin Physiol* **18** (5), 399 (1998).
- 313 Scarpace, P. J., Nicolson, M., and Matheny, M., UCP2, UCP3 and leptin gene expression: modulation by food restriction and leptin. *J Endocrinol* **159** (2), 349 (1998).
- 314 Montague, C. T. et al., Depot- and sex-specific differences in human leptin mRNA expression: implications for the control of regional fat distribution. *Diabetes* **46** (3), 342 (1997).
- 315 Kern, P. A. et al., Adiponectin expression from human adipose tissue: relation to obesity, insulin resistance, and tumor necrosis factor-alpha expression. *Diabetes* **52** (7), 1779 (2003).
- 316 Abbasi, F. et al., Discrimination between obesity and insulin resistance in the relationship with adiponectin. *Diabetes* **53** (3), 585 (2004).
- 317 Pitteloud, N. et al., Relationship between testosterone levels, insulin sensitivity, and mitochondrial function in men. *Diabetes Care* **28** (7), 1636 (2005).
- 318 Awazawa, M. et al., Adiponectin enhances insulin sensitivity by increasing hepatic IRS-2 expression via a macrophage-derived IL-6-dependent pathway. *Cell Metab* **13** (4), 401.

- 319 Bauche, I. B. et al., Overexpression of adiponectin targeted to adipose tissue in transgenic mice: impaired adipocyte differentiation. *Endocrinology* **148** (4), 1539 (2007).
- 320 Boullu-Ciocca, S. et al., Postnatal diet-induced obesity in rats upregulates systemic and adipose tissue glucocorticoid metabolism during development and in adulthood: its relationship with the metabolic syndrome. *Diabetes* **54** (1), 197 (2005).
- 321 Veilleux, A. et al., Expression of genes related to glucocorticoid action in human subcutaneous and omental adipose tissue. *J Steroid Biochem Mol Biol* **122** (1-3), 28.
- 322 Seckl, J. R., Morton, N. M., Chapman, K. E., and Walker, B. R., Glucocorticoids and 11beta-hydroxysteroid dehydrogenase in adipose tissue. *Recent Prog Horm Res* **59**, 359 (2004).
- 323 Kannisto, K. et al., Overexpression of 11beta-hydroxysteroid dehydrogenase-1 in adipose tissue is associated with acquired obesity and features of insulin resistance: studies in young adult monozygotic twins. *J Clin Endocrinol Metab* **89** (9), 4414 (2004).
- 324 Wake, D. J. et al., Local and systemic impact of transcriptional up-regulation of 11beta-hydroxysteroid dehydrogenase type 1 in adipose tissue in human obesity. *J Clin Endocrinol Metab* **88** (8), 3983 (2003).
- 325 Purinton, S. C. and Wood, C. E., Oestrogen augments the fetal ovine hypothalamus- pituitary-adrenal axis in response to hypotension. *J Physiol* **544** (Pt 3), 919 (2002).
- 326 Davies D, Symonds ME and Gardner D, 11 β hydroxysteroid dehydrogenase type 2 (11 β HSD2) is expressed in omental fat of week old lambs. *Endocrine abstracts* **8**, p58 (2004).
- 327 Milagro, F. I., Campion, J., and Martinez, J. A., 11-Beta hydroxysteroid dehydrogenase type 2 expression in white adipose tissue is strongly correlated with adiposity. *J Steroid Biochem Mol Biol* **104** (1-2), 81 (2007).
- 328 Zhang, H. M. et al., Macrophage infiltrates with high levels of Toll-like receptor 4 expression in white adipose tissues of male Chinese. *Nutr Metab Cardiovasc Dis* **19** (10), 736 (2009).
- 329 Chudek, J. et al., Plasma adiponectin concentration before and after successful kidney transplantation. *Transplant Proc* **35** (6), 2186 (2003).
- 330 Keller, C., Keller, P., Marshal, S., and Pedersen, B. K., IL-6 gene expression in human adipose tissue in response to exercise--effect of carbohydrate ingestion. *J Physiol* **550** (Pt 3), 927 (2003).
- 331 Beutler, B. A., Milsark, I. W., and Cerami, A., Cachectin/tumor necrosis factor: production, distribution, and metabolic fate in vivo. *J Immunol* **135** (6), 3972 (1985).
- 332 Galatos, A. D., Anesthesia and analgesia in sheep and goats. *Vet Clin North Am Food Anim Pract* **27** (1), 47.

- 333 Hotta, O. et al., Possible relationship between hyperinsulinemia and glomerular hypertrophy in nephrosclerosis. *Ren Fail* **18** (2), 271 (1996).
- 334 Gaffney, E. F. and Panner, B. J., Membranous glomerulonephritis: clinical significance of glomerular hypercellularity and parietal epithelial abnormalities. *Nephron* **29** (5-6), 209 (1981).
- 335 Benz, K. et al., Early glomerular alterations in genetically determined low nephron number. *Am J Physiol Renal Physiol* **300** (2), F521.
- 336 Janmahasatian, S. et al., Lean body mass normalizes the effect of obesity on renal function. *Br J Clin Pharmacol* **65** (6), 964 (2008).
- 337 Bak, M., Thomsen, K., Christiansen, T., and Flyvbjerg, A., Renal enlargement precedes renal hyperfiltration in early experimental diabetes in rats. *J Am Soc Nephrol* **11** (7), 1287 (2000).
- 338 Praga, M., Synergy of low nephron number and obesity: a new focus on hyperfiltration nephropathy. *Nephrol Dial Transplant* **20** (12), 2594 (2005).
- 339 Griffin, K. A., Kramer, H., and Bidani, A. K., Adverse renal consequences of obesity. *Am J Physiol Renal Physiol* **294** (4), F685 (2008).
- 340 Mangos, G. J., Whitworth, J. A., Williamson, P. M., and Kelly, J. J., Glucocorticoids and the kidney. *Nephrology (Carlton)* **8** (6), 267 (2003).
- 341 Jaenisch, R. and Bird, A., Epigenetic regulation of gene expression: how the genome integrates intrinsic and environmental signals. *Nat Genet* **33 Suppl**, 245 (2003).
- 342 Wang, X. et al., Obesity related methylation changes in DNA of peripheral blood leukocytes. *BMC Med* **8**, 87.
- 343 Brasier, A. R., The NF-kappaB regulatory network. *Cardiovasc Toxicol* **6** (2), 111 (2006).
- 344 Kaminsky, Z., Wang, S. C., and Petronis, A., Complex disease, gender and epigenetics. *Ann Med* **38** (8), 530 (2006).

Appendices

Appendix A – Abstracts, original presentation and conferences attended

Gender differences of inflammatory cytokine expression in kidney using an ovine model of obesity

Ian Bloor, David Gardner, Ravi Mahajan, Sylvain Sebert and Michael Symonds, Department of Academic Child Health School of Clinical Sciences, The University of Nottingham, UK.

Oral presentation by Ian Bloor - Anaesthesia Research Society winter meeting, The Royal College of Anaesthetists, London, UK, December 2009. *British Journal of Anaesthesia* 104 (4): 517-31P (2010)

Obesity has long been linked to a low level pro-inflammatory state which may contribute to numerous clinical manifestations¹. This study aims to investigate expression of two key regulators in the inflammatory apoptosis pathway² MCP-1 (monocyte chemo-attractant protein 1) and its receptor CCR2 in kidney tissue to investigate inflammation within a localised organ system using a sheep model of obesity. At the post-weaning stage of development, male (n=19) and female (n=16) sheep were separated into two experimental groups of physical activity and raised in either an obesogenic (O) or lean (L) environment. Renal tissue RNA was extracted from these sheep and expression of MCP-1 and MCP-1 receptor (CCR2) was analysed using quantitative reverse transcriptase polymerase chain reaction (RT-PCR) and expression quantified using the $2^{-\Delta ct}$ method. Expression of MCP-1 showed a 2 mean fold increase in obese males (n=9) when compared to lean males (n=10) ($p < 0.05$) but not in females (n=9). CCR2 expression showed a 2.5 mean fold increase between lean and obese male sheep ($p < 0.005$) and an 8 mean fold increase in obese males when compared to obese females ($p < 0.0005$). With regards to inflammation in kidney tissue of obese sheep, this study shows that expression of MCP-1 and CCR2 are increased in comparison to lean sheep in males. However this elevation is not seen in the female sheep, suggesting a possible protective effect in obese females which future work in the study aims to investigate further.

Impact of gender on glomerular responses and inflammatory gene expression following juvenile onset obesity in sheep

*Ian Bloor, Sylvain P Sebert, Ravi Mahajan and Michael E Symonds
Department of Academic Child Health, School of Clinical Sciences, The
University of Nottingham, United Kingdom.*

Oral presentation by Ian Bloor – The Physiological Society main summer meeting, The University of Manchester, Manchester, UK, June 2010. *Proceedings of the Physiological Society*, 19, C140

Clinical and experimental evidence suggests that obesity mediated low grade inflammation may contribute towards organ damage and other adverse clinical effects¹ that may be gender dependent. The present study aims to investigate whether obesity modifies kidney glomeruli physiology and gene expression of key regulators involved in activation of the inflammatory immune response, such as cluster of differentiation 14 (CD14)², a lipopolysaccharide binding protein. In addition, we examined the impact of gender on these outcomes. Three months after birth, male (n=12) and female (n=10) sheep were randomly separated into two experimental groups, comprising of restricted and unrestricted activity and thus raised in either a lean (L) or obesogenic (O) environment. At \approx 17 months of age all animals were humanely euthanised and all major organs and tissues sampled. Gene expression was determined using quantitative reverse transcriptase polymerase chain reaction (RT-PCR) and expression quantified using the $2^{-\Delta ct}$ method. Histological staining was performed using haematoxylin and eosin on paraffin-embedded renal tissue sectioned at 5 μ m. Glomerular area and nucleated cell count were quantified using image analysis software Volocity. Kidney weight was increased ($p < 0.05$) with obesity in males (Obese - 140.1 ± 5.044 , (n=7); Lean 120.2 ± 7.276 g, (n=5)), but not females, as was mean glomerular area (Obese - 19790 ± 1094 ; lean - $14280 \pm 430.5 \mu\text{m}^2$ ($p < 0.05$)). This adaptation was accompanied by raised mRNA abundance of CD14 with obesity in males only (Obese - 3.214 ± 0.913 ; Lean - 0.992 ± 0.168 $2^{-\Delta ct}$ ($p < 0.01$)). Our study suggests that males are much more sensitive to the adverse effects of obesity on both glomeruli physiology and inflammatory responses. The mechanisms by which females may be protected from these effects are currently being explored.

This study was funded by the British Journal of Anaesthesia and the Royal College of Anaesthetists.

Influence of gender on the inflammatory response to the kidney following juvenile onset obesity

*Ian Bloor, Sylvain P Sebert, Ravi Mahajan and Michael E Symonds
Department of Academic Child Health, School of Clinical Sciences, The
University of Nottingham, United Kingdom.*

Oral presentation by Michael Symonds – Federation of American Societies for Experimental Biology (FASEB) Renal Haemodynamics 2010, Vermont Academy, Vermont, USA.

Extensive studies in small animals indicate that gender has a major influence on a majority of the long term cardiovascular and metabolic outcomes in the offspring following a change in either the amount or composition of the mother's diet through pregnancy and/or lactation. These differential responses may be mediated by either changes in growth rate and body composition between genders in conjunction with different effects of sex steroids. In large mammals and humans differences in growth through pregnancy, lactation and juvenile life are much more subtle which may explain why the effects of gender on cardiovascular control and kidney function are not so prominent. These effects in large mammals, such as sheep, may also not be dependent on sex steroids as the increased fat mass in females is present from the neonatal period and is accompanied by raised plasma leptin. We have also shown, in the sheep, that maternal nutrient restriction targeted at the stage of early kidney development has little, if any, effect on blood pressure of the resulting offspring when they are maintained with a free-living natural environment. When these offspring are then exposed to a low activity obesogenic environment then all offspring become equally hypertensive although the adverse effects in the kidney in terms of inflammatory and angiogenic adaptations appear to be blunted.

We therefore examined the impact of gender on the kidneys response to obesity as we found that male sheep appear to be much more sensitive to the hypertensive effects of obesity than females. This is despite the fact that they possess approximately one-third less perirenal adipose tissue, one potential risk factor for kidney dysfunction following obesity. In lean animals there is very little difference in kidney structure or gene expression of inflammatory and related markers of apoptosis and macrophage function between males and females.

Following obesity however, we only find structural damage in the kidney of males that is accompanied by a pronounced increase in gene expression of key gene regulators in the inflammatory apoptosis pathway such as monocyte chemoattractant protein 1, its receptor CCR2 and the lipopolysaccharide receptor involved in the inflammatory response, toll-like receptor 4. Obesity, therefore, results in a pronounced increase in the inflammatory response in the kidney in males but not females, suggesting possible protection in females. The extent to which this response may be seen in other tissues and the mechanisms by which females may be protected from some of the adverse effects of obesity is currently under investigation.

Sex differences in adiposity and inflammatory gene expression in kidney following juvenile onset obesity in sheep

*Ian Bloor, Sylvain P Sebert, Ravi Mahajan and Michael E Symonds
Department of Academic Child Health, School of Clinical Sciences, The
University of Nottingham, United Kingdom.*

Poster presentation by Ian Bloor – Federation of American Societies for Experimental Biology (FASEB) 2011, Walter E Washington Convention Center, Washington DC, USA, April 2011. *The FASEB Journal*, 2011; 25: 835.1

The study aimed to investigate whether obesity affects inflammatory gene expression in kidney using a sheep model of obesity. In addition, we also explored the impact of gender on these outcomes.

Three months after birth, male (n=19) and female (n=16) sheep were randomly separated into two experimental groups, comprising of restricted and unrestricted activity, thus raised in either a lean (L) or obesogenic (O) environment. Gene expression was determined using quantitative reverse transcriptase PCR and expression quantified using the $2^{-\Delta\text{ct}}$ method. Perirenal adipose tissue per g/kg of body weight was increased ($p < 0.05$) with obesity in females compared to males (Obese females – 17.05 ± 1.84 , (n=9); Obese Males 11.41 ± 1.29 g, (n=9)), as was renal triglyceride deposition mg/g (Females – 0.219 ± 0.016 : males – 0.140 ± 0.019 mg ($p < 0.05$)). mRNA abundance of Toll like receptor 4 was elevated with obesity only in males (Obese - 33.11 ± 5.89 : Lean – 17.24 ± 2.27 , (n=10) $2^{-\Delta\text{ct}}$ ($p < 0.01$)). Our study suggests that despite increased renal adiposity and triglyceride deposition in females, only males appear to respond to obesity through elevated inflammatory gene expression, thus possibly displaying increased sensitivity to obesity. The mechanisms by which females may be protected from these effects are currently being explored.

This study was funded by the British Journal of Anaesthesia and the Royal College of Anaesthetists.

Appendix B – Details of suppliers

Abcam[®], 330 Cambridge Science Park, Cambridge, CB4 0FL, UK;

www.abcam.com

Abgene Ltd, Abgene House, Blenheim Road, Epsom, KT19 9AP, UK;

www.abgene.com

Actigraph[™], 15 W Mainstreet, Pensacola, Florida (FL), 32502, USA;

www.theactigraph.com

Alpha Laboratories Ltd, 40 Parnham Drive, Eastleigh, Hampshire, SO50 4NU, UK; www.alphalabs.co.uk

Anglia Scientific Ltd, 94 Fordham Road, Soham, Ely, Cambridgeshire, CB7 5AJ, UK; <http://www.angliainst.co.uk/>

Antec International Ltd, Windham Road, Chilton Industrial Estate, Sudbury, Suffolk, CO10 2XD, UK; www.ahs.dupont.com

Applied Biosystems, 5791 Van Allen Way, PO Box 6482, Carlsbad, California (CA), USA; www.appliedbiosystems.com

Bibby Scientific Ltd, Beacon Road, Stone, Staffordshire, ST15 0SA, UK; www.techne.com

Biotek UK, 6 Bull Street, Pottton, Bedfordshire, SG19 2NR, UK; www.biotek.com

Bio-Rad Laboratories Ltd, Bio-Rad House, Maxted Road, Hemel Hempstead, Hertfordshire, HP2 7DX, UK; www.bio-rad.com

Bioron, Rheingoenheimer Str. 36, D-67065, Ludwigshafen, Germany; www.bioron.net

Cell Biolabs Inc., 7758 Arjons Drive, San Diego, California (CA), 92126, USA; www.cellbiolabs.com

Diagnostic Products Corporation, Llanberis, Glyn Rhonwy, Caernarfon, Gwynedd, LL55 4EL, UK; www.pharmaceutical-int.com

Ecolabs[®], 370 Wabasha St N, Saint Paul, Minnesota (MN), 55102, USA; www.ecolab.com

Fisher Scientific UK Ltd, Bishop Meadow Road, Loughborough,
Leicestershire, LE11 5RG, UK; www.fisher.co.uk

GE Healthcare Ltd, Amersham Place, Little Chalfont, Buckinghamshire, HP7
9NA, UK; www.gehealthcare.com

Genetex Inc., 2456 Alton Parkway, Irvine, California (CA), 92606, USA;
www.genetex.com

GraphPad Software Inc., 2236 Avenida de la Playa, La Jolla, California (CA),
92037, USA; www.graphpad.com

Grenier Bio-One Ltd, Brunel Way, Stroudwater Business Park, Stonehouse,
GL10 3SX, UK; www.greinerbioone.com

Hofer® Inc., 84 October Hill Road, Holliston, Massachusetts (MA), 01746,
USA; www.hoferinc.com

IBM UK Ltd, PO Box 41, North Harbour, Portsmouth, Hampshire, PO6 3AU,
UK; www.spss.com

Invitrogen Ltd, 3 Fountain Drive, Inchinnan Business Park, Paisley, PA4 9RF,
UK; www.invitrogen.com

Leica Microsystems (UK) Ltd, Davy Avenue Knowlhill, Milton Keynes,
Buckinghamshire, MK5 8LB, UK; www.leica-microsystems.com

Linton Instrumentation, 1 Forge Business Centre, Upper Rose Lane,
Palgrave, Diss, Norfolk, IP22 1AP, UK; www.lintoninst.co.uk

Manor Farm Feeds Ltd, Owston, Oakham, Rutland, LE15 8DH, UK;
www.manorfarmfeeds.co.uk

Mercodia, Sylveniusgatan 8A, SE-754 50, Uppsala, Sweden;
www.mercodia.se

Menzel-Gläser Inc., Glasbearbeitungswerk GmbH & Co., Saarbrückener Str.
248, D-38116, Braunschweig, Germany; www.menzel.de

Microsoft Corporation, One Microsoft Way, Redmond, Washington (WA),
98052, USA; www.microsoft.com

Millipore, 290 Concord Road, Billerica, Massachusetts (MA), 01821, USA;
www.millipore.com

Minitab Ltd, Brandon Court, Unit E1-E2, Progress Way, Coventry, CV3 2TE, UK; www.minitab.com

PerkinElmer, Saxon Way Bar Hill, Cambridge, Cambridgeshire, CB23 8SL, UK; www.perkinelmer.co.uk

Premier Biosoft International, 3786 Corina Way, Palo Alto, California (CA), 94303, USA; www.premierbiosoft.com

Primer Design Ltd, Millbrook Technology Campus, Second Avenue, Southampton, Hampshire, SO15 0DJ, UK; www.primerdesign.co.uk

Qiagen UK Ltd, Qiagen House, Fleming Way, Crawley, West Sussex, RH10 9NQ, UK; www.qiagen.com

Randox Laboratories Ltd, 55 Diamond Road, Crumlin, County Antrim, BT29 4QY, UK; www.randox.com

Raytek Corporation, 1201 Shaffer Road, Santa Cruz, California (CA), 95061, USA; www.raytek.com

Roche Diagnostics Ltd, Applied Science, Charles Avenue, Burgess Hill, West Sussex, RH15 9RY, UK; www.rocheuk.com

Scientific Laboratory Supplies (SLS) Ltd, Orchard House, The Square, Hessle, East Riding of Yorkshire, HU13 0AE, UK; www.scientificlabs.co.uk

Severn Biotech Ltd, Unit 2, Park Lane, Kidderminster, Worcestershire, DY11 6TJ, UK; www.severnbiotech.com

Sigma-Aldrich Company Ltd, Fancy Road, Poole, Dorset, BH12 4QH, UK; www.sigmaaldrich.com

Simport Ltd, 2588 Bernard-Pilon, Beloeil, Quebec (QC) J3G 4S5, Canada; www.simport.com

VWR International, Hunter Boulevard, Magna Park, Lutterworth, Leicestershire, LE17 4XN, UK; www.vwr.com

Wolf Laboratories Ltd, Colenso House, 1 Deans Lane, Pocklington, York, YO42 2PX, UK; www.wolflabs.co.uk

